



Brunel
University
London

**CLUSTERING CLASSIFICATION AND HUMAN PERCEPTION
OF AUTOMOTIVE STEERING WHEEL TRANSIENT
VIBRATIONS**

By

Sabariah Mohd Yusoff
1322339

Dissertation submitted in partial fulfilment for the degree of
Doctor of Philosophy

College of Engineering, Design and Physical Sciences
Brunel University London, UK

June 2017

ABSTRACT

In the 21st century, the proliferation of steer-by-wire systems has become a central issue in the automobile industry. With such systems there is often an objective to minimise vibrations on the steering wheel to increase driver comfort. Nevertheless, steering wheel vibration is also recognised as an important medium that assists drivers in judging the vehicle's subsystems dynamics as well as to indicate important information such as the presence of danger. This has led to studies of the possible role of vibrational stimuli towards informing drivers of environment conditions such as road surface types. Numerous prior studies were done to identify how characteristics of steering wheel vibrational stimuli might influence driver road surface detection which suggested that there is no single, optimal, acceleration gain that could improve the detection of all road surface types. There is currently a lack of studies on the characteristics of transient vibrations of steering wheel as appear to be an important source of information to the driver road surface detection. Therefore, this study is design to identify the similarity characteristics of transient vibrations for answering the main research question: ***“What are the time-domain features of transient vibrations that can optimise driver road surface detection?”***

This study starts by critically reviewing the existing principles of transient vibrations detection to ensure that the identified transient vibrations from original steering wheel vibrations satisfy with the definition of transient vibrations. The study continues by performing the experimental activities to identify the optimal measurement signal for both identification process of transient vibrations and driver road surface detection without taking for granted the basic measurement of signal processing. The studies then identify the similarity of transient vibrations according to their time-domain features. The studies done by performing the high-dimensional reduction techniques associated with clustering methods. Result suggests that the time-domain features of transient vibrations that can optimise driver road surface detection were found to consist of duration (Δt), amplitude (m/s^2), energy (*r.m.s*) and Kurtosis.

ACKNOWLEDGEMENT

In the name of God, the Most Gracious, the Most Merciful.

First and above all, I would like to express my endless praise and glory to ALLAH (الله), the One and only One, the Merciful and the Passionate God who gave me the courage, strength and patience to complete this research journey.

Many thanks are given to my supervisor, Professor Joseph Giacomini, for his help, research direction, and great encouragement during the completion of this work. Thanks are also dedicated to my second supervisor, Dr Marco Ajovalasit, for his much invaluable help and advice. As a team we have always had an excellent working relationship, and I very much look forward to continuing collaboration in the future.

Special thanks also go to Roslan Bakri+Shahidatul Azirah, Mohd Fathullah+Nurul Hayati, Mohd Anuar Ismail+Fatimatuzzahra, Yona Falinie, Nuraiman Syafiqah, BTB 3.0 buddies and Girls HealthyClub. Being thousands kilometre away from family, having friends who were always there for support and who helped me a lot in overcoming obstacles and staying focused on my studies was such a blessing. Not forgotten, to my officemates (MCST-351), Voula, Kyungjoo, Marlene and Dani for their support and valuable discussions throughout this journey.

There are no words to express how grateful I am to my mother and father for their support, encouragement, patience and prayers for accomplishing my educational goals throughout my life. I would like to thank all my sisters, brothers, niece and nephews for believing in me. Also, I do not forget to mention my gratitude to my in-laws for their concern and support. Finally I would like to express appreciation to my beloved one, Abdul Farhan bin Ibrahim, for his love, patience, sacrifice, and trust.

TABLE OF CONTENTS

ABSTRACT	i
ACKNOWLEDGEMENT	ii
TABLE OF CONTENTS	iii
LIST OF FIGURES	vi
LIST OF TABLES	xiv
CHAPTER 1 MOTIVATION BEHIND THE RESEARCH	1
1.1 Introduction	1
1.2 Evolution of Automobile Steer-By-Wire Systems	3
1.3 Steering Wheel Vibration Stimuli to Automobile Drivers	7
1.4 The 21 st Century Steering System	8
1.5 Research Aim, Objectives and Questions.....	12
CHAPTER 2 HAND-ARM TRANSMITTED AUTOMOBILE STEERING WHEEL VIBRATION	14
2.1 Introduction	14
2.2 Subjective Response to Hand-Arm Transmitted Vibrations	15
2.3 Subjective Response to Hand-Arm Transmitted Steering Wheel Vibrations.....	24
2.4 Conclusion	28
CHAPTER 3 HUMAN COGNITION	29
3.1 Introduction	29
3.2 The Information-Processing Model.....	31
3.3 Human Decision-Making Process	36
3.4 Signal Detection Theory	39
3.5 Conclusion	51

CHAPTER 4 CLUSTER ANALYSIS	53
4.1 Introduction	53
4.2 Visualising Clusters	54
4.3 Clustering Techniques	58
4.4 Conclusion	62
CHAPTER 5 LABORATORY ROAD SURFACES STIMULI AND FACILITIES	64
5.1 Introduction	64
5.2 Laboratory Road Surfaces Stimuli	64
5.3 Laboratory Facilities.....	75
5.4 Conclusion	80
CHAPTER 6 PRINCIPLES OF TRANSIENT VIBRATIONS ROAD SURFACE DETECTION.....	82
6.1 Introduction	82
6.2 MNMS Algorithm for Road Surfaces Transient Vibrations	83
6.3 Towards Better Principles of Transient Vibrations Road Surface	88
6.4 Conclusion	95
CHAPTER 7 VIBRATION ENERGY DISTRIBUTION ON DRIVER ROAD SURFACE DETECTION.....	97
7.1 Introduction	97
7.2 Test Stimuli	99
7.3 Test Protocol.....	102
7.4 Test Participants	104
7.5 Results and Analysis.....	106
7.6 Discussion.....	111
7.7 Conclusion	113

CHAPTER 8 INTEGRATION AND DIFFERENTIATION OF STEERING WHEEL VIBRATION SIGNALS	114
8.1 Introduction	114
8.2 The Effect of Time-domain Integration on Transient Vibrations Steering Wheel Road Surface	116
8.3 The Effect of Time-domain Differentiation on Drivers' Steering Wheel Transient Vibrations Detection.....	125
8.4 Conclusion.....	142
CHAPTER 9 CLUSTERING CLASSIFICATION ON HIGH-DIMENSIONAL OF TRANSIENT VIBRATIONS	144
9.1 Introduction	144
9.2 Clustering Classification of Steering Wheel Transient Vibrations	145
9.3 Discussion.....	164
9.4 Conclusion.....	165
CHAPTER 10 CONCLUSIONS AND FUTURE RESEARCH	166
10.1 Introduction	166
10.2 Key Conclusions of Research Findings.....	166
10.3 Research Limitations	172
10.4 Research Contributions	174
10.5 Future Research	175
REFERENCES.....	177
APPENDICES	204

LIST OF FIGURES

Figure 1.1	
Automotive application of drive-by-wire systems	2
Figure 1.2	
Hydraulic power steering system	4
Figure 1.3	
Electric power steering system.....	4
Figure 1.4	
Steering-by-wire power system.....	5
Figure 1.5	
An approach of a perception enhancement system using by-wire steering	9
Figure 1.6	
Identified research questions (Left) and the approaches to answer those questions (Right)	13
Figure 2.1	
Location four of the mechanoreceptors (Pacian corpuscles, Meissner corpuscles, Merkel discs and Ruffini endings) in hairy and glabrous skin of the human	16
Figure 2.2	
The adaptation properties, relative innervation densities and the typical receptive field sizes of the four mechanoreceptors in the glabrous skin of the hand.....	17

Figure 2.3	
Four-channel psychophysical model showing the threshold frequency response of each channel	18
Figure 2.4	
Curve subjective response magnitude of suprathreshold vibration presented at the fingertip at frequencies of 25, 100, 250 and 500 Hz.....	19
Figure 2.5	
Equal sensation magnitude contours which each curve describes the combinations of frequency and intensity that give rise to equal sensation magnitudes..	21
Figure 2.6	
The anatomical coordinate system for the handgrip position	22
Figure 2.7	
Median perception threshold contours overlaid between the three axes.....	23
Figure 2.8	
Equal sensation data from translational and rotational vibration studies	26
Figure 2.9	
Effect of frequency and grip force on median of growth of sensation.....	27
Figure 3.1	
Elements of the cognitive driving task.....	30
Figure 3.2	
Atkinson and Shiffrin's Model of Memory	31
Figure 3.3	
Working Memory Model	33

Figure 3.4	
Theoretical probability distributions of ‘noise’ and ‘signal plus noise’ for two different values of signal strength.....	39
Figure 3.5	
The signal detection diagram	42
Figure 3.6	
Distributions of noise and signal plus noise expressed in <i>Z</i> scores	44
Figure 3.7	
Receiver operating characteristics (ROC) graph.....	45
Figure 3.8	
ROC curve for the signal plus noise and the noise distribution ($d'=1$), obtained over different observers’ criteria.....	46
Figure 3.9	
A basic ROC graph showing discrete observers	46
Figure 3.10	
Presentation of vibrations through the vibrator embedded in a small frame house	48
Figure 3.11	
Subject undertaking the task projected on the screen	49
Figure 3.12	
Hand posture and axis of vibration. The lateral axis is defined as parallel to the handle axis	50
Figure 3.13	
Participant performing the road surface detection task.....	51
Figure 4.1	
Data clustering techniques	58

Figure 4.2	
Demonstration of <i>k</i> -means clustering process.....	62
Figure 5.1	
Position of steering wheel measurement point	65
Figure 5.2	
Road surfaces and vehicle speeds, whose stimuli were used for laboratory tests.....	66
Figure 5.3	
The time history segments extracted from the road test recordings for laboratory tests	70
Figure 5.4	
The vibration frequency-domain analysis of road surfaces by PSD	72
Figure 5.5	
Distribution of <i>r.m.s</i> and VDV for all ten road surfaces	74
Figure 5.6	
Facility used for laboratory tests, available at Human Centred Design Lab, Brunel University	75
Figure 5.7	
Comparison between target and bench response of time history and PSD before (a & c) and after (b & d) the compensation process.....	78
Figure 6.1	
Possible trigger level values of the transient vibration	84
Figure 6.2	
Decay envelope of the transient vibrations	85
Figure 6.3	
Transient vibrations of Lowbump identified and extracted within the target frequency interval of 20 to 60 Hz	87

Figure 6.4	
Morphological approach to signals using a flat structuring element	92
Figure 6.5	
Diagram of morphological filter	93
Figure 6.6	
Post-processed transient vibrations results using flat structuring elements with different widths	94
Figure 7.1	
Example of original and manipulated Butterworth filter of Country Lane (left) and Tarmac (right) road surfaces used in the laboratory test stimuli.....	101
Figure 7.2	
Posture of participant at the steering wheel simulator	102
Figure 7.3	
Experiment design.....	103
Figure 7.4	
Rate of hit detection for all ten road surfaces studied	106
Figure 7.5	
Observer sensitivity, d' for all ten road surfaces studied	108
Figure 7.6	
ROC points (n=20) for the experiment on the effect of vibration energy distribution .	109
Figure 8.1	
The comparison of the magnitudes of the accuracy transfer function	117

Figure 8.2

Comparison time histories between first (left) and double (right) time-domain integration of steering wheel acceleration by LMS® CADA-X 3.5E software and MATLAB R2014a software..... 118

Figure 8.3

Comparison PSD showing the four wavelet groups distribution between first (left) and double time-domain integration (right) of steering wheel acceleration by LMS® CADA-X 3.5E software and MATLAB R2014a software..... 119

Figure 8.4

Transient vibrations of Tarmac surface identified and extracted within the target frequency interval of 20 to 60 Hz for original steering wheel acceleration vibration ..122

Figure 8.5

Comparison of time histories and PSD of acceleration by double time-domain differentiation of displacement process by LMS® CADA-X 3.5E software and MATLAB R2014a software..... 127

Figure 8.6

Comparison of time histories and PSD between original acceleration by accelerometer and acceleration by double time-domain differentiation of displacement..... 128

Figure 8.7

Transient vibrations of Tarmac surface identified and extracted within the target frequency interval of 20 to 60 Hz for the acceleration by double time-domain differentiation of displacement 131

Figure 8.8

Transient vibrations of Broken surface identified and extracted within the target frequency interval of 20 to 60 Hz for the acceleration by double time-domain differentiation of steering wheel displacement vibration..... 132

Figure 8.9

Experiment design..... 135

Figure 8.10	
Bar chart showing the rate of hit detection for different approaches of steering wheel acceleration vibration	137
Figure 8.11	
Observer sensitivity, d' for different approaches of steering wheel acceleration vibration	138
Figure 8.12	
ROC points (n=20) for different approaches of steering wheel acceleration vibration	140
Figure 9.1	
Results of seven-dimensional mapping into two-dimensional visualisation of transient vibrations data sets with different perplexity parameter values	148
Figure 9.2	
Comparing results of 7, 89, 90 and 91-dimensional mapping into 2-dimensional visualisation of transient vibrations data sets with perplexity values of 7	151
Figure 9.3	
Silhouette index plotting shows the number of cluster of 7 and 89-dimensional mapping into 2-dimensional visualisation of transient vibrations data sets with perplexity values of 7	152
Figure 9.4	
Silhouette index plotting shows the number of cluster of 90 and 91-dimensional mapping into 2-dimensional visualisation of transient vibrations data sets with perplexity values of 7	153
Figure 9.5	
Implementation of k -means algorithm to partition the new 2D variables output of 7 and 89-dimensional into cluster	153

Figure 9.6	
Implementation of <i>k</i> -means algorithm to partition the new 2D variables output of 90 and 91-dimensional into cluster	154
Figure 9.7	
Classification of transient vibrations of 7 vibrational statistics of time-domain features	158
Figure 9.8	
Classification of transient vibrations of 89 original time-domain features (1 Δ t, 88amplitudes).....	159
Figure 9.9	
Classification of transient vibrations of 90 time-domain features (1 Δ t, 88amplitudes, 1 <i>r.m.s</i>)	160
Figure 9.10	
Classification of transient vibrations of 91 time-domain features (1 Δ t, 88amplitudes, 1 <i>r.m.s</i> , 1Kurtosis).....	161
Figure 10.1	
Groups that could benefit from the research	174

LIST OF TABLES

Table 3.1	
The four response outcome of signal detection theory	42
Table 5.1	
Most relevant parameters for vibration signal analysis.....	69
Table 5.2	
The vibration time-domain analysis of road surfaces	71
Table 5.3	
Geometric simulator parameters of the steering wheel rotational vibration	76
Table 5.4	
Physical characteristics of participants for accuracy signal reproduction	79
Table 5.5	
Absolute maximum percent error of signal reproduction	80
Table 7.1	
The <i>r.m.s.</i> values (m/s^2) for original and manipulated Butterworth filters used to produce the laboratory test stimuli	100
Table 7.2	
Anthropometrics and driving experience of test participants	105
Table 8.1	
Number of transient vibrations identified in each wavelet group (WG) from different measures of steering wheel road surface signals.....	121

Table 8.2

Absolute maximum percent errors between acceleration by accelerometer and acceleration by double time-domain differentiation of displacement..... 128

Table 8.3

Number of transient vibrations identified in each wavelet group (WG) for the signal of acceleration by double time-domain differentiation of displacement..... 129

Table 8.4

Anthropometrics and driving experience of test participants 136

Table 9.1

Number of transient vibrations in each cluster of t-SNE mapped 154

Table 9.2

Classification error of each of 7 89, 90-dimensional t-SNE mapped 155

Table 9.3

Vibrational statistics of transient steering wheel vibrations in each cluster for the 91 time-domain features ($1\Delta t$, 88amplitudes, 1*r.m.s*, 1Kurtosis) 162

Table 9.4

Number of transient vibrations of steering wheel road surface contained in each cluster for the 91 time-domain features ($1\Delta t$, 88amplitudes, 1*r.m.s*, 1Kurtosis)..... 163

CHAPTER 1

MOTIVATION BEHIND THE RESEARCH

1.1 Introduction

In the automobile industry, electronic control systems are increasingly being developed with integrated electronic sensors, actuators, microcomputers and information processing for single components, engines, drivetrains, suspension, and brake systems (Isermann *et al.*, 2002). The benefits of applying electronic control systems in automobiles are clear, such as improved performance, safety, and reliability with reduced manufacturing and operating costs (Noguchi, 2002).

The progression of electronic control systems in modern automobiles has progressed quite quickly from anti-lock braking system (ABS) and stability control, via brake-force distribution and automatic proximity braking, to electric power steering systems (EPS) which allow the stability enhancing of steering tie-rod loads (Miles, 2014). These so-called basic mechatronic systems were then overtaken by the innovation of extensive mechatronic systems, called drive-by-wire systems, where vehicular behaviour and driver feedback can be designed without mechanical links between the input and output (Eskandarian, 2012). For instance, instead of using cables, hydraulic pressure, and other means for providing the driver with direct, physical control over the speed or direction of a vehicle, drive-by-wire technology uses electronic controls to activate the brakes, control the steering, and operate other systems. Most of the mechanical control is replaced by electrical wires.

The applications of drive-by-systems used in automobiles are throttle-by-wire, brake-by-wire and steer-by-wire (Parsania and Saradava, 2012), as illustrated in Figure 1.1.

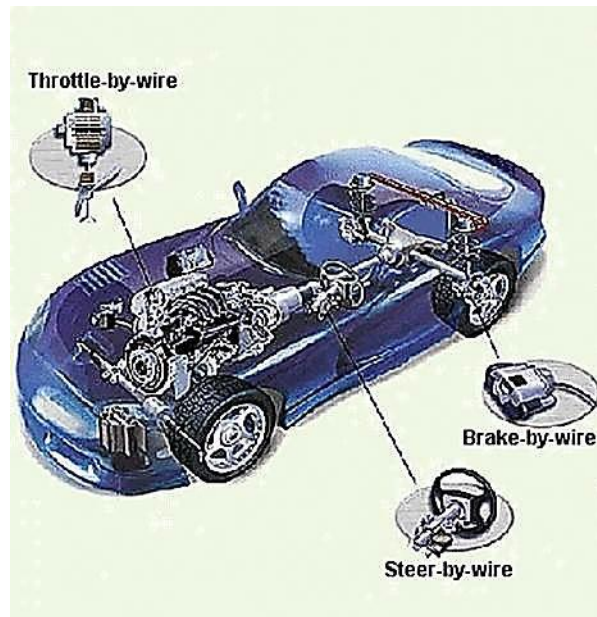


Figure 1.1 Automotive application of drive-by-wire systems (Source: KAIST, 2014)

Throttle-by-wire, or accelerate-by-wire systems, were the first type of drive-by-wire units introduced. These systems use a pedal unit and an engine management system. The pedal uses sensors that measure how much or how little the driver moves the accelerator, and the sensors send that information to the engine management system. The main advantage of throttle-by-wire is that it allows the engine computer to integrate torque management with cruise control, traction control and stability control (AA1Car, 2016)

Brake-by-wire systems involve a spectrum of technologies that range from electro-hydraulic to electro-mechanical, and both can be designed with fail-safes in mind. These systems still use sensors to determine how much brake force is required, but that force is not transmitted via hydraulics. Instead, electro-mechanical actuators are used to activate the brakes located in each wheel. The main benefit of brake-by-wire systems is that they are able to react more quickly, resulting in shorter stopping distances and increased safety (Brakebywire, 2016)

Steer-by-wire systems provide steering control of a car with fewer mechanical components/linkages between the steering wheel and the wheels. The control of the wheels' direction is established through electric motors, which are actuated by electronic control units monitoring the steering wheel inputs from the driver. The first production automobile to implement this was the Infiniti Q50 (Alex, 2014). The system in the Q50,

in development for more than 10 years, is relatively straightforward. Turning the steering wheel sends an electronic signal to the steering force actuator, which sends data to the electronic control unit, which forwards it to the steering angle actuator, which then finally turns the wheels.

This thesis embodies research related to the steering wheel feedback system. In this very first chapter, the thesis will discuss the motivation behind the research, which originated from the limitations of steer-by-wire systems. Before an in-depth discussion is presented, the evolution of steer-by-wire system will be discussed. The following sections will provide an overview of 21st-century steering wheel feedback, including Perception Enhancement for the Steer-by-Wire System. Next in this chapter will present the aims, objectives and end by providing the research questions includes the details of which chapter organise to answer all those research questions.

1.2 Evolution of Automobile Steer-By-Wire Systems

In automotive steering, electronic control systems began in the form of electronically controlled variable assist and fully electric power assist (Peter and Gerhard, 1999; Amberkar *et al.*, 2000). The basic design of automotive steering systems has changed little since the invention of the steering wheel whereby the driver's steering input is transmitted by a shaft through some type of gear reduction mechanism. This is most commonly rack and pinion or recirculating ball bearings to generate steering motion at the front wheels. One of the most prominent developments in the history of the automobile occurred in the 1950s when hydraulic power steering (Figure 1.2) assist was first introduced (Harter *et al.*, 2000). Since then, power assist has become a standard component in modern automotive steering systems. Using hydraulic pressure supplied by an engine-driven pump, power steering amplifies and supplements the driver-applied torque at the steering wheel so that steering effort is reduced. In addition to improved comfort, reducing steering effort has important safety implications as well, such as allowing a driver to more easily swerve to avoid an accident.

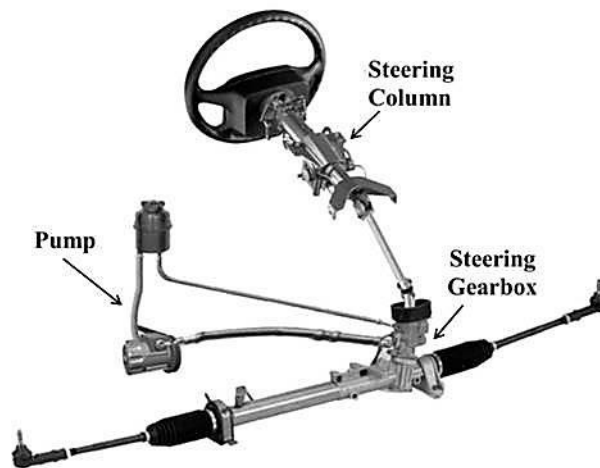


Figure 1.2 Hydraulic power steering system (Source: Harter *et al.*, 2000)

The recent introduction of electric power steering (Figure 1.3) in production vehicles eliminates the need for the hydraulic pump. Electric power steering is more efficient than conventional power steering, since the electric power steering motor only needs to provide assistance when the steering wheel is turned, whereas the hydraulic pump must run constantly. The assist level is also easily tuneable to the vehicle type, road speed, and even driver preference (Badawy *et al.*, 1999; McCann, 2000). An added benefit is the elimination of environmental hazards posed by the leakage and disposal of hydraulic power steering fluid.

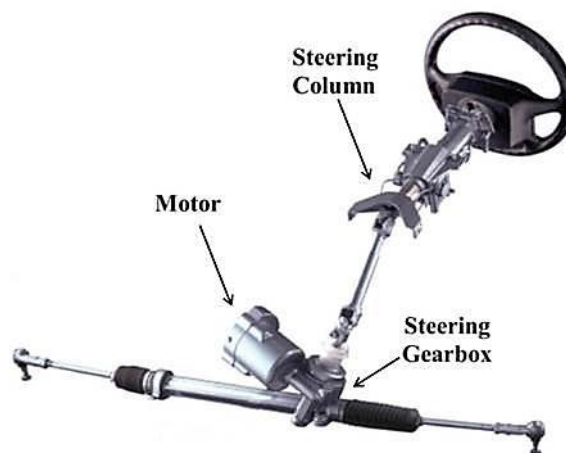


Figure 1.3 Electric power steering system (Source: Harter *et al.*, 2000)

The next step in steering system evolution was the steering-by-wire system (SBW) (Figure 1.4). This is a relatively new development compared to the traditional mechanical, hydraulic, or electric steering systems that are currently used for motor vehicles. It provides the potential benefits of enhanced vehicle performance (Tajima *et al.*, 1999), improved handling behaviour, and fully integrated vehicle dynamic control.

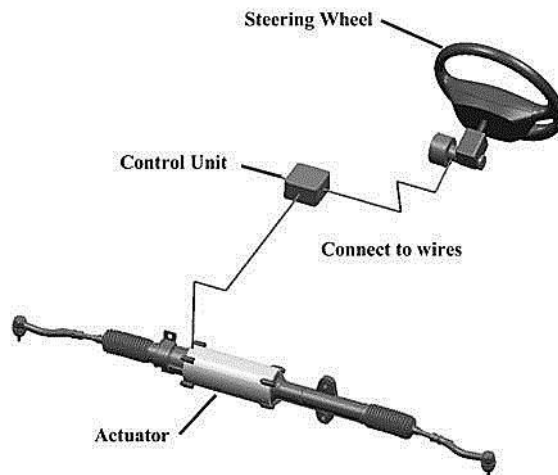


Figure 1.4 Steering-by-wire power system (Source: Berber-Solano, 2008)

In a steer-by-wire system, there is no mechanical coupling between the steering wheel and the steering mechanism. In other words, the vehicle's steering wheel is disengaged from the steering mechanism during normal operation. Even though the mechanical linkage between the steering wheel and the road wheels is eliminated, a steer-by-wire steering system is expected not only to implement the same functions as a conventional mechanically linked steering system, but is also expected to provide advanced steering functions.

Some manufacturers supplement conventional front-wheel steering with rear steer-by-wire to improve low-speed manoeuvrability and high-speed stability (Taneda and Yamanaka, 1998; Bedner and Chen, 2004). Completely replacing conventional steering systems with steer-by-wire, while a more daunting concept than throttle- or brake-by-wire for most drivers, holds several advantages such as larger space in the cabin, freedom in car interior design, no oil leaking, and less injury in case of car accidents. The advantages also open the possibility for an alternative to the traditional steering wheel (Ward and Woodgate, 2004).

The absence of a steering column greatly simplifies the design of car interiors. The steering wheel can be assembled modularly into the dashboard and located easily for either left- or right-hand drive. The absence of a steering shaft allows much better space utilization in the engine compartment. Furthermore, the entire steering mechanism can be designed and installed as a modular unit. Without a direct mechanical connection between the steering wheel and the road wheels, noise, vibration, and harshness (NVH) from the road no longer have a path to the driver's hands and arms through the steering wheel. In addition, during a frontal crash, there is less likelihood that the impact will force the steering wheel to intrude into the driver's survival space. Finally, with steer-by-wire, previously fixed characteristics such as steering ratio and steering effort are now infinitely adjustable to optimize steering response and feel (Parsania and Saradava, 2012).

1.2.1 Projected Future Market of Automobile Steer-By-Wire System

According to Mordor Intelligence, the global automotive power steering systems market was valued at USD 17.16 billion in 2015, and it is projected to reach USD 41.24 billion by 2020, at a CAGR of 15.73% during the forecast period of 2015 to 2020 (Mordor Intelligence, 2016). Meanwhile, Technavio's market research analysts predicts that the global automotive steer-by-wire market will grow at a CAGR of more than 28% by 2020 (Technavio, 2016) from a CAGR of 5.89% over the period of 2014 to 2019 (PR Newswire Association, 2015).

Indeed, one in three current new cars that are under development feature electronic steer-by-wire steering systems (Leen and Heffernan, 2002) and this led to the decision of JTEKT Corp., the biggest supplier of steering systems, to diversify with steer-by-wire systems technology (Automotive news, 2016). Factors such as technological advancement and the customers' demand for safer and fuel-efficient vehicles are the key factors driving the market growth.

1.3 Steering Wheel Vibration Stimuli to Automobile Drivers

According to the definition by Griffin (1990), vibrations are a mechanical phenomenon whereby oscillations occur about an equilibrium point. The oscillations may be periodic, such as the motion of a pendulum, or random, for instance the movement of a tyre on a road surface. Stimuli, as defined by the Dictionary of Psychology (2015) are any event, agent, or influence, internal or external, that excites or is capable of exciting a sensation or feeling receptor and of causing a physical or psychological reaction of an organism. In this research context, the vibration stimuli reach automobile drivers by means of the pedals, the gearshift, the seat, the floor and the steering wheel; the latter is the principal sensory link between the driver and the automobile (Pak *et al.*, 1991; Giacomini and Abrahams, 2000; Amman *et al.*, 2001; Bianchini, 2005).

Loomis and Lederman (1996) have suggested that touch facilitates or makes possible virtually all motor activity, permits the identification and interpretation of nearby objects, supports the understanding of spatial layout when viewing is not feasible, and informs about object properties such as temperature that are not accessible by means of the other senses. In other words, Loomis and Lederman (1996) were simplifying the process known as a haptic perception. According to the Dictionary of Psychology (2015), haptic is related to sense of touch, while perception can be defined as a process to characterise and understand the environment by the organisation, identification and interpretation of sensory information (Grunwald, 2008).

In this research context, the haptic perception is the information that is transmitted to the driver by means of the steering wheel vibration stimuli. It can be assumed that drivers recognise the road through the mechanical link to the wheels. For example, a grooved pavement makes the wheels vibrate; hence the mechanical links between the wheels and steering wheel vibrate in turn. Similarly, the mechanical links provide a certain feel to the steering wheel when the driver turns it. In the case of a steer-by-wire system that needs to emulate the feel of a traditional mechanical steering system, it must use sensors on the wheel hub, suspension components and electrical motor, in order to produce realistic and informative steering wheel motion. This requires an active system that is constantly changing its response based on the road conditions.

1.4 The 21st Century Steering System

In the 21st century, as a sector that has evolved along mainly technological lines, the automotive industry has not always analysed stimuli from the point of view of their uniqueness, ecological characteristics and information carrying potential (Giacomin, 2005). The natural vibration, sound and other stimuli that are produced by the automobile as part of its normal operation are usually simply optimised in terms of comfort or pleasantness. While detailed comparative studies of automobile stimuli are now part of routine Noise, Vibration and Harshness (NVH) testing, the efforts are usually focused on matters of comfort, pleasantness or sensory branding, but unfortunately ignore a feel for the road, which in other words is a lack of information (Giacomin and Woo, 2005). The information from the vibration stimuli is important to the driver because it could help him/her to interpret information, including the type of road surface, the presence of water or snow, tyre slip and the dynamic state of subsystems such as the engine, the steering and the brakes (Giacomin and Woo, 2004). Given the above, the question of which information an automobile subsystem should transmit to the driver is not a simple one. For many years, psychologists, cognitive scientists, and others have established the relation between stimuli and information (Gibson and Gibson, 1955; Gibson, 1969; Simon, 1979; Newell, 1990; Loomis and Lederman, 1996; Nakayama *et al.*, 1999).

According to both Verhoeff *et al.* (2004) and Giacomin (2005), the main challenge for electrical steering systems and for steer-by-wire systems is achieving a steering feel similar or better than that of conventional systems. One means of improving the flow of information to the driver, thus making the driving task easier, is to incorporate a perception enhancement systems (PES) into the design of the automobile steering wheel (Giacomin and Woo, 2005; Berber-Solano and Giacomin, 2005). This is further expected to permit the designer to achieve perception enhancing interfaces.

1.4.1 Perception Enhancement of Steer-by-Wire System

Perception Enhancement Systems (PES) can be defined as any device that optimises feedback to a driver regarding information about the vehicle's interaction with the environment (Giacomin and Woo, 2005). Perception enhancement systems lead the automobiles to distribute the information to drivers and passengers in a clearer and more easily understood manner. In 2005, Giacomin proposed the perception enhancement of steer-by-wire systems, as illustrated in Figure 1.5.

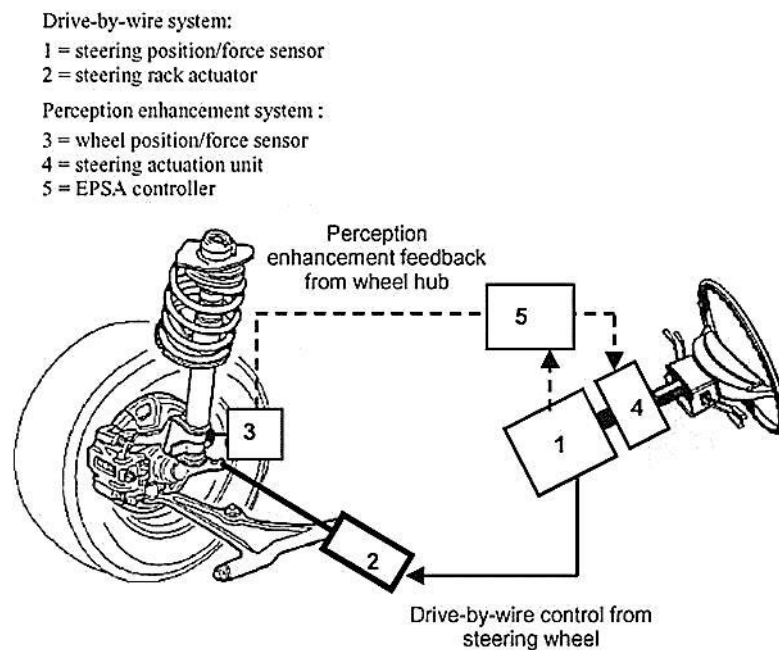


Figure 1.5 An approach of a perception enhancement system using by-wire steering
(Source: Giacomin, 2005)

The PES of the by-wire steering system comprised electronic systems that had the function of identifying significant vibration stimuli occurring at the tyres and suspension, which are required by the driver. These stimuli were then transferred and transformed in order to optimise detection and awareness (Giacomin and Woo, 2004).

1.4.2 Towards Perception Enhancement of Steer-by-Wire System Application

Although it is clear that not all vibration must be retained to clarify to the driver the environmental conditions, it is probable that some of the vibration must be maintained. In the case of information perceived by means of the steering wheel vibration, the increasing vibration level felt can help to clarify the nature of the road surface or the vehicle's dynamic state (Giacomin and Woo, 2004). This process could be used to evaluate how people assimilate the information transmitted by means of the vibrational stimuli occurring in automobile subsystems.

Given the above, a methodology for quantifying the human ability to detect a road surface appears useful (Giacomin and Woo, 2004). This was also the conclusion of a questionnaire-based study (Gnanasekaran *et al.*, 2006), which suggested that the respondents considered steering wheel vibration to be particularly useful in the task of detecting road surface types.

Working towards this goal, several laboratory-based experiments have been performed in order to achieve a first methodology for identifying the parameters or features used by drivers to detect the road surface types. A series of studies within this context have been performed to date, and they suggest that the driver's response to steering wheel vibration depends on factors such as the amplitude, frequency bandwidth (Giacomin and Woo, 2004; 2005) and frequency distribution (Berber-Solano *et al.*, 2013) of the steering wheel vibration. In addition, the repetition rate of transient vibrations caused by road surface irregularities also plays a role (Berber-Solano and Giacomin, 2005; Giacomin and Berber-Solano, 2006; Berber-Solano *et al.*, 2010). The results suggest that there is no single, optimal, acceleration gain that could improve the detection of all road surface types (Giacomin and Woo, 2005; 2004), while manipulation of the transient vibrations contained in the steering wheel vibration were not always statistically significant for all road surface types (Berber-Solano and Giacomin, 2006; 2005; Berber-Solano *et al.*, 2010). The experimental results are useful for both future steer-by-wire systems and also for current steering power systems.

All of the previous studies mentioned seem to be consistent with the nature of the supernormal stimuli concept, which has been defined by the Dictionary of Psychology

(2015) as an exaggerated sign stimulus that evokes a stronger response than the normal sign stimulus. On the other hand, the concept of supernormal stimuli is also defined as a process of manipulating the features of an original stimuli to obtain an artificial stimuli (Pittenger and Shaw, 1975; Hill and Pollick, 2000; Costa and Corrazza, 2006; Goodwin *et al.*, 2016) and identifying how the receiver responds to the artificial stimuli (Dawkins and Guilford, 1995; Drănoiu *et al.*, 2002; ten Cate and Rowe, 2007). For instance, these concepts can be found in studies by Berber-Solano *et al.* (2010) whereby the signal was exaggerated by modifying the transient vibrations so that they were smaller and larger. The aim of this was to develop guidelines for enhancing the communication between the steering systems and the driver.

Based on a review of the research performed on finding the steering wheel vibration feedback till date, it can be seen that there is a lack of studies and understanding on how the characteristics of incoming road surface data signals contribute to driver road surface detection (Giacomin, 2005). The time-domain features known as a basic and simple technique in a signal processing which can provide the behaviour of the signal (Inman and Singh, 2014), thus were chosen to identify the characteristics of incoming road surface data. This can be achieved by classifying the time-domain features of road surface transient vibrations, whereby transient vibrations are defined as high amplitude transient which can cause the overall time history to deviate from a stationary Gaussian model (Giacomin *et al.*, 2000). Next, the optimal driver road surface detection measured by checking human subjective responses to steering wheel vibration. According to the Cambridge Advanced Learner's Dictionary (2008), 'optimise' refers as to make something as good as possible. Therefore, the optimise driver road surface detection in this study refers to the human ability to detect various of road surface types. Therefore, the main question of this research is:

“What are the time-domain features of road surface transient vibrations that can optimise driver road surface detection?”

1.5 Research Aim, Objectives and Questions

The research aim is to classify the transient vibrations of steering wheel road surface, focusing on identifying the time-domain features of transient vibrations that can improve driver road surface detection. Therefore, in order to achieve the aim of this study, the following objectives were set:

- i. To critically review the existing principles of transient vibrations detection in order to establish a better principle for transient vibrations steering wheel road surface
- ii. To validate the previous guidelines related to the frequency bandwidth of steering wheel vibration feedback
- iii. To define the optimal approach for the detection of transient vibrations steering wheel road surface, according to their time-domain waveform
- iv. To classify the transient vibrations steering wheel road surface, according to the similarity of their time-domain features
- v. To provide a definition of design guidelines for perception-enhancing steering wheel vibration feedback

1.5.1 Research Questions

Considering the significant need to identify the time-domain features of road surface transient vibrations, and the objectives set for the study, the questions aimed to be addressed by this research thesis were further defined to give a better understanding of the process carried out and the transition path of each activity.

Figure 1.6 shows each of the research questions defined includes the details of which chapter aims to answer each question.

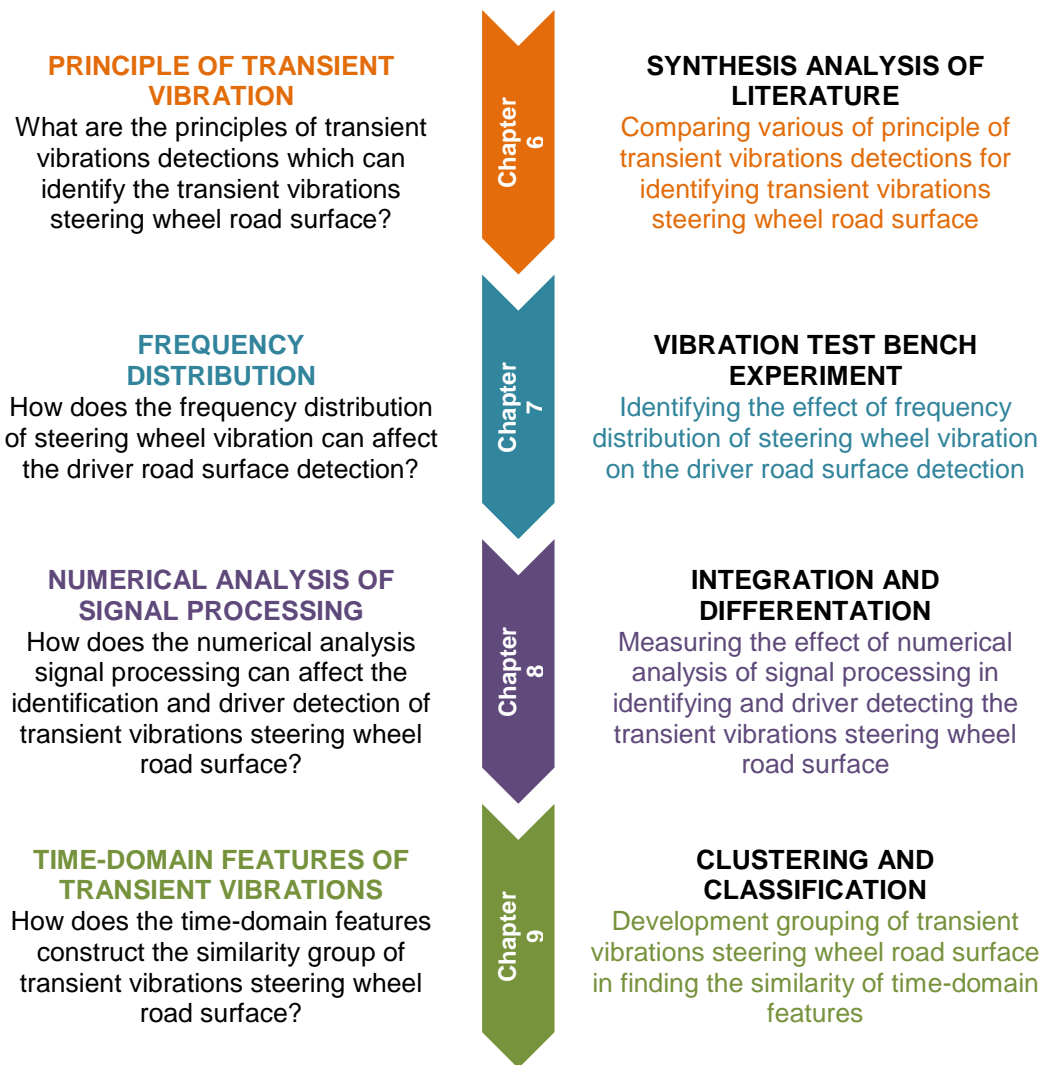


Figure 1.6 Identified research questions (Left) and the approaches to answer those questions (Right)

CHAPTER 2

HAND-ARM TRANSMITTED AUTOMOBILE STEERING WHEEL VIBRATION

2.1 Introduction

Vibrations can produce a wide variety of different effects in humans. According to the definition by Griffin (1990), vibrations are a mechanical phenomenon whereby oscillations occur about an equilibrium point. The oscillations may be periodic, such as the motion of a pendulum, or random, such as the movement of a tyre on a road surface.

In practice, the human body is exposed to various kinds of vibrations, which are transmitted by different sensations into the body. These different sensations of vibrations can be separated into two principal sections – the perception of whole-body vibrations and the perception of hand-arm transmitted vibrations. For instance, when driving on an irregular road surface, drivers are exposed to whole-body vibrations through the backrest (Bellmann, 2002). They are also simultaneously exposed to hand-arm transmitted vibrations that are felt by the hand and fingers as a result of contact with the steering wheel vibration (Griffin, 1990).

The term hand-arm transmitted vibrations can be defined as a vibration entering the body directly usually through the hand or fingers (Oxford University Press, 2004). This is also known as vibrotactile vibration (Griffin, 1990). This definition is consistent with the European Directive (2002), which defines hand-arm transmitted vibrations as a mechanical vibration that when transmitted to the human hand-arm system, entails risks to the health and safety of workers, in particular vascular, bone or joint, neurological or muscular disorders.

This study focuses on hand-arm transmitted vibrations due to the high sensitivity of the skin's tactile receptors on the hand, as well as the lack of intermediate structures such as shoes and clothing, which can attenuate the transmission of vibration to the drivers (Gescheider *et al.*, 2004). For these reasons, the fundamental measurement and evaluation methods of hand-arm transmitted vibrations are presented in this chapter. Additionally, this chapter also presents an evaluation of hand-arm transmitted vibrations in the context of steering wheel vibration.

2.2 Subjective Response to Hand-Arm Transmitted Vibrations

According to Cambridge Advanced Learner's Dictionary (2008), 'subjective' refers to something that is realised more on personal beliefs or feelings, rather than based on facts, while 'response' is judgement or reaction to something. Therefore, the term 'subjective response' in this study refers to human reaction with something which varies dependent on an individual (Griffin, 1990).

The subjective response to hand-arm vibrations has been found to depend on four main physical parameters of the vibration namely quality, intensity, locus and effect (Reynolds *et al.*, 1977, Griffin, 1990). Quality is the subjective difference that capable to name the sensation, such as heat, cold, taste or smell. Intensity represents the size of energy that been perceived. Locus refers to the position of the sensation originates, and effect is the characteristic of the sensation that allows a subject to classify the sensation for instance pleasant or unpleasant. This section therefore provides an overview of the independent physical parameters that affect the subjective response to hand-arm vibrations.

2.2.1 Vibration Contact Location

The biodynamic of the human hand-arm system is one of the most important foundations for the measurement, evaluation and risk assessment of exposure to hand-arm transmitted vibrations. The vibrotactile stimuli received by vehicle drivers are detected by the mechanoreceptors in the skin and mediated by the sensation channels

related to these mechanoreceptors. Colman (2015) defined a mechanoreceptor as a sensory receptor that responds to mechanical stimulation including touch, pressure and vibrations. Four types of mechanoreceptors are found in the glabrous skin (Bolanowski *et al.*, 1988) as shown in Figure 2.1, namely Pacinian corpuscles, Meissner corpuscles, Merkel discs and Ruffini endings.

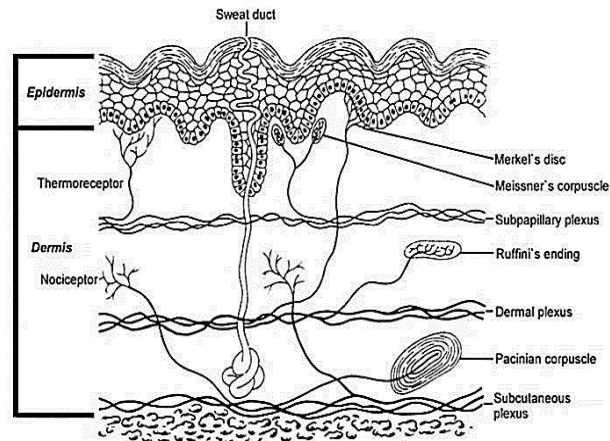


Figure 2.1 Location four of the mechanoreceptors (Pacinian corpuscles, Meissner corpuscles, Merkel discs and Ruffini endings) in hairy and glabrous skin of the human
(Source: Griffin, 1990)

The vibrations normally activate multiple information processing channels, starting from different types of mechanoreceptors, and the most sensitive channel differs, depending on the range of the vibration frequency (Békésy, 1940; Verrillo, 1966; Gescheider, 1976; Verrillo, 1985; Bolanowski *et al.*, 1988; Lamoré and Keemink, 1988; Hollins and Roy, 1996; Gescheider *et al.*, 2001; Bellmann, 2002). The mechanoreceptor fibres are thus classified into two groups which are fast acting (FA) or slow acting (SA) by depending on how quickly they response to a steady stimulus. Slow-acting units will respond all the time of the stimulus duration, whereas the immediate response in the case of the fast-acting units (Johansson *et al.*, 1982). Figure 2.2 summarises the adaptation properties, relative innervation densities and the typical receptive field sizes of the four mechanoreceptors found in the glabrous skin of the hand.

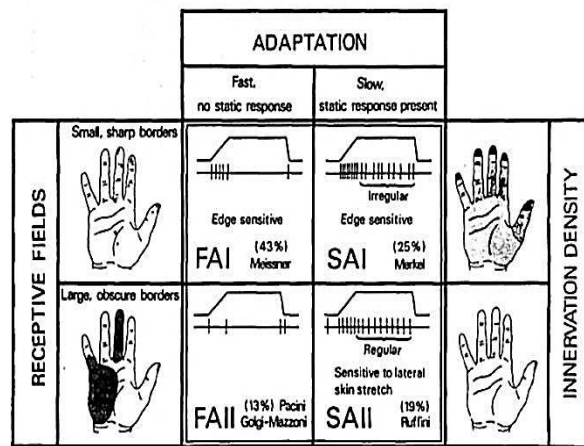


Figure 2.2 The adaptation properties, relative innervation densities and the typical receptive field sizes of the four mechanoreceptors in the glabrous skin of the hand
(Source: Roberts, 2002)

- i. Meissner corpuscles – Non-Pacinian I (Fast Adapting I): Only respond to moving skin stimulus.
- ii. Pacinian corpuscles – Pacinian (Fast Adapting II): Very rapidly adapting sensors.
- iii. Merkel discs – Non-Pacinian III (Slow Adapting I): Produce action potentials in afferent fibres if a long stimulus occurs.
- iv. Ruffini endings – Non-Pacinian II (Slow Adapting II): Produce action potentials in afferent fibres if a long stimulus occurs.

Morioka and Griffin (2007; 2008; 2009) suggested that a frequency greater than approximately 16 Hz or 20 Hz may be mediated by Pacinian corpuscles (FA-II), which provide sensations at high frequencies of vibration. The NP channels include the Meissner corpuscles, Merkel discs and Ruffini endings (i.e. FA-I, SA-I and SA-II, respectively), and show enhanced sensitivity with increasing stimulus gradients at frequencies less than around 16 Hz to 20Hz. The authors also concluded that at least three channels (Pacinian, NP-I and NP-II channels) may be involved in detecting hand-arm transmitted vibrations.

Research by Griffin (2012) stated that the slow-adapting non-Pacinian II channel is likely to be most sensitive at frequencies less than about 2 Hz. The fast-adapting non-Pacinian I channel may mediate perception at threshold levels between approximately 2 Hz and 40 Hz, and the fast-adapting Pacinian channel often mediates perception at frequencies greater than about 40 Hz. The slow-adapting non-Pacinian II channel is sensitive in a frequency range similar to the P channel, but has a sensitivity lower than the P channel in most contact conditions (Figure 2.3).

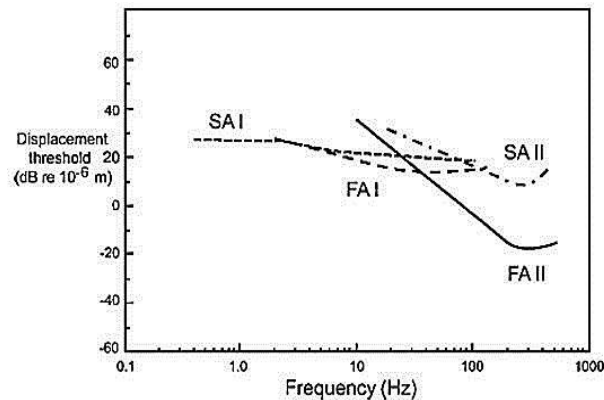


Figure 2.3 Four-channel psychophysical model showing the threshold frequency response of each channel (Source: Griffin, 2012)

The Pacinian corpuscle is strongly implicated as the mechanoreceptor primarily responsible for the perception of transmitted vibration, and the limits of the vibratory detection at high frequencies depend on the activity in the Pacinian afferents. Mechanoreceptor fibres have different to respond to specific frequency ranges of vibratory stimuli which been proven in various of studies areas such as electrophysiological recordings (Talbot *et al.*, 1968; Mountcastle *et al.*, 1972), direct recordings from human nerves (Knibestol and Vallbo, 1970; Johansson *et al.*, 1982; Phillips *et al.*, 1992) and psychophysics (Verrillo, 1966; Gescheider, 1976; Verrillo, 1985; Bolanowski *et al.*, 1988; Lamoré and Keemink, 1988; Hollins and Roy, 1996; Gescheider *et al.*, 2001).

2.2.2 Vibration Magnitude

The comfort contours strongly depend on vibration magnitude, indicating that a frequency weighting for predicting sensation should be dependent on vibration magnitude. The magnitude of the vibration to which the body is exposed can be expressed in terms of physical measurements (e.g. displacement, velocity or acceleration). For practical convenience, the magnitude of vibration is usually expressed in terms of acceleration, whose units are m/s^2 , normally measured by means of accelerometers (ISO 5349-1, 2001). The primary quantity used to describe the magnitude of the vibration shall be the root-mean-square (*r.m.s.*) frequency-weighted acceleration expressed in metres per second squared (m/s^2).

Verrillo *et al.* (1969) determined how subjective intensity affected by vibration amplitude of sinusoidal stimuli, which were applied to the skin of the index finger by means of a vibrating needle. The resulting curves, shown in Figure 2.4, suggest that the subjective magnitude increased as the physical intensity of the vibration was increased. At low intensities, the subjective response was found to grow approximately linearly with respect to the intensity of the vibration (at frequencies from 25 Hz to 250 Hz). This result is consistent with Zwislocki's theory of vibration sensitivity (Zwislocki, 1960), which states that sensory magnitude is approximately proportional to the stimulus intensity near threshold.

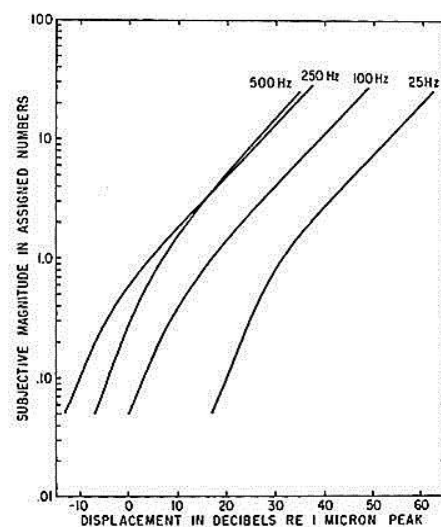


Figure 2.4 Curve subjective response magnitude of suprathreshold vibration presented at the fingertip at frequencies of 25, 100, 250 and 500 Hz (Source: Verrillo et al., 1969)

Adewusi *et al.* (2010) concluded that the magnitudes of transmitted vibration under an extended-arm posture were observed to be nearly twice those for the bent-arm posture in the low frequency region. The results further showed that variations in the grip force mostly affected vibration transmissibility and the characteristic frequencies of the forearm, while changes in the push force influenced the dynamic characteristics of the entire hand-arm system. The magnitudes of transmitted vibration in the vicinity of the characteristic frequencies were influenced by the handle vibration magnitude.

2.2.3 Vibration Frequency

The perceived intensity of hand-arm transmitted vibration is dependent on the frequency of vibration. Frequency analysis in octave bands may appear to be quick, cheap and convenient, but it does not provide sufficient spectral detail. It is now becoming common for the frequency content of vibration signals to be determined using constant bandwidth analysis rather than one-third octave band analysis. When assessing hand-arm transmitted vibrations, the frequency resolution used for constant bandwidth analysis should be less than 10 Hz, but normally needs to be narrower than 1 Hz.

Research related on measuring the response of perception thresholds and annoyance thresholds towards stimuli of different frequencies shown that a constant vibration magnitude produces different intensity at all frequencies (Stevens, 1986; Griffin, 1990). Figure 2.5 presents a set of contours of equal sensation magnitude obtained by Verrillo *et al.* (1969) using sinusoidal vibration stimuli applied to the skin of the index finger by means of a vibrating needle. Each curve is the combinations of both frequency and amplitude that result in judgements of equal subjective intensity. At threshold, the curve is U-shaped, resembling the vibrotactile perception threshold of the hand (Verrillo, 1985), and has a flattened portion in the smoother shape over the high-frequency range of 100 Hz to 1000 Hz. The flattening of the equal sensation curves, as the vibration intensity increases, is analogous to the behaviour of the well-known equal loudness contours for hearing (Moore, 1997), indicating that high-intensity sounds appear equally loud regardless of the frequency.

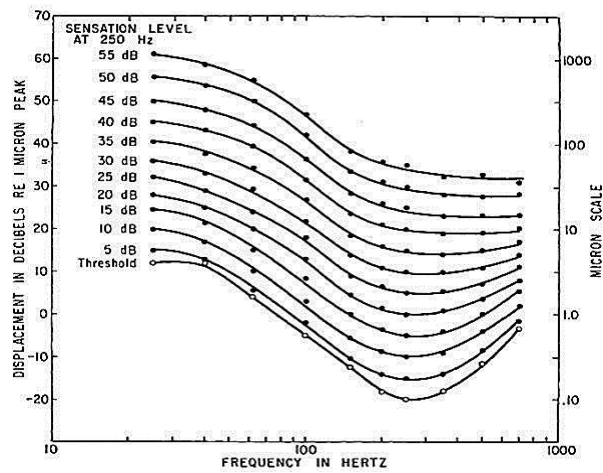


Figure 2.5 Equal sensation magnitude contours which each curve describes the combinations of frequency and intensity that give rise to equal sensation magnitudes (Source: Verrillo *et al.*, 1969)

Griffin (2012) showed that the frequency-dependence of discomfort caused by hand-arm transmitted vibration, depending on vibration magnitude, is similar to absolute thresholds at low magnitudes, but the discomfort at higher magnitudes is similar when the vibration velocity is similar (at frequencies between 16 Hz and 400 Hz). Frequency weighting at current standards extends from 8 Hz to 1000 Hz; frequencies greater than 400 Hz rarely increase the weighted value on tools and there is currently little psychophysical or physiological evidence of their effects.

2.2.4 Vibration Direction

British Standard 6842 (1987) and the International Organization for Standardization 5349-1 (2001) provide general requirements for measuring and reporting hand-arm transmitted vibrations exposure in three orthogonal axes. The directions of vibration transmitted to the hand should be reported in the appropriate directions of the orthogonal coordinate axes, as shown in Figure 2.6.

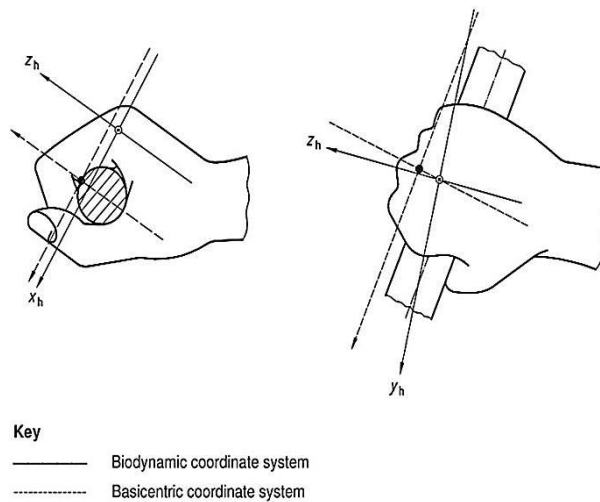


Figure 2.6 The anatomical coordinate system for the handgrip position (Source: BS 6842, 1987; ISO 5349-1, 2001)

The origin of the biodynamic coordinate system is the head of the third metacarpal (distal extremity). The z_h -axis (i.e. hand axis) is defined as the longitudinal axis of the third metacarpal bone and is oriented positively towards the distal end of the finger. The x_h -axis passes through the origin, is perpendicular to the z_h -axis, and is positive in the forwards direction when the hand is in the normal anatomical position (palm facing forwards). The y_h -axis is perpendicular to the other two axes and is positive in the direction towards the fifth finger (thumb). In practice, the basicentric coordinate system is used: the system is generally rotated in the y - z plane so that the y_h -axis is parallel to the handle axis.

Morioka and Griffin (2006) studied the effect of vibration direction (fore-and-aft, lateral and vertical) on predicting the perception of hand-arm transmitted vibrations and the discomfort caused by hand-arm transmitted vibrations. The study found that thresholds for the perception of hand-arm transmitted vibrations in each of the three axes are U-shaped with the greatest sensitivity to acceleration in the range 80 Hz to 160 Hz, as shown in Figure 2.7.

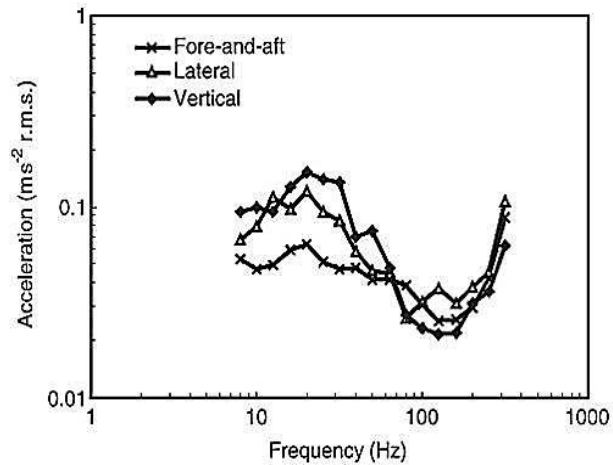


Figure 2.7 Median perception threshold contours overlaid between the three axes
(Source: Morioka and Griffin, 2006)

Figure 2.7 suggests that at frequencies less than 50 Hz, thresholds are lowest for fore-and-aft vibration, while at frequencies greater than 125 Hz, thresholds for vertical vibration are lower than thresholds for lateral vibration.

2.2.5 Vibration Duration

Vibration exposure is dependent on the magnitude of the vibration and the duration of the exposure. Exposure duration can be quantified both on a daily basis and over a lifetime. In both cases it is necessary to recognise that exposures are non-continuous, that the magnitude of adverse effects may grow during exposures, that there may be some recovery between exposures, and that there may be some recovery after the final end to exposure. It may be expected that there will be different ‘time constants’ for both the effects and the recoveries associated with each type of injury. The daily limit exposure stated in the International Organization for Standardization 5349-1 (2001), based on eight hours energy equivalent acceleration value, is 3.4 m/s^2 .

Previous research has suggested that the vibrotactile sensitivity at threshold (Verrillo, 1965; Gescheider, 1976; Checkosky and Bolanowski, 1992) and at suprathreshold levels of stimulation (Verrillo *et al.*, 1969; Gescheider, 1997) can be affected by stimulus duration. According to Verrillo (1965) and Gescheider (1976), the phenomenon of temporal summation or temporal integration were happened at the

threshold amplitude for detection has been found to decrease monotonically with stimulus duration when stimuli frequencies are greater than 40 Hz and stimuli durations shorter than approximately 1.0 seconds. Meanwhile, for stimuli frequencies greater than 40 Hz and stimuli durations longer than approximately 1.0 seconds, the perception threshold was constant with increases in stimulus duration (Verrillo, 1965; Gescheider, 1976). For vibration frequencies less than 40 Hz, no temporal summation has been observed (Gescheider, 1976).

Cohen and Kirman (1986) have performed an experiment to measure the vibrotactile frequency discrimination at durations of 30, 50, 100 and 200 milliseconds (*ms*) with a standard frequency of 100 Hz. From the experimental results they suggested that 50 *ms* is the minimum vibratory duration for good frequency discrimination. Other research studies (Craig, 1985; Gescheider *et al.*, 1990; Biggs and Srinivasan, 2002) have suggested that only a few *ms* are needed to perceive stimuli in human tactile vibration.

2.3 Subjective Response to Hand-Arm Transmitted Steering Wheel Vibrations

In the context of the steering wheel, many aspects of the subjective response to hand-arm transmitted vibrations have been studied in great detail, such as detection thresholds and level of annoyance (Miura *et al.*, 1959; Miwa, 1967; Reynolds *et al.*, 1977; Verrillo, 1985; Griffin, 1990; Giacomini *et al.*, 2004; Morioka and Griffin, 2006; 2009), perception of strength and equal sensation curve (Giacomini and Onesti, 1999; Giacomini *et al.*, 2004; Ajovalasit and Giacomini, 2009) the influence of grip force (Schröder and Zhang, 1997; Morioka and Griffin, 2007) and the influence of duration of the vibrotactile exposure (Miwa, 1968; Giacomini and Onesti, 1999; Giacomini *et al.*, 2004; Morioka, 2004; Morioka and Griffin, 2006).

Studies by Morioka and Griffin (2006; 2009) suggested that equivalent comfort contours for steering wheel vibration determined over a range of frequencies (4 Hz to 250 Hz) and magnitudes (0.1 m/s^2 *r.m.s.* to 1.58 m/s^2 *r.m.s.*) were strongly dependent on vibration magnitude. At magnitudes greater than around 1.0 m/s^2 *r.m.s.*, the sensitivity to acceleration decreased as the vibration frequency increased above 20 Hz. At magnitudes less than around 0.5 m/s^2 *r.m.s.*, the sensitivity to acceleration increased

with increasing frequency. The changes in the shapes of the equivalent comfort contours with vibration magnitude might be due to multiple channels being responsible for the mediation of perception at suprathreshold levels. At suprathreshold levels, the frequency-dependence of the equivalent comfort contours in each of the three axes was highly dependent on vibration magnitude. The authors also suggested that the currently standardised frequency weighting, W_h , does not provide a good prediction of the perception of steering wheel vibration at magnitudes less than approximately $1.5 \text{ m/s}^2 \text{ r.m.s.}$

Research has suggested that, when plotted in terms of acceleration amplitude, the human subjective response to hand-arm vibration decreases almost monotonically as a function of frequency (Miura *et al.*, 1959; Miwa, 1967; Reynolds *et al.*, 1977; Verrillo, 1985; Griffin, 1990; Giacomini *et al.*, 2004). Studies performed by Miwa (1967) to measure equal sensation and perception threshold which participant by 10 test subjects who holding their palm flat against a vibration plate, for vertical and horizontal vibration suggested that the acceleration threshold was found to reach maximum sensitivity at 100 Hz. Meanwhile Reynolds *et al.* (1977) studied the subjective response to vertical and axial direction translational handle vibration by measuring perception and annoyance threshold curves for eight test subjects. For fixed acceleration amplitude, their results showed a general trend of reduced sensitivity with increasing frequency.

Giacomini and Onesti (1999) produced equal sensation curves for the frequency range of 8 Hz to 125 Hz using a sinusoidally rotating steering wheel at reference amplitudes of 1.86 m/s^2 and 5.58 m/s^2 . From the results they suggested that the subjective response was found to be linear as a function of frequency over the frequency range considered. They also suggested that the grip tightness did not have a great effect on the subjective response.

Giacomini *et al.* (2004) investigated the hand-arm perception of rotational steering wheel vibration by means of four equal sensation tests and one annoyance threshold test. All equal sensation curves showed that the human sensitivity will decrease when exposed to hand-arm vibration with increasing frequency. Apart from that, they also suggested that there were two characteristic transition points existed in the curves of equal subjective response which are at frequencies of 6.3 Hz and in the interval from 50 Hz to 80 Hz

(Refer Figure 2.8). The first transition points were suspected to be due to the mechanical decoupling of the hand-arm system, while another one of transition points was claimed to be due to the onset of Pacinian receptor output. Giacomini *et al.* (2004) also suggested that human sensitivity decreased by 6 dB and 10 dB per octave in the frequency ranges of 6.3 Hz to 50 Hz and 160 Hz to 315 Hz respectively, while a 0 dB per octave corresponding constant acceleration was observed in both frequency ranges of 0 Hz to 6.3 Hz and 50 Hz to 160 Hz.

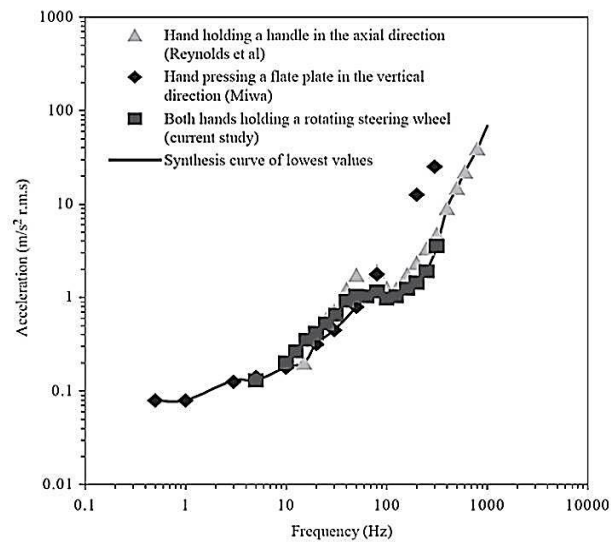


Figure 2.8 Equal sensation data from translational and rotational vibration studies
(Source: Giacomini *et al.*, 2004)

Morioka and Griffin (2007) investigated the effect of grip force on the frequency-dependence of the perception of steering wheel vibration applied to the hands. They found that the growth of sensation depended on vibration frequency, with generally the highest exponent at 31.5 Hz for all three grip conditions which were minimum, light and tight grips with a systematic decrease in exponent with increasing frequency from 31.5 Hz to 125 Hz, as shown in Figure 2.9.

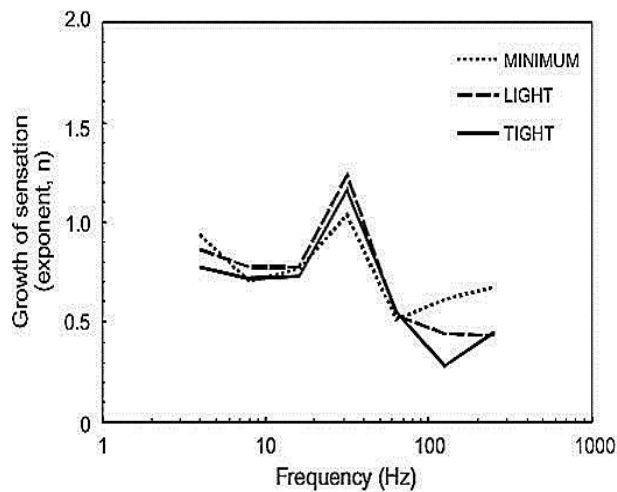


Figure 2.9 Effect of frequency and grip force on median of growth of sensation
(Source: Morioka and Griffin, 2007)

In the case of perceived intensity relative to an automobile steering wheel, Schröder and Zhang (1997) investigated the subjective response to steering wheel acceleration stimuli measured along the three orthogonal axes on a mid-sized European passenger car. This was done for different driving speeds, ranging from 30 km/h to 70 km/h, over three different road surfaces. The results suggested that the vibration along the vertical direction of the steering wheel correlates best with the subjective ratings of the drivers in the frequency range of 30 Hz to 90 Hz whereby the frequency range known as the most of the vibration energy is present at the steering wheel (Peruzzetto, 1988; Amman *et al.*, 2001; Giacomini *et al.*, 2004).

Most of laboratory-based experiment related to the hand-arm vibration has involved protocols in which the test subjects judged the subjective intensity of the vibration duration of 2 seconds to 10 seconds (Miwa, 1968; Giacomini and Onesti, 1999; Giacomini *et al.*, 2004; Morioka, 2004; Morioka and Griffin, 2006). For instance, studies by Miwa (1968) were asked subjects to judge the relative subjective intensity produced by short periods of sinusoidal vibration, and pulsed sinusoidal vibration, for signal durations up to 6 seconds. The test results, suggested that for vibration in the frequency range of 2 Hz to 60 Hz there is no further increase in sensation intensity for stimuli durations greater than approximately 2 seconds, whereas for vibration in the frequency range of 60 Hz to 200 Hz the same limit is approximately 0.8 seconds.

2.4 Conclusion

This present chapter has described the fundamental measurement and evaluation methods of hand-arm transmitted vibrations. Hand-arm transmitted vibrations are caused by mechanical vibration, such as that of the steering wheel, being transferred to the adjacent areas of the hand, arm and shoulder. Subjective responses to the vibrations are varied; they may be quantified by location, direction, magnitude, frequency and durations.

The subjective response appears to be best correlated with vertical direction (Schröder and Zhang, 1997) and an exposure duration between 2 and 10 seconds (Miwa, 1968; Giacomini and Onesti, 1999; Giacomini *et al.*, 2004; Morioka, 2004; Morioka and Griffin, 2006) with the use of a logarithmic transformation for both magnitude and frequency values (Miwa, 1967; Verrillo *et al.*, 1969; Reynolds *et al.*, 1977; Giacomini and Onesti, 1999; Giacomini *et al.*, 2004) for hand-arm transmitted steering wheel vibrations.

Given the above, it is important to review and explain the questions of how humans acquire, interpret, select and organise the vibration information felt by the means of hand-arm transmitted steering wheel vibration. Therefore, the following chapter will focus on human information processing systems that form the basis of detection decision making.

CHAPTER 3

HUMAN COGNITION

3.1 Introduction

The term cognition, also known as mental activity, refers to a group of mental processes that includes attention, memory, producing and understanding language, learning, reasoning, problem solving, and decision making (Wickens *et al.*, 1998). The specific related term used in cognition is cognitive psychology, which describes a theoretical orientation that emphasizes human knowledge and mental processes (Matlin, 2005).

The concept of cognition has spread to various disciplines, such as psychology (Wyer, 1998), education (Rayner *et al.*, 2001; Halpern and Hakel, 2002), social sciences (Kunda, 1999), medicine (Corrigan and Penn, 2001), and health (Brannon and Feist, 2000). However, the usage of the term ‘cognition’ varies across disciplines. For example, in psychology, cognition usually refers to an information processing view of an individual's psychological functions (Wyer, 1998; Matlin, 2005). Meanwhile, in social disciplines, the term ‘cognition’ is used to explain attitudes, attribution, and group dynamics (Kunda, 1999).

In the driving context, cognition usually refers to a cognitive driving task (Hollnagel and Woods, 2005). The concept of a cognitive driving task always appears in the development of car-driving models (Hollnagel and Woods, 2005). For example, when a car approaches an intersection with poor visibility, the driver treats the intersection as an important thing, and the driver also predicts situations where people come from a street intersection (cognition) (Yoshida *et al.*, 2014). Other than that, the concept of cognition is also used by drivers to identify the vibration transmitted to the driver via steering

wheel vibration (Giacomin and Woo, 2004; 2005; Berber-Solano and Giacomin, 2005; Giacomin and Berber-Solano, 2006; Bellet *et al.*, 2007; Berber-Solano *et al.*, 2013). For example, the vibration felt by the driver on the steering wheel helps with the interpretation of many things including the type of road surface, the presence of water or snow, tyre slip (both longitudinal and lateral) and the dynamic state of subsystems such as the engine, the steering and the brakes. The vibrations are perceived, compared to models from long-term memory and interpreted, with the consequent interpretation then influencing decision taking (Giacomin and Woo, 2004). Figure 3.1 shows the elements of the cognitive driving task that are used to discriminate the vibration transmitted to the driver via steering wheel vibration.



Figure 3.1 Elements of the cognitive driving task (Source: Giacomin and Woo, 2004)

According to Dror (2005), the cognitive driving task involves the processes through which a stimulus is detected. The stimulus can be perceived as a discrete event or as a stream of events and can be adjusted in terms of sensitivity thresholds, stimulus segmentation and other parameters (Dror and Dascal, 1997). However, the vibrational stimulus experienced depends on several factors such as the person's past experiences, the person's memory and on a large variety of other psychological variables (Dror, 2005)

After this discussion of the best measurements of the subjective response to hand-arm transmitted steering wheel vibrations, it is important to review and explain how humans acquire, interpret, and organise the vibration information. Therefore, this chapter focuses on three topics. The chapter begins by outlining the information-processing model, which will explain the human working memory model and also emphasise its limitations. This will be followed by an explanation of the process through which

different information is assessed and selected from a number of alternatives, together with the factors that make this process more and less effective. A related theory that provides a means of analysing the critical structure of human detection decision processes in a given task is also examined in the final section of this chapter.

3.2 The Information-Processing Model

The information-processing model is a model used to represent, describe and explain memory, its components and processes (Matlin, 2005). Researchers have proposed a number of information-processing models to explain human memory, which has been categorised into three different classes: Sensory Memory, Short-term Memory and Long-term Memory (Atkinson and Shiffrin, 1968; Tulving, 1972; Anderson, 1990; Baddeley, 1992; Massaro and Cowan, 1993; Reed, 1997; Groome, 1999; Palmer, 1999). Despite this, the proposed model by Atkinson and Shiffrin (1968) has become the best known example within the emerging field of cognitive psychology (Squire *et al.*, 1993) because the theory quickly became the standard approach to the information-processing model. Figure 3.2 shows the Atkinson-Shiffrin model, with arrows to indicate the transfer of information.

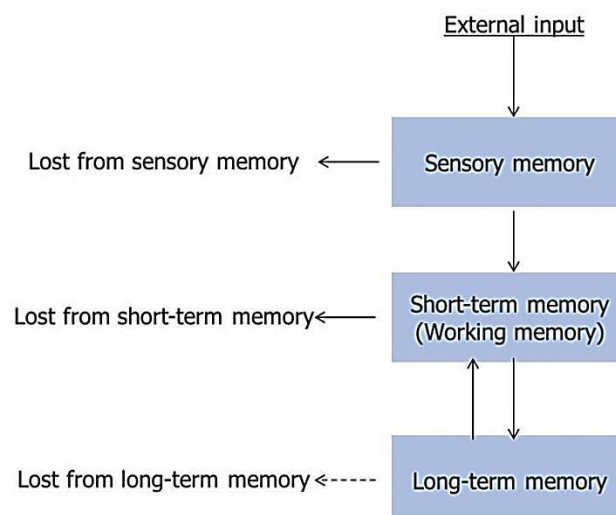


Figure 3.2 Atkinson and Shiffrin's Model of Memory
(Source: Atkinson and Shiffrin, 1968)

External stimuli from the environment first enter sensory memory. Sensory memory is a large capacity storage system that records information from each of the senses with reasonable accuracy. Atkinson and Shiffrin (1968) proposed that information is stored in sensory memory for 2 seconds or less, and then most of it is forgotten. Miller (1956) stated that the sensory information store has unlimited capacity, and reacts to both visual and auditory information. Norman (1970) assumed that sensory memory has the capacity to transform physical environmental stimuli into physiological representations. In this form information can be temporarily retained in the memory system.

Some material from sensory memory will then pass in to the short-term memory, now commonly called working memory, which contains only the small amount of information that the human is actively using (Atkinson and Shiffrin, 1968). Memories in short-term memory are fragile, but not as fragile as those in sensory memory; these memories can be lost within about 30 seconds unless they are somehow repeated (Atkinson and Shiffrin, 1968; Baddeley, 1986; 1990; Cowan, 2001).

According to the Atkinson-Shiffrin's model, material that has been rehearsed passes from short-term memory to long-term memory. Long-term memory is defined as a system for permanently storing, managing and retrieving information for later use, whereby the items of information stored as long-term memory may be available for a lifetime (Atkinson and Shiffrin, 1968; Wickens *et al.*, 1998 Matlin, 2005).

This study will focus on the working memory due to the fact that most of laboratory-based experiment related to the hand-arm vibration has involved protocols in which the test subjects judged the subjective intensity of the vibration duration of 2 seconds to 10 seconds (Miwa, 1968; Giacomini and Onesti, 1999; Giacomini *et al.*, 2004; Morioka, 2004; Morioka and Griffin, 2006). Apart from that, previous researchers have also indicated that human working memory is related to poorer driving performance (Louie and Mouloua, 2015). In light of this, the following subtopic will discuss the fundamentals of human working memory and its capacity limits for processing information.

3.2.1 Human Working Memory

The term working memory is a relatively new name for short-term memory (Matlin, 2005). Working memory refers to the system or systems that are assumed to be necessary in order to keep things in mind while performing cognitive tasks such as reasoning, comprehension and learning (Baddeley, 1992; 2000; Smith, 2000; Cowan, 2001; Engle, 2001). Figure 3.3 illustrates the working model proposed by Baddeley (2000), featuring the phonological loop which deals with verbal information, the visuospatial sketchpad concerned with visual information, the central executive system allowing the manipulation and control of information in working memory, and the episodic buffer, which enables the different components of working memory to interact with long-term memory (Dempere-Marco *et al.*, 2012).

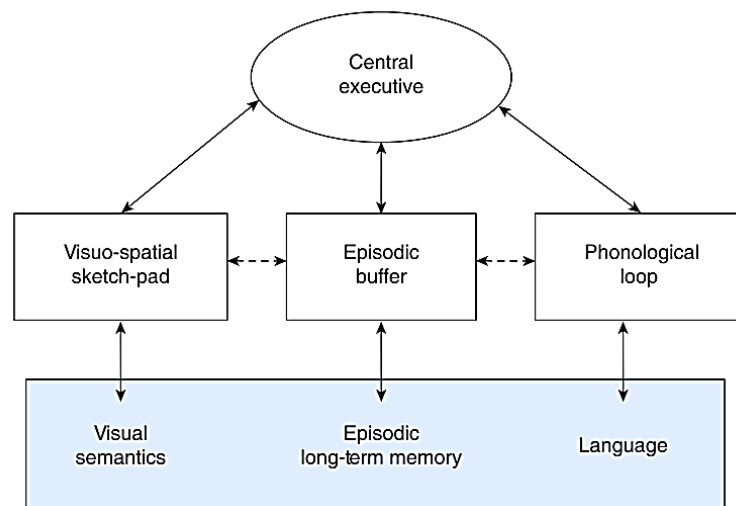


Figure 3.3 Working Memory Model (Baddeley, 2000)

In human working memory (Baddeley, 2000), the central executive is a system that integrates information from the phonological loop, the visuospatial sketchpad and the episodic buffer. The central executive system also plays a major role in attention, planning strategies and coordinating behaviour, as well as suppressing irrelevant information. The central executive directs attention and gives priority to particular activities. In other words, the central executive enables the working memory system to selectively attend to some stimuli and ignore others. For example, transients, such as the onset of brake lights, may orient the driver's attention automatically (Johannsdottir and Herdman, 2010).

The phonological loop and the visuospatial sketchpad are viewed as limited-capacity storage and processing systems for verbal (Sebastián-Gallés, 2006; Johannsdottir and Herdman, 2010; Heenan *et al.*, 2014) and visual information (Baddeley, 1986; Baddeley and Logie, 1999; Logie *et al.*, 2001; Heenan *et al.*, 2014). For example, when driving along a familiar route under stressful weather conditions, a phonological system maintaining the number and direction of the next turn can be a simple and very effective strategy (Baddeley, 2003). Meanwhile, the visuospatial sketchpad system is used when a driver tries to construct a mental map of necessary turns from a set of spoken navigational instructions (Wickens *et al.*, 1998). Previous research has also found that drivers' abilities to locate other vehicles and to avoid hazards were correlated with measures of phonological and visuospatial working memory – for instance, awareness of another vehicle that suddenly moved from behind the driver's vehicle to enter the lane in front of it (Gugerty and Tirre, 2000; Heenan *et al.*, 2014).

The episodic buffer serves as a temporary capacity for gathering and combining information from the phonological loop, the visuospatial sketchpad and long-term memory (Johannsdottir and Herdman, 2010). The episodic buffer actively manipulates information in order to interpret an earlier experience, solve new problems, and plan future activities (Baddeley, 2000; Matlin, 2005). The episodic buffer system is assumed to form a basis for the conscious awareness of drivers (Baddeley, 2003).

3.2.2 Limitation of Working Memory

The working memory model is a basic aspect of cognition; therefore the limitations have been well studied in humans (Schacter, 2002; Dempere-Marco *et al.*, 2012). According to Miller (1956) and Brown (1958), as well as Peterson and Peterson (1959), the working memory has a very limited capacity and duration when humans are dealing with unfamiliar information. Likewise, McLeod (2009), Schacter (2002) and Wickens *et al.* (1998) suggested that the ability to maintain the information in working memory is limited in two interrelated respects, which are how much information can be kept active and how long information can be kept active.

A number of researchers have suggested that the capacity of working memory is limited to around 7 ± 2 chunks of information (Bellezza, 1994; Miller, 1956; Cowan, 2001; Yang and Fricker, 2001; Schacter, 2002). A chunk is a memory unit that consists of several components that are strongly associated with one another (Bellezza, 1994; Cowan, 2001). For example, the sequence of four unrelated letters, X F D U, consists of four chunks, while the four letters DOOR consist of only one chunk, because these can be coded into a single meaningful unit. As a result, each occupies only one 'slot' in working memory, and so our working memory could hold $7(\pm 2)$ words or familiar dates as well as 7 ± 2 unrelated letters or digits. Yang and Fricker (2001) conducted an experiment to determine the amount of information that is considered to be too much for a driver to process, and to determine which method of conveyance is most effective. They used a driving simulator to simulate familiar and unfamiliar areas to the subjects. The responses when given twelve different information combinations for both familiar and unfamiliar areas were evaluated. Their findings showed that when a driver is in a familiar area, the need for a visual display related to the area is not necessary due to the fact that a driver will rely on their prior knowledge of the area. The opposite is observed when the driver is in an unfamiliar area. They also found that a visual display was more effective when accompanied with an auditory message that alerted drivers.

The capacity limits of working memory are closely related to the second limitation of working memory, the limit on how long information may remain. The strength of information in working memory decays over time (Cowan, 2001). To help predict working memory decay for differing numbers of chunks, Card *et al.* (1986) combined data from several studies to determine the half-life of items in working memory. The half-life was estimated to be approximately 7 seconds for a memory store of three chunks and 70 seconds for one chunk. Meanwhile, according to Atkinson and Shiffrin (1971), the duration of working memory seems to be between 15 and 30 seconds if the chunks are repeated. In order to investigate the effect of test subjects judged the subjective intensity of steering wheel hand-arm vibration, (Giacomin and Fustes, 2005; Hacaambwa and Giacomin, 2007; Ajovalasit and Giacomin, 2009; Jeon *et al.*, 2009; Ajovalasit *et al.*, 2012) and to identify the ability of drivers to detect the road surfaces (Giacomin and Woo, 2004; Berber-Solano and Giacomin, 2005; Berber-Solano *et al.*, 2010), test signal durations of between 7 and 10 seconds were used so as to provide a test signal that remained within human short-term memory (Atkinson and Shiffrin,

1971; Sinclair and Burton 1996; Baddeley 1997) This therefore did not rely upon the test participants' long-term storage of information.

The limitation of working memory has been the subject of significant research effort in connection with vehicle technology in order to address operational, safety and environmental related issues (Osman *et al.*, 2015). In addition, some studies have focused on the drivers' behaviour and response to the existence of the technology and how they handle the information load in their vehicle. It has been determined that providing too much information in the form of multiple warnings and/or information in multiple displays may overwhelm and distract the driver. In fact, too much information being presented affects the drivers' reaction times and may lead to inappropriate responses in emergency situations (Blincoe *et al.*, 2015).

3.3 Human Decision-Making Process

The term decision-making was defined as the process of reducing the gap between the existing situation and the desired situation by solving problems and making use of opportunities (Medin and Ross, 1992; Saroj, 2009). Meanwhile, March (1991) and Weick (2012) defined decision-making as a transformation of knowledge and information into managerial action. The importance of the human decision-making process has been the subject of active research from several studies from a psychological and cognitive perspective (Rizun and Taranenko, 2014).

Most initial research on the decision-making process has focused on the study of rational decision-making (Luce and Raiffa, 2012; Fischhoff, 1982). According to McCOWAN *et al.* (1999), the rational decision-making approach is central to the decision and utility theoretic frameworks widely used in the physical sciences and in the behavioural sciences, such as psychology and economics. Towler (2010) suggested that humans generally use a rational decision-making model when they want to make sure that they make the best choice. Rational decision makers seek relevant information, look carefully at future consequences, and act deliberately and logically (French *et al.*, 1993). For instance, rational drivers will drive their car according to the speed limit stated by

the government in both urban and rural environment to avoid the fines and maintain safety when driving (Warner and Åberg, 2008).

Limited cognitive resources, time pressures, and unpredictable changes often make rational processes unworkable (Wickens *et al.*, 1998). Thus, later researchers became interested in describing the cognitive processes associated with human decision-making behaviour and they developed a number of descriptive models (Wickens *et al.*, 1998). These models are often based on laboratory studies, which do not reflect the full range of decision-making situations. A decision maker is thought to act according to his or her understanding of the given situation such as environment and his or her profession (Simon, 1957); therefore, the source of any error is to be found in the person's previous knowledge or in the logical process followed when reaching the decision. Often, decisions are said to be made based on instinct or intuition (Bannister and Remenyi, 2000). The concepts of Simon (1957) and Bannister and Remenyi (2000) are consistent with studies by Perez *et al.* (2015) which suggest that the direction in which a driver will turn (left or right) is made by a driver's preconscious prediction.

3.3.1 Factors Affecting Decision-Making Process

The importance of correct and effective human decision-making is very easy to understand, but at the same time it is difficult to achieve, because it depends on many different and difficult factors (Wickens *et al.*, 1998). For both rational and cognitive decision-making, there exist a number of cognitive and environmental influences that affect the final decision.

Significant factors affecting the decision-making process have been identified, including information bias (Russo *et al.*, 1998; Juliusson *et al.*, 2005), which occurs when a human is asked to choose among alternatives of which they have had previous experience. Russo *et al.* (1998) affirmed that humans unconsciously distort information. In his study, he found that the formation of preferences occurs without instruction, and this leads to subsequent pre-decisional distortion of product information. This is followed by cognitive bias, which can occur when the amount of information available exceeds a decision maker's cognitive processing limits (Duhaime and Schwenk, 1985;

Stanovich and West, 2008). A decision maker is often unable to cope with all the information relevant to a decision, so he or she simplifies the decision-making process by applying cognitive filters or bias.

According to Orasanu and Martin (1998), time constraints can have a critical influence on a decision process. The level of time stress within a situation dictates the level of mental processes incorporated into the decision process. Relative to the amount of information presented, Wright (1974) notes that under high time stress, decision-making performance deteriorates when more, rather than less, information is provided. In high time-stress situations, people tend to restrict their range of focus to environmental cues. Manipulating a large amount of data is not consistent with human information processing capability, especially under stress (Stokes *et al.*, 1992).

Another factor that could affect human decision making is the perception of risk. Miller (2006) defined the perception of risk as a feeling that is psychologically linked to emotion, and these emotions are affected by how decisions are framed. Last but not least, the level of uncertainty is found to be one of the factors that affects human decision making (Wickens *et al.*, 1998). The level of uncertainty surrounding a decision creates bias that alters the way in which information is gathered and the decision is made. Uncertainty is the perceived gap between the information available and the information a decision maker desires (Buchanan and Kock, 2001). Furthermore, uncertainty influences both the decision maker and the outcome of the decision.

Most of the laboratory studies related to judging subjective intensity (Giacomin and Fustes, 2005; Hacaambwa and Giacomin, 2007; Ajovalasit and Giacomin, 2009; Jeon *et al.*, 2009; Ajovalasit *et al.*, 2012) or the detection of road surfaces (Giacomin and Woo, 2004; Berber-Solano and Giacomin, 2005; Berber-Solano *et al.*, 2010) presented the test signals in a random order in order to minimise any possible bias resulting from learning effects.

3.4 Signal Detection Theory

Signal detection theory (SDT) is a framework for understanding accuracy that makes the role of decision processes explicit. This facilitates the quantification of how people behave in detection situations (Tanner and Swets, 1954). SDT emerged as a method for investigating the assumption that expectancy and payoff have a significant influence on people in detection situations. Described in detail by Green and Swets (1966), SDT is a model based on the statistical decision theory and certain ideas about electronic signal detecting devices. The starting point for SDT is the assumption that nearly all reasoning and decision making takes place in the presence of some uncertainty.

Signal detection theory is applicable in any situation that can be considered to consist of two discrete states of the world – signal and noise – that cannot be easily discriminated (Green and Swets, 1966). In a detection situation, the observer must first make an observation (x) and then make a decision about the observation. On each trial, the observer must decide whether x is due to a signal that is present in a noise background or due to the noise alone. According to Gescheider (1997), when the signal is weak the decision becomes difficult and errors are frequent. Figure 3.4 graphically represents two distributions, displaying the random variation of the noise and of the signal plus noise. Since the signal is added to the noise, the average sensory observation magnitude will be greater for the signal plus noise distribution than for the noise distribution. When the distributions are essentially the same, as seen in Figure 3.4, where the signal plus noise distribution is indicated by a dotted line, they greatly overlap and decision-making becomes difficult due to the lack of separation between the two stimuli.

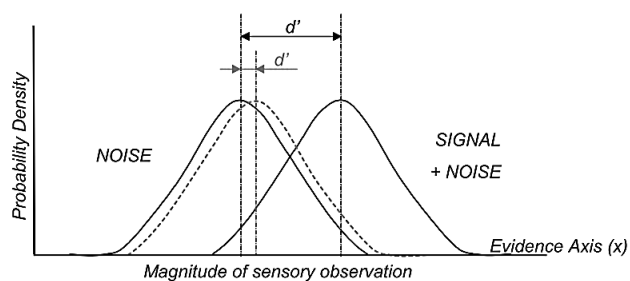


Figure 3.4 Theoretical probability distributions of ‘noise’ and ‘signal plus noise’ for two different values of signal strength (Source: Baird and Noma, 1978)

The theory also takes a stand on the way in which the relevant information is represented by the observer, identifying some aspects of the representation with sensitivity, or inherent accuracy, and others with response factors. The key assumption is that the strength of sensory and cognitive events is continuously variable. An observer who is trying to distinguish two stimulus types in trials, signal and noise for example, is faced with distributions of values for each possibility, as shown in Figure 3.4. Errors arise because the signal and noise distributions overlap, and the degree of overlap is an inverse measure of accuracy, or sensitivity. Improvements in sensitivity can only occur if this overlap is reduced, and such reductions are often not under the immediate control of the observer. By using the decision component of SDT, the solution can be achieved by dividing the strength axis into two regions with a criterion, so that high values lead to 'yes' responses (e.g. there was a signal), and low values lead to 'no' responses (Baird and Noma, 1978). The observer can change the location of the criterion and thus the way in which values of the internal dimension are mapped onto responses. The theory therefore provides a conceptual distinction between sensitivity and response bias.

3.4.1 Ideal Observers

Research has demonstrated that if a subject is attempting to maximise signal identification, the best decision strategy that he or she could employ is that of an ideal observer (Baird and Noma, 1978). The ideal observer derives from a mathematical theory of a detection task where the signal to be detected is noise degraded, and the observation of the signal is limited to a finite period of time. The aim of the theory is to determine to what extent noise limits the detection of the signal.

In order to behave as an ideal observer, a subject must have stored in their memory the signal and noise distributions, or have some other way of gaining access to them. In particular, an ideal observer maps the external stimulus (a 'noise' or a 'signal plus noise') onto a value, x , on the evidence axis and determines the probability of obtaining x from noise distributions, and from signal plus noise distributions, independently. The detectability of the signals is quantified by measuring how the errors are traded off as a function of the subject. SDT assumes that an observer establishes a particular value as a

cut-off point, or criterion, and that the decision is determined by whether a particular observation is above or below the criterion. According to Green and Swets (1966), no observer can make perfect detections of a signal masked by noise if there is overlap between the evidence distributions associated with noise and signal plus noise events. An example in this context was presented in Figure 3.4, where a signal plus noise distribution was drawn with a dotted line.

Peterson *et al.* (1954) derived the Signal Detection Theory and showed that the optimal observer uses the likelihood ratio decision axis, or a decision axis that is strictly monotonic with likelihood ratio, as a basis for decisions about the existence of the signal. If the signal is known to the observer exactly, and the observer can transform the evidence to a quantity that is monotonic with likelihood ratio, then the observer is considered to be an ideal Signal–Known–Exactly (SKE) observer. If the observer does not have an exact representation of a signal, or if the observer is unable to use information about some property of a deterministic signal, the observer is considered to be a Signal–Known–Statistically (SKS) observer.

The early radar engineers considered the concept of the ideal observer as a mathematical theory that predicted the best possible performance for a particular class of signals, with particular restrictions on the information the observer had about the signals (Peterson *et al.*, 1954). When the theory was extended to psychophysics, the emphasis changed. Unlike engineers, psychophysicists were not interested in designing detection systems, but were trying instead to understand existing biological systems that did not necessarily perform ideally, and whose internal processes were usually inaccessible.

3.4.2 Measures of Sensitivity and Response Bias

According to SDT, the separation of the noise and the signal plus noise distributions along the evidence axis is an indication of the level of sensory discrimination. The true sensitivity of the observer is unaffected by criterion location and is reflected instead by the difference between the means of the two distributions, which is denoted by d' , as shown in Figure 3.4.

When an observer is asked to choose between the two possible states (noise and signal plus noise) during the course of a sensory exposure, the combination of two stimulus and two response categories produces a 2x2 matrix (see Table 3.1). It involves four classes of joint events, which are labelled as hits, misses, false alarms and correct rejections.

Table 3.1 The four response outcome of signal detection theory

(Source: Green and Swets, 1966)

		Response alternative	
		Yes	No
Stimulus	Signal+Noise	Hit (Correct detection, $P(S s)$)	Miss (Incorrect rejection, $P(N s)$)
	Noise	False alarm (Incorrect detection, $P(S n)$)	Correct rejection (Correct denial, $P(N n)$)

Figure 3.5 shows the relations between the presence and absence of a stimulus, random variability and the decision criterion. The separation between the means of the two standardised distributions is a measure of detectability, which indicates how well the subject can discriminate between the two events, and it is denoted as d' . The detection task is easier for cases characterised by large separations and/or small variances.

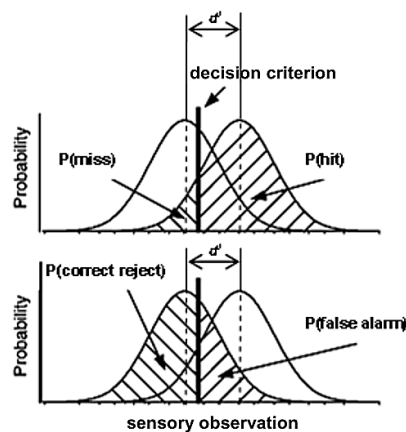


Figure 3.5 The signal detection diagram (Source: Heeger, 1998)

For experimental protocols in which observers are requested to provide a simple 'yes' or 'no' response, the detectability index d' can be estimated from the experimentally determined hit rates and false alarm rates by means of the associated Z-score values using the relations below (Gescheider, 1997). The Z transformation converts a hit or

false alarm rate to a Z (i.e. to standard deviation units). A rate of 0.5 is converted into a Z score of 0, larger rates into positive Z scores, and smaller rates into negative ones.

$$P(\textit{hit}) = \frac{\textit{"number of yes" counted during signals present}}{\textit{number of signals}} \quad (3.1)$$

$$P(\textit{false alarm}) = \frac{\textit{"number of yes" counted during signals present}}{\textit{number of non - signals}} \quad (3.2)$$

$$Z_n = 1.0 - P(\textit{false alarms}) \quad (3.3)$$

$$Z_{sn} = 1.0 - P(\textit{hit}) \quad (3.4)$$

where

$$d' = Z_n - Z_{sn} \quad (3.5)$$

Figure 3.6 presents an example of distributions of ‘noise’ and ‘signal plus noise’ expressed in Z -score values. Once the $P(\textit{hit})$ and $P(\textit{false alarm})$ are determined, the location of the criterion in both distributions is found by the subtraction of $P(\textit{hit})$ and $P(\textit{false alarm})$ from 1.0 and converting this value into Z scores (see Equations 3.3 and 3.4). The value of d' , a measure of the observer’s sensitivity to the signal, is found by subtracting Z_{SN} from Z_N (see Equation 3.5).

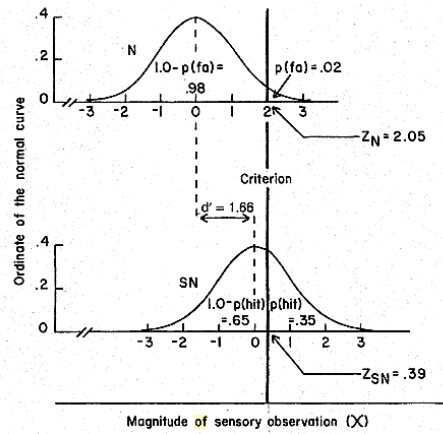


Figure 3.6 Distributions of noise and signal plus noise expressed in Z scores
(Source: Gescheider, 1997)

As shown in Figure 3.6, 1.0 minus the false alarm rate of 0.02 (i.e. 0.98) gives the proportion of the area under the noise distribution below the criterion. Converting 0.98 to a Z score yields a Z_N value of 2.05, which represents the location of the criterion on the abscissa of the noise distribution. The hit rate of 0.35 subtracted from 1.0 (i.e. 0.65) and gives the proportion of the area under the signal plus noise distribution below the criterion. When 0.65 is converted to a Z score, Z_{SN} is found to be 0.39. This value represents the location of the criterion on the abscissa of the signal plus noise distribution. To find d' , the Z_{SN} value of 0.39 is subtracted from the Z_N value of 2.05 to yield a d' value of 1.66. This value of 1.66 is the number of Z-score units between the mean of the noise distribution and the mean of the signal plus noise distribution.

3.4.3 Receiver Operating Characteristics Analysis

A receiver operating characteristics (ROC) graph is a technique for visualising, organising and selecting observers based on their performance. Illustrated in Figure 3.7, ROC graphs are two-dimensional graphs in which hit rate is plotted on the y-axis and false alarm rate is plotted on the x-axis.

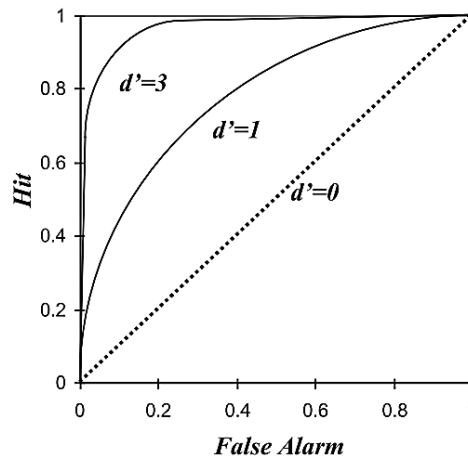


Figure 3.7 Receiver operating characteristics (ROC) graph
 (Source: Green and Swets, 1966)

The ROC curve summarises the observer’s performance as a function of the observer’s decision criterion for all possible criteria (Green and Swets, 1966). As an example, Figure 3.7 shows different ROC curves in which the detectability index values range from 0 to 3.0. An individual ROC curve reflects the response of an observer to a single strength of signal. If signal strength is increased, the ROC curve will have a more pronounced bow, as seen in Figure 3.7. If signal strength is decreased, the ROC curve becomes flatter and approaches the 45-degree diagonal line. Thus the amount of bow in the curve serves as a measure of the perceived signal strength.

Variations in the observer’s criterion result in different points along the ROC curve (see Figure 3.8). A single ROC curve is therefore a representation of detection performance for a situation characterised by a constant detectability index d' between a noise and a signal plus noise, by changing the values of the receiver’s detection criterion. Figure 3.8 presents the relationship between an individual ROC data point and the position of noise and signal plus noise distributions. The points on the curve indicate the mapping of hits and false alarms for different positions of the observer’s criterion, while the dotted diagonal line represents the case where $d'=0$, when noise and signal plus noise distributions are identical.

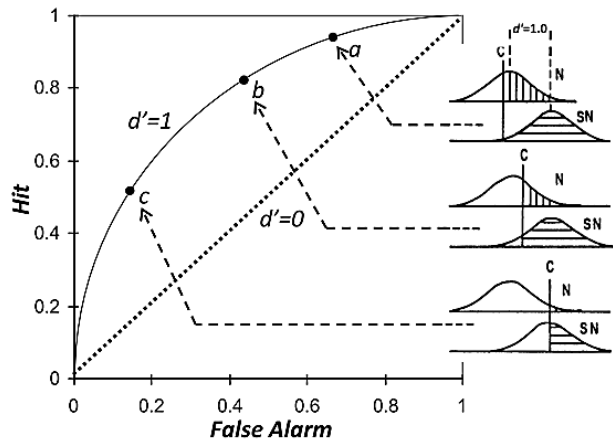


Figure 3.8 ROC curve for the signal plus noise and the noise distribution ($d' = 1$), obtained over different observers' criteria (Source: Green and Swets, 1966)

Algebraically, a ROC curve is calculated by solving Equation 3.5, which means that different curves represent different values of the detectability index. The prediction of SDT states that if a subject in a discrimination experiment produces a (false alarm, hit) pair which belongs on a particular ROC curve (i.e. [0.2, 0.6], $d'=1$), the same subject should be able to display any other (false alarm, hit) pair on the same curve (i.e. [0.4, 0.8], $d'=1$) (Macmillan and Creelman, 2005).

A discrete observer is one that outputs only a class label. Each discrete observer produces a pair corresponding to a single point in ROC space, as shown in Figure 3.9.

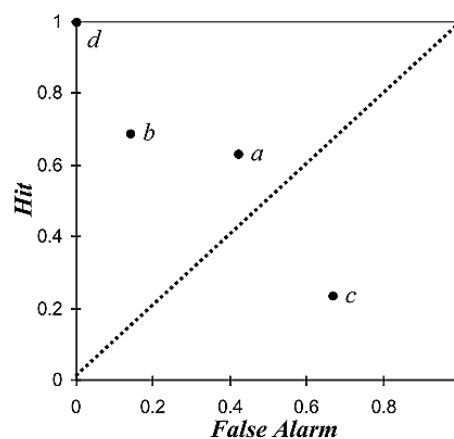


Figure 3.9 A basic ROC graph showing discrete observers (Source: Fawcett, 2006)

Several points in ROC space are important to note. The lower left point (0, 0) represents the strategy of never issuing a positive observation; such an observer commits no false

positive errors but also gains no true positives. The opposite strategy, of unconditionally issuing positive classifications, is represented by the upper right point (1, 1). The d' 's point (0, 1) represents perfect observation. Informally, one point in ROC space is better than another if it is to the northwest (hit rate is higher, false alarm rate is lower, or both) of the first. Observers appearing on the left-hand side of an ROC graph, near the x -axis, may be thought of as conservative: they make positive observations only with strong evidence, so they make few false positive errors, but they often have low true positive rates as well. Observers on the upper right-hand side of an ROC graph may be thought of as liberal: they make positive observations with weak evidence, so they classify nearly all positives correctly, but they often have high false positive rates. In Figure 3.9, b is more conservative than a . Many real-world domains are dominated by large numbers of negative instances, so performance in the far left-hand side of the ROC graph becomes more interesting.

3.4.4 Signal Detection Theory in Human Subjective Response

Researchers in many diverse areas of psychology have begun to employ the SDT to separate the ability of subjects to differentiate between classes of events from motivation effects or response bias. In addition to its extensive application in sensory psychophysics, signal detection has found an application in such diverse areas as vision perception (Tanner and Swets, 1954), vibrotactile perception (Pongrac, 2008), memory perception (Hermawati, 2003) and hand-transmitted vibration perception (Morioka and Griffin, 2006; Giacomini and Woo, 2004; 2005; Berber-Solano and Giacomini, 2005; 2006; Berber-Solano *et al.*, 2013).

Tanner and Swets (1954) measured human observers' behaviour when detecting light signals in a uniform light background. Detection of these signals depends on information transmitted to cortical centres by way of the visual pathways. With a total of 100 experimental observations, the expected form of data collected in 'yes-no' psychophysical experiments was used.

Pongrac (2008) applied the detection theory in vibrotactile perception studies to examine the coding of vibrations and the just-noticeable difference under various

conditions. The stimuli consisted of sinusoidal waves with 500 ms duration, with a total of 16 stimulus vibrations realised. Figure 3.10 shows the laboratory experiment setup for the studies, whereby the accelerometer with a circular contactor was directly attached to the vibrator. A circular piece of foam rubber was glued on to the contactor of the accelerometer. The vibrator with the mounted accelerometer was embedded in a small frame house, and the contactor was passed through a 15 mm-diameter hole in the frame house.



Figure 3.10 Presentation of vibrations through the vibrator embedded in a small frame house (Source: Pongrac, 2008)

The participants were instructed to put the pad of their index finger on the contactor without exerting any pressure on it. It was ensured that every participant adopted the same finger position during the experimental session. White noise was emitted through closed headphones in order to mask any sounds made by the vibrator. The participants had to indicate whether the presented stimulus pair consisted of two ‘same’ or two ‘different’ vibrations.

Hermawati (2003) aimed to investigate the main interaction effects of intermittent noise and random vibration in short-term memory scanning ability; the subjects were exposed to nine different experimental conditions. Task performance and subjective assessment data were collected during the experiment. Memory sets of 2, 4 or 6 letters (set size) were displayed for 1 second on the screen (see Figure 3.11).



Figure 3.11 Subject undertaking the task projected on the screen

(Source: Hermawati, 2003)

After each memory set, a single probe was presented. All letters were taken from the English alphabet and presented in upper case. Upon presentation of the probe, the participants were instructed to press the corresponding button as accurately and quickly as possible. The subject was to press the ‘*yes*’ button if the probe was displayed in the previous memory set (positive probe), and the ‘*no*’ button if the probe was not displayed in the memory set (negative probes). A random presentation with respect to memory set size and positive/negative trials was used with equal probability for each memory set size and response type. The task in each test run consisted of 150 stimuli. The performance of the task was measured through reaction time on correct responses and the number of correct responses.

Morioka and Griffin (2006) determined the absolute threshold of the perception of hand-transmitted vibration using a laboratory experiment, whereby the subjects were exposed to hand-transmitted vibration via a 30 mm-diameter rigid, smooth cylindrical wooden handle mounted on a Derritron VP30 electrodynamic vibrator (for fore-and-aft and lateral vibration), or a Derritron VP 4 electrodynamic vibrator (for vertical vibration) as shown in Figure 3.12.

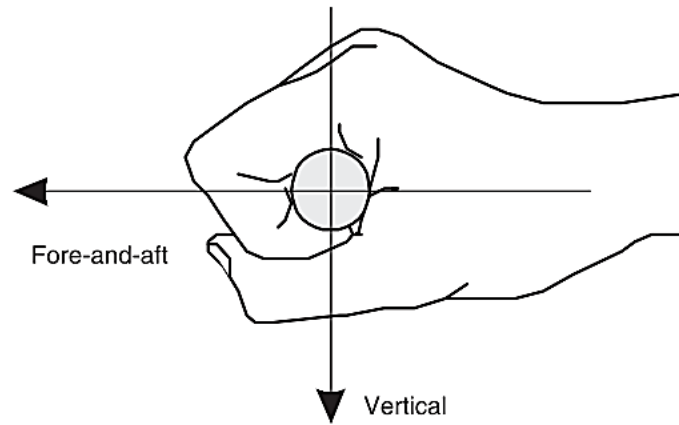


Figure 3.12 Hand posture and axis of vibration. The lateral axis is defined as parallel to the handle axis (Source: Morioka and Griffin, 2006)

A single test stimulus was presented, 2.0 s in duration. The subjects were tasked with indicating whether they perceived the vibration stimulus or not. They responded by saying ‘yes’ or ‘no’. The vibration stimulus increased in intensity by 2 dB (25.8% increment) after a negative (‘no’) response from a subject and decreased in intensity by 2 dB after three consecutive positive (‘yes’) responses.

Giacomin and Woo (2004; 2005), Berber-Solano and Giacomin (2005), Giacomin and Berber-Solano (2006), and Berber-Solano *et al.* (2013) conducted laboratory-based experiments to evaluate the effect of steering wheel vibration on the driver detection of road surface type. The studies used steering wheel tangential direction acceleration time histories, which had been measured in a mid-sized European automobile that was driven over different types of road surfaces. The photograph shown was an image similar to a driver’s view of the road while driving (see Figure 3.13), whereby the test participants were exposed to both non-manipulated and manipulated steering wheel tangential vibration stimuli.



Figure 3.13 Participant performing the road surface detection task
(Source: Woo and Giacomini, 2006)

3.5 Conclusion

This chapter considered the basic mechanism by which humans perceive, think, remember, evaluate and decide which is generally grouped under the label of cognition (Wickens *et al.*, 1998). The term cognition refers to the acquisition, storage, transformation, and use of knowledge, while cognitive psychology is sometimes used as a synonym for cognition and sometimes as a term referring to a theoretical approach to psychology. Within the driving situation, cognition was used to refer to a cognitive driving task.

The information-processing model that explained the human working memory model and its limitations was covered in the first section of this chapter. The best-known example of an information-processing model is the Atkinson-Shiffrin (1968) model. The external stimuli from the environment first enter sensory memory. Some material from the sensory memory will then pass into the short-term memory, now called working memory, which contains only the small amount of information that humans are actively using. Finally, the material that has been rehearsed passes from short-term memory to long-term memory. The working memory model is a basic aspect of cognition; therefore its limitations have been well studied in humans. The ability to maintain the information in working memory is limited in two interrelated respects – how much information can be kept active and for how long information can be kept active.

The second topic presented how different information is assessed and how people choose from a number of alternatives, together with the factors that make this process more or less effective. Most of the initial research on the decision-making process focused on the study of rational decision making and later became interested in cognitive processes associated with human decision making. Rational decision making describes how humans should compare alternatives and make the best decision, while cognitive processes are said to be made based on instinct or intuition. The importance of correct and effective human decision-making is very easy to understand, but at the same time it is difficult to achieve, because it depends on many different and difficult factors including information bias, cognitive bias, time stress, perception of risk, and level of uncertainty.

Together, this chapter describes the general theory of signal detectability and the application of the theory in a number of studies within psychophysical experiments. The signal detection theory provides a means of analysing the critical structure of the human detection decision process in a variety of situation. Furthermore, the theory allows sensitivity to be separated from bias, accuracy to be compared across paradigms, and the extrinsic limitations of an experimental design to be distinguished from intrinsic ones. Ideal observers are those who attempt to maximise signal identification. The psychophysical studies presented in this chapter employed the ‘*yes-no*’ procedure because it yields ROC curves of a monotonically decreasing slope; that is, curves of the general form predicted by the signal detection theory. In addition, the data are fitted well by theoretical curves based on normal probability distributions.

In many ways, both the topic of human cognition and the signal detection theory described in this chapter can be considered as experiment protocols to be used in this research. Explicitly, they provide the appropriate procedures for data collection and analysis in terms of the human subjective response approach.

The following chapter will discuss the method that will be employed to find homogeneous groups of highly similar variables related to the individual transient vibrations of road surfaces. This discussion provides the complete theoretical background that is needed before the data of the individual transient vibrations of road surfaces used in this research are analysed with a numerical approach.

CHAPTER 4

CLUSTER ANALYSIS

4.1 Introduction

Cluster analysis is an activity that groups or classifies a set of objects in such a way that objects in the same group are more similar to each other than to those in other groups (Green *et al.*, 1967; Paykel, 1971; Jain *et al.*, 1999; Kettnering, 2006; Kashef, 2008; Fernández and Gómez, 2008; Amit *et al.*, 2009). The greater the similarity of objects within a group and the greater the difference of objects in different groups, the better the results of data clustering activity (Paykel, 1971).

A study conducted by Jain (2010) suggested that clustering activities have been used for three main purposes. The first purpose is to gain insight into objects, generate hypotheses, detect abnormalities and identify significant features of objects. Following these is the purpose of identifying the degree of similarity among objects. Jain (2010) also suggested that clustering has been used as a method for organising objects and summarising them through cluster prototypes.

The applications of the data clustering approach appear in many disciplines, such as marketing (Green *et al.*, 1967), image and video processing (Conway *et al.*, 1991; Chatterjee and Milanfar, 2009; Yang *et al.*, 2016), and psychology (Bruner *et al.*, 1956; Rosch, 1975; 1978; Rosch *et al.*, 1976; Barsalou, 1983; McClelland and Rumelhart, 1985; Murphy and Medin, 1985; Niedenthal *et al.*, 1999; Niedenthal and Halberstadt, 2000; Brosch *et al.*, 2010). For example, in marketing (Green *et al.*, 1967) the clustering approach was adopted to group 88 cities on the basis of 14 variables, such as city size, newspaper circulation, per capita income and so on. Meanwhile, in radar images

processing (Conway *et al.*, 1991), it is used to segment synthetic aperture radar images as part of a study into crop classification. Furthermore, using clustering activities, the structure of emotional stimuli was classified according to certain principles, such as perceptual similarities (Rosch, 1978), semantic rules or theories (Murphy and Medin, 1985), implications for goal states (Barsalou, 1983) or evoked emotional responses (Niedenthal *et al.*, 1999).

Despite this, clustering activities are yet to be applied in transient vibrations steering wheel road surface (Berber-Solano, 2008). By classifying the structure of each transient vibration of road surfaces, the optimal guidelines of steering wheel feedback can be obtained (Giacomin, 2005; Giacomin and Woo, 2005) and, at the same time, the classification will provide a complete documentation of the road surface features for the purpose of monitoring applications (Giacomin *et al.*, 2000). This situation suggests a need to review the data clustering techniques in order to define an appropriate technique to classify transient vibrations steering wheel road surface. Therefore, the purpose of this chapter is to introduce the techniques that will be considered for use in finding similar groups of highly significant features related to the transient vibrations steering wheel road surface.

4.2 Visualising Clusters

Clusters can be identified in one or two dimensions by looking for separate modes in the estimated density function of the data. Such an approach can be used on dataset where the number of variables is greater than two by first projecting the data into a low-dimensional space using dimensionality reduction techniques (Everitt *et al.*, 2001).

The dimensionality reduction techniques transform the data from the original D -dimensional feature space into a new d -dimensional feature space, with the latter being smaller than the former (Faivishevsky and Goldberger, 2012). The main objective of dimensionality reduction is to preserve as much of the significant structure of the high-dimensional data as possible in the low-dimensional space (Maaten and Hinton, 2008). The advantages of dimensionality reduction are that it makes the data more convenient for humans (Everitt *et al.*, 2001; Faivishevsky and Goldberger, 2012), for instance by

reducing it to a two dimensional space, and it also facilitates automatic inference (Faivishevsky and Goldberger, 2012), since a computationally intensive technique may be manageable only for low dimensional data. Furthermore, dimensional reduction can also reduce the quota limit of computer memory and the time required for dealing with large numbers of features of dataset.

Many techniques have been proposed to perform dimensionality reduction, such as Principal Components Analysis (PCA). PCA is known as one of the most traditional and popular techniques (Faivishevsky and Goldberger, 2012; Platzer, 2013; Saadatpour *et al.*, 2015) because of its straightforward and standard ways of accomplishing the feature transformation (Esteva *et al.*, 2012). PCA is an unsupervised (Diana, 2016; Tang *et al.*, 2016) and linear transformation of high-dimensional data (Maaten and Hinton, 2008; van der Maaten, 2009; Esteva *et al.*, 2012; Mwangi *et al.*, 2014; Saadatpour *et al.*, 2015; Diana, 2016; Zhang *et al.*, 2016; Balamurali and Melkumyan, 2016) which works by decreasing the proportions of the total variance of the original dataset (Everitt *et al.*, 2001; Platzer, 2013).

Despite the successful application of PCA in various studies such as non-destructive testing and evaluation (Johnson, 2002), neural networks and learning systems (Li and Yang, 2016), biological processing (Platzer, 2013), because real-world data are complex and nonlinear, PCA seem powerless to capture nonlinear relationships in a high-dimensional space (Amir *et al.*, 2013; Mwangi *et al.*, 2014; Saadatpour *et al.*, 2015). Therefore, to overcome this limitation, newer techniques of non-linear dimensionality reduction, namely t-Distributed Stochastic Neighbor Embedding (t-SNE), were introduced (Maaten, and Hinton, 2008; van der Maaten, 2009).

The t-SNE techniques are generated through an unsupervised process and are unlikely to have a direct physical interpretation, despite carrying important information (Maaten, and Hinton, 2008; van der Maaten, 2009; Faivishevsky and Goldberger, 2012; Balamurali and Melkumyan, 2016; Diana, 2016). Most notably, t-SNE shows a superior performance for visualising datasets, from high-dimensional to low-dimensional data (Maaten, and Hinton, 2008; van der Maaten, 2009; Esteva *et al.*, 2012; Faivishevsky and Goldberger, 2012; Amir *et al.*, 2013; Platzer, 2013; Frid and Lavner, 2014; Mwangi *et al.*, 2014; Saadatpour *et al.*, 2015; Balamurali and Melkumyan, 2016). This is due to the fact that the majority of dimensionality reduction techniques are not capable of

retaining both local and global structures of the data simultaneously during the dimensionality reduction process (Maaten, and Hinton, 2008; Mwangi *et al.*, 2014; Balamurali and Melkumyan, 2016). Additionally, t-SNE also displays the data in a visual format, which is more understandable and helps to improve inferences, comprehension and decision making.

Taking into account the benefits of using t-SNE over traditional dimensionality reduction processes such as principal component analysis, the next subsection discusses t-SNE techniques, with the assumption that the techniques can be applied for the clustering and classification of transient vibrations steering wheel road surface.

4.2.1 t-Distributed Stochastic Neighbor Embedding (t-SNE)

The t-SNE algorithm transforms the original dataset from a high-dimensional space to a low-dimensional space by minimising the differences in all pairwise similarities between points in high- and low-dimensional spaces. In other words, t-SNE gathers all information in m components (where m is freely chosen, in case of plots $m=2$). The axes of the low-dimensional spaces are given in arbitrary units.

The first step in the t-SNE algorithm is calculating the pairwise distance matrix in the high-dimensional space. The distance matrix is transformed into a similarity matrix using a varying Gaussian kernel so that the similarity between points x_i and x_j represents the conditional probability that x_i will choose x_j as its neighbour or vice versa. The choices are based on the Euclidean distance of x_i and x_j and their local density. Mathematically, the conditional probability of x_i to x_j is given by:

$$p_{(j|i)} = \frac{\exp\left(-\|x_i - x_j\|^2 / 2\sigma_i^2\right)}{\sum_{k \neq i} \exp\left(-\|x_i - x_k\|^2 / 2\sigma_i^2\right)}, \quad (4.1)$$

where σ_i is the variance of the Gaussian that is centered on data point x_i

$$p_{ij} = \frac{p_{j|i} + p_{i|j}}{2n} \quad (4.2)$$

The bandwidth of the Gaussian kernels σ_i , is set in such a way that the perplexity of the conditional distribution equals a predefined perplexity using a binary search. The perplexity is defined as:

$$Perp(P_i) = 2^{H(P_i)}, \quad (4.3)$$

where $H(P_i)$ is the Shannon entropy of P_i measured in bits

$$H(P_i) = - \sum_j p_{j|i} \log_2 p_{j|i} \quad (4.4)$$

The perplexity can be defined as a smooth measure of the effective number of neighbours. The performance of t-SNE is fairly robust but is affected by the value of perplexity, whereby the perplexity decreases monotonically with the variance σ_i . In another words, the lower the value of perplexity, the farther apart the data points will be in the low-dimensional space.

Then, a random low-dimensional mapping is rendered and pairwise similarities are computed for points in the low-dimensional space. In t-SNE, a Student t-distribution is used in order to allow dissimilar objects to be modelled far apart in the space. Using this distribution, the joint probabilities are defined as:

$$q_{ij} = \frac{(1 + \|y_i - y_j\|^2)^{-1}}{\sum_{k \neq l} (1 + \|y_k - y_l\|^2)^{-1}} \quad (4.5)$$

Finally, gradient descent is used to minimise the Kullback-Leibler divergence between the two probability distributions of Student-t based joint probability distribution Q and

distribution P , leading to the final low-dimensional map. The Kullback-Leibler divergence between the two joint probability distributions P and Q is given by:

$$KL(P||Q) = \sum_i \sum_j p_{ij} \log \frac{p_{ij}}{q_{ij}} \quad (4.6)$$

Silverman (1986) suggested that dimensional reduction can be used as the basis for a more formal approach before the clustering analysis begins. Thus, the following section provides the discussion related to the clustering analysis.

4.3 Clustering Techniques

Clustering techniques can be classified in terms of different independent dimensions. For instance, different starting points, methodologies, techniques, points of view, clustering criteria and output representations (Kashef, 2008). The different techniques used to cluster data can be described with the help of the hierarchy shown in Figure 4.1.

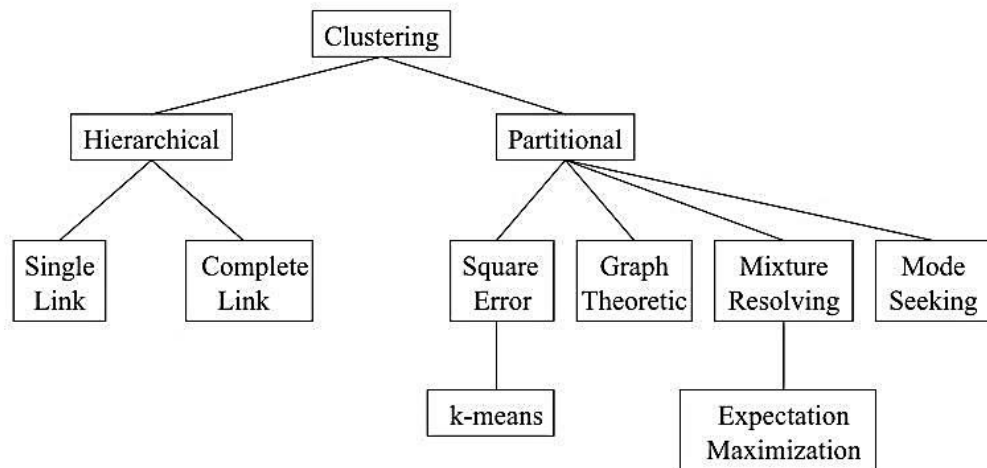


Figure 4.1 Data clustering techniques (Source: Jain *et al.*, 1999)

Clustering techniques can be broadly divided into two groups, hierarchical and partitional (Jain and Dubes, 1988). Hierarchical clustering will find nested clusters either in agglomerative methods or in divisive methods (Jain and Dubes, 1988; Jain *et al.*, 1999; Everitt *et al.*, 2001). An agglomerative method begins with each data point in

its own cluster and the merging of the most similar pair of clusters successively to form a cluster hierarchy. On the other hand, a divisive method begins with all objects in a single cluster and iteratively performs splitting until a stopping criterion is met. In contrast to hierarchical clustering, partitional clustering will divide the data into a particular number of clusters at a single step (Everitt *et al.*, 2001). In addition, partitional clustering has advantages in applications involving large dataset (Jain *et al.*, 1999; Kashef, 2008).

According to Jain *et al.* (1999), the best-known hierarchical algorithms are single-link and complete-link. In the single-link method, the distance between two clusters is the minimum of the distances between all pairs of patterns drawn from the two clusters (one pattern from the first cluster, the other from the second). In the complete-link method, the distance between two clusters is the maximum of all pairwise distances between patterns in the two clusters. Furthermore, Jain *et al.* (1999) concluded that single-link and complete-link methods differ in the way they characterise the similarity between a pair of clusters.

Jain *et al.* (1999) further suggested that the most popular and simplest partitional algorithm is *k*-means. The *k*-means algorithm is popular because it is easy to implement (Jain *et al.*, 1999). Apart from that, the *k*-means algorithm is considered an effective clustering algorithm in producing good clustering results for many practical applications, such as psychiatry (Paykel, 1971; Pilowsky *et al.*, 1969), archaeology (Dellaportas, 1998; Mallory-Greenough *et al.*, 1998; Hodson, 1971), market research (Green *et al.*, 1967) and EEG medical imaging (Orhan *et al.*, 2011; Güneş *et al.*, 2011) in biomedical fields. Another factor that makes the *k*-means algorithm popular and the preferred technique of previous researchers is the ability to apply *k*-means directly to environments without the need for training with the data measured or known as unsupervised technique (Yiakopoulos *et al.*, 2011). It can also be applied without prior information about the associations of data points with clusters (Faraoun and Boukelif, 2007; Hekim and Orhan, 2011; Mwasiagi *et al.*, 2009; Orhan and Hekim, 2007; Orhan *et al.*, 2008).

4.3.1 Choosing Clustering Techniques

As highlighted by Jain and Dubes (1988) and Jain (2010), even though there have been many successful applications of clustering in a number of different studies, defining appropriate clustering techniques remains a difficult problem. In order to minimise this difficulty, therefore, the selection criteria is first predetermined to ensure the clustering techniques for transient vibrations steering wheel road surface can be done easily and are manageable.

As stated in the Introduction (Section 4.1), clustering has not yet been used in the classification of transient vibrations steering wheel road surface (Berber-Solano, 2008), and therefore promising techniques are required. The techniques must be the simplest methods which offer an effective clustering algorithm in producing good clustering results for many practical applications. Clustering techniques do not require sets of prior data to be trained – as in this research situation where there are no dataset of feature information related to the transient vibrations steering wheel road surface available. In a study performed by Berber-Solano (2008), the total number of transient vibrations steering wheel road surface which exceeded the threshold trigger level (TTL) value of 2.6 and were distributed in the frequency band of 20 Hz – 60 Hz, which is known both as a critical trigger level and frequency band for a driver to detect the road surface types, was found to be approximately 600 dataset. Thus, the technique to be used in this research must not only be effective in producing good clustering results, but also needs to be compatible with the larger dataset without prior features information of the dataset.

Refer to selection criteria stated and the discussion on the various techniques of clustering analysis in the previous section of 4.3, it shows that the *k*-means meets all the selection criteria and an appropriate clustering technique to adapt in this research. Therefore, in the following subsection will present an in-depth review of *k*-means clustering.

4.3.2 *k*-means Clustering Algorithm

As stated by Rabiner and Juang (1993), the *k*-means clustering algorithm was developed by Steinhaus in 1957, following which Lloyd proposed a standard algorithm for *k*-means in 1982. Pierson *et al.* (2015) defined the *k*-means clustering as algorithms to subdivide data points of a dataset into clusters based on the nearest mean values. Further explained was the term of *k*-means, where *k* denotes the number of clusters in the data that need to be given a priori. The initial partitioning is randomly generated, that is, the centroids are randomly initialised to some points in the region of the space. The *k*-means partitions the dataset into *k* non-overlapping regions identified by their centroids based on an objective function criterion, where objects are assigned to the closest centroid. The most widely used objective function criterion is the distance criterion, namely Euclidean distance (Jain *et al.*, 1999; Everitt *et al.*, 2001; Jain, 2010).

Referring to the Concise Oxford Dictionary of Mathematics (2014), Euclidean distance can be defined as the straight-line distance between two points, which can be measured using the following equation (Jain *et al.*, 1999; Everitt *et al.*, 2001; Jain, 2010):

$$J = \sum_{j=1}^k \sum_{i=1}^n \|x_i^{(j)} - c_j\|^2 \quad (4.7)$$

where $\|x_i^{(j)} - c_j\|^2$ is a chosen distance measure between a data point $x_i^{(j)}$ and the cluster centre c_j is an indicator of the distance of the n data points from respective cluster centres. Figure 4.2 depicts the process of the standard *k*-means clustering algorithm where $k = 3$.

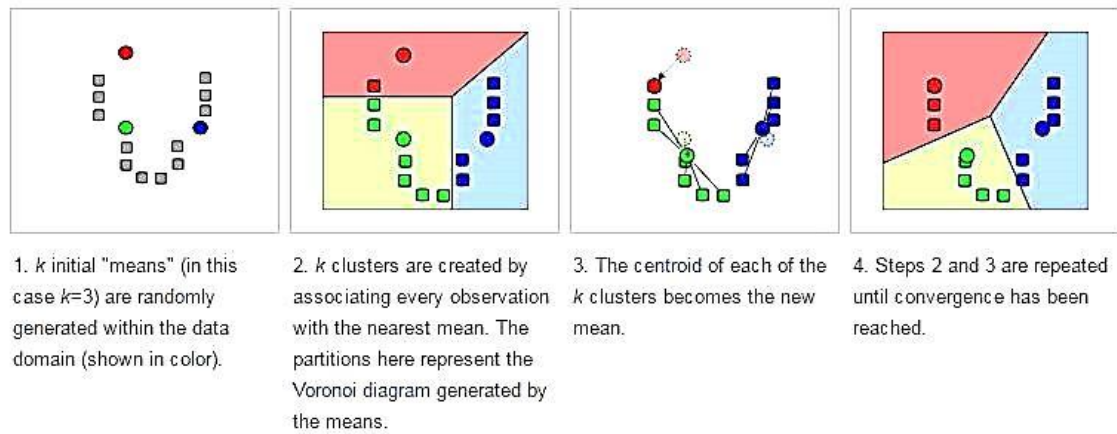


Figure 4.2 Demonstration of k -means clustering process

Figure 4.2 shows that the essential steps in the k -means algorithm will be iterated until convergence or a stopping criterion is met (Everitt *et al.*, 2001). The algorithm converges when re-computing the partitions does not result in a change in the partitioning.

Other than application of k -means in various number of studies of classification objects, the literature reveals that association between dimensionality reduction techniques such as t-SNE with clustering technique will lead to organising large dataset to be more easily understood and information retrieved more efficiently (Faivishevsky and Goldberger, 2012; Saadatpour *et al.*, 2015; Balamurali and Melkumyan, 2016) whereby the k -means technique is implemented as a clustering evaluation (Platzer, 2013; Mwangi *et al.*, 2014).

4.4 Conclusion

This chapter has presented the theory of cluster analysis and it starts by describing the projection of the high-dimensional data into a low-dimensional space using dimensionality reduction techniques. The t-SNE algorithm provided promising results as the technique was capable of retaining the local and global structures of the data simultaneously during the dimensionality reduction process. Following that, the background of clustering techniques in general was discussed. Clustering is a process of grouping data items based on a measure of similarity; the data can be broadly divided into two groups, hierarchical and partitional. As the clustering activities are yet to be

applied in steering wheel road surface vibrations, not only should the technique that is used in this research be effective in producing good clustering results, but it must also be compatible with the larger dataset without requiring prior feature information of the dataset. Therefore, the t-SNE and the k -means technique were chosen to be used for the classification of transient vibrations steering wheel road surface.

Moving forwards, before the proposed classification methods can be implemented in this current research, the choice of road surface types to be used throughout this study must also be considered. It is very important as a research approach, in order to ensure that the objectives can be achieved. Therefore, in the next chapter, the characteristics of the road surface types as well as the laboratory facilities will be presented.

CHAPTER 5

LABORATORY ROAD SURFACES STIMULI AND FACILITIES

5.1 Introduction

Chapter 5 is divided into two main sections. The first section will describe the road surfaces signals that will be used as a laboratory test stimuli. Following this is an explanation related to the laboratory facilities used during this research; the accuracy of the signal reproduction of the laboratory facilities is also presented at the end of this chapter.

5.2 Laboratory Road Surfaces Stimuli

Laboratory road surfaces stimuli are the stimuli used to perform any laboratory tests of human ability to detect road surface type, or of human sensitivity to changes in the statistical properties of the steering acceleration signals. In the process of choosing the laboratory road surface stimuli, the stimuli should satisfy three logical conditions of the selection criteria.

Firstly, the stimuli should be produced by commonly encountered road surfaces, so as to be representative of regular driving conditions (Giacomin and Gnanasekaran, 2005), such as city asphalt, pavé, potholes, bumps, country asphalt and smooth motorway surfaces. Secondly, the automobile test speeds should be reasonable values which are commonly used during driving over each specific type of surface (Department of Transport, 2006). Finally, the steering acceleration signals, if possible, should produce the widest operational envelope of test stimuli which can be achieved in terms of the

steering wheel acceleration root mean square (*r.m.s.*), kurtosis value, crest factor (CF) value and power spectral density (PSD) function.

In this following subtopic, the description of road surface types used during this research is presented, followed by the statistical analysis of each road surface.

5.2.1 Description of Road Surfaces

The laboratory road surfaces signal was selected from an extensive database of previous road test measurements made by the Perception Enhancement Research Group (Gnanasekaran *et al.*, 2006; Ajovalasit *et al.*, 2013; Berber-Solano, 2008; Jeon, 2010; Berber-Solano *et al.*, 2010). The road surfaces signal was provided by MIRA (Motor Industry Research Association), and the Michelin Group, including the directly measured tests over road surfaces in and around Uxbridge, West London, UK (Berber-Solano, 2008). A two-minute recording of road surfaces was measured by steering wheel acceleration using an accelerometer. The accelerometer was clamped tightly at the 60° position (two o'clock position) with respect to the top-centre of the steering wheel, as shown in Figure 5.1. This location corresponds with the typical grip position of the driver's hand when holding an automotive steering wheel (Giacomin and Gnanasekaran, 2005).



Figure 5.1 Position of steering wheel measurement point
(Source: Berber-Solano, 2008)

Figure 5.2 (a) to (j) presents the road surfaces as viewed from directly above and as seen from a distance when driving, along with the automobile velocity at which they were measured.



(a) Broken road;
Vehicle speed: 40km/h



(b) Broken Concrete;
Vehicle speed: 50km/h



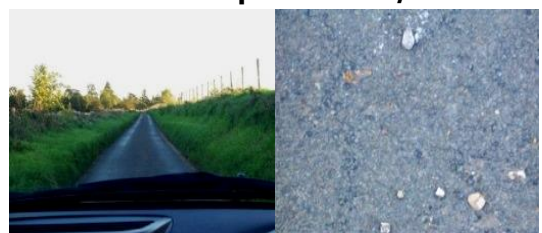
(c) Broken Lane;
Vehicle speed: 50km/h



(d) Cobblestone;
Vehicle speed: 30km/h



(e) Concrete;
Vehicle speed: 96km/h



(f) Country Lane;
Vehicle speed: 40km/h



(g) Harsh;
Vehicle speed: 40km/h



(h) Low Bump;
Vehicle speed: 50km/h



(i) Noise;
Vehicle speed: 80km/h



(j) Tarmac;
Vehicle speed: 96km/h

Figure 5.2 Road surfaces and vehicle speeds, whose stimuli were used for laboratory tests

In Figure 5.2 there are four steering wheel acceleration signals provided by MIRA, namely Cobblestone surface, Concrete surface, Low Bump and a Tarmac surface. The road surfaces were measured at MIRA's proving ground in Nuneaton, Warwickshire, UK, which has a comprehensive range of circuits and facilities used to carry out a wide range of tests. The automobile used by MIRA during the experimental vibrational test was an Audi A4 model, year 2000, type 4/5S SAL (4 doors, 5-speed manual transmission, saloon sedan). Meanwhile, for Harsh and Noise surfaces, the steering wheel acceleration signals were provided by the Michelin Group, whose measurements were performed at the Claremont-Ferrand proving ground in the province of Auvergne, France using a Renault Megane 1.9 dTi model, year 1996, type 2+2 FHC (Fixed-Head Coupé), with 3 doors and a 5-speed manual transmission. The remaining road surfaces such as Broken surface, Broken Concrete surface, Broken Lane surface and a Country Lane surface were measured using a VW Golf 1.9 TDI model, year 2005, type 5/5S HBK (5 doors, 5-speed manual transmission, Hatchback) in and around Uxbridge, West London, UK.

Furthermore, all ten road surfaces presented in Figure 5.2 can be divided into two major categories. The first category includes the Harsh and Low Bump surfaces. Both surfaces contained significant transient vibrations, which greatly exceeded the magnitude when compared to the previous and future sections' magnitude (Ajovalasit *et al.*, 2013). The Harsh and Low Bump surfaces were basically obstacles placed across a surface in the path of the automobile. According to the Department of Transport (2006), in the UK this kind of obstacle is used in urban areas such as town centres, high streets, residential roads and in the vicinity of schools; therefore, the automobile speed should be less than 40 km/h when driving over the obstacle.

The remaining eight road surfaces were measured with a random vibration process with a stable magnitude throughout the overall acceleration recording, but containing a few high peaks due to short duration transients, which can be broadly classified as mildly non-stationary signals (Giacomin *et al.*, 2000). The Broken road, Broken Concrete and Broken Lane were damaged surfaces, which are commonly found in many areas in the UK. Speeds to drive over damaged surfaces can reach levels of up to 50 km/h (Department of Transport, 2006). The cobblestone surface is formed by rectangular stones such as those found in many Italian and French cities or in the city centre road surfaces in the UK. The Department of Transport (2006) in the UK establishes a speed

of less than 40 km/h to drive over such surfaces; the aim of this limit is to reduce vehicle speed due to the possible presence of vulnerable road users such as cyclists, children or the elderly. The concrete surface is formed by pieces of plain concrete which are coupled by means of expansion joints. The Tarmac surface, properly referred to as bituminous macadam, or "Bitmac" for brevity, has the characteristic of being a smooth surface which is widely used to surface pavements, highways and even internal floors. Both concrete and tarmac surfaces are predominantly used in non-built-up areas or in built-up areas where a higher speed is both safe and appropriate. Speeds above 90 km/h are common for these two types of road surfaces (Department of Transport, 2006). The country lane surface, which is commonly found in rural areas, is a type of road where stones and pieces of wood can be found across the asphalt surface. According to the Department of Transport, in the UK the speed limit in rural areas can vary from 32 km/h to 50 km/h. The Noise surface is a form of asphalt road which is widely encountered on pavements and highways. Speeds above 90km/h are common for this kind of road surface.

5.2.2 Vibration Signal Analysis of Road Surfaces

Vibration signal analysis has always been a crucial part of many vibration practical applications (Peng *et al.*, 2005). In the context of road surfaces, the main purpose of the vibration signal analysis is to provide the road profile data of different surface types to describe the irregularities of the road (Bruscella *et al.*, 1999; Rouillard *et al.*, 2001; Eriksson *et al.*, 2008; Hu-ming *et al.*, 2010), as well as the testing and monitoring of applications (Giacomin *et al.*, 2000).

The possible methods used to analyse a vibration signal are in the time-domain (Erdreich, 1986; Bendat and Piersol, 2011) or the frequency-domain (Bruscella *et al.*, 1999). In the time-domain, Bellmann (2002) suggested the most relevant statistical parameters to quantify the vibration signal, as shown in Table 5.1. Moreover, Bellmann (2002) also suggested that analysis in the frequency-domain can be done by a Fast Fourier Transformation (FFT) or in the power spectral density (PSD).

Table 5.1 Most relevant parameters for vibration signal analysis

(Source: Bellmann, 2002)

Parameter	Mathematical Notation	Descriptions
Mean	$\bar{x} = \frac{1}{N} \sum_{j=1}^N x_j$	Considered as the first statistical ‘moment’ of the random process to quantify the overall energy of a signal.
Standard deviation	$\sigma = \left\{ \frac{1}{N} \sum_{i=1}^N [x(i) - \bar{x}]^2 \right\}^{\frac{1}{2}}$	Considered as the second statistical ‘moment’ of the random process to quantify the overall energy of a signal.
Root-mean-square	$r.m.s = \left\{ \frac{1}{N} \sum_{j=1}^N x_j^2 \right\}^{\frac{1}{2}}$	Quantifies and characterises the strength of energy content in a signal.
Skewness	$\lambda = \frac{1}{N} \sum_{j=1}^N \left(\frac{x_j - \bar{x}}{\sigma} \right)^3$	Characterises the degree of asymmetry of a distribution around its mean value.
Kurtosis	$\gamma = \frac{1}{N} \sum_{j=1}^N \left(\frac{x_j - \bar{x}}{\sigma} \right)^4$	Characterises the relative peakedness or flatness of a distribution in relation to the normal Gaussian distribution.
Crest factor	$CF = \frac{x_{jmax}}{r.m.s}$	Quantifies the severity of peaks in a waveform. The higher the peaks, the greater the crest factor.
Vibration Dose Value	$VDV = \left[\frac{T_s}{N} \sum_{j=1}^N x^4(t) \right]^{1/4}$	Quantifies the severity of exposure of a human to vibration.

5.2.2.1 Vibration Signal Analysis in the Time-Domain

Vibration signal analysis in the time-domain will provide the behaviour of the signal over time, which allows predictions and regression models for the signal (Inman and Singh, 2014). Therefore, a ten-second data segment was chosen to serve as a test stimulus, as presented in Figure 5.3, used to perform the time-domain analysis.

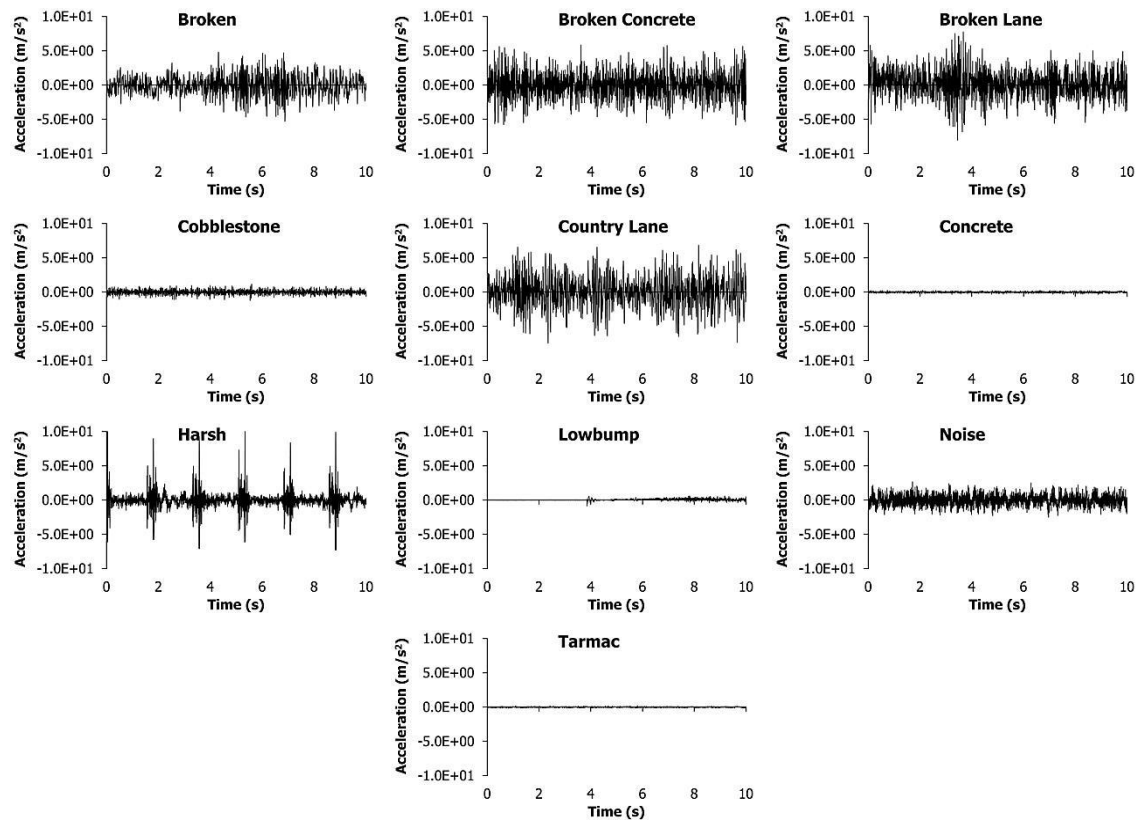


Figure 5.3 The time history segments extracted from the road test recordings for laboratory tests

The segment length was selected so that the root mean square values, the kurtosis, crest factor value and the power spectra density were close and statistically representative to those of the complete time history (Giacomin *et al.*, 2000). Additionally, the ten-second duration of data segments was chosen so as to remain within human short-term memory (Atkinson and Shiffrin, 1971).

Furthermore, the time-domain analysis was calculated based on the most relevant statistical parameters for vibration signal analysis, described in Table 5.1. However, in this thesis all the data calculation has been performed by using the Time Monitoring (T-MON) module of the LMS[®] CADA-X 3.5E software (LMS International, 2002). The results of vibration time-domain analysis of each road surface are presented in Table 5.2. The value of each parameter is presented in two decimal places as suggested by rule of thumb of statistics in presenting the decimal places by Spatz (2008) for the accuracy of calculation results.

Table 5.2 The vibration time-domain analysis of road surfaces

Road Surfaces	Mean	Standard deviation	<i>r.m.s.</i> (m/s ²)	Skewness (Dimensionless)	Kurtosis (Dimensionless)	Crest Factor (Dimensionless)	VDV (m/s ^{1.75})
Broken	-0.01	1.32	1.32	-0.05	3.48	3.84	3.20
Broken Concrete	0.00	1.73	1.73	0.01	3.21	3.36	4.13
Broken Lane	0.19	1.77	1.78	-0.03	3.63	4.40	4.36
Cobblestone	0.00	0.31	0.31	0.01	3.16	3.89	0.74
Concrete	-0.01	0.09	0.09	0.05	3.08	3.47	0.22
Country Lane	0.02	2.05	2.05	-0.07	3.27	3.49	4.90
Harsh	-0.03	1.26	1.26	1.14	18.83	7.28	4.69
Low Bump	0.06	0.13	0.14	0.33	6.43	5.35	0.36
Noise	-0.02	0.75	0.75	0.09	2.93	3.46	1.73
Tarmac	0.00	0.06	0.06	0.07	3.00	3.64	0.13

Table 5.2 suggested that vibration signals of road surfaces achieved root mean square (*r.m.s.*) acceleration levels from a minimum of 0.06 m/s² (for the Tarmac surface) to a maximum of 2.05 m/s² (for the Country Lane surface). Maximum crest factor (CF) was obtained in the case of the Harsh surface, which produced a value of 7.28, while the minimum CF was found for the Broken Concrete surface with a value of 3.36. Results for the vibration dose value (VDV) varied from 0.13 m/s^{1.75} for the Tarmac surface to 4.90 m/s^{1.75} for the Country Lane surface.

The results in Table 5.2 also suggested that all road surfaces, except for Low Bump and Harsh, have a stable magnitude throughout the overall acceleration recording, but containing a few high peaks due to short duration transients which, indeed, can be broadly classified as mildly non-stationary signals (Giacomin *et al.*, 2000) where it is shown that the acceleration data were Gaussian distributed, with a kurtosis value close to 3.0 and a skewness value close to 0.00.

5.2.2.2 Vibration Signal Analysis in the Frequency-Domain

Vibration signal analysis in the frequency-domain can be done by a Fast Fourier Transformation (FFT) or in the power spectral density (PSD). FFT is a method that capable to transforming a signal in the time-domain into the frequency-domain, while PSD is common technique for analysing the frequency content of signals for human vibration (Mansfield, 2005). However, both methods provided the characteristic distribution of vibration energy to be identified (Inman and Singh, 2014). By using the Time Monitoring (T-MON) module of the LMS[®] CADA-X 3.5E software, the vibration

signal analysis of road surfaces in the frequency-domain by PSD can be achieved and the results are presented in Figure 5.4 (i) to (x), accordingly.

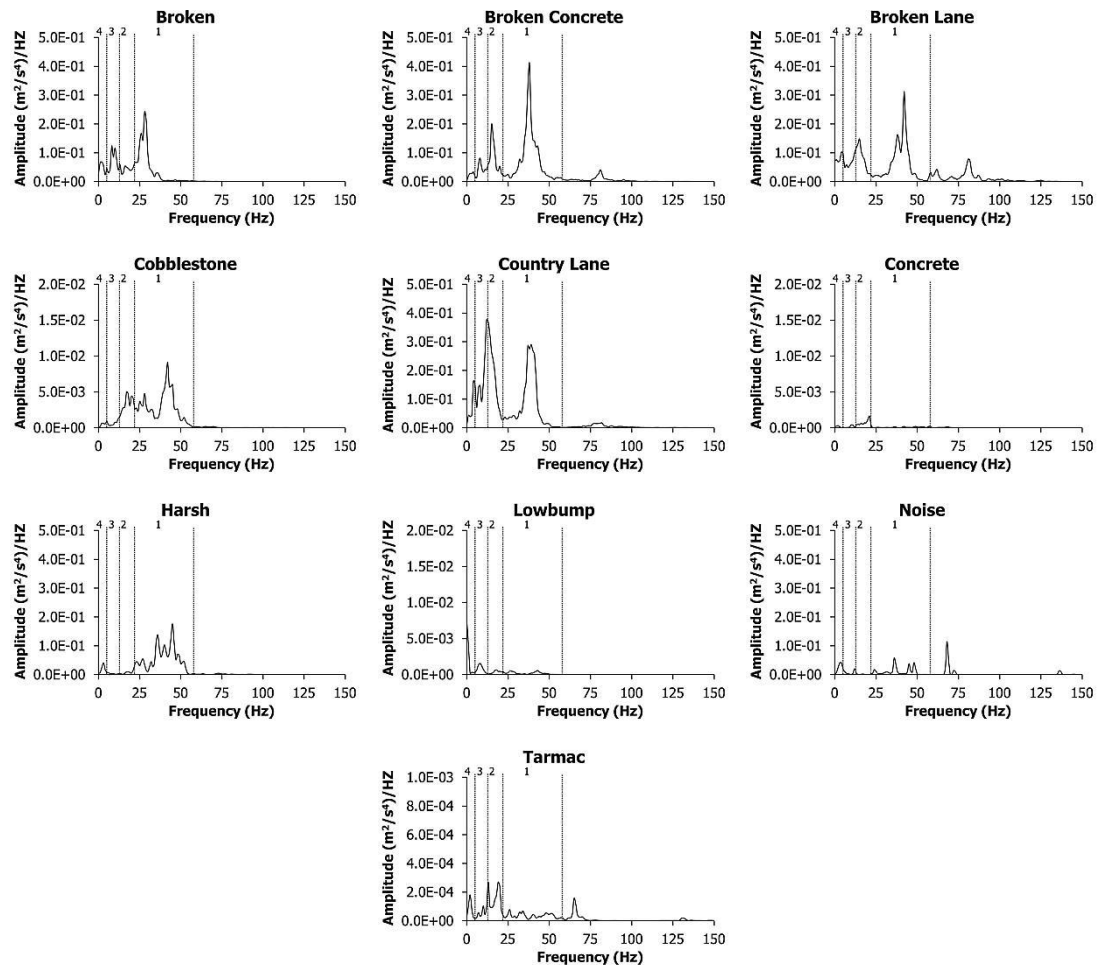


Figure 5.4 The vibration frequency-domain analysis of road surfaces by PSD

As can be observed in Figure 5.4, the results suggest that the principal frequency content is mostly in the range from 0 Hz to 80 Hz for all road surfaces. The highest peaks in the vibrational energy were found for the Broken Concrete surface, while the lowest peaks were found for the Tarmac surface. Moreover, the frequency distributions suggest that the higher peaks of energy correspond to the typical automobile resonance frequencies, which can be divided into four main regions (Pottinger *et al.*, 1986; Giacomini *et al.*, 1999; Hamilton, 2000; Kulkarni and Thyagarajan, 2001).

The first region of frequency distribution, which is from 20 Hz to 60 Hz, is mostly defined by higher frequency modes of the chassis and by tire resonances (Pottinger *et al.*, 1986; Giacomini *et al.*, 1999). Meanwhile, the vibration energy distributed in the range of 13 Hz and 20 Hz may reflect low frequency flexible body modes of the chassis.

This is followed by the regions which can be related to the behaviour of suspension units separately or with the rigid body motion of the engine/transmission unit distributed within 5 Hz and 13 Hz. Finally, the region between 0 Hz and 5 Hz is associated with the rigid body motion of the automobile chassis on the main suspension.

5.2.3 Evaluation Selection of Road Surfaces

At the beginning of this chapter (Section 5.2), the road surfaces to serve as laboratory test stimuli were stated, satisfying three logical conditions of selection criteria. Description of the road surfaces (in Section 5.3) explained that most of the road surfaces can be easily found around the UK, including both rural and urban areas. For instance, Cobblestone surface can be found in urban areas, and Country Lane in rural areas. Other than that, from Figure 5.2 (a) to (j), it can be seen that all the road surfaces were encountered with ordinary driving conditions, with both smooth surfaces, such as Tarmac, and damaged road, including Broken road, Broken Concrete and Broken Lane.

During the measurement of road surfaces by MIRA Group, the Michelin Group, and direct measurements by Berber-Solano (2008), it was found that the automobile test speeds were comparable and followed the prescribed speed limit of the Department of Transport (2006).

As presented in Table 5.2, most of the road surfaces were classified as mildly non-stationary signals, where the acceleration data were Gaussian distributed, with a kurtosis value close to 3.0 and a skewness value close to 0.00. These results were comparable with the study done by Giacomini *et al.* (2000), which showed that 65 % of the recorded road surface data around the UK were mildly nonstationary vibration data signals.

Moreover, the results suggested that the road surfaces differ significantly in terms of the *r.m.s.* and the VDV ($p = 0.01 < 0.05$). Therefore, the comparative scatter plotting of *r.m.s.* and VDV are illustrated in Figure 5.5 to identify the distribution pattern of the road surfaces.

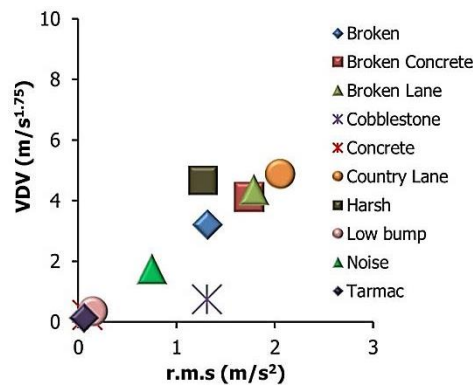


Figure 5.5 Distribution of *r.m.s* and VDV for all ten road surfaces

As can be seen in Figure 5.5, the distribution of the ten road surfaces suggested that the acceleration road surfaces may provide a wide statistical base of steering wheel magnitudes when compared to the vibration acceleration magnitude ranges from the previous research studies (Giacomin and Woo, 2004; Giacomin and Berber-Solano, 2005; Ajovalasit *et al.*, 2013; Berber-Solano *et al.*, 2013).

The studies of both Giacomin and Woo (2004), and Giacomin and Berber-Solano (2005) performed psychophysical laboratory experimental tests using steering wheel vibration stimuli with the acceleration magnitude range of 0.05 m/s^2 *r.m.s* to 0.27 m/s^2 *r.m.s*. Meanwhile, Ajovalasit *et al.* (2013) used the acceleration magnitude range of 0.06 m/s^2 *r.m.s* to 1.97 m/s^2 *r.m.s* to quantify the human responses towards the steering wheel vibration stimuli. The psychophysical laboratory experimental tests by Berber-Solano (2013) applied the steering wheel vibration stimuli with the acceleration magnitude range of 1.15 m/s^2 *r.m.s* to 2.36 m/s^2 *r.m.s*.

From the comparison of vibration acceleration magnitude ranges, the acceleration data from the road surfaces described in Section 5.2.1 can be considered a wide and representative operating envelope for use in laboratory-based experiments of automotive steering wheel vibration.

5.3 Laboratory Facilities

The laboratory facility used during this research for applying rotational vibration to seated test participants was the existing steering wheel simulator shown in Figure 5.6 (a), which was built in the Human Centred Design Lab, Brunel University. A schematic of the steering wheel simulator and the associated signal conditioning and data acquisition system is shown in Figure 5.6 (b).

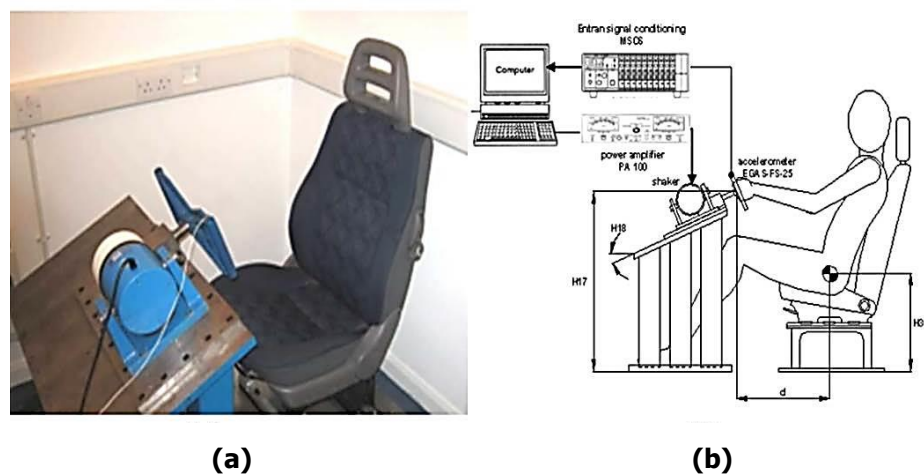


Figure 5.6 Facility used for laboratory tests, available at Human Centred Design Lab, Brunel University

The rotational system consisted of a 325 mm-diameter aluminium steering wheel attached to a steel shaft. The shaft was connected to the electro-dynamic shaker head by means of a copper stinger-rod. Rotational vibration was applied by means of a G&W V20 electro dynamic shaker driven by PA100 amplifier. The steering wheel tangential acceleration was measured by means of an Entran EGAS-FS-25 accelerometer attached to the top-left side of the wheel. The accelerometer signal was amplified by means of an Entran MSC6 signal conditioning unit. Control and data acquisition are performed using the Time Monitoring (T-MON) module of the LMS[®] CADA-X 3.5E software coupled with a DIFA SCADASIII unit (LMS International, 2002).

Table 5.3 details the main geometric dimensions of the steering simulator, which were based on the average data taken from a small European automobile, and the car seat was directly taken from a 1997 Fiat Punto.

Table 5.3 Geometric simulator parameters of the steering wheel rotational vibration

Geometric Parameter	Value
Steering column angle (H18)	23°
Steering wheel hub centre height above floor (H17)	710 mm
Steering wheel diameter (W9)	325 mm
Steering wheel tube diameter	25 mm
Horizontal distance from H point to steering wheel hub centre (d= L11-L51)	390-550 mm

The simulator has been designed to incorporate the maximum vibration limit levels felt every day by the participants in their cars. These features are to avoid and minimise the discomfort or pain felt by the participants. Apart from that, these features also allow participants to release their grip immediately from the steering simulator, whenever they feel discomfort or at any time they wish to do so during the test. In addition, the simulator also incorporates an emergency stop shutdown in case the excessive vibration limit is reached. These features are to avoid any harm to the participants. Furthermore, the car seat is fully adjustable, similar to those in actual cars, without any obstruction (e.g. no seat belts built-in), which permits the participants to get up and leave at any time. The safety features of the steering wheel simulator and the acceleration levels used conform to the health and safety recommendations outlined by British Standard 7085 (1989).

5.3.1 Accuracy of Signal Reproduction

The Oxford University Press (2013) defined accuracy as the degree of correctness of a measurement, for instance, the values produced are close to the true value of a measured quantity. In order to determine the accuracy of the steering wheel rotational vibration simulator when reproducing the test stimuli, hence an accuracy test needs to be performed.

5.3.1.1 Test Stimuli

All of the ten road surfaces base stimuli described in Section 5.2.1 were used as the target signals. The *r.m.s.* values of the target stimuli ranged from a minimum of $0.06 \text{ m/s}^2 \text{ r.m.s}$ to a maximum $2.05 \text{ m/s}^2 \text{ r.m.s}$ (see Table 5.2). Referring to the figure of PSDs presented in Figure 5.4, none of the steering wheel acceleration time histories contained significant vibrational energy at frequencies greater than 125 Hz. Therefore, the decision was taken to apply a bandpass digital Butterworth filter to limit the vibrational energy in the frequency range from 3 Hz to 125 Hz; the lower cut-off value of 3 Hz was chosen in recognition of the frequency response limitations of the electrodynamic shaker unit of the laboratory steering wheel rotational vibration simulator.

Pretesting discovered that both time history (Figure 5.7a) and Power Spectral Density (Figure 5.7c) of the reproduced stimuli did not match the target values, due to the frequency response of the shaker and the bench mechanical components. Compensated drive voltage signals were therefore applied, which included the effect of the frequency response of the shaker. The compensated drive signals were created by scaling the FFT amplitudes of the carrier and the sideband frequencies of the test signals, and by subsequently applying the inverse FFT to obtain the drive signal in the time-domain. The compensatory process was iterated so as to equalise the harmonic sidebands to the desired target values.

To illustrate the example of the compensator process, Figure 5.7 presents the Country Lane, which recorded the highest energy level among the ten road surfaces studied before and after applying the compensatory process.

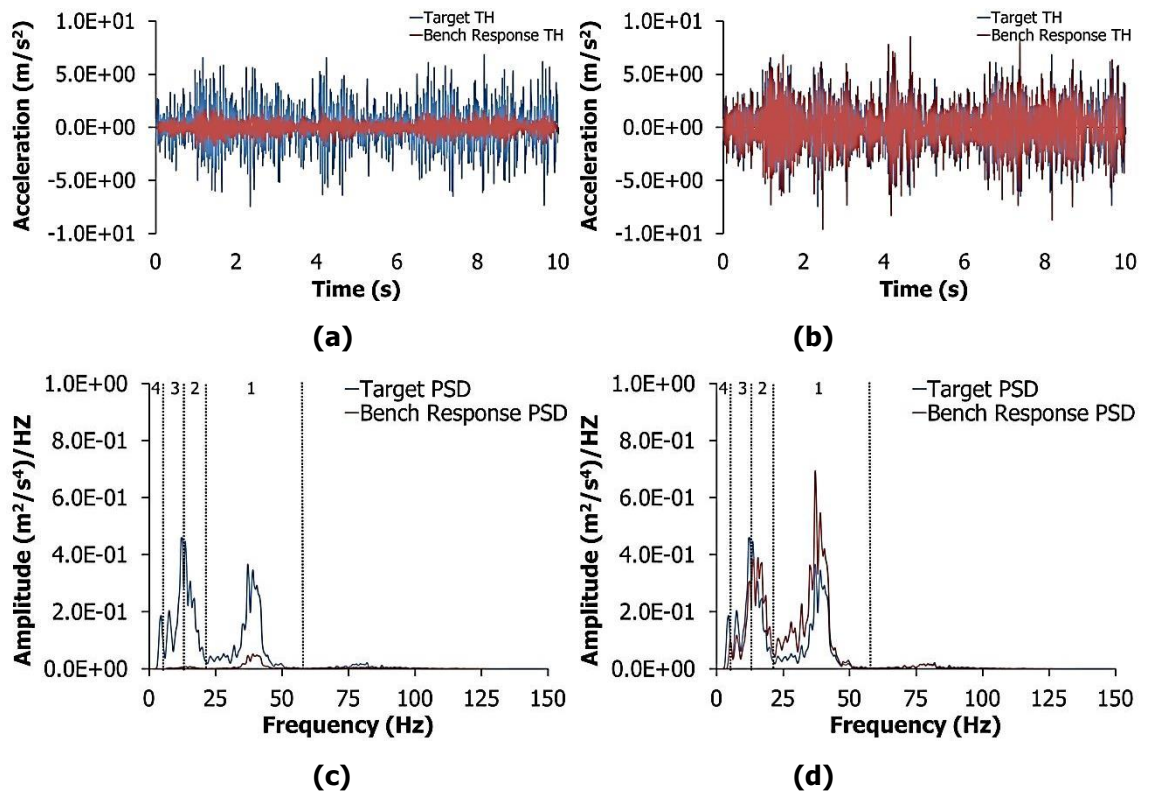


Figure 5.7 Comparison between target and bench response of time history and PSD before (a & c) and after (b & d) the compensation process.

5.3.1.2 Test Protocol

The test procedure evaluated the ensemble of the LMS software, the front end electronics unit, the shaker, the accelerometer and the signal conditioning units. The participant used in the accuracy signal reproduction so as to consider also the possible differences in bench response which are caused by differences in impedance loading on the steering wheel from people of different size. All participants were volunteers and they have the right to withdraw from the experiment at any time.

Before commencing testing, each of the participants was presented with a short questionnaire to gather information regarding their anthropometry, health and history of previous vibration exposures. Prior to the experiment, each participant was given instructions pertaining to the experimental method, as well as to the laboratory's health and safety procedures. They were required to remove any articles of heavy clothing such as coats as well as any watches or jewellery. They were then asked to adjust the

position of the seat and the angle of the backrest to simulate a driving posture that was as realistic as possible.

In the experiment, the participants were only asked to load their hands during the actuated acceleration stimulus transmitted to them. The maximum and minimum response *r.m.s.* acceleration values were obtained. The response *r.m.s.* values were then expressed as a percentage of the target *r.m.s.* value.

5.3.1.3 Test Participants

Seven participants, consisting of 3 males and 4 females, were used in the accuracy signal reproduction process. The physical characteristics of the test participants are summarised in Table 5.4.

Table 5.4 Physical characteristics of participants for accuracy signal reproduction

	Male (n=3)				Female (n=4)			
	Min	Max	Mean	SD	Min	Max	Mean	SD
Age (years)	22	41	31.67	9.50	20	35	27.25	7.85
Weight (kg)	80.20	95	86.73	7.55	62.30	74	67.33	5.02
Height (m)	1.69	1.77	1.74	0.04	1.55	1.66	1.61	0.06

It can be seen from the data in Table 5.4 that the mean values and standard deviations of the height and mass of the test participants were approximately at the 50th percentile value for the UK population (Pheasant and Haslegrave, 2005). Therefore, the degree of accuracy of the test signal reproduction is the maximum possible, caused by the impedance loading on the steering wheel from people of average size.

5.3.1.4 Result and Analysis

The accuracy of the target stimuli reproduction was quantified by measuring the *r.m.s.* difference between the actuated signal and the target signal, and the results are shown in Table 5.5. The value of each parameter is presented in two decimal places as suggested by rule of thumb of statistics in presenting the decimal places by Spatz (2008) for the accuracy of calculation results.

Table 5.5 Absolute maximum percent error of signal reproduction

Road Surfaces	<i>r.m.s.</i> (m/s ²)		
	Original Signal	Mean Bench Response	Absolute Maximum Percent Error (%)
Broken	1.32	1.31	0.76
Broken Concrete	1.73	1.74	0.58
Broken Lane	1.78	1.63	8.43
Cobblestone	0.31	0.36	16.13
Concrete	0.09	0.09	0.00
Country Lane	2.05	2.19	6.83
Harsh	1.26	1.17	7.14
Low Bump	0.14	0.12	14.29
Noise	0.75	0.68	9.33
Tarmac	0.06	0.05	16.67

The results of the signal reproduction of the bench response signal, shown in Table 5.5, varied between 1 % and 17 % with respect to their target signal value. The absolute maximum percent error is found comparable with the just-noticeable-difference value for human perception of hand-arm vibration of 15 % to 18 %, determined by Morioka (1998).

5.4 Conclusion

This chapter was divided into two sections. The first section presented all ten chosen road surfaces, namely Broken, Broken Concrete, Broken Lane, Cobblestone, Country Lane, Concrete, Harsh, Low Bump, Noise and Tarmac. Based on the vibration signal analysis of road surfaces both in the time-domain and frequency-domain, together with the comparison of vibration acceleration magnitude ranges from the previous studies, all ten road surfaces met the selection criterion to serve as laboratory test stimuli.

In the second section, the laboratory facilities of the Human Centred Design Lab, Brunel University were discussed. The safety features of the steering wheel simulator and the acceleration levels used conform to the health and safety recommendations outlined by British Standard 7085 (1989), and the accuracy of signal reproductions was comparable with the just-noticeable-difference value for human perception of hand-arm vibration, hence, the facilities were appropriate for use in this research.

In the next chapter, the critical review of principles in identifying the transient vibrations from various areas of study will be presents. The main objective is to ensure that the principle use in the current research in order to identify the transient vibrations contained in road surfaces data signals is the best principle.

CHAPTER 6

PRINCIPLES OF TRANSIENT VIBRATIONS ROAD SURFACE DETECTION

6.1 Introduction

In signal processing, the transient signal is generally defined as a signal whose duration is short compared to the observation interval. Transients can be either deterministic or random, and in the latter case they are nonstationary (Friedlander and Porat, 1989). The transient detection analysis is considered highly useful in different areas of study, such as in early earthquake detection in the seismology field, cardiac disease diagnosis in the biomedical field, defects detection in the machinery field, and fatigue analysis as well as human comfort analysis in the automotive field.

The purpose of this chapter is to explore the potential alternatives for identifying the transient vibrations contained in road surfaces data signals. The chapter begins with the current Mildly Nonstationary Mission Synthesis (MNMS) algorithm used for identification of transient vibrations in road surfaces. We provide an overview of the MNMS algorithm and the limitations in identification of transient vibrations processes. This is followed by a selective and critical review of alternative principles in identifying the transient vibrations from various areas of study. Before the final remarks are presented at the end of this chapter, the potential principle, based on the critical review, is applied to all of the ten road surfaces base stimuli described in previous Chapter 5.

6.2 MNMS Algorithm for Road Surfaces Transient Vibrations

The Mildly Nonstationary Mission Synthesis (MNMS) algorithm developed by Giacomini *et al.* (2000) is a method of summarising mildly nonstationary vibration records to obtain short mission signals that can be used for experimental or numerical testing purposes.

The MNMS algorithm is based on well-known signal processing algorithms and the use of simple peak correcting. The signal processing algorithms used are the Discrete Fourier Transform (DFT), the Orthogonal Wavelet Transform (OWT) and correlation functions.

The MNMS algorithm consists of three processing stages, which begin with the application of the Discrete Fourier Transform, which is widely used in digital random controllers for shakers and similar test benches (Vandeurzen *et al.*, 1988). In the signal processing, the DFT known as a mathematical technique to decompose a signal into sinusoidal components of various frequencies ranging from 0 frequency up to the maximum frequency of sampling rate (Sinha, 2012). The DFT was applied to the road surfaces data to determine the overall Power Spectral Density function, and, next, the results of spectral function were used to contrast a short artificial basis signal. This approach guarantees that the short test signal precisely reproduces the PSD of road surfaces data prescribed (Giacomini *et al.*, 2000).

In the second stage of the MNMS algorithm, the process starts with the application of Orthogonal Wavelet Transform to the road data, followed by grouping of wavelet level into a small number of filter banks, which subdivide the vibrational energy. The mildly non-stationary mission synthesis algorithm splits an original signal into wavelet levels (Chui, 1992; Daubechies, 1992). The OWT used when the wavelet form a set of orthonormal functions (Burrus *et al.*, 1998). Twelfth order Daubechies wavelets have been used in the analysis performed to date (Giacomini *et al.*, 2000) because of its successful application in several previous studies involving automotive road data (Abdullah *et al.*, 2006). Wavelet levels consist of time histories which are obtained from the wavelet decomposition, and contain the signal energy which is specific to a particular frequency band. MNMS uses the orthogonal wavelet transform to divide the

overall energy into individual signals, in a manner analogous to a parallel bank of band-pass filters. A feature which is specific to MNMS is a wavelet grouping stage which permits the user to group individual wavelet levels into larger regions of significant energy.

Stage 3 of the MNMS algorithm consists of two processes. Firstly, the transient vibrations for each wavelet group in both the original road data and the synthetic Fourier signal is counted. The wavelet group of the road surfaces data is analysed separately to locate and count all transient vibrations.

For the purpose of the MNMS, transient vibrations are defined as high amplitude transient which can cause the overall time history to deviate from a stationary Gaussian model. Formally, a point is considered a transient vibrations if the road data signal is at a local maximum or minimum, and the wavelet group time history exceeds the trigger level prescribed (for each wavelet group) by the user in terms of standard deviations. Experience suggests that wavelet group trigger levels at 3.5 standard deviations have been found to produce accurate vibration missions for most road data signals analysed to date (Giacomin *et al.*, 2000). Once an event is identified which exceeds the trigger level, the time duration of the transient vibrations is determined, as shown in Figure 6.1.

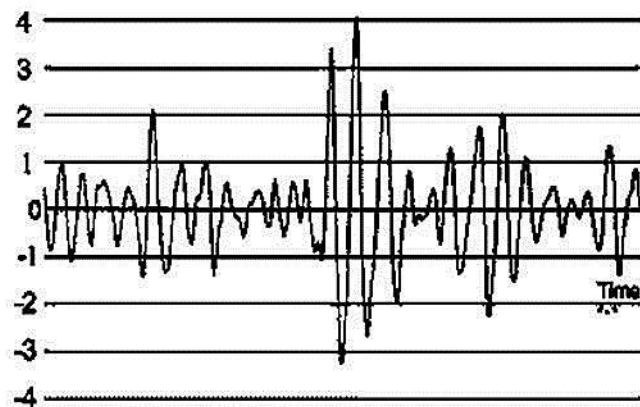


Figure 6.1 Possible trigger level values of the transient vibration
(Source: Giacomin and Berber-Solano, 2006)

To determine the time extent of individual transient vibrations, it is assumed that the event represents the system response to a single isolated impulse. The algorithm checks the monotonic decay envelope of the signal on either side of the peak value and

identifies the points where the signal amplitude begins, again, to increase. The inversion points at which the monotonic decay process ends are taken to signal the time duration of the transient vibrations. The transient start and end points are then taken to be a fixed distance (in data points) from the points of envelope inversion, as shown in Figure 6.2.

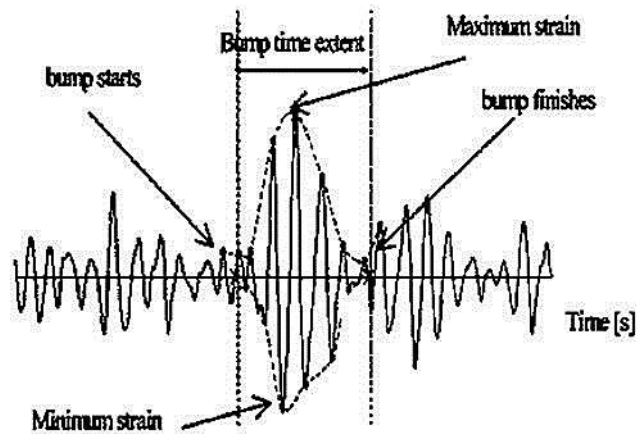


Figure 6.2 Decay envelope of the transient vibrations

(Source: Giacomini and Berber-Solano, 2006)

The second process in stage 3 is peak correction of the artificial basis signal to introduce necessary transient vibrations. If all transient vibrations extracted from long road data records were introduced into the short mission signal, the correction would be excessive, and the final mission signal would deviate from the original data in several statistics. Therefore, it was decided to introduce a number of transient vibrations, selected to be in direct proportion to the signal compression ratio.

During the process of transient vibrations counting, a ranking based on the size of the maximum peak value is performed for the events found in the particular wavelet group of the original road data. All identified transients are ranked in descending order according to their peak value. Having ranked all transient vibrations, and having specified a compression ratio of n , transient vibrations are selected by moving down the ranking list with a step equal to n . In order to reduce the impact of bump correction on the PSD of the synthetic Fourier basis signal, each selected transient vibrations are introduced at a location in time where the synthetic signal most closely resembles the bump event. This location is determined by means of a correlation procedure in which the transient vibrations are moved along the whole time history of the synthetic signal and compared with it in terms of *r.m.s.* difference at each position.

When all required transient vibrations are introduced, the synthetic Fourier signal can be considered to be upgraded to mission signal status, and the total sum of all wavelet group time histories produces the final mission signal. The final output mission signals replicate the fundamental vibration characteristics of the input signal in terms of the fundamental global signal statistics such as *r.m.s.*, skewness, kurtosis, crest factor and the power spectral density.

6.2.1 Evaluation of the MNMS Algorithm for Transient Vibrations

Apart from acting as a compression tool to produce a shortened stimuli sequence, the purpose of the MNMS algorithm was to aid engineers in defining vibration mission signals for vehicle components, such as comfort testing of automotive seats (Giacomin *et al.*, 2000).

The proliferation of the MNMS algorithm can be found in the studied to facilitate driver-road detection (Berber-Solano *et al.*, 2010). The outcome from the study was to provide the guideline for the optimisation of the steering wheel acceleration signal, which was unfortunately not universally optimal to all road surface types. Apart from the lack of acoustical stimuli in a laboratory task, the process of transient vibrations identification and extraction from road data signals is also suspected to be a contributing factor leading to the results.

As this MNMS algorithm has, to date, been used for road surfaces signals, the technique of transient vibrations identification and extraction in road surfaces data signals based on the MNMS algorithm needs to be evaluated. The main purpose of evaluation is to ensure that the classification of transient vibrations in this current research can be performed without any doubt – for instance, to ensure that the shape of the transient vibrations identified and extracted fulfils the definition and criteria of transient vibrations stated by the MNMS algorithm.

The Lowbump road surface data signal has been applied with MNMS for the purpose of transient vibrations identification and extraction evaluation. The MNMS algorithm is currently written in MATLAB R2014a software, and runs on Windows-compatible PCs.

Using the MNMS algorithm, the Lowbump road surface data signal was decomposed into 12 wavelet levels in the frequency range from 0 to 60 Hz, which were grouped according to the natural frequency energy distribution of the signal into four wavelet groups (see Figure 5.4). Next, the transient vibrations are identified and extracted within the target frequency interval of 20 to 60 Hz, as the frequency range plays a key role in human cognitive detection of the road surface type and signal threshold trigger level value of 2.6 (Berber-Solano *et al.*, 2010). Figure 6.3 (a) to (c) presents examples of the results for transient vibrations in the Lowbump road surface data signal that have been identified and extracted together with the details of the criteria.

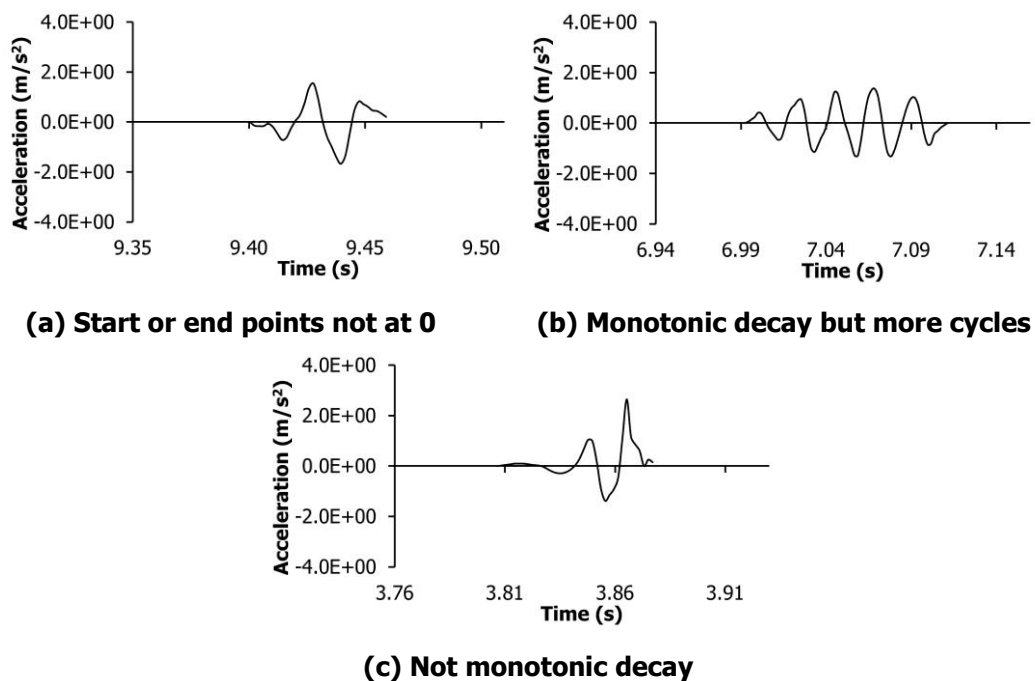


Figure 6.3 Transient vibrations of Lowbump identified and extracted within the target frequency interval of 20 to 60 Hz

As shown in Figure 6.3, the transient vibrations identified and extracted did not fulfil the definition and criteria of transient vibrations stated by the MNMS algorithm. This result may cause conflict in the current research, which is the classification of transient vibrations of road surfaces data signals.

The following section presents the possible potential or alternative principles that can provide the better results in identify the transient vibrations steering wheel road surface. To investigate the possibilities, hence the literature review survey was conducted.

6.3 Towards Better Principles of Transient Vibrations Road Surface

In this section, the possible processes to identify the transient vibrations to be applied in the steering wheel vibration road surfaces data signals will be described. In conjunction with that, the literature survey has been conducted, which focused on the description of the principles. Prior to the literature survey, the criteria of selection for alternative principles of transient vibrations detection are first predetermined in order to ensure that the survey can be easily manageable. Apart from that, the search criteria were also very important to ensure that the alternative algorithm was compatible with the transient vibrations of road data signals, and can also provide better results in identifying the transient vibrations of road surfaces data signals. The alternative principles of transient vibrations are determined by applying two criteria.

The main search criterion chosen was the nature of transient vibrations in signal processing. The transient vibrations of road surfaces data signals are defined as high amplitude transient vibrations which can cause the overall time history to deviate from a stationary Gaussian model, which exceeds a prescribed trigger level. Other than that, the transient vibrations in the road surfaces data signals were assumed to occur repeatedly, corresponding to the vehicle moving over irregular road surfaces until arriving at the destination. Therefore, the nature of transient vibrations in signal processing must be that of transient vibrations which deviate from the normal background and also need to be repetitive events.

The second search criterion was the principles of transient vibrations detection. In the MNMS algorithm, the principle of wavelet transform has been used to identify the transient vibrations of road surfaces data signals, and the results did not really fulfil the definition and criteria of transient vibrations. For that reason, during the literature survey, an alternative principle of wavelet transform was found in order to gather better results in identifying the transient vibrations of road surfaces data signals. However, although the principles were not directly applied to the transient vibrations of road surfaces data signals, the principles may be useful in both the processing and post-processing stages of the transient vibrations of road surfaces data signals.

6.3.1 Criterion 1: Nature of Transient Vibrations

Firstly, the literature survey started with a search using the first criterion, resulting in the discovery of a total of 23 pieces of literature, consisting of 6 pieces from biomedical studies, 9 pieces from machinery and 5 pieces from seismology studies. The remaining pieces were from radar echo studies (2 pieces) and a fatigue automotive study.

In the 1980s to 2010s, the analysis of transient vibrations to detect large earthquakes proved effective in estimating the expected amount of ground shaking (Nakamura, 1988; Bouchon *et al.*, 2001; Botella, 2003; Horiuchi *et al.*, 2005; Satriano *et al.*, 2011). Moreover, the value of social wellbeing was also improved by decreasing the number of deaths, injuries and level of economic loss, as well as preventing the construction from collapsing as a result of the earthquake.

In the 1980s to 1990s, the studies on QRS shape detection in Electrocardiogram (ECG) waveforms show that detection was important to diagnose cardiac disease, and also represents the different heart functions (Chu and Delp, 1989; Trahanias, 1993; Li *et al.*, 1995; Köhler *et al.*, 2002; Raphisak *et al.*, 2004; Song *et al.*, 2010)

In the 1990s to 2000s, the application of transients detection analysis in ultrasonic flaw detection was used, whereby the analysis was performed by isolating the flaw echo from noise background and estimating the exact location of the flaw. Laterally, ultrasonic flaw detection assures the quality of materials non-destructively (Saniie and Mohamed, 1994; Hu *et al.*, 2006; Song and Que, 2006).

In the 2000s, inrush current detection in transformers had proven to have great practical importance to operators, as it permits the scheduled shutdown and repair of a system, as well as monitoring the life cycles of machines to avoid faulty replacement of components (Jiang *et al.*, 2000; Zhang *et al.*, 2002; Cheng *et al.*, 2004, Sedighi and Haghifam, 2005; Jing *et al.*, 2006; Wu *et al.*, 2013a; 2013b).

In the 2000s, radar detection within the underwater acoustic was performed and proved that detection strengthens coastal security, improves navigational safety and helps in

environmental monitoring (Davidson and Griffiths, 2002; Panagopoulos and Soraghan, 2004).

Again, in the 2000s, the analysis of transient detection spread widely in automotive study fields regarding fatigue damage in variable amplitude ground vehicles (S. Abdullah *et al.*, 2006). As one of the key stages in the design of vehicle structure, the analysis proved that manufacturers can produce better components in the vehicle. While, for the purpose of NVH testing or for human comfort, the detection of transient analysis led to the algorithm development of the Mildly Nonstationary Mission Synthesis (MNMS).

All the 23 literatures were weighted first by the nature of transient vibrations occurring in the particular study areas. As stated previously, the transient vibrations of road surfaces data signals were assumed to be occurring repeatedly, hence, the studies of early earthquake and inrush current detection were eliminated, as the possible alternative of nature was to be considered. Even though early earthquake detection provides very important information to people and several previous studies suggested an algorithm for detection of the events that was very comprehensive, unfortunately the nature of the early earthquake detection was not the same as bump events detection, because the *P*-wave only happened once within a period of time before the real wave came, the *S*-wave. Meanwhile, inrush currents are instantaneous input currents drawn by an electrical device when first turned on.

After the elimination of two areas of study which do not satisfy the first criterion, the remaining areas of study, such as biomedical, radar echo and fatigue studies, are considered further in terms of the next criterion in the process of searching for better principles of transient vibrations steering wheel road surface.

6.3.2 Criterion 2: Measurement of Transient Vibrations

The remaining 9 literature surveys considered in this second criterion suggested two different principles, namely wavelet transform and mathematical morphology. As in the MNMS algorithm, the principle of wavelet transform has been used to identify the

transient vibrations of road surfaces data signals, and the results did not really fulfil the definition and criteria of transient vibrations, hence, the wavelet transform was omitted and mathematical morphology will be further explored.

Mathematical morphology is widely used in studies by Chu and Delp (1989), Trahanias (1993), Saniie and Mohamed (1994), Zhang *et al.* (2002), Panagopoulos and Soraghan (2004), Jing *et al.* (2006) and Wu *et al.* (2013a; 2013b). Wu *et al.* (2013a; 2013b) used mathematical morphology because the application of the technique involved the processes of the shape of a signal waveform in the time-domain, which means it can avoid the influence of phase shifting and amplitude decaying. Besides using a much shorter data window for calculation, mathematical morphology seems a more appropriate technique with better performance in treating sudden changes and the transient process compared with the wavelet transform (Zhang *et al.*, 2002; Jing *et al.*, 2006). In addition, morphology filters have better performance because of their flexibility in changing the shape of the structuring elements to preserve certain patterns of the original signal (Saniie and Mohamed, 1994). Provided with the wider use of mathematical morphology and the advantages offered in transient detection analysis, this technique has been chosen to be studied in depth, in order to assess how this technique can contribute to solving the current problem of transient vibrations road surfaces data signals.

6.3.3 Mathematical Morphology for Transient Vibrations

Mathematical morphology (MM) is a set of nonlinear signal transformation tools that transform the shape of signals, which is based on set operation signals of dilation and erosion as fundamental operators, as shown in Figure 6.4(c) and Figure 6.4(d), respectively, and was originally introduced by Matheron and Serra in the late 1970s (Panagopoulos and Soraghan, 2004).

Mathematical morphology has been used in the field of image processing, and is known for its robust performance in preserving the shape of a signal (Chu and Delp, 1989) while rejecting the white noise and pulse noise. In another words, MM filters unwanted

shapes of the signal while leaving the other parts of the signal unchanged (Raphisak *et al.*, 2004).

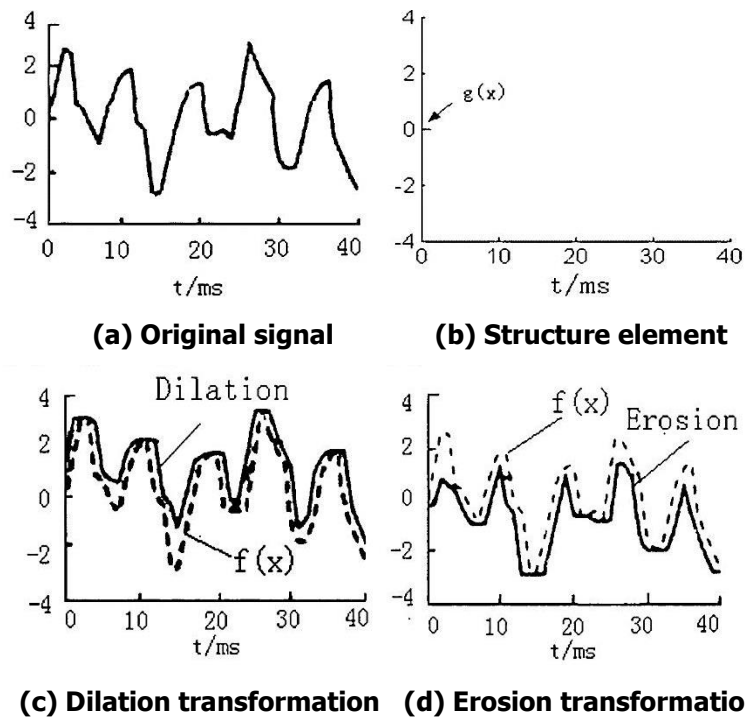


Figure 6.4 Morphological approach to signals using a flat structuring element

(Source: Jing *et al.*, 2006)

The concepts of dilation and erosion in mathematical morphology are the expansion and shrinking of a particular shape into another shape (Jing *et al.*, 2006); therefore, this technique was chosen to solve the problems of start and end points for transient vibrations which were not at zero (see Figure 6.3a). The hypothesis was that by using the dilation and erosion concepts in mathematical morphology, both the start and end points of each transient vibration can be closer to zero.

The morphology filter program was written in MATLAB R2014a software by referring to the concept diagram suggested by Raphisak *et al.* (2004), as shown in Figure 6.5 below. The concept used the derivation operation of erosion and dilation, namely opening and closing (Saniie and Mohamed 1994). Opening is defined as erosion followed by dilation, while closing is vice versa. In most applications, opening is used to suppress peaks, while closing is used to suppress pits (Chu and Delp, 1989).

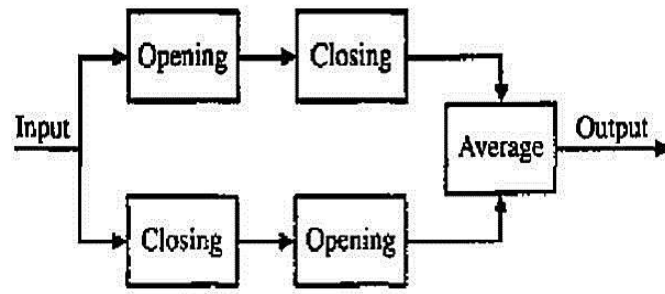


Figure 6.5 Diagram of morphological filter (Raphisak *et al.*, 2004)

Apart from dilation and erosion, Structure Element (SE) is also a key element in mathematical morphology (Panagopoulos and Soraghan, 2004), which will interact with the signal and extract information (Chu and Delp, 1989; Saniie and Mohamed, 1994). Mathematical morphology is a time-domain tool and does not quantify the frequency content of a signal (Gautam and Brahma, 2012), hence, the structuring element interacts with the signal under study and transforms it into a new signal, which is, in some way, more expressive than the original. Other than that, SE also acts as a lowpass filter; therefore, the effects of the width of flat structuring elements can influence the results of the shapes (Saniie and Mohamed, 1994).

To identify the optimal width of flat structuring elements that can be compatible for all ten road surface data signals used in this research, the random suggested values of the width of flat structuring elements from 1 to 10 were tested as the number is the best values to preserve the original shape without severe distortion (Saniie and Mohamed, 1994). Figure 6.6 presents the post-processed transient vibrations results using flat structuring elements with different widths.

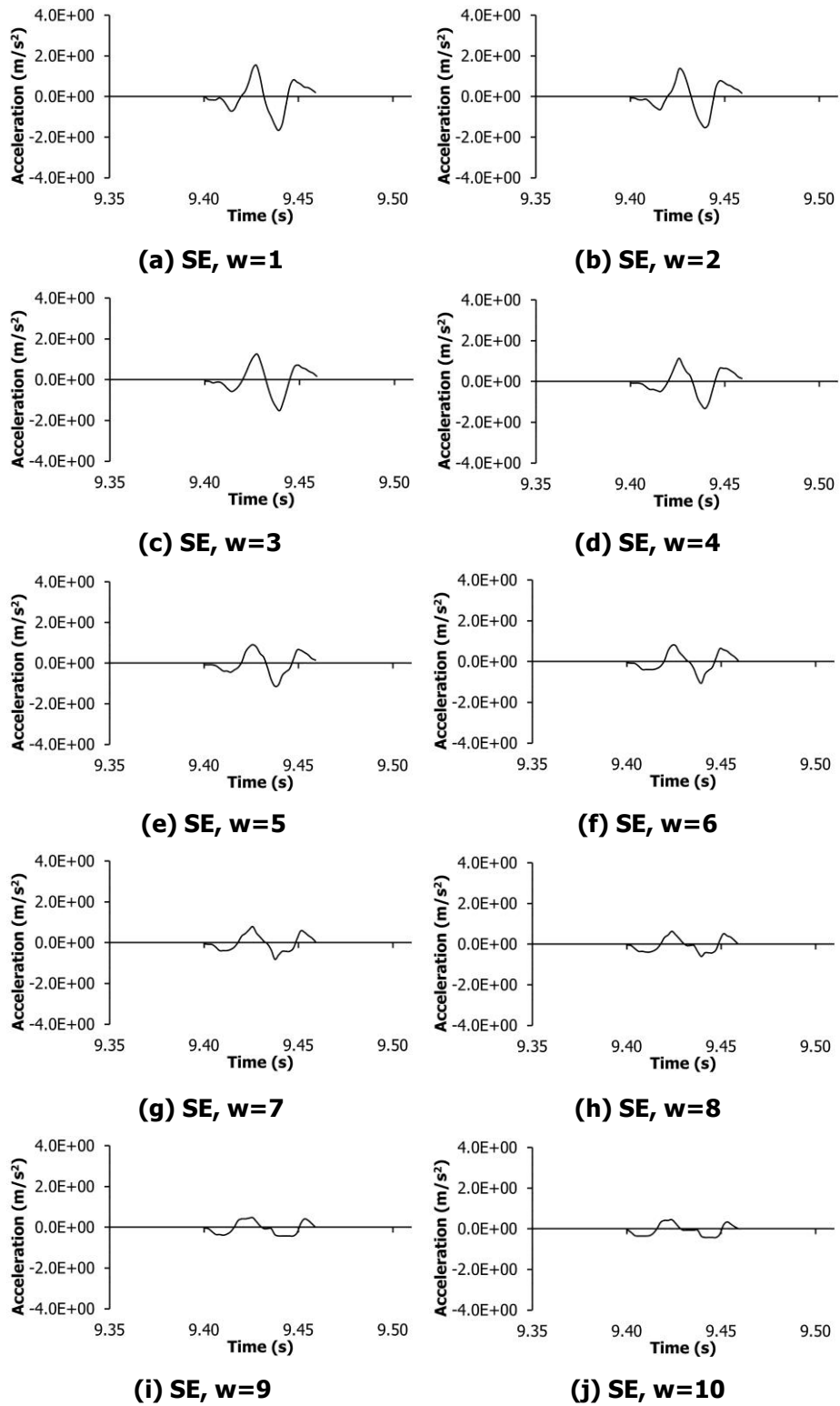


Figure 6.6 Post-processed transient vibrations results using flat structuring elements with different widths

As shown in Figure 6.6, the start and end points for the transient vibrations were close to the zero, as the width of structure elements is larger, however the transient vibrations become smaller and the original shape was missing. From the post-processed results, it

is suggests that the width of flat structuring elements can influence the results of the transient vibrations shapes.

6.3.4 Discussion

In the test of mathematical morphology for road surfaces transient vibrations detection it was shown that the shapes of transient vibrations were missing, as the width of flat structuring elements becomes bigger. Moreover, the post-processed results displayed how the start and end points for transient vibrations did not show any changes, which suggested that the mathematical morphology operation of dilation and erosion did not solve the problems of expanding and shrinking both the start and end points of bump events closer to zero.

This result may be explained by the fact that the mathematical morphology operation provides techniques that can potentially be used to suppress noise, and therefore the increasing value of width of structuring elements can possibly suppress noise excessively, which laterally removes the important information contained in transient vibrations (Chu and Delp, 1989; Trahanias, 1993). Other than that, the performance of the mathematical morphology is dependent on three factors, which are amount of noise, choice of structuring elements, and sampling rate of the signal (Panagopoulos and Soraghan, 2004).

6.4 Conclusion

The main goal of the current chapter was to determine alternative opportunities to identify and extract the transient vibrations steering wheel road surface. As shown in Figure 6.3, the transient vibrations identified and extracted did not really fulfil the definition and criteria of transient vibrations stated in the MNMS algorithm. Furthermore, the results shown in Figure 6.3 may also present conflict with the next step, which is classification based on the similarity of information content in transient vibrations steering wheel road surface.

To address the issue, the literature review survey, related to the principle of transient vibrations detection, was conducted to gather better results in identifying the transient vibrations steering wheel road surface. The survey on transient vibrations detection analysis included various areas of study, such as seismology studies, biomedical studies and also machinery studies. The alternative principle was measured based on two selection criteria. Firstly, the nature of transient vibrations in signal processing must be the transient vibrations that deviate from the normal background, and also need to be repetitive events before an alternative technique can be found.

Results from the literature review survey suggested that mathematical morphology can be used as an alternative technique to identify and measure the transient vibrations steering wheel road surface. The technique has been used as a post-processing technique to solve the problems of transient vibrations, whereby the start and end points were not at zero. The different widths of structuring elements in mathematical morphology were tested on transient vibrations, but unfortunately the results showed that mathematical morphology does not solve the current problems, and the decision was made to proceed with the MNMS algorithm in identifying the transient vibrations of road surfaces data signals.

The next chapter will present the first study in this research, in which the aim is to perform validation of previous guidelines related to the frequency bandwidth of steering wheel vibration feedback to driver road surface detection.

CHAPTER 7

VIBRATION ENERGY DISTRIBUTION ON DRIVER ROAD SURFACE DETECTION

7.1 Introduction

In 2013, Berber-Solano *et al.* identified drivers' detection of road surface types. They measured the sensitivity of this detection by eliminating regions of vibrational energy from the original power spectral density of the steering wheel acceleration signal. In their experiment, the power spectral density analysis of time histories suggested the presence of five important frequency bands within 0 Hz to 150 Hz, which were characterised by their significant vibrational energy. They hypothesised that eliminating the energy from any of the five regions might cause driver detection of the road surface type to be more difficult, due to the elimination of vital vibrational cues. Therefore, in order to test this hypothesis, each time history was manipulated so as to eliminate, in turn, each of the five frequency bands (0 Hz – 6 Hz, 6 Hz – 13 Hz, 13 Hz – 27 Hz, 27 Hz – 60 Hz, 60 Hz – 150 Hz).

An ensemble composed of both the original and modified steering wheel acceleration stimuli was used to perform detection of road surface type via a laboratory-based experiment. The participants' task was to detect the road surface type by considering whether the stimulus transmitted by the steering test bench originated from the road surface that was displayed in front of them by means of a large photograph on a board. The confidence of the detection was indicated by the participants using a binary response procedure of 'yes' or 'no'.

The results of Berber-Solano *et al.*'s study (2013) suggested that the elimination of vibrational energy in the frequency band of 20 Hz to 60 Hz was highly detrimental to the task of detecting road surface types. This in turn suggested that this specific frequency range has a significant impact on the steering wheel feel and on the drivers' situation awareness.

However, the frequency band suggested was too large, as in automotive terms the frequency range of 20 Hz to 60 Hz is known to contain the resonance behaviours of numerous chassis and steering systems (Giacomin *et al.*, 2000). Moreover, during driving, steering wheel power spectral densities can reach up to 350 Hz, with vibrational energy mostly present in the range between 10 Hz and 60 Hz (Fujikawi, 1998). This is typically characterised by low-frequency excitation in the range of 8 Hz to 20 Hz, due to first-order tyre non-uniformity forces and tyre-wheel unbalance, and due to second-order engine and mechanical imbalance in the frequency range between 20 Hz and 200 Hz (Ajovalasit and Giacomin, 2003).

Furthermore, the alternative procedure in which detection is indicated using a continuum, rather than a binary response procedure, might prove beneficial. It may improve the detection accuracy and resolution because there is no absolute judgement when it comes to human responses because all responses are based on an individual's restricted opinions and past experiences (Laming, 2003). Additionally, individuals tend to have a preference for giving feedback in greater detail than a binary response in order to measure the quality of human judgement (Gescheider *et al.*, 1971; Green and Swets, 1966).

The primary objective of the study, as described in this chapter, was to identify a more specific frequency band (within 20 Hz to 60 Hz) that contains the most vibrational energy that corresponds closely to steering wheel feedback. This was done by measuring the effect of vibrational energy distribution (within 20 Hz to 60 Hz) on the human cognitive detection of road surface types based on steering wheel vibration. The secondary objective was to measure the quality and accuracy of the detection results when adopting a more fine-grained and continuum-based procedure, as it was hypothesised that this can improve the quality of data gathered as well as yield better statistical results. In addition, this study is also an exposure exercise for the researcher

due to the lack of information in this field; it was considered important to perform a check and validation of the previous results.

7.2 Test Stimuli

All of the ten road surface base stimuli described in Section 5.2.1 were used as test stimuli whereby four different frequency bands within 20 Hz to 60 Hz were eliminated. The selection of the bands to be eliminated was based on the estimated locations of the higher peaks of vibrational energy, which is mostly defined by higher frequency modes of the chassis and by tyre resonances (Pottinger *et al.*, 1986; Giacomini *et al.*, 1999). The assumption was made that the elimination of information from one of the most important subsystems might limit the driver as it would deprive him/her of an important source of information about the road surfaces (Berber-Solano *et al.*, 2013).

The calculation steps to identify which frequency bands to eliminate within the range of 20 Hz to 60 Hz were adopted from the studies by Bau *et al.* (2010). In the study performed by Bau *et al.* (2010), the participants were requested to identify test stimuli that were different to the two identical reference stimuli. Five reference frequencies equally spaced on a logarithmic scale (80, 120, 180, 270, and 400 Hz) were selected, and their magnitudes were adjusted to equal intensities (approximately 15 dB above the threshold). Bau *et al.* (2010) used the Weber fraction to differentiate the test stimuli from the frequency of the reference stimuli, as shown below:

$$JNDF = \frac{\Delta f}{f} \quad (7.1)$$

Further, Morioka and Griffin (2000) suggested that vibration intensity needs to be reduced by at least 10 per cent for the changes to be detected by a person; hence Equation 7.1 can be simplified to:

$$JNDF = \frac{f_{n+1}-f_n}{0.1f_n}, n = 1,2,3,4 \quad (7.2)$$

Where n is the total number of the frequency bands that were eliminated. Since $f_1 = 20$ and $f_4 = 60$, by simplifying Equation 7.2, the value for the frequency bands interval was found as a logarithmic scale of 3.1610. After all values were substituted, the general formula to determine the frequency band intervals was identified as follows:

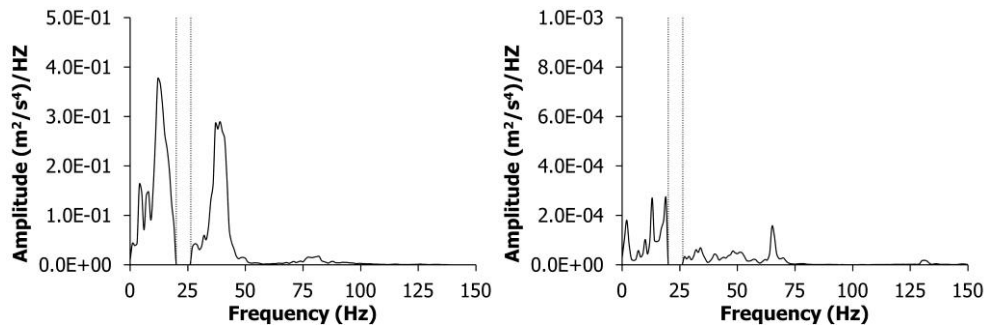
$$JNDF = 20(1.31610)^{n-1}, n = 1,2,3,4 \quad (7.3)$$

Therefore, from Equation 7.3, the frequency bands to be eliminated were 20 to 26.32 Hz, 26.32 to 34.64 Hz, 34.64 to 45.59 Hz and 45.59 to 60 Hz. The elimination process for each of the frequency bands successfully applied high-pass filters and band-pass filters by means of digital Butterworth filters, which were constructed in the LMS[®] TMON software (LMS TMON, 2002).

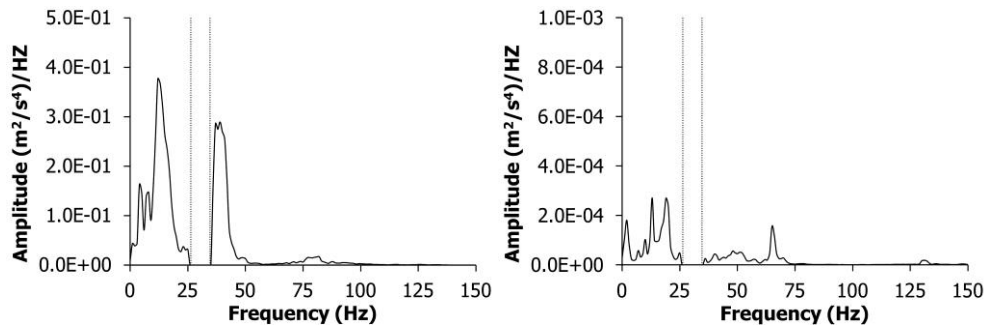
As described in Table 5.1, the *r.m.s.* acceleration value (m/s^2) was quantified to show the strength of the energy content in a signal. Therefore, the *r.m.s.* values for each of the ten test stimuli obtained after the elimination of the chosen frequency bands are shown in Table 7.1. Further, Figure 7.1 presents an example of the power spectral density (PSD) data of the manipulated high-pass filter and band-pass filter for Country Lane and Tarmac, which recorded the highest and the lowest energy levels among the ten road surface studied, respectively.

Table 7.1 The *r.m.s.* values (m/s^2) for original and manipulated Butterworth filters used to produce the laboratory test stimuli

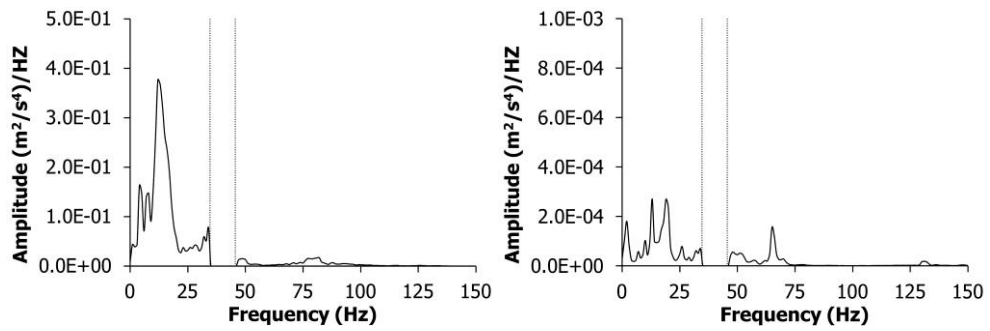
Road Surfaces	<i>r.m.s.</i> (m/s^2)				
	Original	First band eliminated (20 Hz – 26.32 Hz)	Second band eliminated (26.32 Hz – 34.64 Hz)	Third band eliminated (34.64 Hz – 45.59 Hz)	Fourth band eliminated (45.59 Hz – 60 Hz)
Broken	1.32	1.11	1.02	1.23	1.24
Broken Concrete	1.73	1.68	1.60	1.25	1.66
Broken Lane	1.78	1.69	1.67	1.37	1.67
Cobblestone	0.31	0.29	0.28	0.24	0.29
Concrete	0.09	0.08	0.09	0.09	0.08
Country Lane	2.05	1.98	1.96	1.67	2.00
Harsh	1.26	1.18	1.15	0.89	1.10
Low Bump	0.14	0.10	0.10	0.10	0.10
Noise	0.75	0.68	0.67	0.61	0.65
Tarmac	0.06	0.05	0.05	0.05	0.05



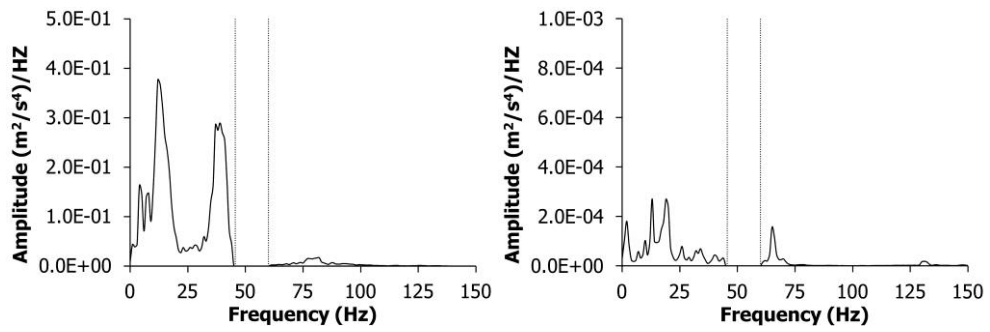
(a) Eliminated PSD within 20 Hz – 26.32 Hz



(b) Eliminated PSD within 26.32 Hz – 34.64 Hz



(c) Eliminated PSD within 34.64 Hz – 45.59 Hz



(d) Eliminated PSD within 45.59 Hz – 60 Hz

Figure 7.1 Example of original and manipulated Butterworth filter of Country Lane (left) and Tarmac (right) road surfaces used in the laboratory test stimuli

7.3 Test Protocol

Following an email invitation sent to the students' general mailing list of the College of Engineering, Design and Physical Sciences, Brunel University, London, the potential participants were approached by the researcher. Each potential participant was given an information sheet and a consent form describing the purpose, procedures, risks and time commitment entailed in their participation. Next, an appointment was made to carry out the experiment with those who declared an interest in participating, and who met the primary requirements of the study (details described in Section 7.4). All participants were volunteers and they have the right to withdraw from the experiment at any time.

Upon their arrival at the laboratory, each of the participants was presented with a short questionnaire to gather information regarding their anthropometry, health and history of previous vibration exposures. Prior to the experiment, each participant was given instructions pertaining to the experimental method, as well as to the laboratory's health and safety procedures. They were required to remove any articles of heavy clothing such as coats as well as any watches or jewellery. They were then asked to adjust the position of the seat and the angle of the backrest to simulate a driving posture that was as realistic as possible. An example of the participants' posture during the experiment is shown in Figure 7.2.



Figure 7.2 Posture of participant at the steering wheel simulator

Since the grip force applied to the steering wheel has been known to affect the transmission of vibrations to the hand-arm system (Morioka and Griffin, 2009), the participants were required to keep a constant palm grip on the steering wheel using both

hands. Finally, they were asked to fix their eyes on a board placed directly in front of the steering wheel simulator, which displayed a photograph of the road surface being studied (see Figure 5.2). The room temperature in the laboratory was maintained within the range of 20 to 25°C to avoid any significant environmental effects on the participants' skin sensitivities (ISO13091-1, 2001).

Each of the ten road surfaces studied consisted of three repetitions for each of the four manipulated and the original base stimulus from the displayed road surface plus a further 25 stimuli chosen randomly from other stimuli sets of the other nine road surfaces used as background noise stimuli. Five different series of eight acceleration stimuli were applied to evaluate each road surface type. The duration of each individual test stimulus was ten seconds. Prior to commencing formal testing, the 20 seconds exposure stimuli of each of the four stimuli types which would be used later were provided to participant in order to become acquainted with the detection task. Figure 7.3 illustrate the experiment design adapted during this experiment.

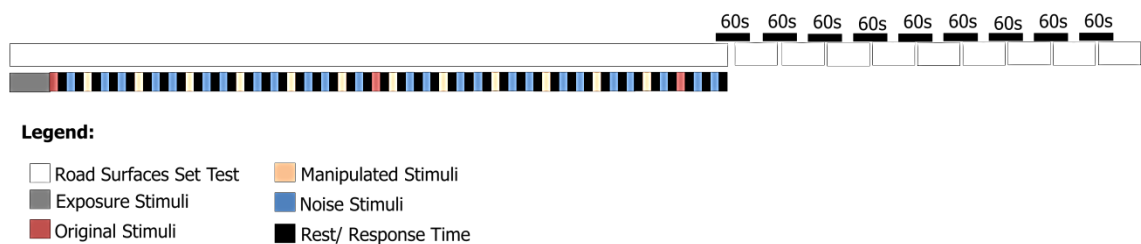


Figure 7.3 Experiment design

During the experiment, the participants were asked to judge whether the actuated acceleration stimulus transmitted to them through the steering wheel was coming from the road surface shown on the photograph on the board directly in front of the test bench. They were also asked to rate the confidence of their judgement on a five-point scale. They were instructed to report “one” if they were very sure it was not the same signal, “two” if they were fairly sure it was not the same signal, “three” if they were not sure either way, “four” if they were fairly sure that it was the corresponding signal, and “five” if they were very sure it was the same signal. Each series of stimuli was separated by a five-second gap to allow participants enough time to indicate their detection responses to the stimuli directed at them.

Each participant performed 40 detections for each road surface studied, with a total of 400 detections over the course of the one and half hours allocated to complete the experiment. Due to the large total number of stimuli detection and the time required, the experiment was designed to take into consideration learning (Giacomin and Woo, 2004) and fatigue effects (Giacomin and Abrahams, 2000; Giacomin and Screti, 2005). Hence the order of stimuli arrangements in each series was fully randomised for each participant, and the participants were asked to attend on two separate sessions to complete the experiment, with 200 detections in each session.

The facility and the protocol of the experiment was approved by the College of Engineering, Design and Physical Sciences Research Ethics Committee, Brunel University (Ref No: EC/507).

7.4 Test Participants

In order to minimise the margin of error in the detection tasks, driving experience was identified as one of the main factors considered in this experiment. A study performed by Zhao *et al.* (2014) identified the capability of performance in a change detection task of both experienced and novice drivers. Their findings suggested that experienced drivers were better able to identify changes in a detection task and they had more knowledge of the road than novice drivers. According to the Department of Transport (2013), a person is a novice driver until they have held a driver's licence for at least two years or periods adding up to two years. Meanwhile, an experienced driver is a person who has held a driver's licence for more than ten years (Craen *et al.*, 2011).

According to Kumar (2005), sampling strategies can be categorised into probability and non-probability designs. He also stated that probability sampling design is used when the sample is representative of the population, while non-probability sampling is suitable when the number of elements in a population is either unknown or cannot be individually identified. Additionally, the most commonly used non-probability sampling strategies are convenience, accidental, purposive and snowball sampling (Coolican, 2009).

Therefore, the current study described here used a non-probability purposive sampling strategy (Coolican, 2009) with participants who had driving experience of a minimum of two years as primary characteristic for sample selection and also were served as controlled parameter. Meanwhile, parameters relating to gender and physical body mass (weight and height) were not controlled in the current study, as previous research suggested that there were no significant differences between genders in the subjective experience of hand-arm vibration (Mansfield and Griffin, 2000; Neely and Burström, 2006; Jeon *et al.*, 2009).

Apart from the controlled and uncontrolled parameters in this experiment, the chosen minimum number of participants followed the statistical rule of thumb guiding sample size for detecting differences, as suggested by VanVoorhis and Morgan (2007). They suggested that participant numbers need to be between 14 and 30 in order to maintain the adequate power of 80 per cent when using statistics designed to detect differences between variables.

A total of twenty (n=20) university students participated in this experiment. Both controlled and uncontrolled parameters of the participants are summarised in Table 7.2 below.

Table 7.2 Anthropometrics and driving experience of test participants

		Male (n=10)				Female (n=10)			
		Min	Max	Mean	SD	Min	Max	Mean	SD
Controlled parameters	Driving experience (years)	2	20	8.63	7.44	2	10	4.5	2.45
Uncontrolled parameters	Weight (kg)	61	90	79.75	9.88	50	83	61.69	13.25
	Height (m)	1.62	1.90	1.77	0.10	1.57	1.67	1.62	0.04

The mean values and standard deviations of the height and mass of the test participants were close to the 50th percentile values for the UK population (Pheasant and Haslegrave, 2005). The average driving experience of participants in Table 7.2 is over 8 years, which means they can be categorised as experienced drivers, comparable with studies done by Borowsky *et al.* (2010) who suggested that novice drivers had an average of 2.7 months of driving experience, experienced drivers had an average of 7.3 years, and older drivers had an average of 37.5 years.

7.5 Results and Analysis

The results of the experimental tests were analysed using the Theory of Signal Detection of Rating Procedure (Green and Swets, 1966) as the analytical framework. They were summarised by the Hit Rate (%), Detectability Index (d') and Receiver Operating Curve (ROC) points.

The reduction of the rating procedure matrix to a binary response was used in the analysis of this study (Green and Swets, 1966). For each frequency bands analysed in this study, the hit rate, $P(S|s)$ was taken based on the proportion of “four and five” scale responses which were obtained from the stimuli of the road surfaces that was shown on the board while the false alarm, $P(S|n)$ was taken from the proportion of “one, two and three” scale responses.

Figure 7.4 illustrates the results obtained from the experiment, which investigates how changes in vibrational energy cause changes in the human cognitive detection of road surfaces, based on steering wheel vibration. The results are presented in the line graph format which following Spatz (2008) who suggested that line graphs are suitable for comparing changes over the same period of time for more than one group. The hit rate percentage is presented along the ordinate, while the five different frequency bands for each road are presented along the abscissa.

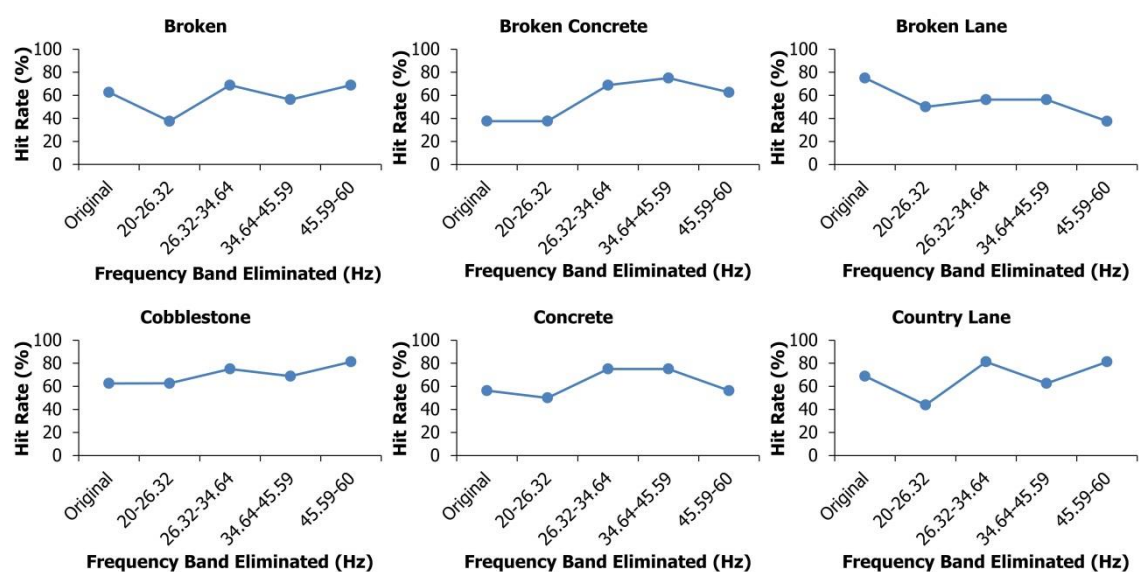


Figure 7.4 Rate of hit detection for all ten road surfaces studied

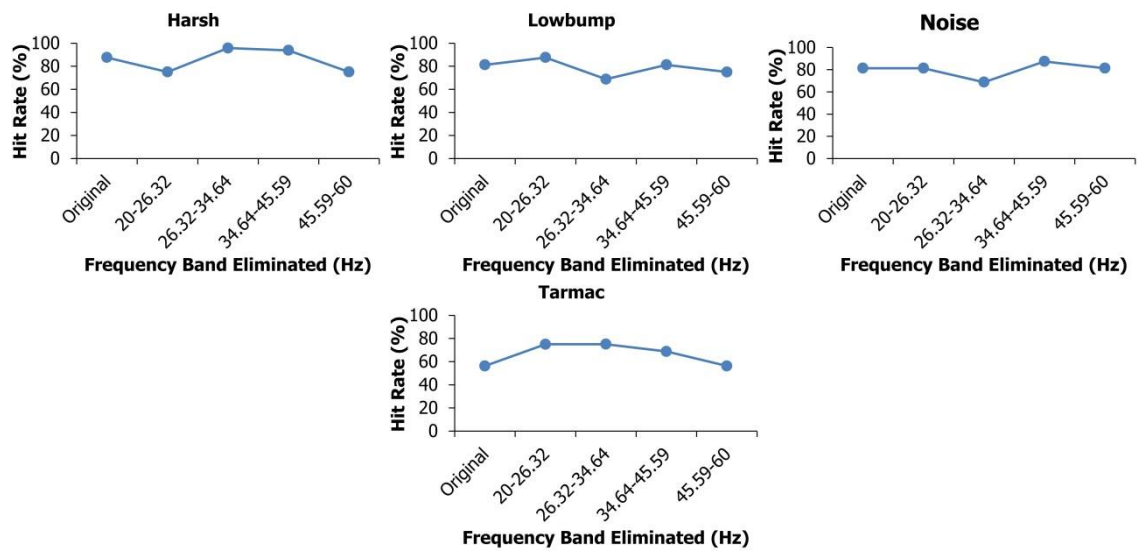


Figure 7.4 (continued) Rate of hit detection for all ten road surfaces studied

Refer the results in Figure 7.4 shown that the hit rates for the original base stimuli for Broken, Broken Lane, Cobblestone, Country Lane, Concrete, Low Bump, Harsh, Noise and Tarmac were higher than 50 per cent in each case. Broken Concrete was lower, as the hit rate was 37.6 per cent. Qualitatively, the results from the Broken Concrete showed a very different behaviour from that of the other nine test stimuli, suggesting important differences in the underlying energy content.

Next, when the participants were exposed to the frequency band of 20 to 26.32 Hz, which was eliminated from the original time histories, it was found that the hit rates decreased by 12 to 25 per cent for Broken, Broken Lane, Country Lane, Concrete and Harsh surfaces. In contrast, there was a slight increase for Broken Concrete, Cobblestone, Low Bump, Noise and Tarmac surfaces of 5 to 19 per cent. From the hit rates reported, it can be claimed that the detection ability increased sharply in the frequency band of 26.32 to 34.64 Hz for all the ten road surfaces except for Low Bump, Noise and Tarmac.

The data can also be quantified in terms of signal detection sensitivity. Figure 7.5 illustrates detectability index as a function of the frequency bands eliminated. In signal detection theory, the sensitive of the observer is denoted as d' and the higher the d' value, the higher the hit rate and lower the number of false alarms (Woo and Giacomini, 2006). In other words, the greater the d' value, the more sensitive is the observer's reaction to the particular signal.

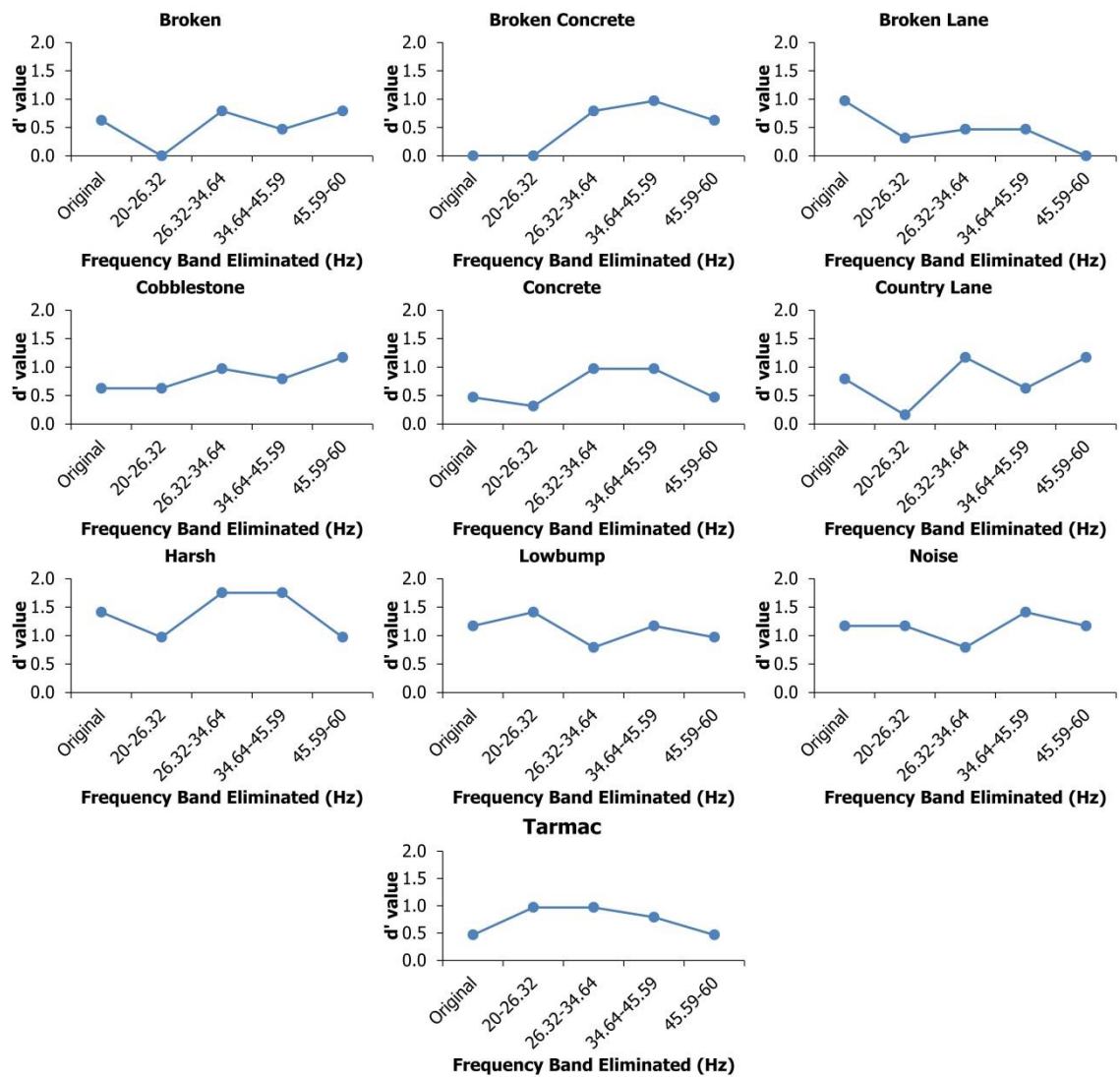


Figure 7.5 Observer sensitivity, d' for all ten road surfaces studied

Figure 7.5 indicates that the highest value rate of changes of d' in the elimination of frequency bands was between 26.32 and 34.64 Hz for most of the road surfaces studied, for instance, Broken, Broken Lane, Country Lane, Concrete and Harsh.

The pattern of the curve and the qualitative human responses for both hit rate (Figure 7.4) and d' (Figure 7.5) value showed similarities. It can be concluded that the frequency band of 26.32 to 34.64 Hz in this experiment played an important role in the participants' cognitive detection of the road surface for all the road surfaces studied.

Further analyses were conducted by means of ROC distribution points to verify which frequency bands contain vibrational information that can prevent human cognitive detection of the road surface (Green and Swets, 1966). Figure 7.6 presents the receiver operating characteristic points obtained for each of the 20 test participants for each of the frequency bands elimination, as well as for the original stimulus of the road surfaces studied. The plots contain less than 20 individual points due to the occasional outcome of more than one subject producing identical hit and false alarm rates.

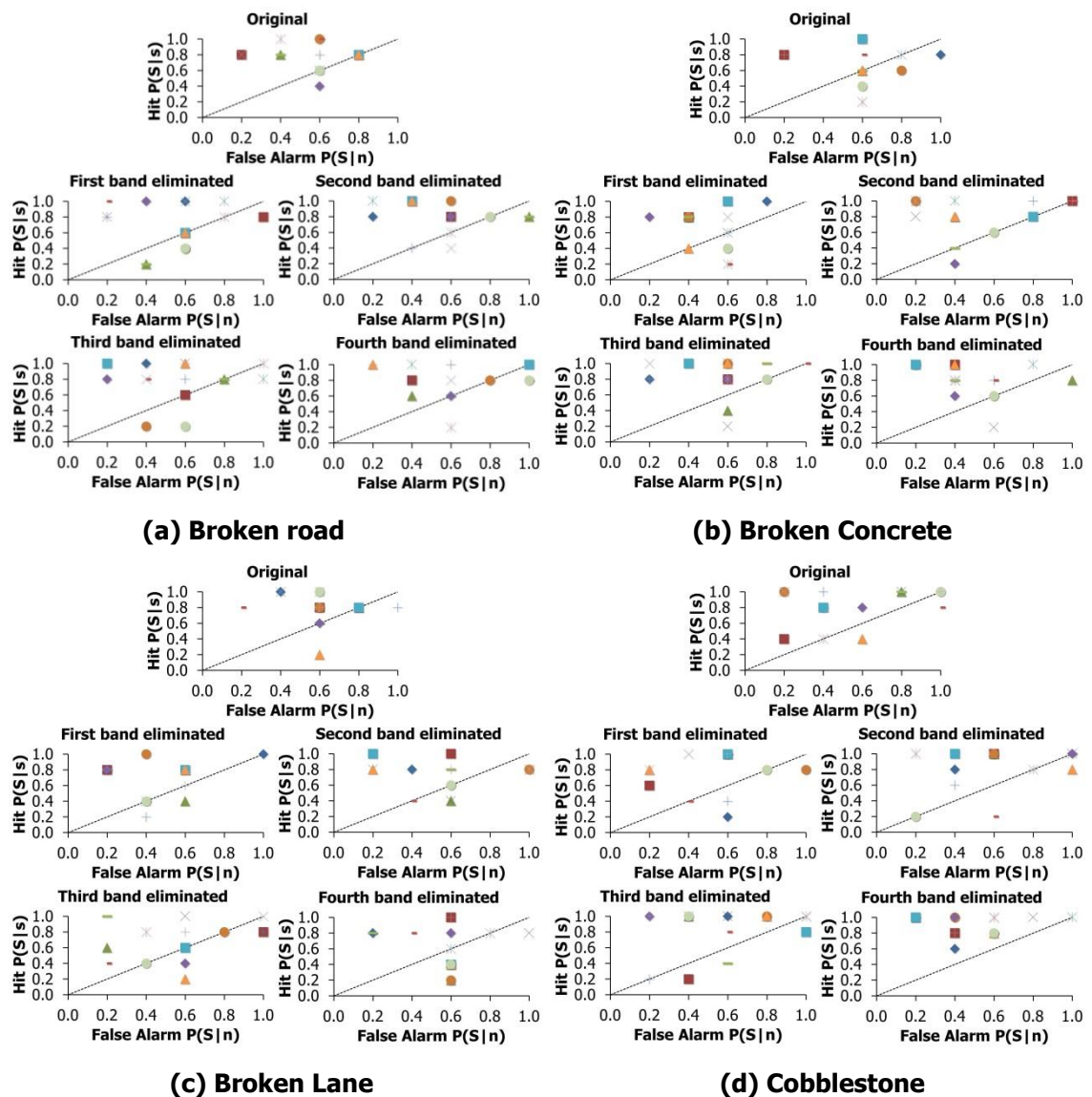


Figure 7.6 ROC points ($n=20$) for the experiment on the effect of vibration energy distribution

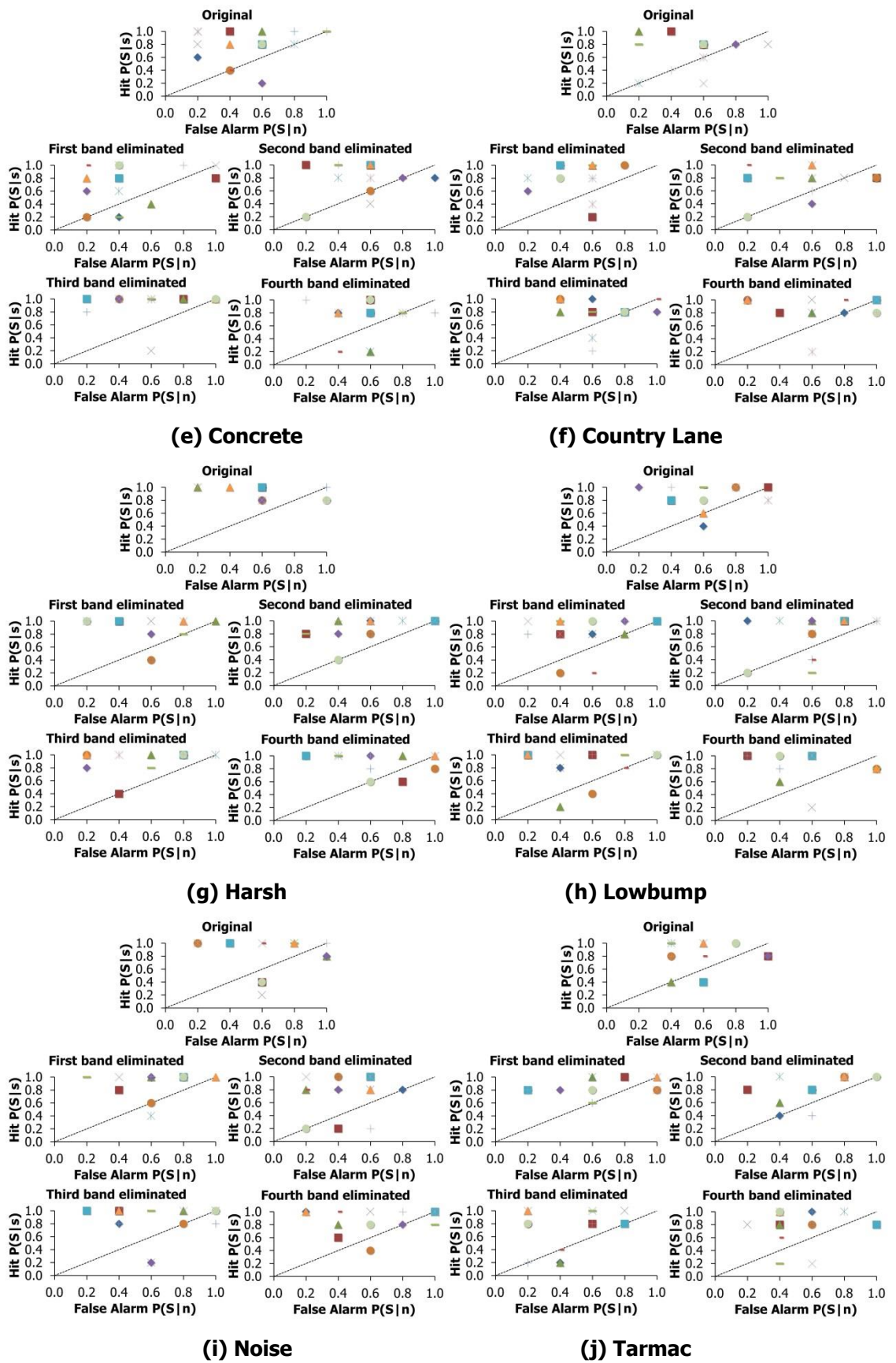


Figure 7.6 (continued) ROC points ($n=20$) for the experiment on the effect of vibration energy distribution

From Figure 7.6, there is a large number of ROC points located in the region of 26.32 to 34.64 Hz. The results shows that the elimination of this frequency band made it impossible to correctly detect smooth surfaces, namely, Tarmac, Cobblestone and Concrete. On the other hand, it caused noticeably sensitive levels of human cognitive detection for uneven surfaces, namely, Broken, Broken Concrete, Broken Lane, Country Lane, Noise, Harsh and Low Bump surfaces. The results suggest that the long-term memory model used by average drivers to judge road surface type contains information about oscillatory frequencies between 26.32 and 34.64 Hz.

Based on the similarities in the results of the hit rate percentages (Figure 7.4), the detectability value d' (Figure 7.5) and the ROC point distributions (Figure 7.6), it can be noted that all of the results suggest that the elimination of the frequency band 26.32 to 34.64 Hz made it almost possible for the participants to make correct detections of the road surfaces. This was imperative in increasing the sensitivity of the human cognitive ability to detect road surface conditions

7.6 Discussion

The study discussed in this chapter was designed to measure the effect of vibrational energy distribution on the human ability to detect road surfaces based on steering wheel vibration. This study was inspired by previous research carried out by Berber-Solano *et al.* (2013) who investigated drivers' detection of road surface types by measuring the sensitivity of this detection by eliminating regions of vibrational energy from the power spectral density of the steering wheel acceleration signal.

As illustrated in Figure 7.4, the percentage hit rate of less than 100 per cent for all ten road surfaces suggests the difficulty of achieving fully accurate detection through a laboratory task. A possible explanation for these results may be the lack of the presence of several key stimuli such as acoustical stimuli (Berber-Solano *et al.*, 2013). Other possible causes of low detection include the signal reproduction up to 18% as shown in Table 5.5 due to the signal distortion, which is defined as an error phenomenon that causes the appearance of extraneous signals in the output of test equipment (BS 6840-2, 1993). Moreover, the road surface detection problem that appears to emerge from the

current findings is a complex human detection mechanism. The measured human responses to changing stimuli bandwidth suggest that the long-term memory model (or cognitive interpretation mechanism) differed for different road surfaces (Giacomin and Woo, 2005).

This study aims to measure how changes in the vibrational energy within the frequency band of 20 Hz to 60 Hz may affect human cognitive detection of road surface types based on steering wheel vibration. The results in Figure 7.4 and Figure 7.5 suggest that the elimination of the frequency band of 26.32 Hz to 34.64 Hz from the original stimuli played a key role in the human cognitive detection of the relevant road surface. These relationships may be partly explained by the fact that the elimination of this frequency band appeared to produce the highest peaks of vibrational energy resulting from the resonance in the vehicle's dynamic systems such as tyres and steering wheel (Berber-Solano *et al.*, 2013). Moreover, these results are also consistent with those reported by Fujikawi (1998), Pak *et al.* (1991) and Giacomin *et al.* (2000), who suggested that a frequency band of 23 Hz to 58 Hz is the largest range of frequency that contributes to vehicle dynamics, whereas the band of 20 Hz to 35 Hz is defined by steering wheel resonance (Kulkarni and Thyagarajan, 2001).

The distribution of the ROC points presented in Figure 7.6 shown that the distributions were scattered which was not consistent with the theory pertaining to the advantages of applying more binary procedures proposed by Swets *et al.* (1961). The theory suggested that the distribution data points of more binary procedures were less scattered than those from binary procedures. This result may be explained by the fact that the requirement of a minimum of two years' driving experience was not sufficient to help the participants detect the vibrations in the different road surface types based on the steering wheel vibrations. Zhao *et al.* (2014) suggested that experience interacts with the location of the change and the relevance of the change to driving. It is also in line with Patten *et al.* (2006) which claimed that drivers with an average driving experience of five to ten years have more knowledge about the road and changing cognitive tasks than the novice drivers.

7.7 Conclusion

This study involved twenty participants who were exposed to vertical steering wheel vibration stimuli in a laboratory test bench from ten different road surfaces, namely, Broken, Broken Concrete, Broken Lane, Cobblestone, Country Lane, Concrete, Low Bump, Harsh, Noise and Tarmac. The objective was to establish the most pertinent frequency band from 20 Hz to 60 Hz which, if eliminated from the vibrational energy, might affect the level of driver road surface detection.

The responses given by the participants were collected using the more binary response scale from one to five to indicate whether the signal perceived matched the road surface shown in front of them. Next, the Theory of Signal Detection Rating Procedure was applied to analyse the results. For each frequency bands analysed in this experiment, the hit rate, $P(S|s)$ was taken at the proportion of “four and five” scale responses obtained from the stimuli which were actually derived from the road surface shown on the board while the false alarm, $P(S|n)$ was taken at the proportion of “one, two and three” scale responses.

The findings suggested that the elimination of vibrational energy in the frequency band of 26.32 Hz to 34.64 Hz can be highly detrimental to human cognitive detection of road surface types. The findings also demonstrate that the frequency band of 26.32 to 34.64 compromises steering wheel feedback the most, and that the elimination of these frequency bands can lead to the correct detection of road surfaces. Meanwhile as the results of distribution of the ROC points were scattered, therefore in the next studies suggested to just remain the binary response procedure.

The next chapter will define the optimal approach for the detection transient vibration of steering wheel road surface in the frequency band of 20 Hz to 60 Hz according to their time-domain waveform. The study will start by applying the signal transformations of steering wheel vibration level based on Trapezium numerical integration rules of signal processing to measures the process of identification steering wheel vibration road surfaces transient vibrations. Next, the study continue by determine the effects of signal transformations of steering wheel vibration level based on centred differentiation filter of signal processing towards driver road surface detection.

CHAPTER 8

INTEGRATION AND DIFFERENTIATION OF STEERING WHEEL VIBRATION SIGNALS

8.1 Introduction

Integration and differentiation are basic numerical analysis with a wide range of applications in many areas of science including signal processing. Three well-known measured data that interrelated through differentiation and integration are acceleration, velocity and displacement (Marchesiello and Fasana, 2001; Kerschen *et al.*, 2001; Ding *et al.*, 2011) which is often needed when it comes to the application of vibration signal data especially in conjunction with numerical modelling systems (Mercer, 2011).

As concluded in Chapter 6, in order to identify the transient vibrations of road surface data signals it has been decided to follow the procedure stated in the Mildly Nonstationary Mission Synthesis algorithm. Next, the data will be used as the input for automation machine learning to classify the transient vibrations into their similarity groups. However, before the classification process begins, it is crucial to ensure that the pre-processing data provided is appropriate and simple, as the automation machine will be very sensitive while performing the task learning (Everitt *et al.*, 2001; Hair, 2006).

Previous studies carried out by S. Abdullah *et al.* (2006) and Berber-Solano *et al.* (2010) used an MNMS algorithm to identify and extract the transient vibrations of steering wheel vibration. In both studies, they used the original steering wheel vibration that had been measured by an accelerometer in an acceleration quantities unit. Similarly, from literature related to the human subjective response to steering wheel vibrations, reveals that the human subjective response is very sensitive to acceleration (Miura *et al.*,

1959; Miwa, 1967; Reynolds *et al.*, 1977; Verrillo, 1985; Griffin, 1990; Morioka and Griffin, 2006; 2009). The effects of steering wheel acceleration signals on driver road surface detection have also been discussed in the previous chapter. In fact, the International Organization for Standardization 5349-1 (2001) also suggested that for practical convenience, the magnitude of vibration needs to be measured by means of an accelerometer in terms of acceleration units.

In spite of that, the question arises as to what would happen if we consider two other measurement data of velocity and displacement, as a steering wheel vibration signal measurement data? Would these measurements facilitate the MNMS algorithm to identify the transient vibrations of steering wheel vibration? Also, would another two measurement types facilitate the human subjective response to steering wheel vibration for detection of road surfaces?

In the context of this thesis, the original steering wheel acceleration vibration will be integrated twice to give velocity and displacement. It was performed based on the assumption that the original steering wheel acceleration vibration contained a great deal of noise, whereas the numerical integration analysis applied to the signal, which functions as a filter (Worden, 1990), will reduce the noise and consequently allow the MNMS algorithm to easily identify the transient vibrations road surface signals. Meanwhile, the differentiation numerical analysis will be used to compare both test stimuli of original steering wheel acceleration measured by accelerometer, and steering wheel acceleration measured by double time-domain differentiation of displacement to identify the optimal approach used by humans to detect the road surface type.

Therefore, without taking for granted of velocity and displacement, this chapter describes a set of experimental testing activities performed in order to measure the effect of integration and differentiation of steering wheel vibration road surface signals, for the identification of transient vibrations by MNMS algorithm and humans' ability to detect the road surface type. This chapter has been divided into three sections. The first will be concerned with determining which signal measurement should be used to perform the identification of transient vibrations contained in steering wheel vibration road surface signals. Following this, the effect of the signal will be measured with different approaches in order to assess the ability of humans to detect the road surface

type. Finally, the conclusion provides a summary and critique of the findings related to the optimal measurement signal for both the identification process of transient vibrations and driver road surface detection.

8.2 The Effect of Time-domain Integration on Transient Vibrations Steering Wheel Road Surface

The time-domain integration of steering wheel vibration road surface signals was performed based on the assumption that the original steering wheel acceleration vibration contained a great deal of noise. The numerical integration analysis applied to the signal, which functions as a filter, will reduce the noise and consequently allow the MNMS algorithm to easily identify the transient vibrations road surface signals. To investigate how time-domain integration makes the identification of transient vibrations waveforms easier or harder, the objectives of this experiment are:

- i. To identify the number of transient vibrations from the different measured signals of steering wheel vibration road surfaces based on time-domain integration.
- ii. To perform the evaluation of the identified transient vibrations from the different measured signals of steering wheel vibration road surfaces based on time-domain integration with the criteria of transient vibrations stated in the MNMS algorithm.
- iii. To conclude which measured signal of steering wheel vibration road surfaces will be used to identify the transient vibrations of steering wheel vibration road surfaces.

8.2.1 Numerical Data Sampling

Various methods for achieving integration exist, such as the Trapezium rule, Simpson's rule, Tick's Rule and 3rd Order Corrector (Smyth and Pei, 2000). To examine the accuracy of an integrator, the transfer function of the output of the integrator versus the exact signal expected can be used (Worden, 1990). The comparison magnitude for each transfer function of integration rule is shown in Figure 8.1:

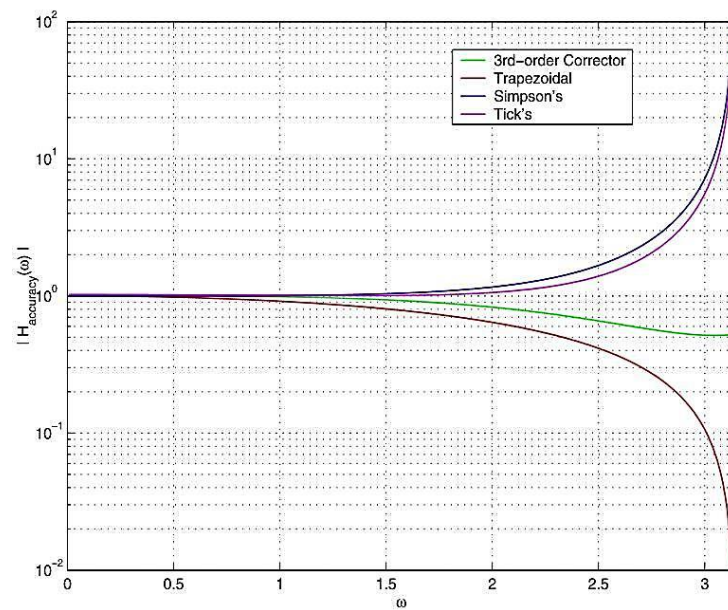


Figure 8.1 The comparison of the magnitudes of the accuracy transfer function
(Source: Worden, 1990; Smyth and Pei, 2000)

In the application of signal processing, integration analysis exposes two main problems, which are the introduction of low- and high-frequency components (Worden, 1990). From Figure 8.1 it can be seen that the Simpson's and Tick's rules behave rather poorly in the higher frequency ranges by going to infinity. In contrast, the Trapezium rule greatly reduces the higher frequency content in the estimated signal and only suffers from the introduction of low frequency components, and does not require the use of a low-pass filter (Smyth and Pei, 2000; Kerschen *et al.*, 2001; Marchesiello and Fasana, 2001). Generally, the Trapezium rule is also very useful for a wide range of numerical integration scenarios because of the easy conceptualisation of derivation (Wicklin, 2011), and it offers a considerable saving in time (Kerschen *et al.*, 2001; Marchesiello and Fasana, 2001). Therefore, for these reasons, the Trapezium rule is considered in this research.

The numerical-based experiment starts by applying the time-domain integration of the Trapezium rule to all ten original steering wheel acceleration vibration signals described in Section 5.2, where the steering vibration velocity will be obtained. Furthermore, the double time-domain integration analysis is performed to obtain the steering vibration displacement.

The time-domain integration of the Trapezium rule calculation has been performed by using both the Time Monitoring (T-MON) module of the LMS[®] CADA-X 3.5E software and MATLAB R2014a software to ensure the signals produced were correct. To illustrate an example of the time-domain integration of the Trapezium rule process, Figure 8.2 presents the Country Lane and Tarmac, which respectively recorded the highest and lowest energy levels among the ten road surfaces studied after applying first and double time-domain integration of the Trapezium rule.

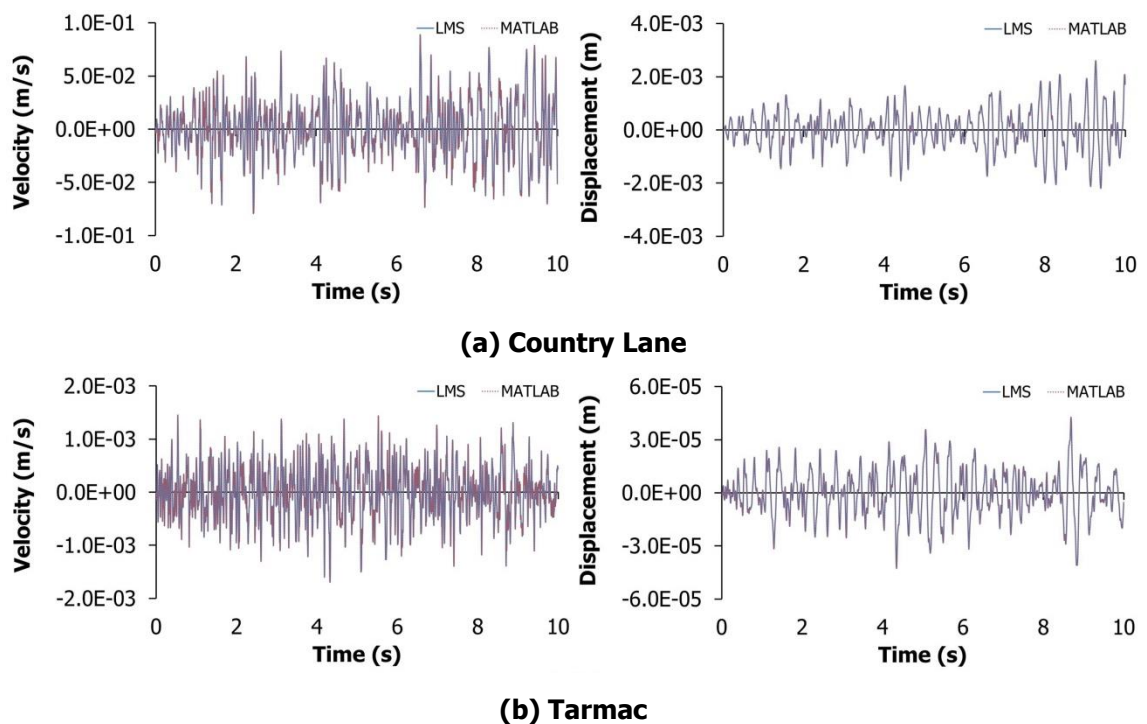


Figure 8.2 Comparison time histories between first (left) and double (right) time-domain integration of steering wheel acceleration by LMS[®] CADA-X 3.5E software and MATLAB R2014a software

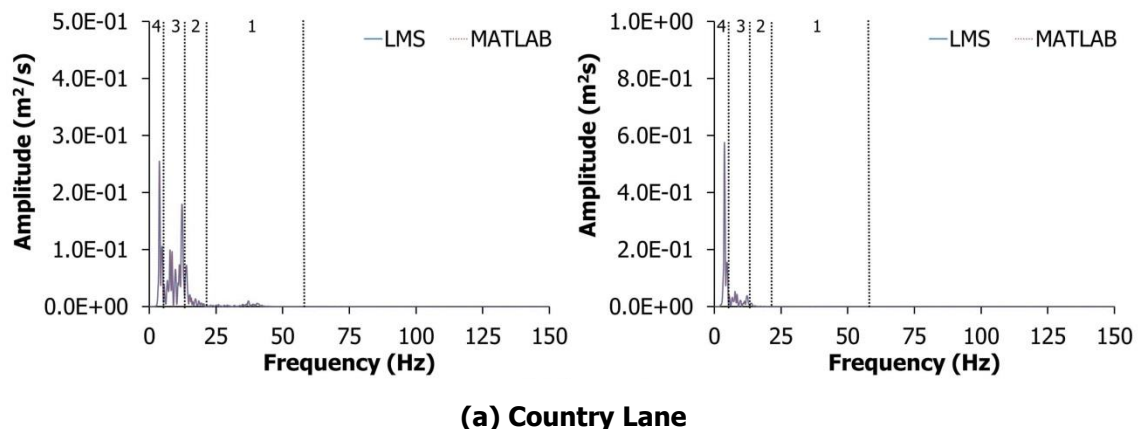
From the comparison between LMS[®] CADA-X 3.5E and MATLAB R2014a software in producing first and double time-domain integration of steering wheel acceleration in Figure 8.2, it is apparent that there are no errors or differences. Hence, since the MNMS

algorithm has also been written in MATLAB R2014a software, and runs on Windows-compatible PCs, in this research the first and double time-domain integration signals produced by MATLAB R2014a software have been chosen to minimise computational errors when associated with the MNMS algorithm later.

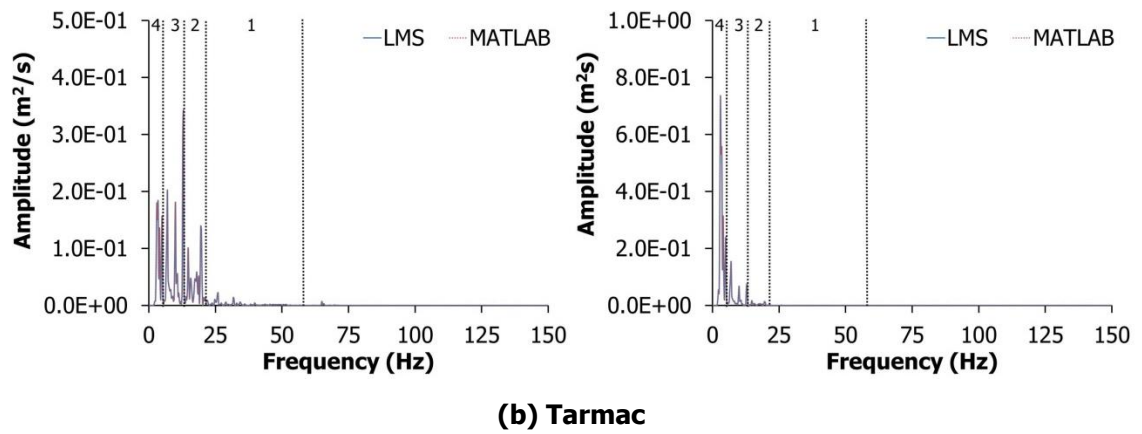
After all ten original steering wheel acceleration vibration signals have been transformed to the velocity and displacement signals, the total number of signals used in this experiment is 30 vibration road surface signals and subsequently the MNMS algorithm is applied to each signals for the purpose of transient vibrations identification and extraction.

By using the MNMS algorithm, all 30 vibration road surface signals were decomposed into twelfth order Daubechies wavelets (Giacomin *et al.*, 2000) in the frequency range of 0 to 60 Hz. These were grouped, according to the natural frequency energy distribution of the signal, into four wavelet groups.

Figure 8.3 presents the power spectral density (PSD) of first (left) and double (right) time-domain integration for Country Lane and Tarmac, which recorded the highest and the lowest energy levels among the ten road surfaces studied, respectively, showing the wavelet group distribution.



(a) Country Lane
Figure 8.3 Comparison PSD showing the four wavelet groups distribution between first (left) and double time-domain integration (right) of steering wheel acceleration by LMS® CADA-X 3.5E software and MATLAB R2014a software



(b) Tarmac
Figure 8.3 (continued) Comparison PSD showing the four wavelet groups distribution between first (left) and double time-domain integration (right) of steering wheel acceleration by LMS® CADA-X 3.5E software and MATLAB R2014a software

The first region of frequency distribution, which is from 20 Hz to 60 Hz, is mostly defined by higher frequency modes of the chassis and by tyre resonances (Pottinger *et al.*, 1986; Giacomini *et al.*, 1999). Meanwhile, the vibration energy distributed in the range of 13 Hz to 20 Hz may reflect the low frequency flexible body modes of the chassis. This is followed by the regions that can be related to the behaviour of suspension units, separately or with the rigid body motion of the engine/transmission unit, distributed within 5 Hz and 13 Hz. Finally, the region between 0 Hz and 5 Hz is associated with the rigid body motion of the automobile chassis on the main suspension.

8.2.2 Results and Analysis

In the MNMS algorithm, transient vibrations identification is achieved in each wavelet group time history by means of a threshold trigger level that is specific to the wavelet group. In this numerical-based experiment, a threshold trigger level (TTL) value of 2.6 is chosen, which is known as a critical trigger level for a driver to detect the road surface types (Berber-Solano *et al.*, 2010). Table 8.1 presents the number of transient vibrations identified in each wavelet group for all 30 vibration road surface signals.

Table 8.1 Number of transient vibrations identified in each wavelet group (WG) from different measures of steering wheel road surface signals

Road Surfaces	Measured signal	Number of transient vibrations				Total
		WG1	WG2	WG3	WG4	
		20 < Hz < 60	13 < Hz < 20	5 < Hz < 13	0.5 < Hz < 5	
Broken	Acceleration, (m/s ²)	19	15	8	2	44
	Velocity, (m/s)	19	15	4	7	45
	Displacement, (m)	13	12	6	2	33
Broken Concrete	Acceleration, (m/s ²)	22	21	7	4	54
	Velocity, (m/s)	16	13	10	2	41
	Displacement, (m)	13	13	7	3	36
Broken Lane	Acceleration, (m/s ²)	30	17	7	5	59
	Velocity, (m/s)	22	9	6	4	41
	Displacement, (m)	14	10	6	1	31
Cobblestone	Acceleration, (m/s ²)	17	14	8	2	41
	Velocity, (m/s)	16	15	10	2	43
	Displacement, (m)	18	5	5	2	30
Concrete	Acceleration, (m/s ²)	24	5	7	5	41
	Velocity, (m/s)	19	7	8	4	38
	Displacement, (m)	23	6	5	2	36
Country Lane	Acceleration, (m/s ²)	30	19	8	5	62
	Velocity, (m/s)	15	11	6	6	38
	Displacement, (m)	16	12	6	3	37
Harsh	Acceleration, (m/s ²)	23	12	7	3	45
	Velocity, (m/s)	17	12	9	4	42
	Displacement, (m)	15	13	8	3	39
Lowbump	Acceleration, (m/s ²)	39	18	4	2	63
	Velocity, (m/s)	23	14	5	3	45
	Displacement, (m)	25	15	2	5	47
Noise	Acceleration, (m/s ²)	21	12	3	3	39
	Velocity, (m/s)	16	14	5	1	36
	Displacement, (m)	16	12	5	1	34
Tarmac	Acceleration, (m/s ²)	31	10	5	4	50
	Velocity, (m/s)	25	13	7	2	47
	Displacement, (m)	24	7	5	4	40

The comparative table above intends to show the effect between the signal produced by the time-domain integration of Trapezium rules of original steering wheel acceleration vibration signals and the number of identified transient vibrations. From Table 8.1 it can be observed that the identification of transient vibrations is decreased up to 38% when steering wheel acceleration vibration is applied by the first time-domain integration for the Country Lane surfaces and decreased another 2% after second time-domain integration. Therefore, it is apparent from Table 8.1 that the total number of transient vibrations decreased when time-domain integration was applied to the original steering wheel acceleration vibration. It seems possible that, while producing velocity and displacement signals, the level of noise contained in the signal has reduced.

Consequently, the important peaks which exceed the TTL value of 2.6 have also been removed.

The transient vibrations distributed in wavelet group 1 for the frequency band of 20 Hz to 60 Hz was then been extracted. The process used to compares the transient vibrations waveforms produced between original acceleration and both signals produced by the first and second time-domain integration. Figure 8.4 presents examples of the results for the first five extracted transient vibrations of the Tarmac road surface. The first five extracted transient vibrations were ordered from the highest amplitude to the lowest amplitude.

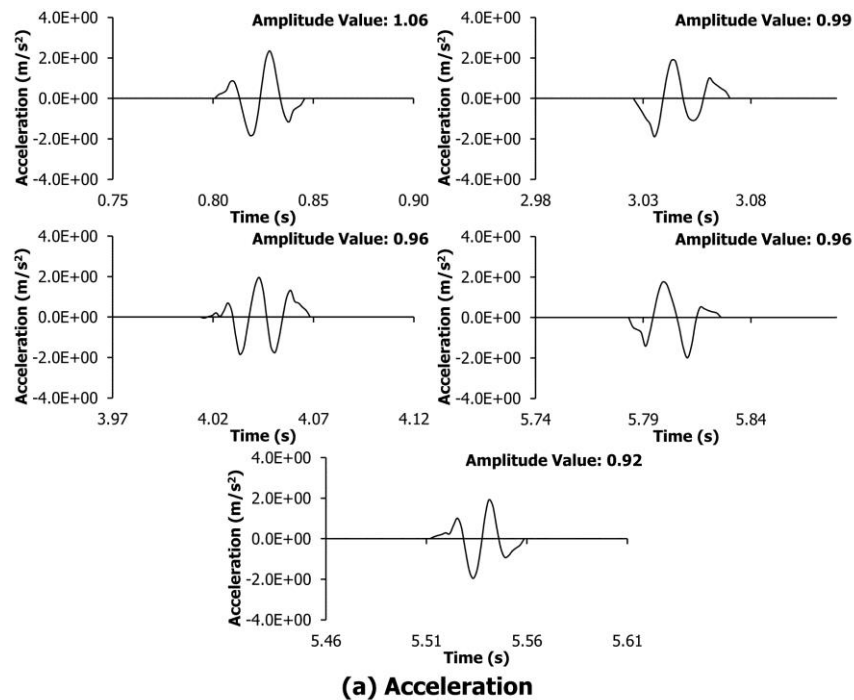
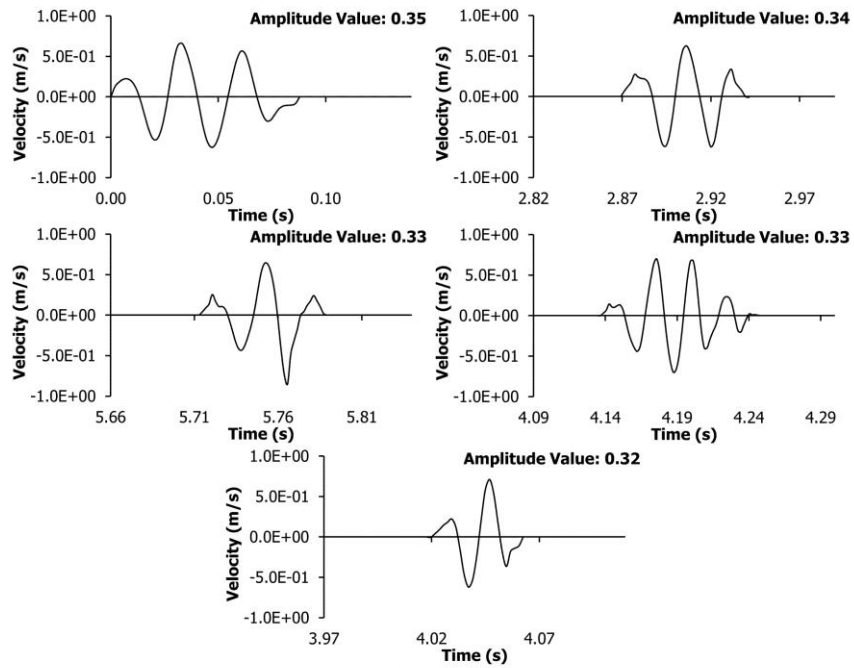
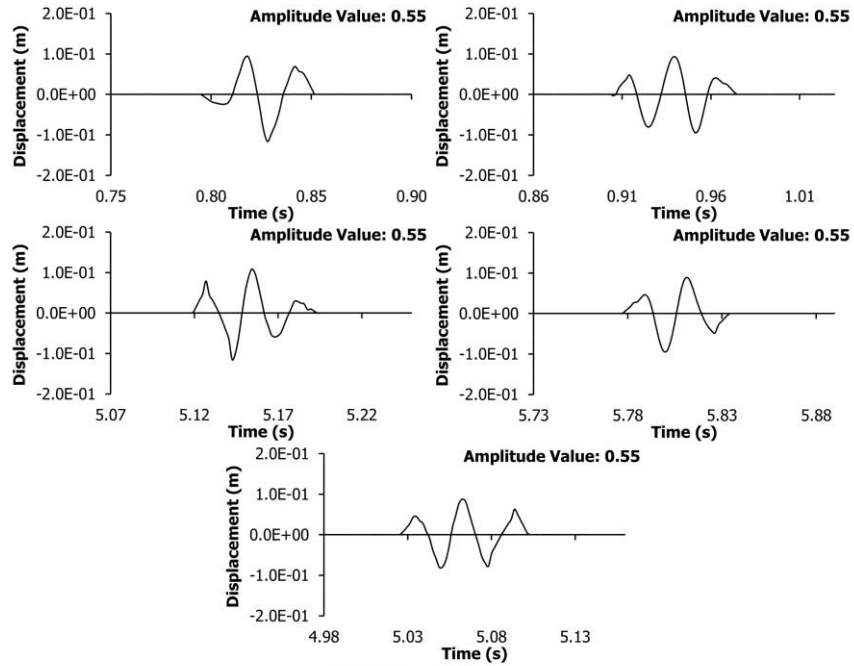


Figure 8.4 Transient vibrations of Tarmac surface identified and extracted within the target frequency interval of 20 to 60 Hz for original steering wheel acceleration vibration



(b) Velocity



(c) Displacement

Figure 8.4 (continued) Transient vibrations of Tarmac surface identified and extracted within the target frequency interval of 20 to 60 Hz for the first (b) and double time-domain integration (c) of steering wheel acceleration vibration

In Figure 8.4 there is a clear trend of decreasing value of amplitude for highest amplitude. For instance, the highest amplitude value for transient vibrations of acceleration is 1.06 m/s^2 , 0.35 m/s^2 for velocity and keeps decreasing to 0.05 m/s^2 for displacement. Other than that, it shows that the first transient vibrations for both

acceleration and displacement are at the same start and end position in the time-domain, starting at 0.80 seconds and ending at 0.85 seconds. Furthermore, both shape and oscillation for all the identified transient vibrations become smoother after applying time-domain integration to the original steering wheel acceleration vibration, whereby transient vibrations of displacement provided the better results both in shape and oscillation, which are closer to the definition of transient vibrations identified by the MNMS algorithm.

Considering the effect of the signal produced by the time-domain integration of Trapezium rules of the original steering wheel acceleration vibration signals on both the number and the waveforms of identified transient vibrations, it can be noted that all of the results suggest that displacement was better at identifying the transient vibrations of steering wheel vibration road surfaces.

8.2.3 Discussion

The present numerical-based experiment was designed to determine the effect of time-domain integration on steering wheel vibration road surfaces in identifying and extracting the transient vibrations. The original steering wheel acceleration vibration was integrated twice to give velocity and displacement. The comparison of results of this numerical-based experiment shows that the total number of transient vibrations (Table 8.1) becomes smaller when time-domain integration is applied, and both shape and oscillation (Figure 8.4) are closer to the definition of transient vibrations stated by the MNMS algorithm. This result may be explained by the fact that the functioning of integration process acts as a filter to the signal, as Worden (1990) suggested that in the Trapezium rules a low-pass Butterworth filter was used on the input to produce a signal in the range 0 to 200 Hz, which will reduce the noise in steering wheel vibration and consequently the MNMS algorithm can easily identify and extract the transient vibrations. These results also seem to be consistent with assumptions stated earlier (Section 8.2) – that the original steering wheel acceleration vibration contained a significant amount of noise, whereas the numerical integration analysis applied to the signal, which functions as a filter, will reduce the noise and consequently make it easy for the MNMS algorithm to identify and extract the transient vibrations.

However, the results still cannot promise that displacement steering wheel vibration is the best measurement signal for a human to detect the road surfaces. Other than that, the main issue is the limitations of the laboratory facility used during this research (previously discussed in Section 4.3), which pertained to the control and data acquisition being measured in the acceleration measurement (LMS International, 2002). Therefore, the displacement signal of steering wheel road surface vibration needs to be transformed back to the acceleration signal. The transformation of the signal will be compared with original signal in order to identify the optimal approach for driver road surface detection – either the test stimuli that originated measured from the accelerometer, as discussed in Chapter 5, or the test stimuli that were produced by the numerical processes. To obtain the answer, therefore, the theory of numerical differentiation of time-domain needs to be explored and applied to the research test stimuli; consequently, both original acceleration by accelerometer (AA) and acceleration by double differentiation of displacement (AD) processes will be tested by humans.

8.3 The Effect of Time-domain Differentiation on Drivers' Steering Wheel Transient Vibrations Detection

Further experiments from the previous numerical-based experiment are required to overcome the limitations of the laboratory facility used during this research, which was built in the Human Centred Design Lab, Brunel University whereby the control and data acquisition being measured in the acceleration measurement (LMS International, 2002). This laboratory-based experiment will compare both test stimuli of steering wheel acceleration measured by accelerometer, as discussed in Section 5.2.1, and the double time-domain differentiation of displacement.

In order to identify the optimal measurement signal for driver road surface detection, the objectives of this experiment are:

- i. To measure both the percentage of hit rate and the detectability index of the detection of transient vibrations steering wheel road surface based on steering wheel acceleration vibration by accelerometer (AA).

- ii. To measure both the percentage of hit rate and the detectability index of the detection of transient vibrations steering wheel road surface based on steering wheel acceleration vibration by double differentiation of displacement (AD).
- iii. To define the optimal approach for the detection of transient vibrations steering wheel road surface.

8.3.1 Test Stimuli

Three common approaches of the difference formula are the backward difference, forward difference and the centred difference. Among the three approaches, centred differences are the most stable because the errors for the forward difference and backward difference tend to have opposite signs, while the centred difference will average the other two approaches, which would give a better result than either alone (Worden or Tomlinson, 2000). Additionally, centred difference formulae also implement the differentiation as a digital filter or recursion relation. In the most practical applications which needed to reduce high frequency components of the signal, suggested that the five-point centred difference is often very useful (Worden, 1990; Worden and Tomlinson, 2000). Therefore, for these reasons, the five-point centred difference is considered in this research.

Firstly, the laboratory-based experiment starts by applying the double time-domain of five-point centred differences to all ten steering vibration displacement signals produced previously by double time-domain integration analysis, described in section 8.2.

The double time-domain of five-point centred differences calculation has been performed by using both the Time Monitoring (T-MON) module of the LMS[®] CADA-X 3.5E software and MATLAB R2014a software to ensure the signals produced were correct. To illustrate the example, Figure 8.5 presents the Country Lane and Tarmac, after applying the double time-domain of five-point centred differences.

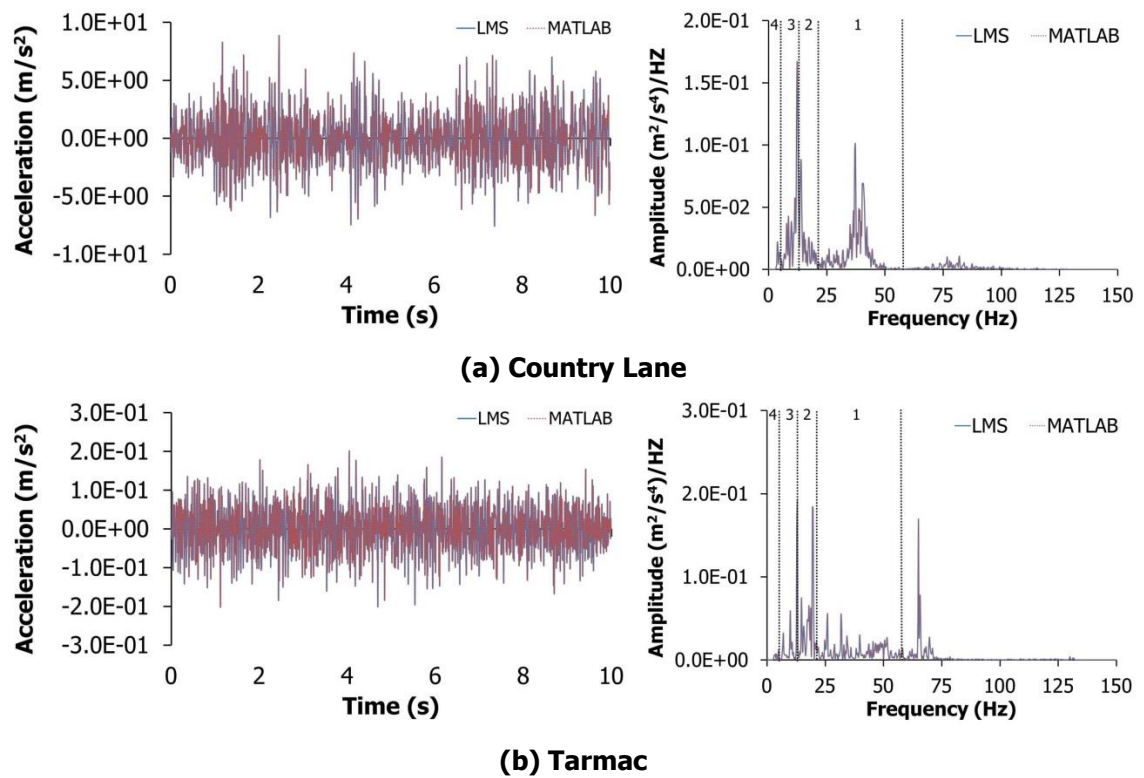


Figure 8.5 Comparison of time histories and PSD of acceleration by double time-domain differentiation of displacement process by LMS® CADA-X 3.5E software and MATLAB R2014a software

From the comparison between LMS® CADA-X 3.5E and MATLAB R2014a software in producing the signals of acceleration by double time-domain differentiation of displacement in Figure 8.5, it is apparent that there are no errors or differences. Hence, since the MNMS algorithm has also been written in MATLAB R2014a software, and runs on Windows-compatible PCs, the signal of acceleration by double time-domain differentiation of displacement produced by MATLAB R2014a software has been chosen to minimise computational errors when associated with the MNMS algorithm later.

Figure 8.6 shows the comparison of time histories and PSD between the original acceleration by accelerometer (AA) and acceleration by double time-domain differentiation of displacement (AD).

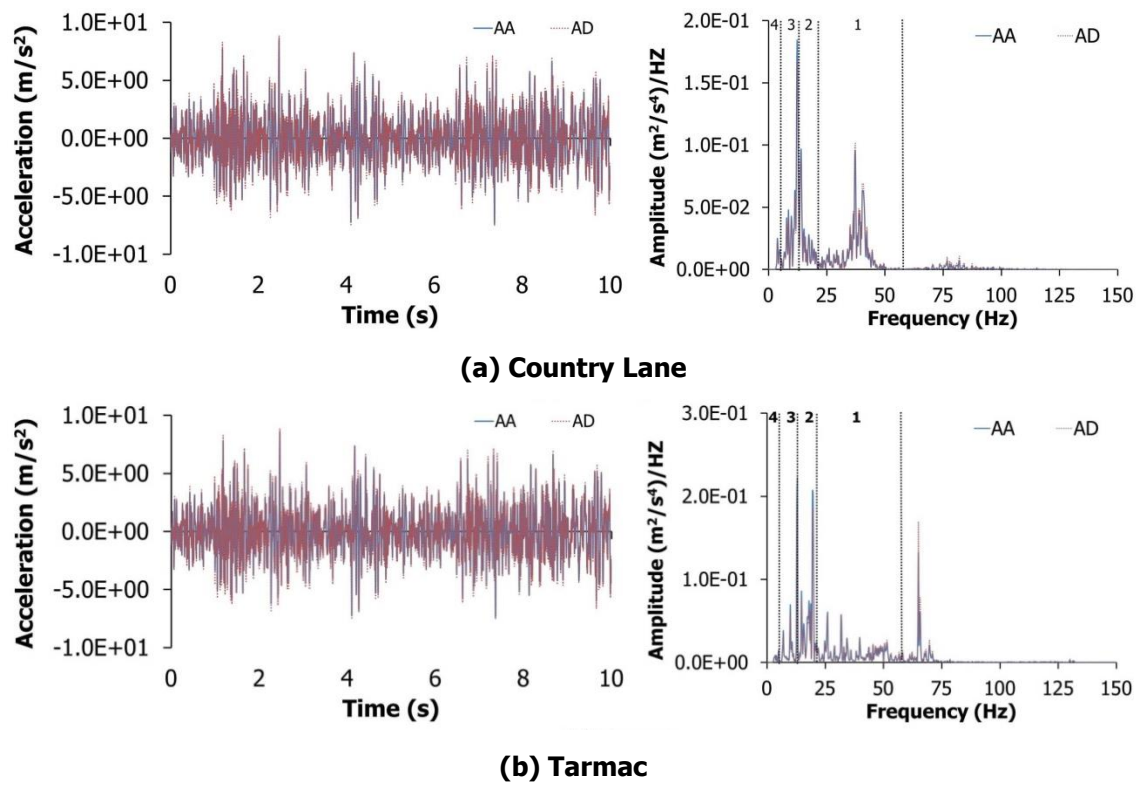


Figure 8.6 Comparison of time histories and PSD between original acceleration by accelerometer and acceleration by double time-domain differentiation of displacement

Meanwhile, the accuracy of the signal produced was quantified by measuring the *r.m.s.* difference between the original acceleration by accelerometer and acceleration by double time-domain differentiation of displacement, and the results are shown in Table 8.2.

Table 8.2 Absolute maximum percent errors between acceleration by accelerometer and acceleration by double time-domain differentiation of displacement

Road Surfaces	<i>r.m.s.</i> (m/s ²)		
	AA	AD	Absolute Maximum Percent Error (%)
Broken	1.32	1.37	3.79
Broken Concrete	1.73	1.88	8.67
Broken Lane	1.78	1.92	7.87
Cobblestone	0.31	0.33	6.45
Concrete	0.09	0.10	11.11
Country Lane	2.05	2.15	4.88
Harsh	1.26	1.37	8.73
Low Bump	0.14	0.13	7.14
Noise	0.75	0.79	5.33
Tarmac	0.06	0.05	16.67

The value of absolute maximum percent error is presented to two decimal places, as suggested by the rule of thumb of statistics in presenting decimal places by Spatz (2008) for the accuracy of calculation results. The results of the acceleration signals produced by double time-domain differentiation of displacement, as shown in Table 8.2, varied between 4% and 17% with respect to the original acceleration by accelerometer. The absolute maximum percent error between AA and AD was consistent with the studies by Worden and Tomlinson (2000) who suggested that the range error between measured and estimated data of the 3.4% to 17% is remarkably good.

Next, in the same manner described in Section 8.2.1, the MNMS algorithm was applied to all the signals of acceleration by double time-domain differentiation of displacement, which were decomposed into 12 wavelet levels in the frequency range of 0 to 60 Hz. The transient vibrations are identified and extracted within the target frequency interval of 20 to 60 Hz, as the frequency range plays a key role in human cognitive detection of the road surface type and signal threshold trigger level value of 2.6 (Berber-Solano *et al.*, 2010). Table 8.3 presents the number of transient vibrations identified and extracted in each wavelet group for the signals of acceleration by double time-domain differentiation of displacement.

Table 8.3 Number of transient vibrations identified in each wavelet group (WG) for the signal of acceleration by double time-domain differentiation of displacement

Road Surfaces	Number of transient vibrations				Total
	WG1	WG2	WG3	WG4	
	20 < Hz < 60	13 < Hz < 20	5 < Hz < 13	0.5 < Hz < 5	
Broken	20	15	8	2	45
Broken Concrete	22	21	7	4	54
Broken Lane	29	16	7	5	57
Cobblestone	17	14	8	2	41
Concrete	25	5	7	5	42
Country Lane	34	19	8	5	66
Harsh	26	12	8	3	49
Lowbump	41	17	4	2	64
Noise	21	12	3	3	39
Tarmac	30	10	5	4	49

Data from Table 8.3 can be compared with the data in Table 8.1 by focusing on wavelet group 1, which is known as the frequency range that plays a key role in human cognitive detection of the road surface type. As shown in Table 8.3, the number of transient vibrations for Broken Concrete, Cobblestone and Noise are the same as in the

original acceleration signal by accelerometer presented in Table 8.1. The number of transient vibrations of Broken and Tarmac identified and extracted in wavelet group 1 for the signal of acceleration by double time-domain differentiation of displacement were decreased, in contrast with Broken, Country Lane, Concrete, Harsh and Low bump.

From the total number of transient vibrations identified and extracted for both acceleration by accelerometer and the double time-domain differentiation of displacement, it is apparent that the total number of transient vibrations identified and extracted from the signal of acceleration by double time-domain differentiation of displacement was decreased with respect to the number of transient vibrations of original acceleration by accelerometer. The results seem consistent with the theory of numerical differentiation processes, whereby the five-point centred difference is capable of reducing high frequency components of the signal (Worden, 1990), which are able to remove the important peak of transient vibrations contained in acceleration by double time-domain differentiation of displacement, which leads to a decreasing number of transient vibrations.

Figure 8.7 presents examples of the results for the first five extracted transient vibrations of the Tarmac road surface. The first five extracted transient vibrations were ordered from the highest amplitude to the lowest amplitude.

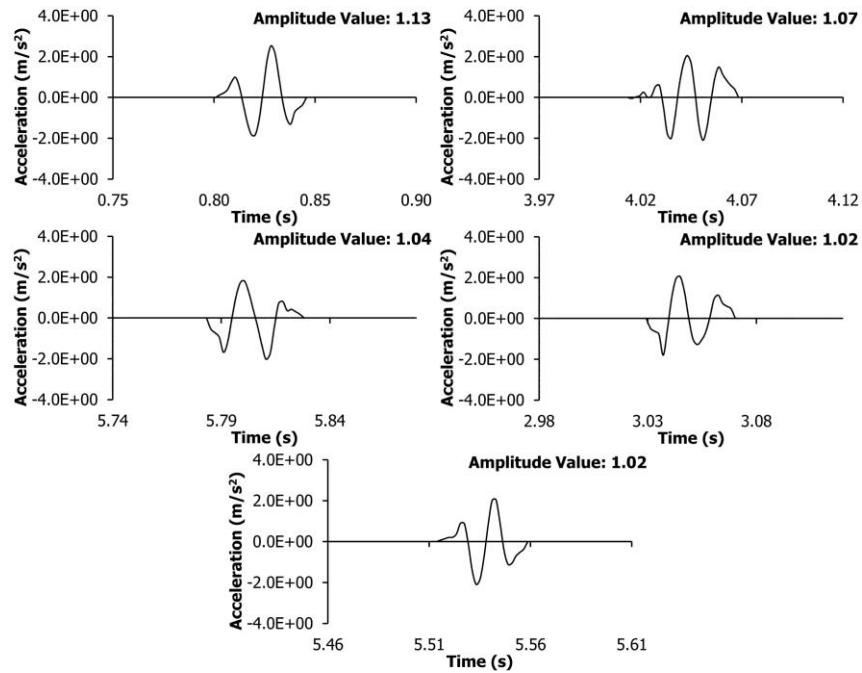


Figure 8.7 Transient vibrations of Tarmac surface identified and extracted within the target frequency interval of 20 to 60 Hz for the acceleration by double time-domain differentiation of displacement

Transient vibrations identified and extracted from the acceleration by double time-domain differentiation of displacement shown in Figure 8.7 can be compared with the transient vibrations in Figure 8.4(a), which show some similar characteristics, such as the same position of transient vibrations in time-domain. For instance, the first transient vibrations in Figure 8.7 have the same position in time-domain with the first transient vibrations in Figure 8.4(a). Meanwhile, some transient vibrations have the same position in time-domain but differ according to the order of their amplitude. For instance, transient vibrations number 2 in Figure 8.7 and transient vibrations number 3 in Figure 8.4(a) have the same position time-domain, but the amplitude of transient vibrations number 2 in Figure 8.7 is higher than transient vibrations number 3 in Figure 8.4(a).

From a comparison of Figure 8.7 and Figure 8.4(a), it is suggested that the transient vibrations identified and extracted from both acceleration by double time-domain differentiation of displacement and accelerometer will lead to different positions in both time-domain and order of amplitude.

The differences in characteristics between transient vibrations identified and extracted from the acceleration by accelerometer and double time-domain differentiation of displacement explained above are used as selection criteria for these test stimuli of the laboratory-based experiment. The stimuli which have less same number of transient vibrations for both position in time-domain and the order of amplitude will be chosen as the test stimuli, namely Country Lane, Broken Lane, Noise and Tarmac.

Meanwhile, Broken road surfaces will be used as a baseline signal because the transient vibrations identified and extracted for both accelerometer and double time-domain differentiation of displacement does not meet with any of the selection criteria stated, as illustrated in Figure 8.8 below:

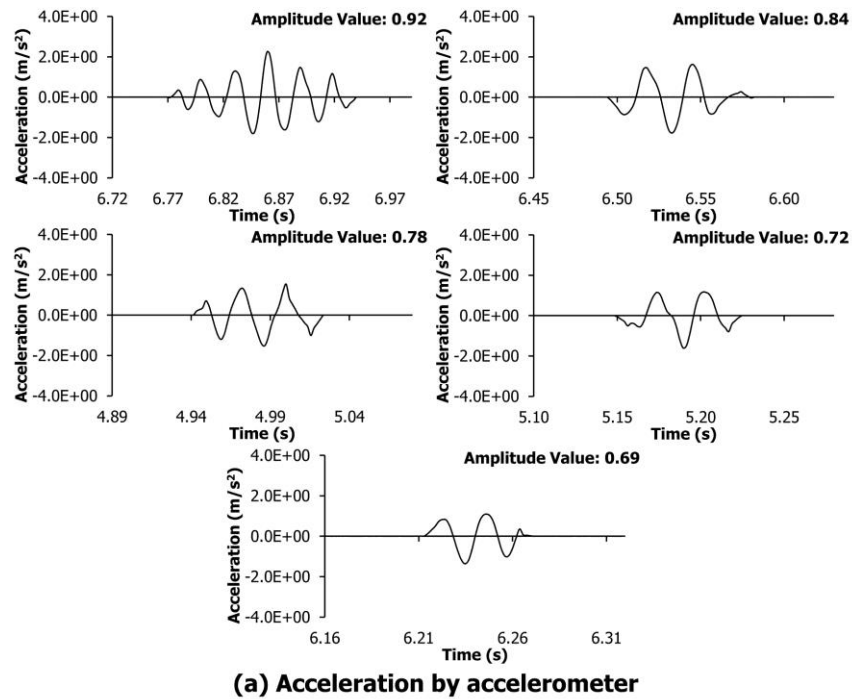
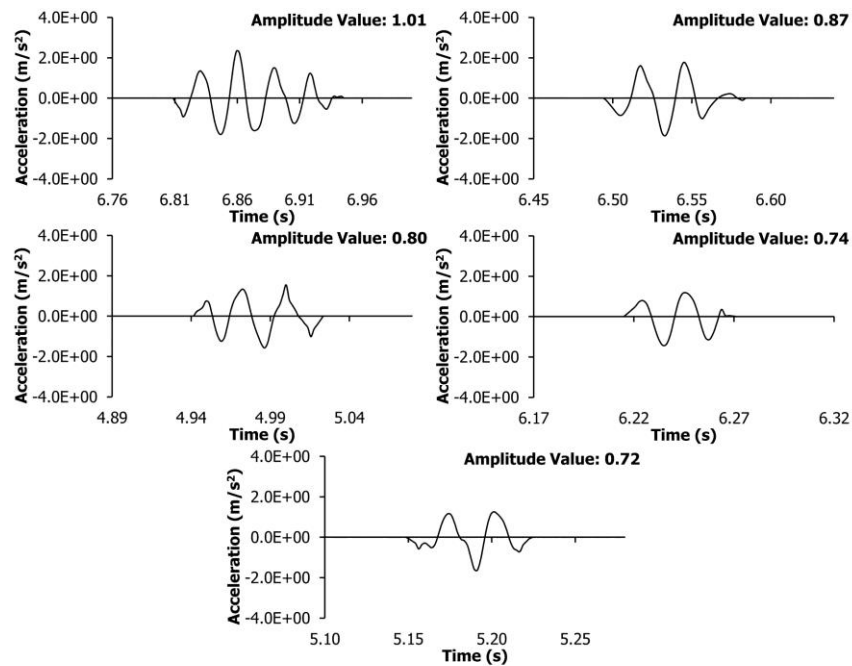


Figure 8.8 Transient vibrations of Broken surface identified and extracted within the target frequency interval of 20 to 60 Hz for the acceleration by double time-domain differentiation of steering wheel displacement vibration



(b) Acceleration by double differentiation of displacement

Figure 8.8 (continued) Transient vibrations of Broken surface identified and extracted within the target frequency interval of 20 to 60 Hz for the acceleration by double time-domain differentiation of steering wheel displacement vibration

From Figure 8.8 it is apparent that two transient vibrations numbers have the same position in time-domain and order of amplitude for both of acceleration by accelerometer and double time-domain differentiation of displacement, these being transient vibrations numbers 2 and 3.

Therefore, the test stimuli used in this laboratory-based experiment will consist of five types of road surfaces for each acceleration vibration signal by accelerometer and double time-domain differentiation of displacement, which is ten test stimuli in total. For each of the ten test stimuli, their first ten transient vibrations have been used to manipulate the signal whereby the transient vibrations were eliminated from the vibration signal. The elimination process for each of the transient vibrations successfully applied high-pass filters and band-pass filters by means of digital Butterworth filters, which were constructed in the LMS[®] TMON software (LMS TMON, 2002).

8.3.2 Test Protocol

Following an advertisement related to the experiment on the “Get Involved” section of the intraBrunel home page, any interested participants were approached by the researcher via email. Each potential participant was given an information sheet and a consent form describing the purpose, procedures, risks and time commitment entailed in their participation. Next, an appointment was made to carry out the experiment with those who declared an interest in participating, and who met the primary requirements of the study (details described in Section 6.4). All participants were volunteers and they had the right to withdraw from the experiment at any time.

Upon their arrival at the laboratory, each of the participants was presented with a short questionnaire to gather information regarding their anthropometry, health and history of previous vibration exposures. Prior to the experiment, each participant was given instructions pertaining to the experimental method, as well as to the laboratory’s health and safety procedures. They were required to remove any articles of heavy clothing such as coats, along with any watches or jewellery. They were then asked to adjust the position of the seat and the angle of the backrest to simulate a driving posture that was as realistic as possible. An example of the participants’ posture during the experiment was shown in Figure 6.2.

Since the grip force applied to the steering wheel has been known to affect the transmission of vibrations to the hand-arm system (Morioka and Griffin, 2009), the participants were required to keep a constant palm grip on the steering wheel using both hands. Finally, they were asked to fix their eyes on a board placed directly in front of the steering wheel simulator, which displayed a photograph of the road surface being studied (see Figure 4.2). The room temperature in the laboratory was maintained within the range of 20 to 25°C to avoid any significant environmental effects on the participants’ skin sensitivities (ISO13091-1, 2001).

Each of the five road surfaces studied consisted of ten manipulated stimuli for both original acceleration vibration by accelerometer and acceleration vibration by double time-domain differentiation of displacement, plus a further ten stimuli chosen randomly from other stimuli sets of the other four road surfaces used as background noise stimuli.

The duration of each individual test stimulus was 10 seconds. Prior to commencing formal testing, the 20-second exposure stimuli of each of the four stimuli types, which would be used later, were provided to participants in order that they could become acquainted with the detection task. Each participant performed 30 detections with approximately 8 minutes for each road surface studied, with a total of 150 detections over the course of the 40 minutes allocated to complete the experiment. Figure 8.9 illustrates the experiment design adapted during this experiment.

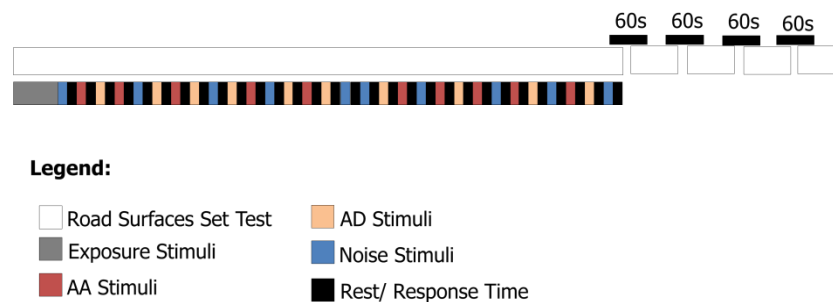


Figure 8.9 Experiment design

During the experiment, the participants were asked to judge the actuated acceleration stimulus transmitted to them through the steering wheel. They were instructed to report “yes” if actuated acceleration stimulus transmitted to them through the steering wheel was coming from the road surface shown on the photograph on the board directly in front of the test bench, and “no” if otherwise. Each series of stimuli was separated by a 5-second gap to allow participants enough time to indicate their detection responses to the stimuli directed at them. Due to the large total number of stimuli detected and the time required, the experiment was designed to take into consideration learning (Giacomin and Woo, 2004) and fatigue effects (Giacomin and Abrahams, 2000; Giacomin and Screti, 2005), and therefore, the order of stimuli arrangements in each series was fully randomised for each participant.

The facility and the protocol of the experiment was approved by the College of Engineering, Design and Physical Sciences Research Ethics Committee, Brunel University (Ref No: 4407-MHR-Nov/2016- 4522-2).

8.3.3 Test Participants

In order to minimise the margin of error in the detection tasks, the laboratory-based experiment described here used a non-probability purposive sampling strategy (Coolican, 2009), with participants who had driving experience of a minimum of two years as a primary characteristic for sample selection, which also served as a controlled parameter because it suggested that they were able to identify changes in a detection task and had more knowledge related to road surfaces (Zhao *et al.*, 2014). Meanwhile, parameters relating to gender and physical body mass (weight and height) were not controlled, as previous research suggested that there were no significant differences between genders in the subjective experience of hand-arm vibration (Mansfield and Griffin, 2000; Neely and Burström, 2006; Jeon *et al.*, 2009).

A total of twenty (n=20) university students participated in this experiment. Both controlled and uncontrolled parameters of the participants are summarised in Table 8.4 below:

Table 8.4 Anthropometrics and driving experience of test participants

		Male (n=10)				Female (n=10)			
		Min	Max	Mean	SD	Min	Max	Mean	SD
Controlled parameters	Driving experience (years)	5	23	10.80	7.27	4	25	8.90	6.90
Uncontrolled parameters	Weight (kg)	58	90	72.54	11.37	48.5	93	60.55	14.37
	Height (m)	1.64	1.80	1.71	0.06	1.56	1.73	1.62	0.05

The mean values and standard deviations of the height and mass of the test participants were close to the 50th percentile values for the UK population (Pheasant and Haslegrave, 2005). The average driving experience of participants in Table 8.4 is over 8 years, which means they can be categorised as experienced drivers, comparable with studies done by Borowsky *et al.*, (2010) who suggested that novice drivers had an average of 2.7 months of driving experience, experienced drivers had an average of 7.3 years, and older drivers had an average of 37.5 years.

8.3.4 Results and Analysis

The results of the experimental tests were analysed using the Theory of Signal Detection of Rating Procedure (Green and Swets, 1966) as the analytical framework. They were summarised by the Hit Rate (%), Detectability Index (d') and Receiver Operating Curve (ROC) points.

Figure 8.10 presents a bar chart containing the percentage of correct detection from both the original steering wheel acceleration vibration by accelerometer and double time-domain differentiation of displacement for each of the five road surfaces investigated in the experiment. A bar chart, or bar graph, is a chart that uses either horizontal or vertical bars to show comparisons among categories (Coolican, 2009). The percentage of correct detection is presented along the ordinate, while the name of the road surface is presented along the abscissa. For each acceleration vibration by accelerometer or acceleration vibration by double time-domain differentiation of displacement road surface stimulus the hit rate was taken to be the proportion of “yes” responses obtained from the stimuli that were actually from the presented road surface. The false alarm rate was taken to be the proportion of “yes” responses obtained from the stimuli that were not derived from the road surface which was being presented.

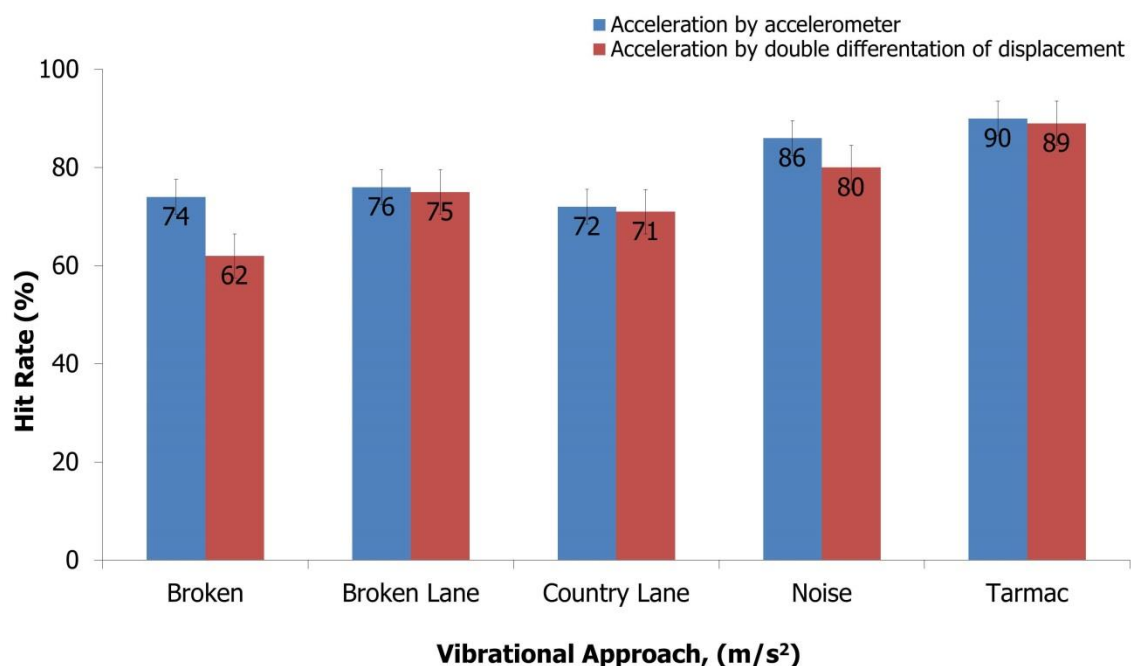


Figure 8.10 Bar chart showing the rate of hit detection for different approaches of steering wheel acceleration vibration

From Figure 8.10 it can be noted that the percentage of correct detection relative to the acceleration vibration by accelerometer was found to be systematically higher than that of the acceleration vibration by double time-domain differentiation of displacement. A two-tailed normally distributed t -test performed between the correct detection response results of the two acceleration vibration approaches suggested that the differences were statistically significant at a 95% confidence level ($p = 0.04 < 0.05$) for all five road surfaces. The results in Figure 8.10 suggest that the correct detection of road surfaces was higher when the original steering wheel acceleration vibration by accelerometer was used as a measurement for the laboratory-based experiment. It seems that these results might be related to the unstable numerical processes that produced a significant amount of noise to the signal produced during the double time-domain differentiation of displacement (Anderssen and Bloomfield, 1974).

Further analysis continues, which is quantified in terms of signal detection sensitivity. Figure 8.11 illustrates the detectability index as a function of the steering wheel acceleration vibration by accelerometer and double time-domain differentiation of displacement. In signal detection theory, the sensitivity of the observer is denoted as d' , and the higher the d' value, the higher the hit rate and lower the number of false alarms (Woo and Giacomini, 2006). In other words, the greater the d' value, the more sensitive is the observer's reaction to the particular signal.

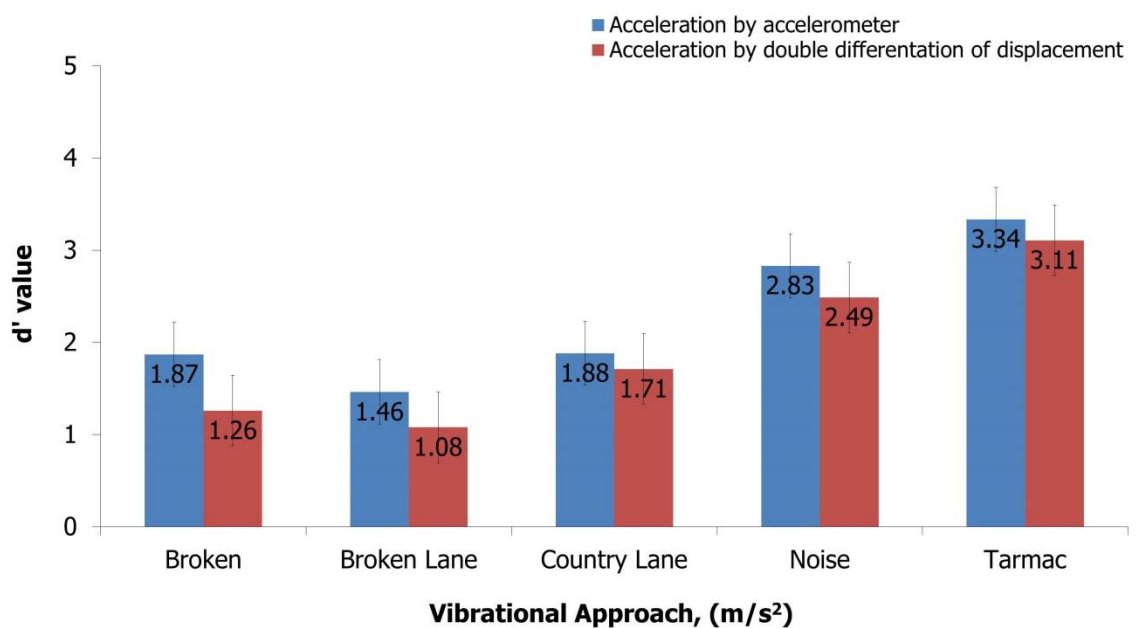


Figure 8.11 Observer sensitivity, d' for different approaches of steering wheel acceleration vibration

Figure 8.11 indicates that acceleration vibration by accelerometer mostly contributes to driver sensitivity in detecting the road surface type. A two-tailed normally distributed t -test performed between the signal detection sensitivity of the two acceleration vibration approaches suggested that the differences were statistically significant at a 95% confidence level ($p = 0.005 < 0.05$) for all five road surfaces. Apart from the unstable signal produced from the double time-domain differentiation processes, these results suggest that the sensitivity of driver road surface detection is affected by the mechanoreceptors in the skin, namely the Pacinian corpuscle receptor.

The pattern of the curve and the qualitative human responses for both hit rate and d' value showed similarities. It can be concluded that the original steering wheel acceleration vibration by accelerometer is the optimal approach for the detection of transient vibrations steering wheel road surface.

Further analyses were conducted by means of ROC distribution points to verify which approaches of steering wheel acceleration vibration can optimise human cognitive detection of the road surface (Green and Swets, 1966).

Figure 8.12 presents the receiver operating characteristic points obtained for each of the 20 test participants for both steering wheel acceleration vibration by accelerometer (●) and double time-domain differentiation of displacement (✕) for each of the five road surfaces studied. The plots contain less than 20 individual points due to the occasional outcome of more than one subject producing identical hit and false alarm rates.

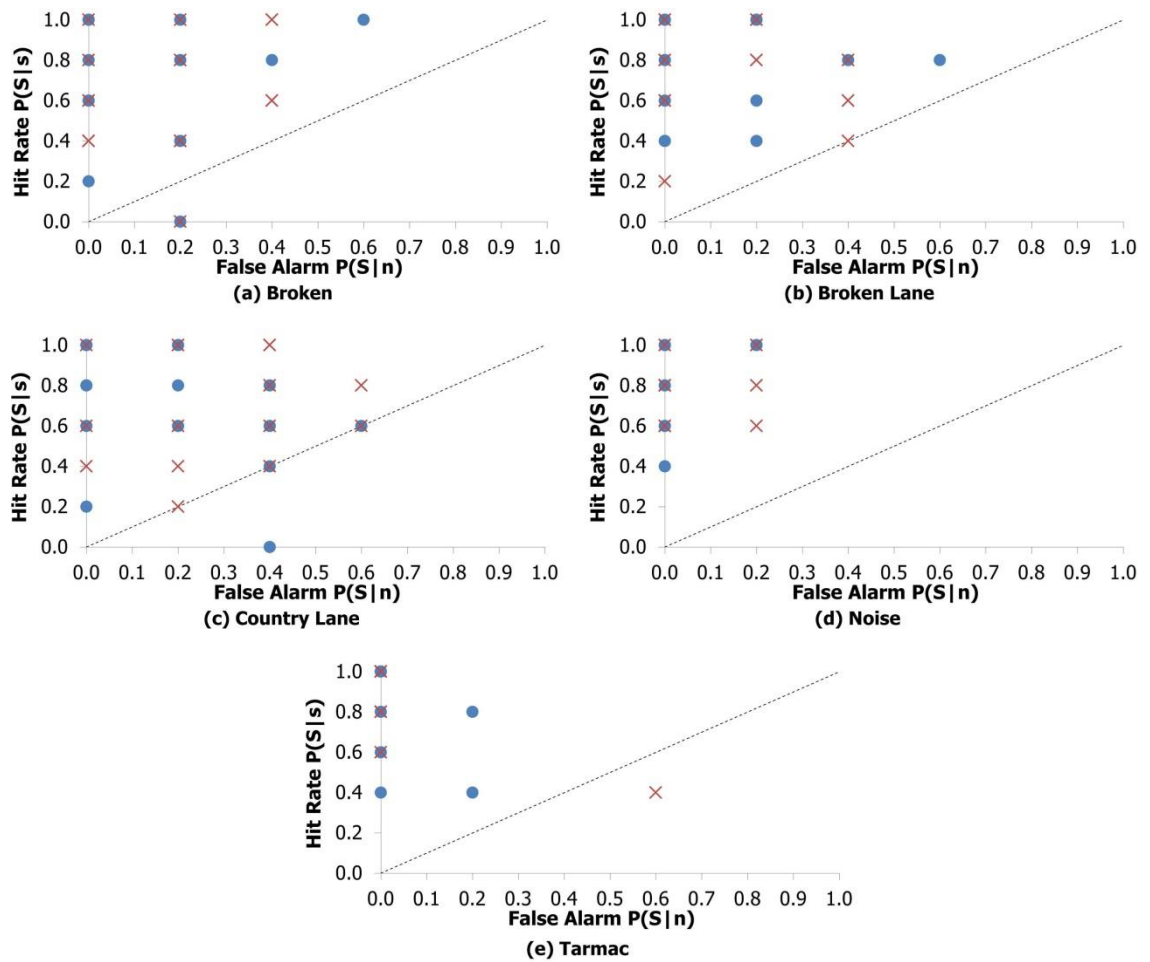


Figure 8.12 ROC points ($n=20$) for different approaches of steering wheel acceleration vibration

In Figure 8.12, the ROC points are distributed closer to the y-axis, which represents a perfect observer (Fawcett, 2006) for both approaches of steering wheel vibration. The experienced drivers who participated in this experiment showed that they were capable of detecting the road surfaces either when vibrations were produced from the original measured by the accelerometer or signals was produced from the double time-domain differentiation of displacement processes.

Taking into account similarities in the results of the hit rate percentages, the detectability index d' and the ROC point distributions, it can be noted that all of the results suggest that the original steering wheel acceleration vibration by accelerometer made it possible for the participants to make correct detections of the road surfaces.

8.3.5 Discussion

This laboratory-based experiment set out to determine which approach of acceleration steering wheel vibration is optimal regarding driver road surface detection. Taking into account the similarities of the results, the findings from this study suggest that acceleration by the accelerometer is the optimal approach for humans to detect road surfaces. In general, the findings of the current study met the general requirement for practical convenience provided by the International Organization for Standardization 5349-1 (2001), by which the magnitude of vibration is measured by means of accelerometers.

According to the biodynamic of the human hand-arm system, the subjective response will increase when the magnitude of the vibration increases (Morioka and Griffin, 2006; 2009), which is affected by the well-known response of the Pacinian mechanoreceptors (Verrillo, 1966; Reynolds *et al.*, 1977). With reference to Table 8.2, the magnitude of vibration for the acceleration by double time-domain differentiation of displacement is higher than that by accelerometer; however, in this laboratory-based experiment it suggests that the higher magnitude of the vibration is not used for driver road surface judgement. A possible explanation of this situation is the numerical differentiation procedures known to lead to unstable processes (Anderssen and Bloomfield, 1974) because the measurements yield intrinsic errors, which are often much less accurate than the limit of the machine used, and there exists the effect of loss of significance (Worden, 1990; Ahnert and Abel, 2007). The unstable processes also contributed to more noises to the signal produced (Worden, 1990), which will lead to excessive artificial stimuli. Therefore, the results are consistent with the nature of the supernormal stimuli concept suggesting that excessive artificial stimuli will eventually lead to a negative response (Dawkins and Guilford, 1995; Drănoiu *et al.*, 2002; ten Cate and Rowe, 2007) to the receiver.

Regarding the excessive artificial stimuli, which in this study is stimuli produced by the double time-domain differentiation of displacement, the experienced drivers who participated in this experiment successfully differentiated between that and the original acceleration by accelerometer. The average driving experience of participants in this experiment is over 8 years, which means they can be generally categorised as

experienced drivers; therefore, it is consistent with previous results suggested by Zhao *et al.* (2014) and Patten *et al.* (2006) stating that those with average driving experience of five to ten years have more knowledge about the road and changing cognitive tasks than novice drivers.

8.4 Conclusion

This chapter described a set of experimental testing activities performed in order to measure the effect of integration and differentiation of steering wheel vibration signals on the identification of transient vibrations and the ability of humans to detect the road surface type.

The first section of this chapter is concerned with determining which signal measurement should be used to perform the identification of transient vibrations contained in steering wheel vibration signals. The numerical-based experiment was designed to determine the effect of time-domain integration on steering wheel vibration road in identifying and extracting the transient vibrations. The original steering wheel acceleration vibration was integrated twice to give velocity and displacement. The comparison of results of this numerical-based experiment shows that the total number of transient vibrations becomes smaller when the time-domain integration is applied, and both shape and oscillation are closer to the definition of transient vibrations stated by the MNMS algorithm.

However, concerning the limitations of the laboratory facility used during this research and for practical convenience, those displacement vibration signals were applied to the double differentiation to produce the acceleration vibration signal. Therefore, the laboratory-based experiment was designed to compare both test stimuli of steering wheel acceleration measured by accelerometer and double time-domain differentiation of displacement, which eventually suggested that the acceleration steering wheel vibration by accelerometer is the optimal approach to be used by humans to detect the road surface type.

Taking into account the findings from both the numerical and laboratory-based experiments in this chapter, the transient vibrations identified and extracted from the original steering wheel acceleration by accelerometer will be used to explain the main time-domain features of steering wheel vibration road surface transient vibrations. An activity to classify the transient vibrations into the same group will bring the research to the answer, which will be discussed in the next chapter.

CHAPTER 9

CLUSTERING CLASSIFICATION ON HIGH-DIMENSIONAL OF TRANSIENT VIBRATIONS

9.1 Introduction

The classification of high-dimensional data is an important problem in many different areas and deals with data of widely varying dimensionality (Maaten and Hinton; 2008) such as difficult to classify such high numbers of dimensional in a meaningful manner (Amir *et al.*, 2013). According to Banchoff (1990), high-dimensional data are known whenever the dataset contains more than four features to describe the dataset itself.

In 2014, Mwangi *et al.* has performed the classification of high-dimensional data to identify hidden population patterns of healthy brain dataset. A dimensionality reduction techniques as a proposed method was able to classify 93 study subjects into two very distinct groups which corresponded to subjects' gender labels. The application of dimensionality reduction techniques can be also found broadly in Geological domain (Balamurali and Melkumyan, 2016) to detect the quality of mineral resources. Since the dimensionality reduction technique allows to easily see the patterns of the dataset, the most significant information within the dataset can be well captured.

Studies that align with the classification of vibrations used different features of time-domain to describe and represent their dataset. For example, Jiang *et al.*, (2014) used twelve features of time-domain to measure the sensitivity of fault diagnosis of rotating machinery which included a most relevant vibrational statistics, namely mean, standard deviation, root mean square, skewness, kurtosis crest factor and Vibration Dose Value (Bellmann, 2002). Those vibrational statistics of time-domain features also have been

used in few studies related to the vibrations data previously such as Güneş *et al.* (2011), Yiakopoulos *et al.* (2011), Soualhi, *et al.* (2014) and Hanus *et al.* (2016).

In spite of that, some questions still remain to be answered such as could the vibrational statistics of time-domain features in previous studies be used to describe the transient vibrations of steering wheel road surface scenarios? What are the possible time-domain features that help to describe the transient vibrations of steering wheel road surface? What are the similarities within the identified transient vibrations of steering wheel road surface?

In this chapter, the high-dimensional reduction techniques associated with clustering methods were used to identifying the possible time-domain features to describe the transient vibrations of steering wheel road surface. It will then go on to the classification process which describing the similarities characteristics of transient vibrations according to their time-domain features.

9.2 Clustering Classification of Steering Wheel Transient Vibrations

Towards Perception Enhancement of steer-by-wire system, several previous studies have put their main objective of studies to determine the optimal steering wheel feedback to drivers (Giacomin and Woo, 2004; 2005; Berber-Solano and Giacomin, 2005; Giacomin and Berber-Solano, 2006; Berber-Solano *et al.*, 2010; Berber-Solano *et al.*, 2013) by quantifying the sensitivity and ability of driver to detect a road surface types. However, the optimal steering wheel vibration feedback gain could not be defined without considerate the features of transient vibrations of road surface. The proposed process is important because the transient vibrations of road surface might comprises the similar features of vibration stimuli which hence bring the similar information and consequently influence sensitivity and ability of driver to detect road surface types.

Thus, the objectives of this numerical-based experiment describes in this chapter are:

- i. To identify the possible time-domain features that can describe the transient vibrations steering wheel road surface
- ii. To cluster the high dimensionality of time-domain features of the transient vibrations steering wheel road surface dataset
- iii. To classify the transient vibrations steering wheel road surface according to their similarity of time-domain features

9.2.1 Pre-processing and Features Extraction of Transient Vibrations

In this numerical-based experiment, the first step is to identify and extract the transient vibrations of steering wheel road surface by using the MNMS algorithm. A total of 256 transient vibrations that been found previously discussed in Chapter 8 (Refer Table 8.1) will be used for classification process. The transient vibrations are deviated from the normal time-domain condition (Giacomin *et al.*, 2000) which abundant importance transient information (Jiang Jiang *et al.*, 2014), hence can be used to describe and represent the dataset to describe the similarities within the identified transient vibrations of road surface.

As till the date, the time-domain features in the context of transient vibrations steering wheel road surface is not yet been fully discussed anywhere, thus, as many as possible features that can be indicate and describe the transient vibrations will be used. However, it is difficult to cluster such high numbers of dimensions in a meaningful manner (Amir *et al.*, 2013). Therefore, t-Distributed Stochastic Neighbor Embedding (t-SNE) is applied to reduce the high numbers of dimensions of transient vibrations dataset into a possible two-dimensional space.

There are two parameters for the implementation of t-SNE namely initial dimensions and perplexity value. Initial dimensions are a preprocessing reduction with PCA to eliminate the most likely noise with skipping components with virtually no variance

which makes the computation faster. In this numerical-based experiment, the initial dimension is set to be seven vibrational statistics of time-domain features, namely mean, standard deviation, root mean square, skewness, kurtosis crest factor and Vibration Dose Value (Bellmann, 2002) since most previous studies used this parameter to describe their vibrations dataset (Güneş *et al.*, 2011; Yiakopoulos *et al.*, 2011; Soualhi *et al.*, 2014; Jiang *et al.*, 2014; Hanus *et al.*, 2016).

Whereas, perplexity value is define as a smooth measure of the effective number of neighbours. According to Maaten and Hinton (2008) typical values of perplexity parameter vary between 5 and 50. The perplexity parameter values of 5, 10, 30 and 50 have been used in this numerical-based experiment. The value of 30 defined as a default value of the Gaussian kernel (Maaten and Hinton, 2008) while 10 is most used in the literatures (Frid and Lavner, 2014; Mwangi *et al.*, 2014).

An implementation of t-SNE algorithm in this study been written in MATLAB R2014a software, and runs on Windows-compatible PCs which provided elsewhere at Maaten and Hinton (2008) used to reduce the seven-dimensionality of time-domain features of transient vibrations to a two-dimensional space and the results shows in Figure 9.1. As suggested by Maaten and Hinton (2008), the minimum times to run the t-SNE was ten times and selects the solution with the lowest Kullback-Leibler divergence of the objective function as a final visualisation. Notably, the axes of the low-dimensional spaces are given in arbitrary units (Maaten and Hinton, 2008) while the label represents the total number of road surfaces (n=10).

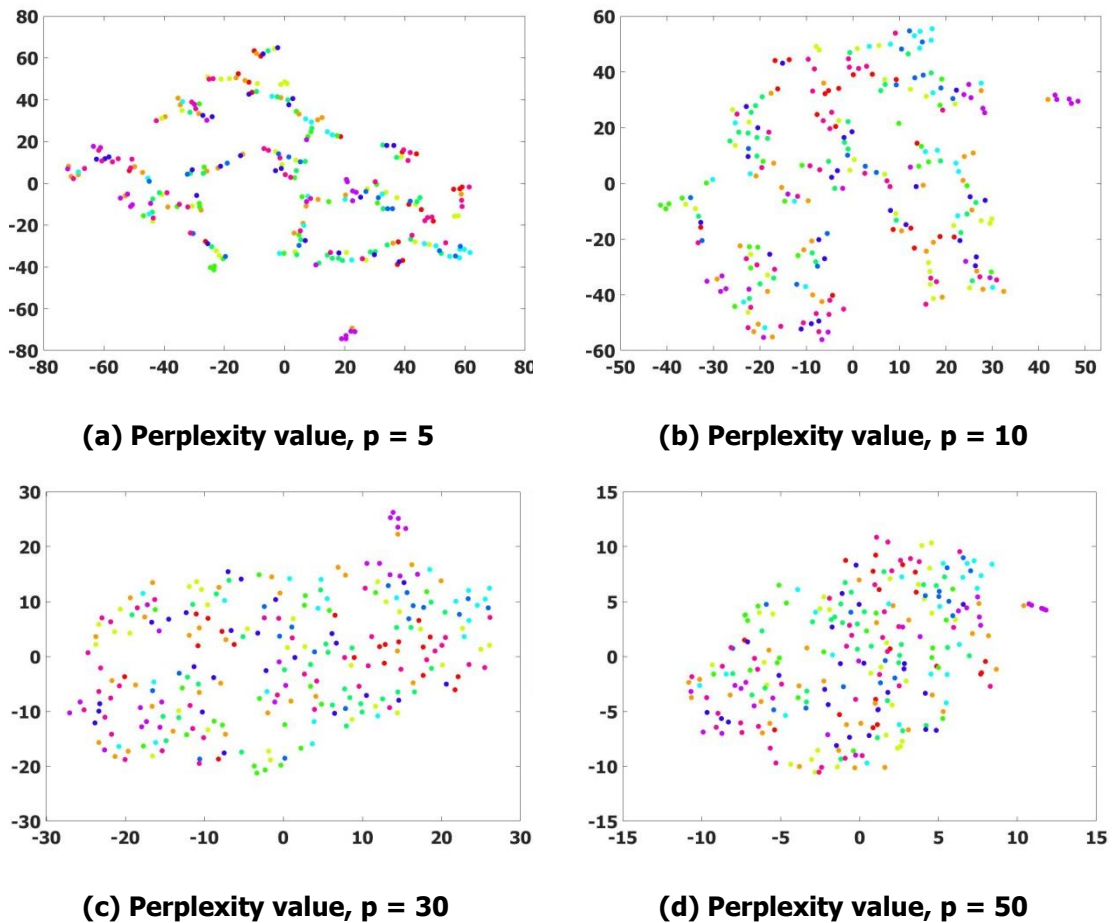


Figure 9.1 Results of seven-dimensional mapping into two-dimensional visualisation of transient vibrations data sets with different perplexity parameter values

In Figure 9.1, the visualisation of the seven-dimensional time-domain features of transient vibrations dataset were constructed by transforming the datasets using different perplexity value to two-dimensional space which clearly shows two different situations of results.

The first situation is the perplexity value 30 and 50, construct a “ball” (Maaten and Hinton, 2008) in which the structure of transient vibrations data is too complex to be captured well in two-dimensional space. In particular, the perplexity values of 30 and 50 are very chaotic which is almost without any class information. Meanwhile, for lowest perplexity value of 5 and 10 outperforms perplexity value of 30 and 50 whereby they reveal that much of the local structure of the datasets is captured however the boundaries of the cluster are ambiguous of which are difficult to identify and interpreted.

From Figure 9.1, the results created two assumptions. In the context of machine learning method performance, the dimensionality reduction techniques can be seen as a loss of information, which could be described by how much these methods lose in constructing models (Platzer, 2013). Hence the first assumption created from the result is by increasing the number of time-domain features to describe transient vibrations dataset, the possibility of information loss will be reduced eventually the dataset can be captured and structured well in two-dimensional space.

In fact, the selection value of perplexity affects the robustness of performance in mapping the high-dimensional into low-dimensional space (Maaten and Hinton, 2008) whereby the lower the value of perplexity, the farther apart the data points will be in the low-dimensional space. Hence, the second assumption created from Figure 9.1 is by decreasing the perplexity value within the range of 5 and 10 the performance of datasets mapping two-dimensional space will increase. The transient vibrations dataset will be able to fit separately and distribute in the two-dimensional space and concurrently allows to easily see the cluster boundaries.

To answer both assumptions, the perplexity value of seven was chosen, while for the initial dimension of transient vibrations dataset will be increased by attempting to use the original time-domain features. Throughout this activity, the original time-domain features are both maximum of the length of transient vibrations (Δt) and the amplitude for each data point. The maximum length of transient that has been identified and extracted from steering wheel road surface vibration was 88 data points, hence the initial dimension of transient vibrations according to the original time-domain vibration brings up to 89 features ($1\Delta t$, 88 amplitudes).

With the purpose of identifying possible time-domain features in describing the similarity of transient vibrations, other than vibrational statistics and original time-domain features, the input of original time-domain features has also been added one by one with the *r.m.s* and the kurtosis of transient vibrations to measure the stability of the classification process. The *r.m.s* will describe the overall energy content of the oscillatory signal, while the kurtosis is used to describe the peak phenomena of the transient vibrations. Therefore, the following section will present the comparison of 1) 7 vibrational statistics of time-domain features; 2) 89 original time-domain features ($1\Delta t$,

88amplitudes); 3) 90 time-domain features which consists of (1 Δ t, 88amplitudes, 1 *r.m.s*); 4) 91 time-domain features which consists of (1 Δ t, 88amplitudes, 1 *r.m.s*, 1 Kurtosis) with perplexity value of seven.

9.2.2 Clustering of Transient Vibrations Using Various of Time-Domain Features

The experiment begins by all possible four time-domain features of transient vibrations as stated previously which are 1) 7 vibrational statistics of time-domain features; 2) 89 original time-domain features (1 Δ t, 88amplitudes); 3) 90 time-domain features which consists of (1 Δ t, 88amplitudes, 1 *r.m.s*); 4) 91 time-domain features which consists of (1 Δ t, 88amplitudes, 1 *r.m.s*, 1 Kurtosis) with perplexity value of seven being input into the t-SNE algorithm. After that, the algorithm returned a new set of variables for each transient vibration in a 'reduced' 2D space.

Figure 9.2 compares the results of two-dimensional space based on 7, 89, 90 and 91-dimensionality of transient vibrations dataset by using t-SNE algorithm with value of perplexity of 7.

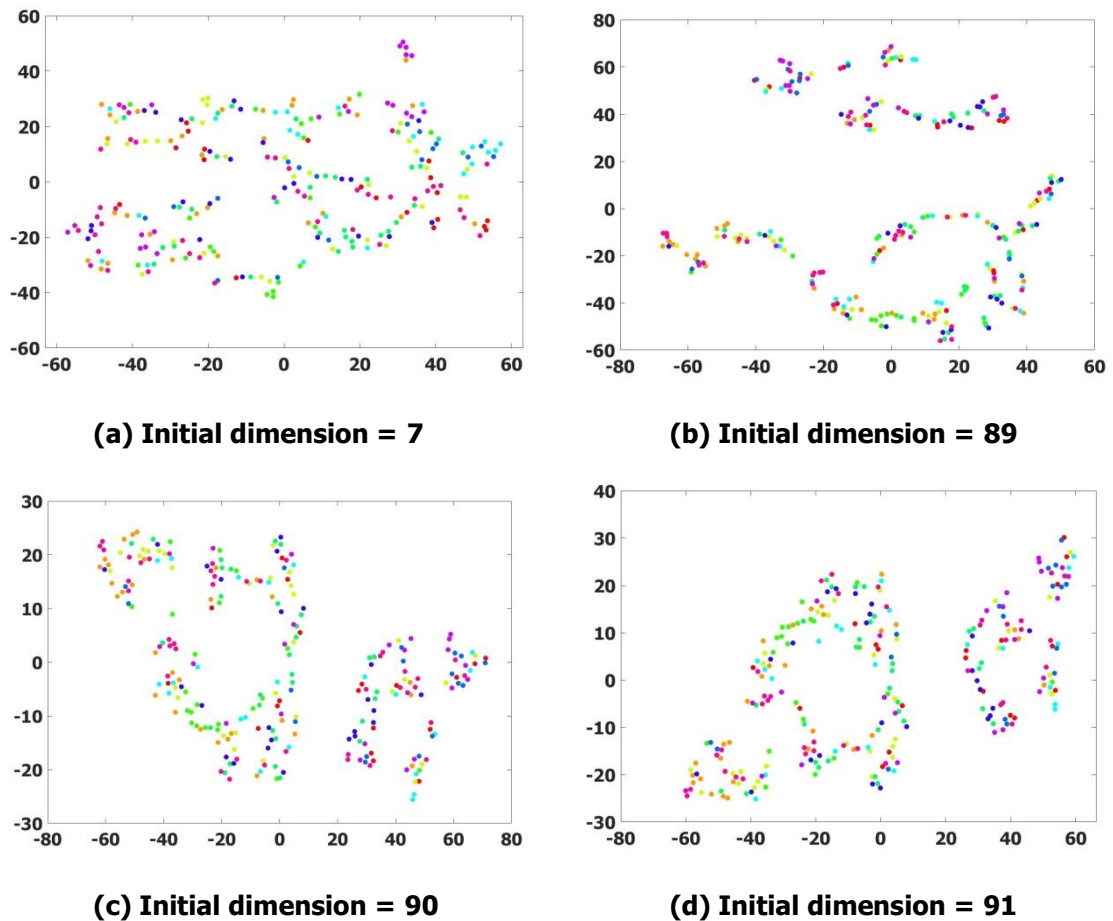


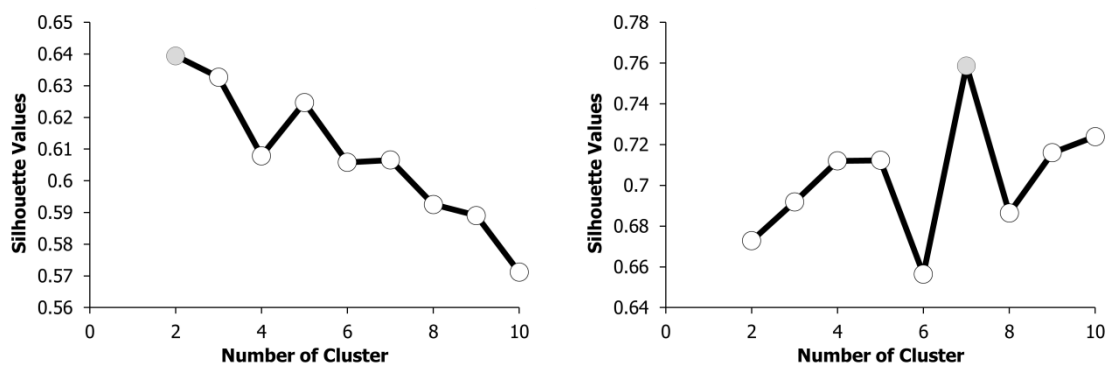
Figure 9.2 Comparing results of 7, 89, 90 and 91-dimensional mapping into 2-dimensional visualisation of transient vibrations data sets with perplexity values of 7

From Figure 9.2, result shown that the 89, 90 and 91 of original time-domain features provided a better clustering in two-dimensional space compared to 7 vibrational statistics of time-domain features. It can be seen from the Figure, the transient vibrations were farther apart in the low-dimensional space. Furthermore, the transient vibrations were able to fit separate and distribute in the two-dimensional space and concurrently allows to easily see the cluster boundaries. These results may suggest that the transient vibrations were well described by the original time-domain features.

9.2.3 Evaluation on 2D Clustering of Time-Domain Features of Transient Vibrations

The evaluation on 2D clustering transient vibrations was done to measuring the consistency of clustering produced by t-SNE algorithm. One approach to measuring the consistency of the clustering structure is by silhouette width index value (Platzer, 2013; Mwangi *et al.*, 2014). The silhouette index value is used to assessing the quality of a cluster solution, enabling to identifying misclassified objects and so distinguishing clear-cut clusters from weak ones (Everitt *et al.*, 2001). The value of silhouette index is range between -1 to 1 whereby the higher value of silhouette index associated with well-defined clusters (Everitt *et al.*, 2001; Mwangi *et al.*, 2014).

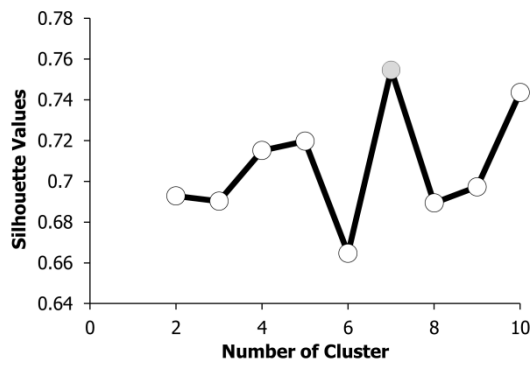
Figure 9.3 and 9.4 shows the silhouette index plotting which reveal the number of cluster of the transformed data of 7, 89, 90 and 91-dimensionality of transient vibrations mapping into 2-dimensional visualisation by using t-SNE algorithm with value of perplexity of 7.



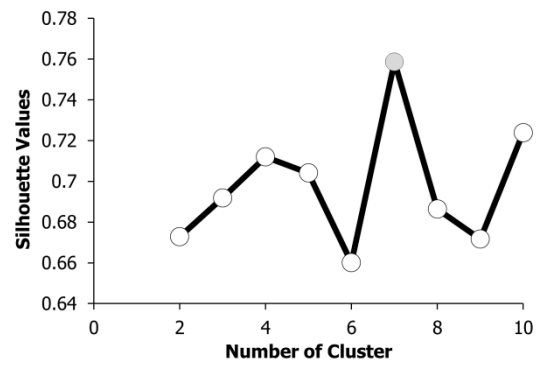
(a) Initial dimension = 7

(b) Initial dimension = 89

Figure 9.3 Silhouette index plotting shows the number of cluster of 7 and 89-dimensional mapping into 2-dimensional visualisation of transient vibrations data sets with perplexity values of 7



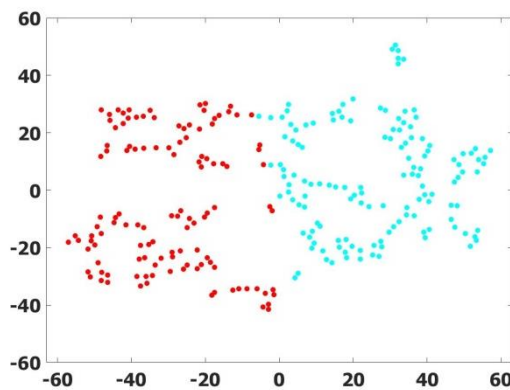
(c) Initial dimension = 90



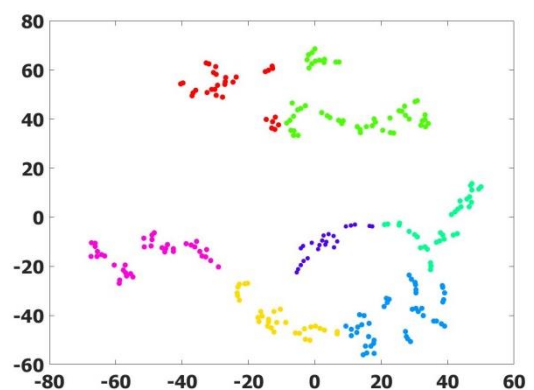
(d) Initial dimension = 91

Figure 9.4 Silhouette index plotting shows the number of cluster of 90 and 91-dimensional mapping into 2-dimensional visualisation of transient vibrations data sets with perplexity values of 7

Following that, the *k*-means algorithm written in MATLAB R2014a software, and runs on Windows-compatible PCs was used to partition the new 2D variables output from t-SNE into cluster (Mwangi *et al.*, 2014). Figure 9.5 and 9.6 below shows the results of the partition process. Notably, the axes of the low-dimensional spaces are given in arbitrary units (Maaten and Hinton, 2008) while the label represents the total number of cluster.

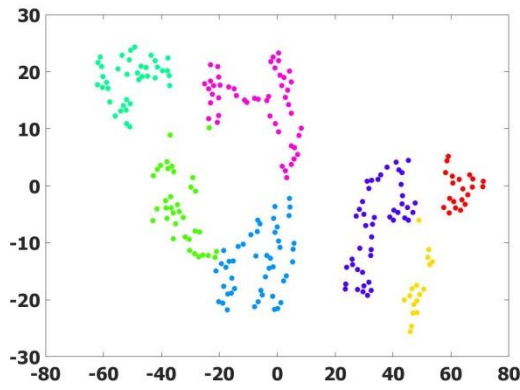


(a) Initial dimension = 7

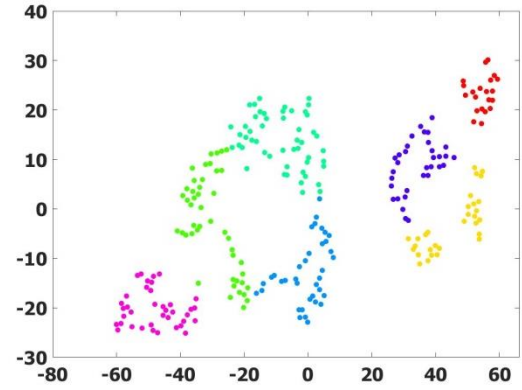


(b) Initial dimension = 89

Figure 9.5 Implementation of *k*-means algorithm to partition the new 2D variables output of 7 and 89-dimensional into cluster



(c) Initial dimension = 90



(d) Initial dimension = 91

Figure 9.6 Implementation of *k*-means algorithm to partition the new 2D variables output of 90 and 91-dimensional into cluster

From both silhouette index plotting partition of 2D t-SNE mapped were clearly shown that the number of cluster become stable when the original time-domain features were used to describe the transient vibrations dataset. Table 9.1 presents the number of transient vibrations in each cluster of 7, 89, 90 and 91-dimensional.

Table 9.1 Number of transient vibrations in each cluster of t-SNE mapped

Cluster	Number of transient vibration for each initial dimension			
	7	89	90	91
1	119	31	21	21
2	137	31	17	30
3		53	36	46
4		34	38	51
5		45	48	37
6		23	46	33
7		39	50	38

Further, a classification error of transient vibrations was measured for each cluster by comparing the Kullback-Leibler (KL) divergences (Maaten and Hinton, 2008). Table 9.2 will shows the classification error of each of 7 89, 90 and 91-dimensional t-SNE mapped clustering. Notably, the figures in the parenthesis are the similar number and percentage of transient vibrations in corresponding cluster.

Table 9.2 Classification error of each of 7 89, 90-dimensional t-SNE mapped

Level of classification error	Classification error on transient vibrations of features = 7		
	KL divergences = 0.08	KL divergences = 0.09	KL divergences = 0.09
Accurate	2 (137)	1 (2; 1.68%)	2 (137; 95.80%)
		2 (135; 98.54%)	
Inaccurate	1 (119)	1 (117; 98.32%)	1 (113; 100%)
		2 (2; 1.46%)	2 (6; 4.20%)

Level of classification error	Classification error on transient vibrations of features = 89		
	KL divergences = 0.71	KL divergences = 0.73	KL divergences = 0.74
Accurate	3 (53)	1 (1, 3.13%) 7 (52, 100%)	1 (12, 32.43%) 7 (41, 87.23%)
	4 (34)	5 (3, 9.09%) 6 (31, 91.18%)	2 (4, 14.81%) 6 (30, 96.77%)
	5 (45)	4 (15, 38.46%) 5 (30, 90.91%)	5 (44, 95.65%) 6 (1, 3.23%)
	7 (39)	2 (38, 100%) 3 (1, 3.57%)	4 (39, 100%)
Inaccurate	6 (23)	3 (20, 71.43%) 6 (3, 8.82%)	2 (23, 100%)
	2 (31)	3 (7, 25%) 4 (24, 61.54%)	3 (29, 100%) 5 (2, 4.35%)
	1 (31)	1 (31, 96.88%)	1 (25, 67.57%) 7 (6, 12.77%)

Level of classification error	Classification error on transient vibrations of features = 90		
	KL divergences = 0.46	KL divergences = 0.44	KL divergences = 0.45
Accurate	4 (38)	7 (38, 100%)	4 (38, 100%)
	5 (48)	5 (47, 95.92%) 6 (1, 3.13%)	2 (14, 28.57%) 5 (34, 87.18%)
	7 (50)	4 (19, 95%) 6 (31, 96.88%)	5 (5, 12.82%) 7 (45, 97.83%)
	1 (21)	1 (21, 84%)	1 (21, 95.45%)
Inaccurate	6 (46)	2 (46, 77.97%)	1 (1, 4.55%) 3 (5, 22.73%) 6 (40, 100%)
	2 (17)	1 (4, 16%) 2 (13, 22.03%)	3 (17, 77.27%)
	3 (36)	3 (33, 100%) 4 (1, 5%) 5 (2, 4.08%)	2 (35, 71.43%) 7 (1, 2.17%)

Level of classification error	Classification error on transient vibrations of features = 91		
	KL divergences = 0.44	KL divergences = 0.46	KL divergences = 0.47
Accurate	7 (38)	7 (38, 97.44%)	7 (38, 97.44%)
	1 (21)	1 (21, 95.45%)	1 (21, 75%)
	4 (51)	3 (1, 3.23%) 5 (50, 98.04%)	3 (6, 17.14%) 5 (45, 98.73%)
	3 (46)	3 (30, 96.77%) 6 (15, 29.41%) 7 (1, 2.56)	3 (29, 82.86%) 4 (16, 69.57%) 7 (1, 2.56%)
Inaccurate	5 (37)	5 (1, 1.96%) 6 (36, 70.59%)	4 (7, 30.43%) 5 (1, 2.17%) 6 (29, 100%)
	2 (30)	2 (16, 45.71%) 4 (14, 51.85%)	1 (4, 14.29%) 2 (26, 46.43%)
	6 (33)	1 (1, 4.55%) 2 (19, 54.29%) 4 (13, 48.15%)	1 (3, 10.71%) 2 (30, 53.57%)

The classification error of transient vibrations measured by calculated the distribution of transient vibration when t-SNE algorithm been run several time. The lowest value of KL been compared with another two lowest values. For example, refer to the table that presented the classification error on transient vibrations of 91 time-domain features, for instance all the 38 transient vibration Cluster 7 (KL = 0.44) was been in the same cluster even if the t-SNE algorithm been run several times. Meanwhile for Cluster 6 (KL=0.44), the transient vibrations separated into three different cluster (1 transient vibration in Cluster 1, 19 transient vibration in Cluster 2, 4 transient vibration in Cluster 4) and two different cluster (3 transient vibration in Cluster 1, 30 transient vibration in Cluster 2) for KL divergence value of 0.4634 and 0.4654, respectively. Consistency of transient vibrations in Cluster 7 is more that 90% which can be categorise as an accurate membership of cluster (Subasi, 2007).

Apart from the classification error, the important information that can be extracted was the value of KL divergences. From the Table shown that the value of KL divergences becomes smaller when the total features of transient vibrations was increase. As mentioned previous, the smaller number of KL divergences describe the best classification of the high-dimensional dataset. Therefore, the result can be suggested that the value of 91 time-domains features (1 Δt , 88amplitudes, 1*r.m.s*, 1 Kurtosis) provided the possible time-domain features that can describe the transient of steering wheel vibrations.

9.2.4 Similarity Characteristics of Transient Vibrations

In the previous section, it can be seen that by using t-SNE algorithm and 91 time-domain features (1 Δt , 88amplitudes, 1*r.m.s*, 1 Kurtosis) was able to clustered the transient vibrations of steering wheel. However, is also important to measure at what level the features can separate the transient vibrations in terms of shape. The shape of transient vibrations is assumed to be important in order to identify the phenomena of driving situation.

Figure 9.7 to 9.10 illustrates the graphic of transient vibrations for each 7 vibrational statistics of time-domain features; 89 original time-domain features (1 Δt ,

88amplitudes); 90 time-domain features which consists of ($1\Delta t$, 88amplitudes, $1r.m.s$);
4) 91 time-domain features which consists of ($1\Delta t$, 88amplitudes, $1r.m.s$, 1Kurtosis).
Because of space limitation, both figure and explanation can be found out at the next few pages.

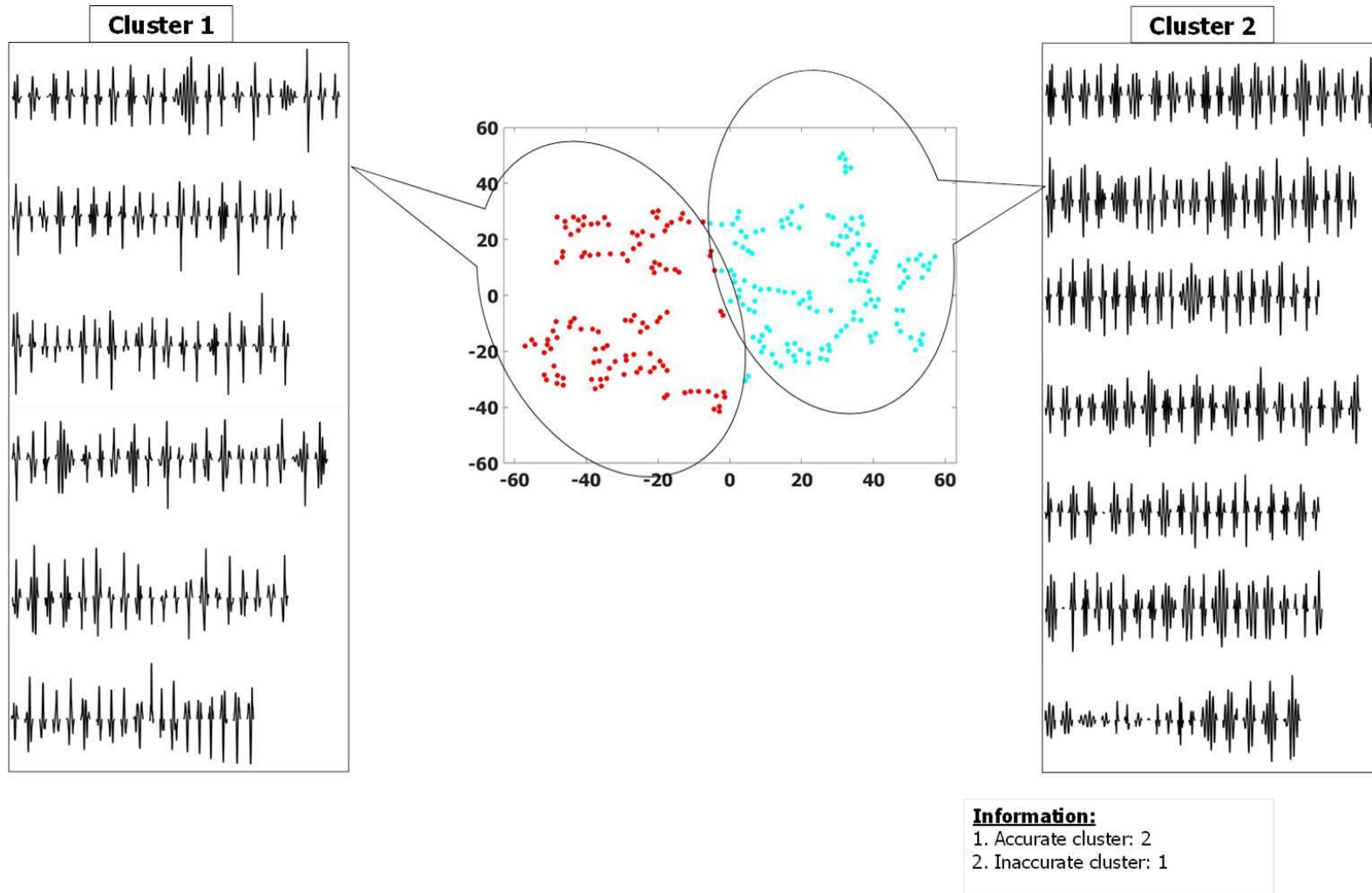


Figure 9.7 Classification of transient vibrations of 7 vibrational statistics of time-domain features

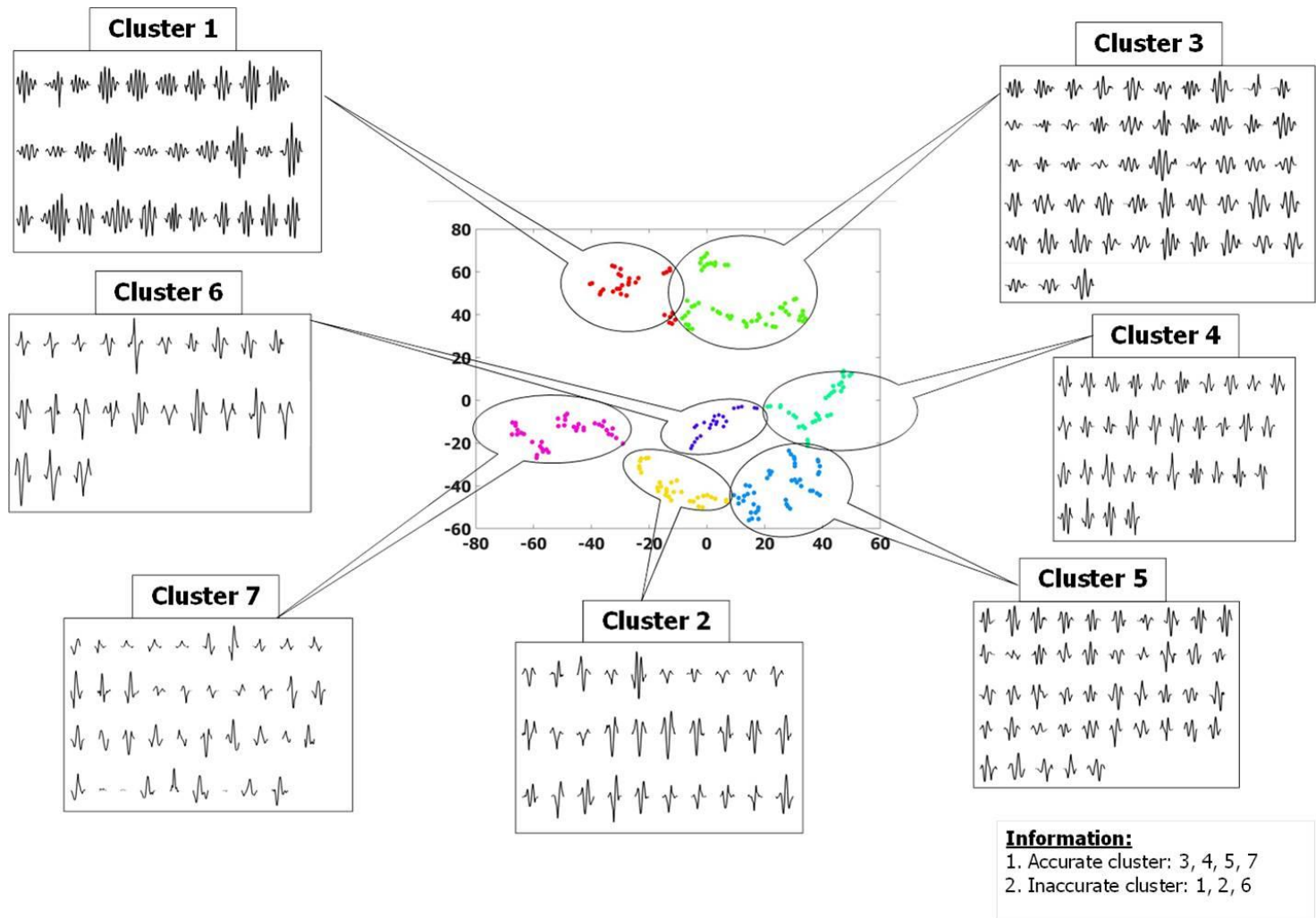


Figure 9.8 Classification of transient vibrations of 89 original time-domain features ($1\Delta t$, 88amplitudes)

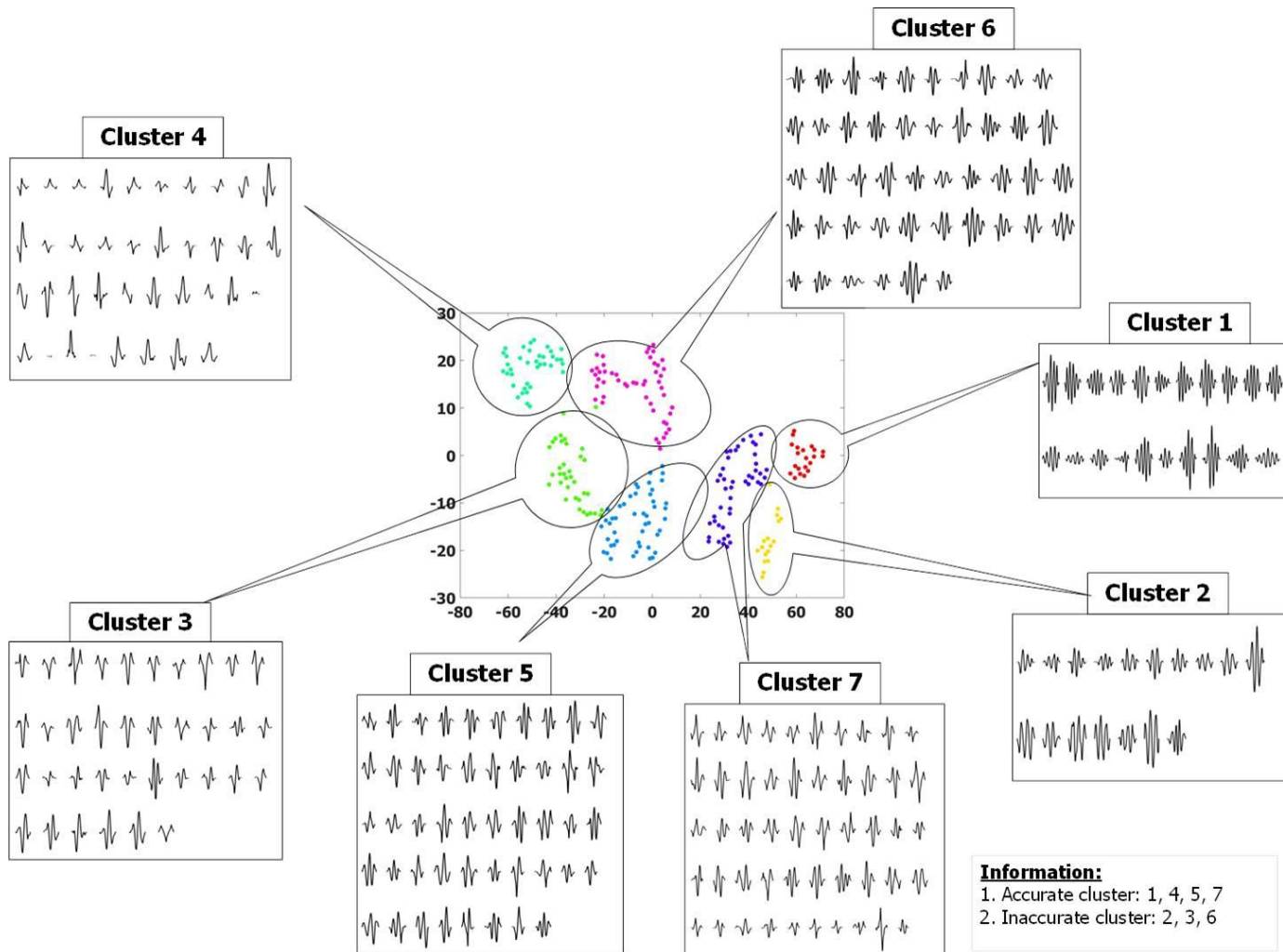


Figure 9.9 Classification of transient vibrations of 90 time-domain features ($1\Delta t$, 88amplitudes, $1r.m.s$)

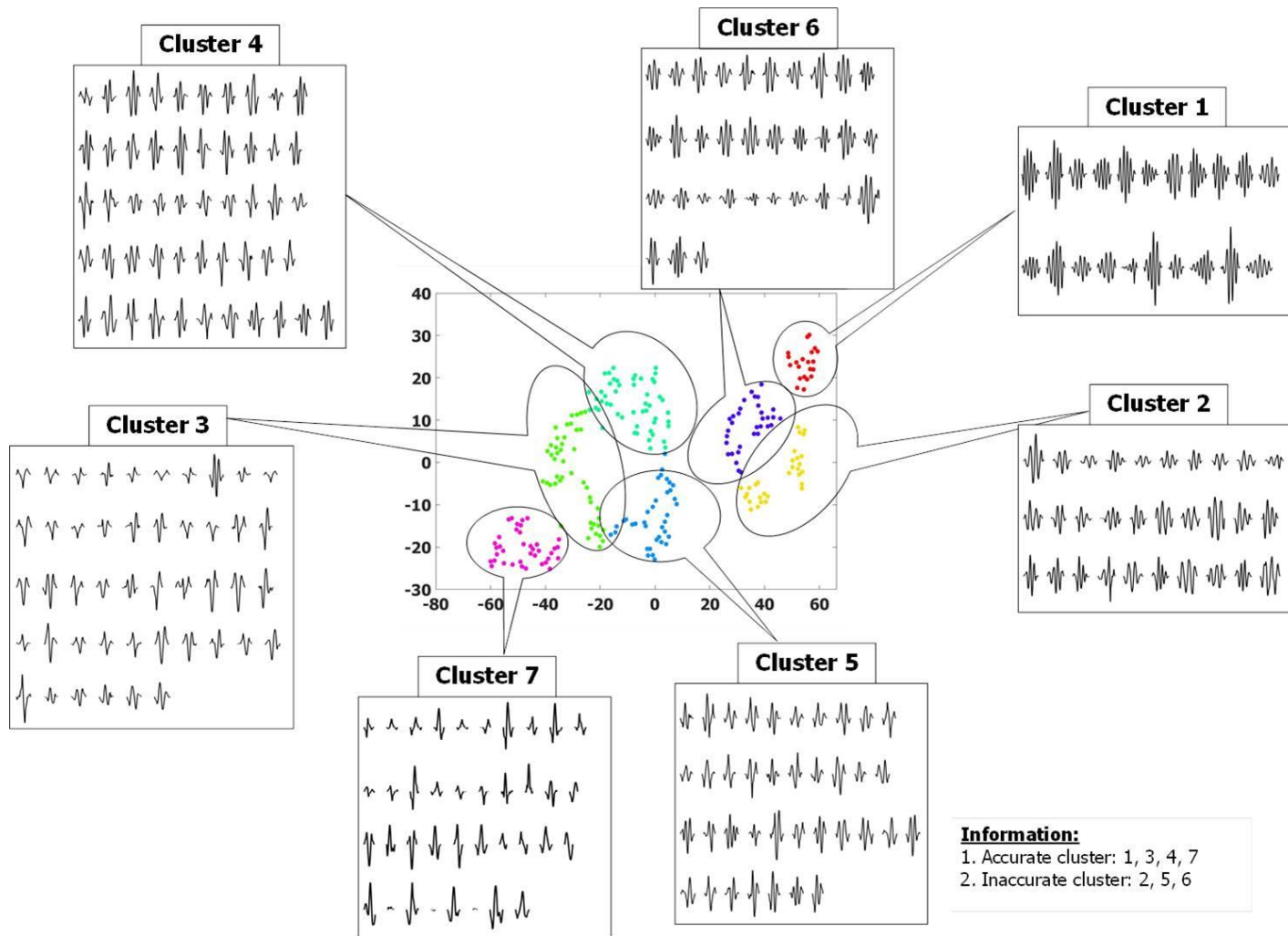


Figure 9.10 Classification of transient vibrations of 91 time-domain features ($1\Delta t$, 88amplitudes, $1r.m.s$, 1Kurtosis).

From the graphics mapping of transient vibrations clustering shown in Figure 9.7 to 9.10, it can be seen that the 91 time-domain features (1 Δt , 88 amplitudes, 1 *r.m.s.*, 1 Kurtosis) are able to separate the transient vibrations significantly more than the other three features (7, 80, 90 time-domain features). By adding the energy (*r.m.s.*) and Kurtosis in the original time-domain features, we can see that the transient vibrations started moving and separated well. For example, transient vibrations in Cluster 1 (89 original time-domain features) mixed up the energy of transient vibration, however after the new features adding up constantly the transient vibrations separated to new Cluster of 1, 2 and 6 for both 90 and 91 time-domain features.

Table 9.3 and Table 9.4 summarise the characteristics of transient vibrations for each cluster resulted by 91 time-domain features (1 Δt , 88 amplitudes, 1 *r.m.s.*, 1 Kurtosis) which shown the best graphic mapping amongst others features (7, 80, 91 time-domain features).

Table 9.3 Vibrational statistics of transient steering wheel vibrations in each cluster for the 91 time-domain features (1 Δt , 88 amplitudes, 1 *r.m.s.*, 1 Kurtosis)

Cluster	Statistics Descriptions									
	np		Δt		No. of cycles		RMS		Kurtosis	
	Min	Max	Min	Max	Min	Max	Min	Max	Min	Max
1	53	88	0.71	1.19	3	6	0.49	2.63	2.07	7.25
2	36	49	0.46	0.66	2	3	0.65	2.50	1.72	5.44
3	19	25	0.25	0.33	1	2	0.45	1.92	2.38	5.38
4	24	34	0.37	0.45	1	3	0.36	1.20	2.11	4.96
5	24	33	0.31	0.44	1	3	0.42	1.29	2.15	4.69
6	35	54	0.72	0.48	2	4	0.47	2.33	2.05	6.07
7	7	23	0.08	0.30	0	2	0.06	1.38	1.64	4.98

Table 9.3 shown that Cluster 1 is contains of transient vibrations with the higher number of cycles and the longest transient, while the Cluster 7 is belongs to transient vibrations with shortest transient. Inaccurate cluster which is Cluster 2, 5 and 6 lies with those transient vibrations which have lowest energy. The higher kurtosis of transient vibration is the membership of Cluster 1. From Table 9.3 can be suggested that Cluster 1 which categorise as accurate cluster membership contained with the transient vibrations which have higher number of duration, cycles, *r.m.s.* and kurtosis.

Table 9.4 Number of transient vibrations of steering wheel road surface contained in each cluster for the 91 time-domain features (1 Δt , 88amplitudes, 1*r.m.s*, 1Kurtosis)

Cluster	Number of transient vibrations of road surfaces									
	Broken	Broken Concrete	Broken Lane	Cobblestone	Concrete	Country Lane	Harsh	Low Bump	Noise	Tarmac
1	3	-	2	6	-	2	6	2	-	-
2	4	1	4	4	3	2	4	5	1	2
3	2	8	3	-	4	2	3	9	11	4
4	3	6	6	2	6	6	2	5	5	10
5	3	2	3	1	4	7	3	3	2	9
6	4	2	2	2	5	3	4	7	-	4
7	-	11	2	2	2	8	1	8	2	2

It can be seen from the data in Table 9.4 that, for accurate cluster (cluster 1,3,4,7), the transient vibrations were most from the Broken Concrete road surfaces value of 25, while the lowest is eight transient vibrations of Broken road surfaces. The results suggest that, the accurate cluster lies with road surfaces which can be broadly classified as mildly non-stationary signals (Giacomin *et al.*, 2000). In additions, Cluster 1, 3, 4 and 7 contained with damaged surfaces, which are commonly found in many areas in the UK. Speeds to drive over damaged surfaces can reach levels of up to 50 km/h (Department of Transport, 2006).

Meanwhile, for inaccurate cluster (cluster 2, 5 and 6) contained significant transient vibrations which greatly exceeded the magnitude when compared to the previous and future sections' magnitude (Ajovalasit *et al.*, 2013) such as Low bump. Low Bump surfaces were basically obstacles placed across a surface in the path of the automobile. According to the Department of Transport (2006), in the UK this kind of obstacle is used in urban areas such as town centres, high streets, residential roads and in the vicinity of schools; therefore, the automobile speed should be less than 40 km/h when driving over the obstacle.

9.3 Discussion

The purpose of the current study discussed in this chapter was to determine the possible features that can be used to clustering and classify the transient vibrations of steering wheel road surface into the similarity of group based on the time-domain features. Notably, t-SNE algorithm provided the 91 time-domains features (1 Δt , 88amplitudes, 1*r.m.s*, 1Kurtosis) with perplexity value of 7 managed to cluster the transient vibrations of steering wheel road surface into their similarity of groups.

The results from the correct classification rate presented in Table 9.1 shows that the accurate classification rate was more than 90% comparable with the classification rate used in the evaluation of EEG signal classification, 94% (Subasi, 2007), audio classification, 90% (Lambrou *et al.*,1998), and image classification, 85% (Foody, 2005). From the results provided, an accurate cluster of 91 time-domain features such as Cluster 1 contained the minimum transient vibrations up to 6 cycles. According to Parsons and Griffin (1988), the perception of vibration for human will be increase when exposed to the multi oscillation of vibration in the range of 0.25 to 0.5-second.

Accurate clusters are mostly contained the damage road surfaces, while inaccurate cluster consists of the significant transient vibrations of the road surfaces signal. These finding are consistent with studies by Yiakopoulos *et al.* (2011), Soualhi, *et al.* (2014) and Hanus *et al.* (2016) which used Kurtosis to distinguish between damaged and healthy transient vibrations of bearing. Moreover, the transient vibrations than been identified and extracted from Broken Concrete using MNMS algorithm which categorise as the most detectable by drivers (Berber-Solano, 2008; Berber-Solano *et al.*, 2010) is also lies in the accurate cluster.

9.4 Conclusion

This chapter has presented the capability of t-SNE algorithm in uncovering relevant natural grouping of transient vibration of steering wheel using high-dimensional time-domain features.

This study was performed in order to identify the possible time-domain features that can describe the transient of steering wheel vibrations. Four different type of features have been compared which were 1) 7 vibrational statistics of time-domain features; 2) 89 original time-domain features ($1\Delta t$, 88amplitudes); 3) 90 time-domain features ($1\Delta t$, 88amplitudes, $1r.m.s$); 4) 91 time-domain features ($1\Delta t$, 88amplitudes, $1r.m.s$, 1 Kurtosis) being input into the t-SNE algorithm with perplexity value of seven. The algorithm returned a new set of transient vibrations in a 'reduced' 2D space. The silhouette index, k -means clustering algorithm and classification error rate were used to evaluate the cluster membership presented in the new 2D space. The results of this study suggest that the transient vibrations of steering wheel road surface can be separated into seven different of groups by using t-SNE algorithm. The possible time-domain of 91 features which contained both original and two most vibrational statistics ($1\Delta t$, 88amplitudes, $1r.m.s$, 1 Kurtosis) with perplexity value of 7 managed to cluster the transient vibrations of steering wheel road surface into their similarity of groups. Furthermore, the characteristics of transient vibrations in accurate clusters might be able to increase the driver road surface detection.

In the next final chapter, this thesis is summarised by revisiting the objectives of this research in order to examine the extent to which they have been achieved. The thesis concludes by highlighting the contributions to the knowledge, discussing the limitations and future research directions.

CHAPTER 10

CONCLUSIONS AND FUTURE RESEARCH

10.1 Introduction

This chapter summarises the main findings and attempts to provide an answer to the research questions posed in the Figure 1.6, Chapter 1. Research activities described from Chapter 6 to Chapter 9 of this thesis were performed in order to answer the research questions and to use the findings to define the time-domain features of road surface transient vibrations that can optimise driver road surface detection. Finally, the research limitations are presented and, accordingly, further research is recommended.

10.2 Key Conclusions of Research Findings

This section presents a summary of the research findings organised in relation to the research questions presented in Section 1.5.1, divided into subsections that address each of the four research questions. Together in this section presents the answer for the main research question constructed for this research.

10.2.1 Research Question 1

What are the principles of transient vibrations detections which can identify the transient vibrations steering wheel road surface?

The main goal of Chapter 6 was to critically review the existing principles of transient vibrations in order to establish a better principle for transient vibrations of steering wheel road surfaces (Objective 1).

Firstly, the transient vibrations of steering wheel road surfaces were identified and extracted by using MNMS algorithm which the results did not really fulfil the definition and criteria of transient vibrations stated in the MNMS algorithm.

To address the issue, the literature review survey related to the principle of transient vibrations detection was conducted to gather better results in identifying the transient vibrations steering wheel road surface. The survey on transient detection analysis included various areas of study, such as seismology studies, biomedical studies and also machinery studies. The alternative principle was measured based on two selection criteria. First, the nature of transient vibrations in signal processing should be the transient vibrations that deviate from the normal background, and also need to be repetitive events before an alternative technique can be found.

Results from the literature review survey suggested that mathematical morphology can be used as an alternative technique to identify and measure the transient vibrations steering wheel road surface. The technique has been used as a post-processing technique to solve the problems of transient vibrations, whereby the start and end points were not at zero. The different widths of structuring elements in mathematical morphology were tested on transient vibrations, but unfortunately the results showed that mathematical morphology does not solve the current problems, and the decision was made to proceed with the MNMS algorithm in identifying the transient vibrations of road surfaces data signals.

10.2.2 Research Question 2

How does the frequency distribution of steering wheel vibration can affect the driver road surface detection?

The main goal of Chapter 7 was to validate the previous guidelines related to the frequency bandwidth of steering wheel vibration feedback. The study has been also ideated as an exposure exercise for the researcher due to the lack of information in this field; therefore it was considered important to perform a check and validation of the previous results.

This study aimed to measure how changes in the vibrational energy within the frequency band of 20 Hz to 60 Hz may affect human cognitive detection of road surface types based on steering wheel vibration. The results suggested that the elimination of the frequency band of 26.32 Hz to 34.64 Hz from the original stimuli played a key role in the human cognitive detection of the relevant road surface. These relationships may be partly explained by the fact that the elimination of this frequency band appeared to produce the highest peaks of vibrational energy resulting from the resonance in the vehicle's dynamic systems such as tyres and steering wheel. Moreover, these results are also consistent with those reported by Fujikawi (1998), Pak *et al.* (1991) and Giacomini *et al.* (2000), who suggested that a frequency band of 23 Hz to 58 Hz is the largest range of frequency that contributes to vehicle dynamics, whereas the band of 20 Hz to 35 Hz is defined by steering wheel resonance (Kulkarni and Thyagarajan, 2001). Therefore, steering feel may be compromised by any reductions or elimination in vibrational energy at the steering wheel in this interval which meet and satisfied with the previous guidelines related to the frequency bandwidth of steering wheel vibration feedback.

The results of ROC points were found scattered which was not consistent with the theory pertaining to the advantages of applying more binary procedures proposed by Swets *et al.* (1961). This result may be explained by the fact that the requirement of a minimum of two years' driving experience was not sufficient to help the participants

detect the vibrations in the different road surface types based on the steering wheel vibrations.

10.2.3 Research Question 3

How does the numerical analysis signal processing can affect the identification and driver detection of transient vibrations steering wheel road surface?

Both numerical and laboratory-based experiment were conducted and discussed in Chapter 8 whereby the objective for both studies were to define the optimal approach for the transient vibrations detection of steering wheel vibration road surface, according to their time-domain waveform (Objective 3). Without taking for granted of the basic numerical analysis of signal processing measurement such as velocity and displacement, hence a set of experimental testing activities performed in order to measure the effect of integration and differentiation of steering wheel vibration signals on the identification of transient vibrations and the ability of humans to detect the road surface type.

The first section of this chapter is concerned with determining which signal measurement should be used to perform the identification of transient vibrations contained in steering wheel vibration signals. The numerical-based experiment was designed to determine the effect of time-domain integration on steering wheel vibration road surface in identifying and extracting the transient vibrations. The original steering wheel acceleration vibration was integrated twice to give velocity and displacement. The comparison of results of this numerical-based experiment shows that the total number of transient vibrations becomes smaller when the time-domain integration is applied, and both shape and oscillation are closer to the definition of transient vibrations stated by the MNMS algorithm.

However, concerning the limitations of the laboratory facility used during this research and for practical convenience, those displacement vibration signals were applied to the double differentiation to produce the acceleration vibration signal. Therefore, the laboratory-based experiment was designed to compare both test stimuli of steering

wheel acceleration measured by accelerometer and double time-domain differentiation of displacement, which eventually suggested that the acceleration steering wheel vibration by accelerometer is the optimal approach to be used by humans to detect the road surface type.

Taking into account the findings from both the numerical and laboratory-based experiments, the transient vibrations identified and extracted from the original steering wheel acceleration by accelerometer will be used to explain the main time-domain features of transient vibrations steering wheel road surface.

10.2.4 Research Question 4

How does the time-domain features construct the similarity group of transient vibrations steering wheel road surface?

The final questions addressed in this research involved with the high-dimensional reduction technique to cluster the transient vibrations steering wheel road surface, according to the similarity of their time-domain features (Objective 4).

In this study, in order to identify the possible time-domain features that can describe the transient of steering wheel vibrations, four different type of features have been compared which were 1) 7 vibrational statistics of time-domain features; 2) 89 original time-domain features (1 Δ t, 88amplitudes); 3) 90 time-domain features (1 Δ t, 88amplitudes, 1r.m.s); 4) 91 time-domain features (1 Δ t, 88amplitudes, 1r.m.s, 1 Kurtosis) being input into the t-SNE algorithm with perplexity value of seven. The algorithm returned a new set of transient vibrations in a 'reduced' 2D space. The silhouette index, *k*-means clustering algorithm and classification error rate were used to evaluate the cluster membership presented in the new 2D space.

From Figure 9.2, result shown that the 89, 90 and 91 of original time-domain features provided a better clustering in two-dimensional space compared to 7 vibrational statistics of time-domain features. It can be seen from the Figure, the transient

vibrations were farther apart in the low-dimensional space. Furthermore, the transient vibrations were able to fit separate and distribute in the two-dimensional space and concurrently allows to easily see the cluster boundaries. These results may suggest that the transient vibrations were well described by the original time-domain features which can be separated into seven different of groups by using t-SNE algorithm.

10.2.5 Main Research Question

What are the time-domain features of road surface transient vibrations that can optimise driver road surface detection?

In Chapter 9 also presented characteristics of time-domain features that can describe the transient vibrations steering wheel road surface whereby eventually provide a definition of design guidelines for perception-enhancing steering wheel vibration feedback (Objective 5).

From the graphics mapping of transient vibrations clustering shown in Figure 9.7 to 9.10, it can be see that the 91 time-domain features (1 Δt , 88amplitudes, 1*r.m.s*, 1Kurtosis) able to separate the transient vibrations significantly more than the other three features (7, 80, 90 time-domain features). By adding the energy (*r.m.s*) and Kurtosis in the original time-domain features, we can see that the transient vibrations started moving and separated well.

Moreover, the results from the correct classification rate presented in Table 9.1 shows that the accurate classification rate of 91 time-domain features was more than 90% comparable with the classification rate used in the evaluation of EEG signal classification, 94% (Subasi, 2007), audio classification, 90% (Lambrou *et al.*,1998), and image classification, 85% (Foody, 2005). From the results provided, an accurate cluster of 91 time-domain features such as Cluster 1 contained the minimum transient vibrations up to 6 cycles. According to Parsons and Griffin (1988), the perception of vibration for human will be increase when exposed to the multi oscillation of vibration in the range of 0.25 to 0.5-second. Apart from that, accurate clusters are mostly

contained the damage road surfaces such as Broken Concrete using MNMS algorithm which categorise as the most detectable by drivers (Berber-Solano, 2008; Berber-Solano *et al.*, 2010) is also lies in the accurate cluster.

Therefore, result suggests that the time-domain features of transient vibrations that can optimise driver road surface detection were found to consist of duration (Δt), amplitude (m/s^2), energy (*r.m.s*) and Kurtosis.

10.3 Research Limitations

As with all research, there are limitations and sources of error which should be considered, the following is a discussion of some of the main issues:

- i. The first significant **limitation was due to the lack of scientific literature** concerning the non-linear classification of transient vibrations, which made this study a real challenge. The fact of being one of the first studies to describe the similarity of transient vibrations in the context of steering wheel road surfaces gives the opportunity to be the first to state the first findings in this field, but it also leads to difficulties in time-domain features selection and statistical analysis due to the lack of analogous studies. However, there are few studies in the literature which can be used to substantiate the choices which were made (Mwangi *et al.*, 2014; Maaten, and Hinton, 2008).
- ii. **The number and selection of the steering vibration stimuli** used to perform the experimental test activities of the thesis (described in the Chapter 5) can be considered a research limitation. The researcher knows that there are several factors which cause a change in the dynamics of the automobile, consequently there are several factors which also cause changes in the steering wheel stimuli such as the type of the automobile (i.e. sport, luxury, compact, lorry), the type of engine (i.e. diesel, gasoline), the suspension type, the tyres pressure, the driving speeds, the type of road surface and the environmental conditions.

- iii. In the laboratory-based experiment where **humans are the test subjects**, there are few possible source of error that might affect the results and finding of the research. In order to minimise the sources of error happened, hence the calibration of the test facilities, the accuracy of the test stimuli reproduction and the test protocol employed during the test activity, which includes: instructions given to the participant, posture of the participant during the test, the number of repetitions of the test stimuli, the duration of each test stimulus, the way to judge each test stimulus and the environmental conditions. A significant effort was made to achieve the greatest possible repeatability in these parameters, thus the results should be considered reliable.

Apart from that, the **driving experience of test subjects** can be considered a source of error and a limitation of the research. It is happened because of the environment of driving a real car is interlinked and can affect in the perception of what is seen, heard or felt. Nevertheless, the isolation of the steering wheel vibration in this research was necessary in order to determine more clearly how much information of the steering feel is store in the human memory and which are the features carrying the main part of the road surface information to the driver.

- iv. In the numerical-based experiment, **the computational error**, memory spaces and processor speed can be considered a source of error and a limitation of the research. As increased the features of transient vibrations and perplexity value, the time required for t-SNE algorithm to provide the results are also increased. Apart from that, the results needed a bigger space to save all the visualisation results. However, since the computational memory capacity and the processer speed were limited therefore the analysis was needed to be terminated if the time to solve taken too long (ie: 10-min per test). In addition, to overcome any computational error, the activities of clustering were use the same computer.

10.4 Research Contributions

Figure 10.1 summarises the multiple categories of groups that can potentially be benefited from the research described in this thesis:

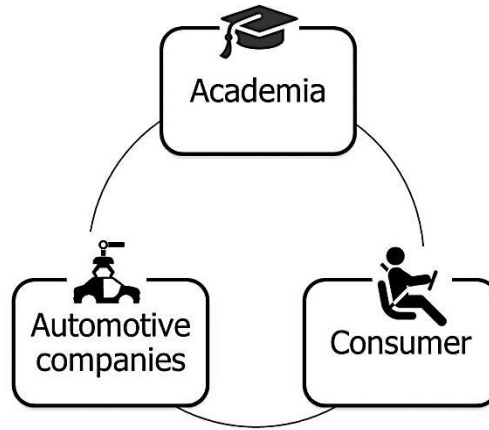


Figure 10.1 Groups that could benefit from the research

For the academia group, this research will enhance the current Mildly Nonstationary Mission Synthesis (MNMS) algorithm. By adding the classification stages in the MNMS algorithm to analyse the structure of each transient vibrations road surface, the complete documentation of road features can be achieved. The combination of transient vibrations analysis and mission synthesis would serve as an intelligent black-box recorder for testing and monitoring applications. Moreover, since the classification process described in this research is the very first work in the context of steering wheel vibration road surfaces, it can be used as a clustering automated method for future work on transient vibration road surface.

Meanwhile, the automotive companies will benefit from this research as it will enable them to provide sophisticated automation steering systems that incorporate both comfort and information from vibration stimuli, in future steer-by-wire systems and also in current steering power systems. By utilising the characteristics of accurate transient vibrations clustered, the real time research development can proposed the production of car body control which able to read the road surfaces such as pothole, big bumps and eventually adjust the suspension system accordingly.

The last group that will potentially benefit from this research are drivers. After the automotive companies have provided steering wheel feedback that incorporates the information transmitted from the steering wheel vibration, the driver will be able to distinguish the vibration stimuli – either the vibration related to the environment or to problems with the vehicle’s components. This can achieve by removing the range of 20 – 60 Hz which the range of transient vibrations of road surfaces been identified and extracted from the original road surfaces vibrations.

10.5 Future Research

In this research work, the necessary process to classify the transient vibrations of steering wheel such as algorithm to identified and extracted the transient vibrations, a better approach human to detected the road surface vibrations and time-domain features to describe the similarity of transient vibrations were wisely been done, further investigation and test experiments are required in order to define the system specifications for a steering perception enhancement system for automobiles. A few important areas in which further research would be beneficial are listened below:

- i. **Completing the documentation of road surfaces:** By adding a classification stage to the MNMS algorithm to analyse the structure of each transient vibrations, hence can provides a complete documentation of the road features. The combination of transient vibrations analysis and mission synthesis would serve as an intelligent black- box recorder for testing and monitoring applications.
- ii. **Human perception on the similarity of transient vibrations:** Despite of successful t-SNE algorithm to distinct the transient vibrations according the time-domain features, human perception should also be consider in the loop of clustering validation to ensure that the machine that been build are suit to user’s subjective viewpoint. The validation is expected to be achieved by means of paired-comparison methods. The criteria of choosing the transient vibrations to be compared need to consider the perceptual moments of vibrations in order to ensure that the vibrations can be perceived by human. Other than that, the pair-

comparison needs to include both within and between the clusters provided by t-SNE algorithm.

REFERENCES

- AA1Car, 2016. Electronic Throttle Control. Available at: <http://www.aa1car.com/library/throttle-by-wire.htm>. (Accessed: 28 December 2016).
- Abdullah, S., Choi, J.C., Giacomini, J.A. and Yates, J.R., 2006. Bump extraction algorithm for variable amplitude fatigue loading. *International Journal of Fatigue*, 28(7), pp.675-691.
- Adewusi, S. A., Rakheja, S., Marcotte, P. and Boutin, J., 2010. Vibration transmissibility characteristics of the human hand-arm system under different postures, hand forces and excitation levels. *Journal of Sound and Vibration*, 329(14), 2953–2971.
- Ahnert, K. and Abel, M., 2007. Numerical differentiation of experimental data: local versus global methods. *Computer Physics Communications*, 177(10), pp.764-774.
- Ajovalasit, M. and Giacomini, J., 2003. Analysis of variations in diesel engine idle vibration. *Proceedings of the Institution of Mechanical Engineers, Part D: Journal of Automobile Engineering*, 217(10), pp.921-933.
- Ajovalasit, M. and Giacomini, J., 2009. Human subjective response to steering wheel vibration caused by diesel engine idle. *Proceedings of the Institution of Mechanical Engineers, Part D: Journal of Automobile Engineering*, 219(4), pp. 499–510.
- Ajovalasit, M. and Giacomini, J., 2009. Non-linear dependency of the subjective perceived intensity of steering wheel rotational vibration. *International Journal of Industrial Ergonomics*, 39(1), pp.58-67.
- Ajovalasit, M., Shabani, A., Tajadura, A. and Giacomini, J., 2012. Affective Reactions to Vibro-Tactile Events: A Case Study in Automotive Applications'. *International Journal of Vehicle Noise and Vibration*.
- Ajovalasit, M., Tajadura-Jiménez, A., Shabani, A. and Giacomini, J., 2013. Human emotional response to steering wheel vibration in automobiles. *International Journal of Vehicle Noise and Vibration*, 9(1-2), pp.109-128.

- Alex, D., 2014. Infiniti's New Steering System is a big step forwards – unless you love cars. Available at: <https://www.wired.com/2014/06/infiniti-q50-steer-by-wire/> (Accessed: 30 August 2016).
- Amberkar, S., Kushion, M., Eschtruth, K. and Bolourchi, F., 2000. *Diagnostic development for an electric power steering system* (No. 2000-01-0819). SAE Technical Paper.
- Amir, E.A.D., Davis, K.L., Tadmor, M.D., Simonds, E.F., Levine, J.H., Bendall, S.C., Shenfeld, D.K., Krishnaswamy, S., Nolan, G.P. and Pe'er, D., 2013. viSNE enables visualization of high dimensional single-cell data and reveals phenotypic heterogeneity of leukemia. *Nature biotechnology*, 31(6), pp.545-552.
- Amit, G., Gavriely, N. and Intrator, N., 2009. Cluster analysis and classification of heart sounds. *Biomedical Signal Processing and Control*, 4(1), pp.26-36.
- Amman, S., Pielemeier, B., Snyder, D. and Toting, F., 2001. *Road vibration investigation using the ford vehicle vibration simulator* (No. 2001-01-1572). SAE Technical Paper.
- Anderson, J.R., 1990. *Cognitive psychology and its implications*. WH Freeman/Times Books/Henry Holt & Co.
- Anderssen, R.S. and Bloomfield, P.E.T.E.R., 1974. Numerical differentiation procedures for non-exact data. *Numerische Mathematik*, 22(3), pp.157-182.
- Atkinson, R. C., and Shiffrin, R. M., 1971. *The control processes of short-term memory*. Institute for Mathematical Studies in the Social Sciences, Stanford University.
- Atkinson, R.C. and Shiffrin, R.M., 1968. Human memory: A proposed system and its control processes. *Psychology of learning and motivation*, 2, pp.89-195.
- Automotive news, 2016. JTEKT targets diversification and steer-by-wire technology. Available at: <http://www.autonews.com/article/20150803/OEM10/308039986/jtekt-targets-diversification-and-steer-by-wire-technology>. (Accessed: 17 October 2016).
- Badawy, A., Zuraski, J., Bolourchi, F. and Chandy, A., 1999. *Modelling and analysis of an electric power steering system* (No. 1999-01-0399). SAE Technical Paper.
- Baddeley, A. D., & Logie, R. H., 1999. Working memory: The multiple-component model. In A. Miyake & P. Shah (Eds.), *Models of working memory* (pp. 28–61). New York: Cambridge University Press.
- Baddeley, A. D., 1990. *Human memory: Theory and practice*. Boston: Allyn and Bacon.
- Baddeley, A. D., 2002. Is working memory still working?. *European psychologist*, 7(2), p. 85.

- Baddeley, A., 1992. Working memory. *Science*, 255(5044), p. 556.
- Baddeley, A., 2000. The episodic buffer: a new component of working memory?. *Trends in cognitive sciences*, 4(11), pp.417-423.
- Baddeley, A., 2003. Working memory and language: An overview. *Journal of communication disorders*, 36(3), pp.189-208.
- Baddeley, A.D., 1986. *Working memory*. Oxford. England: Oxford Uni.
- Baddeley, A.D., 1997. *Human memory; Theory and practice* (Rev. ed.). East Sussex, England: Psychology Press.
- Baird, J.C. and Noma, E.J., 1978. *Fundamentals of scaling and psychophysics*. John Wiley & Sons.
- Balamurali, M. and Melkumyan, A., 2016, October. t-SNE Based Visualisation and Clustering of Geological Domain. In *International Conference on Neural Information Processing* (pp. 565-572). Springer International Publishing.
- Banchoff, T.F., 1990. *Beyond the Third Dimension: Geometry. Computer Graphics and Higher Dimensions*, WH Freeman, New York.
- Bannister, F. and Remenyi, D., 2000. Acts of faith: instinct, value and IT investment decisions. *Journal of information Technology*, 15(3), pp. 231–241.
- Barsalou, L. W., 1983. Ad hoc categories. *Memory & Cognition*, 11, 211–227.
- Bau, O., Poupyrev, I., Israr, A. and Harrison, C., 2010, October. TeslaTouch: electrovibration for touch surfaces. In *Proceedings of the 23rd annual ACM symposium on User interface software and technology* (pp. 283-292). ACM.
- Bedner, E.J. and Chen, H.H., 2004. *A supervisory control to manage brakes and four-wheel-steer systems* (No. 2004-01-1059). SAE Technical Paper.
- Bekesy, G.V., 1940. The neural terminations responding to stimulation of pressure and vibration. *Journal of Experimental Psychology*, 26(5), p.514.
- Bellet, T., Bailly, B., Mayenobe, P. and Georgeon, O., 2007. Modelling Driver Behavior in Automotive Environments. *Critical Issues in Driver Interactions with Intelligent Transportation Systems. Cognitive Modelling and Computational Simulation of Driver Mental Activities*. Benmimoun, A.(2004). *Der Fahrer als Vorbild für Fahrerassistenzsysteme*.
- Bellezza, F., 1994. Chunking. *RAMACHANDRAN, VS (Ed.) Encyclopedia of human behavior*, pp.579-589.
- Bellmann, M.A., 2002. Perception of whole-body vibrations: From basic experiments to effects of seat and steering-wheel vibrations on the passenger's comfort inside

- vehicles. *Fachbereich Physik der Universitaet Oldenburg, Shaker Verlag, Aachen*. PhD thesis.
- Bendat, J.S. and Piersol, A.G., 2011. *Random data: analysis and measurement procedures* (Vol. 729). John Wiley & Sons.
- Berber-Solano, T. P., Ajovalasit, M. and Giacomini, J., 2010. Facilitating the driver detection of road surface type by selective manipulation of the steering wheel acceleration signal. *Proceedings of the IMechE, Part D – Journal of Automobile Engineering*. Vol. 224 (10): 1321–1333.
- Berber-Solano, T. P., Giacomini, J. A. and Ajovalasit, M., 2013. Effect of steering wheel acceleration frequency distribution on detection of road type. *Ingeniería mecánica, tecnología y desarrollo*, Vol. 4, No.4, pp. 145–151.
- Berber-Solano, T.P. and Giacomini, J.A., 2005. Perception enhancement system for automotive steering. *Annual Conference of the European Association of Cognitive Ergonomics (EACE 2005)*. Chania, Crete, Greece. Sept. 29 to Oct. 1.
- Berber-Solano, T.P., 2008. Evaluation of the human cognitive detection of road surfaces based on the feedback vibrations provided by the automobile steering wheel. *The University of Sheffield*. PhD thesis.
- Bianchini, E., 2005. *Active Vibration Control of Automotive Steering Wheels* (No. 2005-01-2546). SAE Technical Paper.
- Biggs, J. and Srinivasan, M.A., 2002. Tangential versus normal displacements of skin: Relative effectiveness for producing tactile sensations. In *Haptic Interfaces for Virtual Environment and Teleoperator Systems, 2002. HAPTICS 2002. Proceedings. 10th Symposium on* (pp. 121-128). IEEE.
- Blincoe, L. J., Miller, T. R., Zaloshnja, E., & Lawrence, B. A., 2015. The economic and societal impact of motor vehicle crashes, 2010. (Revised) (Report No. DOT HS 812 013). Washington, DC: National Highway Traffic Safety Administration.
- Bolanowski Jr., S. J., Gescheider, G. A., Verrillo, R. T. and Checkosky, C.M., 1988. Four channels mediate the mechanical aspects of touch, *Journal of the Acoustical Society of America*, 84(5), pp. 1680–1694.
- Borowsky, A., Shinar, D. and Oron-Gilad, T., 2010. Age, skill, and hazard perception in driving. *Accident Analysis & Prevention*, 42(4), pp.1240-1249.
- Botella, F., Rosa-Herranz, J., Giner, J.J., Molina, S. and Galiana-Merino, J.J., 2003. A real-time earthquake detector with prefiltering by wavelets. *Computers & Geosciences*, 29(7), pp.911-919.

- Bouchon, M., Bouin, M.P., Karabulut, H., Toksöz, M.N., Dietrich, M. and Rosakis, A.J., 2001. How fast is rupture during an earthquake? New insights from the 1999 Turkey earthquakes. *Geophysical Research Letters*, 28(14), pp.2723-2726.
- Brakebywire, 2016. Brake by wire advantages. Available at: <http://www.brakebywire.com/brake-by-wire-advantages.html> (Accessed: 28 December 2016).
- Brannon, L., & Feist, J., 2000. *Health psychology: An introduction to behavior and health*. 4th ed, Belmont, CA: Wadsworth.
- Brosch, T., Pourtois, G. and Sanders, D., 2010. The perception and categorization of emotional stimuli: A review. *Cognition and Emotion*, 24, 377–400.
- Brown, J., 1958. Some tests of the decay theory of immediate memory. *Quarterly Journal of Experimental Psychology*, 10(1), pp. 12–21.
- Bruner, J. S., Goodnow, J. J. and Austin, G. A., 1956. A study of thinking. New York, NY: Wiley.
- Bruscella, B., Rouillard, V. and Sek, M., 1999. Analysis of road surface profiles. *Journal of Transportation Engineering*, 125(1), pp.55-59.
- BS 6840-2:1993, IEC 60268-2:1987: *Sound system equipment. Glossary of general terms and calculation methods* 1993, British Standards Institute.
- BS 6842:1987: *Guide to measurement and evaluation of human exposure to vibration transmitted to the hand* 1987, British Standards Institute.
- BS 7085:1989: *Guide to safety aspects of experiments in which people are exposed to mechanical vibration and shock* 1989, British Standards Institute.
- Buchanan, J. and Kock, N., 2001. Information overload: A decision making perspective. In *Multiple Criteria Decision Making in the New Millennium* (pp. 49–58). Springer Berlin Heidelberg.
- Burrus, C.S., Gopinath, R.A. & Guo, H. 1998, *Introduction to wavelets and wavelet transforms: a primer*, Prentice Hall, Upper Saddle River, N.J
- Cambridge Advanced Learner's Dictionary, 2008, Cambridge Dictionary 3rd Edition, Cambridge: Cambridge University Press.
- Card, S., Moran, T. and Newell, A., 1986. The model human processor. In *Human of perception and human performance*, 2nd Edition. New York: Willey.
- Chatterjee, P. and Milanfar, P., 2009. Clustering-based denoising with locally learned dictionaries. *IEEE Transactions on Image Processing*, 18(7), pp.1438-1451.

- Checkosky, C. M. and Bolanowski Jr S. J., 1992. The effects of stimulus duration on the response properties of Pacinian corpuscles: Implications for the neural code, *Journal of the Acoustical Society of America*, 91, pp. 3372–3380.
- Cheng, C.K., Liang, T.J., Chen, J.F., Chen, S.D. and Yang, W.H., 2004, May. Novel approach to reducing the inrush current of a power transformer. In *Electric Power Applications, IEE Proceedings-* (Vol. 151, No. 3, pp. 289-295). IET.
- Chu, C.H. and Delp, E.J., 1989. Impulsive noise suppression and background normalization of electrocardiogram signals using morphological operators. *IEEE transactions on bio-medical engineering*, 36(2), pp.262-273.
- Chui, C.K. 1992, *Wavelets: a tutorial in theory and applications*, Academic Press, Boston;London.
- Cohen, B. and Kirman, J. H., 1986. Vibrotactile frequency discrimination at short durations, *Journal of General Psychology*, 113(2), pp. 179–186.
- Colman, A., 2015. *Mechanoreceptor*. In *A Dictionary of Psychology*. : Oxford University Press. Available at: <http://www.oxfordreference.com/view/10.1093/acref/9780199657681.001.0001/acref-9780199657681-e-4908>. (Accessed: 15 November 2016).
- Concise Oxford Dictionary of Mathematics, 2014. 5th edn, Oxford University Press.
- Conway, J.A., Brown, L.M.J., Veck, N.J., Wielogorski, A. and Borgeaud, M., 1991, April. A model-based system for crop classification from radar imagery. In *Antennas and Propagation, 1991. ICAP 91., Seventh International Conference on (IEE)* (pp. 616-619). IET.
- Coolican, H. 2009, *Research methods and statistics in psychology*, 5th edn, Hodder Education, London.
- Corrigan, P.W. and Penn, D.L., 2001. *Social cognition and schizophrenia*. American Psychological Association.
- Costa, M. and Corazza, L., 2006. Aesthetic phenomena as supernormal stimuli: The case of eye, lip, and lower-face size and roundness in artistic portraits. *Perception*, 35(2), pp.229-246.
- Cowan, N., 2001. The magical number 4 in short-term memory: a reconsideration of mental storage capacity. *Behavioral & Brain Sciences*, 24, pp. 87–185.
- Craig, J. C., 1985. Tactile pattern perception and its perturbations, *Journal of the Acoustical Society of America*, 77, pp. 238–246.
- Daubechies, I., 1992. *Ten lectures on wavelets* (Vol. 61, pp. 198-202). Philadelphia: Society for industrial and applied mathematics.

- Davidson, G. and Griffiths, H.D., 2002. Wavelet detection scheme for small targets in sea clutter. *Electronics letters*, 38(19), p.1.
- Dawkins, M.S. and Guilford, T., 1995. An exaggerated preference for simple neural network models of signal evolution?. *Proceedings of the Royal Society of London B: Biological Sciences*, 261(1362), pp.357-360.
- De Craen, S., Twisk, D.A.M., Hagenzieker, M.P., Elffers, H. and Brookhuis, K.A., 2011. Do young novice drivers overestimate their driving skills more than experienced drivers? Different methods lead to different conclusions. *Accident analysis & prevention*, 43(5), pp.1660-1665.
- Dellaportas, P., 1998. Bayesian classification of neolithic tools. *Applied Statistics*, pp. 279–297.
- Dempere-Marco, L., Melcher, D.P. & Deco, G. 2012. Effective Visual Working Memory Capacity: An Emergent Effect from the Neural Dynamics in an Attractor Network: e42719", *PLoS One*, vol. 7, no. 8.
- Department of Transport, 2006. *Setting Local Speed Limits*. Available at: <https://www.gov.uk/government/publications/setting-local-speed-limits>. (Accessed: 19 January 2015).
- Department of Transport, 2013. *Who is novice driver?*. Available at: <http://www.transport.wa.gov.au/licensing/novice-drivers.asp>. (Accessed: 1 July 2015).
- Diana, S, 2016. Dimensionality Reduction Techniques: Where to Begin. Available at: <https://blog.treasuredata.com/blog/2016/03/25/dimensionality-reduction-techniques-where-to-begin/>. (Accessed: 26 January 2016).
- Dictionary of Psychology, 2015. 4th edn, Oxford University Press.
- Ding, Y., Zhu, L., Zhang, X. and Ding, H., 2011. Numerical integration method for prediction of milling stability. *Journal of Manufacturing Science and Engineering*, 133(3), p.031005.
- Drăgănoiu, T.I., Nagle, L. and Kreutzer, M., 2002. Directional female preference for an exaggerated male trait in canary (*Serinus canarius*) song. *Proceedings of the Royal Society of London B: Biological Sciences*, 269(1509), pp.2525-2531.
- Dror, I. E. and Dascal, M., 1997. Can Wittgenstein help free the mind from rules? The philosophical foundations of connectionism. In D. Johnson and C. Erneling (eds.), *The Future of the Cognitive Revolution*, pp. 217–226. Oxford University Press.
- Dror, I. E., 2005. Perception is far from perfection: the role of the brain and mind in constructing realities. *Behavioral and Brain Sciences*, 28(06), pp. 763–763.

- Duhaime, I. M. and Schwenk, C. R., 1985. Conjectures on cognitive simplification in acquisition and divestment decision making. *Academy of Management Review*, 10(2), pp. 287–295.
- Engle, R., 2001. What is working memory capacity? In H.L. Roediger, III, J. S. Nairne, I. Neath, & A. M. Surprenant (Eds.), *The nature of remembering* (pp. 297-314). Washington, DC: American Psychological Association.
- Erdreich, J., 1986. A distribution based definition of impulse noise. *The Journal of the Acoustical Society of America*, 79(4), pp.990-998.
- Eriksson, J., Girod, L., Hull, B., Newton, R., Madden, S. and Balakrishnan, H., 2008, June. The pothole patrol: using a mobile sensor network for road surface monitoring. In *Proceedings of the 6th international conference on Mobile systems, applications, and services* (pp. 29-39). ACM.
- Eskandarian, A. ed., 2012. *Handbook of Intelligent Vehicles*. London, UK: Springer.
- Esteva, A., Sampat, A. and Badlani, A., 2012. 2D Visualization of Immune System Cellular Protein Data by Nonlinear Dimensionality Reduction.
- European Directive, 2002. The minimum health and safety requirements regarding the exposure of workers to the risks arising from physical agents. Article 16(1) of Directive 89/391/EEC).
- Everitt, B. S., Landau, S., and Leese, M., 2001. *Cluster Analysis*. 4th edn. New York: Oxford University Press Inc.
- Faivishevsky, L. and Goldberger, J., 2012. An unsupervised data projection that preserves the cluster structure. *Pattern Recognition Letters*, 33(3), pp.256-262.
- Faraoun, K.M. and Boukelif, A., 2007. Neural networks learning improvement using the k-means clustering algorithm to detect network intrusions. *World Academy of Science, Engineering and Technology, International Journal of Computer, Electrical, Automation, Control and Information Engineering*, 1(10), pp.3138-3145.
- Fawcett, T., 2006. An introduction to ROC analysis. *Pattern recognition letters*, 27(8), pp. 861–874.
- Fernández, A. and Gómez, S., 2008. Solving non-uniqueness in agglomerative hierarchical clustering using multidendrograms. *Journal of Classification*, 25(1), pp.43-65.
- Fischhoff, B., 1982. Debiasing. In D. Kahneman, P. Slovic, and A. Tversky (eds.) (1982). *Judgment under uncertainty: Heuristics and biases*. New York: Cambridge University Press.

- Foody, G.M., 2005. Local characterization of thematic classification accuracy through spatially constrained confusion matrices. *International Journal of Remote Sensing*, 26(6), pp.1217-1228.
- French, D.J., West, R.J., Elander, J. and Wilding, J.M., 1993. Decision-making style, driving style, and self-reported involvement in road traffic accidents. *Ergonomics*, 36(6), pp.627-644.
- Frid, A. and Lavner, Y., 2014, April. Spectral and textural features for automatic classification of fricatives. In *Pacific Voice Conference (PVC), 2014 XXII Annual* (pp. 1-4). IEEE.
- Friedlander, B. and Porat, B., 1989. Detection of transient signals by the Gabor representation. *Acoustics, Speech and Signal Processing, IEEE Transactions on*, 37(2), pp.169-180.
- Fujikawi, K. 1998. Analysis of steering wheel column vibration, *Motion & control*, 4, pp 37-41.
- Gautam, S. and Brahma, S.M., 2012, July. Guidelines for selection of an optimal structuring element for mathematical morphology based tools to detect power system disturbances. In *Power and Energy Society General Meeting, 2012 IEEE* (pp. 1-6). IEEE.
- Gerhard, D., 2003. Pitch extraction and fundamental frequency: History and current techniques (pp. 0–22). Regina: Department of Computer Science, University of Regina.
- Gescheider, G. A., 1976. Evidence in support of the duplex theory of mechanoreception, *Sensory Process*, 1, pp. 68–76.
- Gescheider, G. A., Bolanowski Jr., S. J. and Hardick, K. R., 2001. The frequency selectivity of information-processing channels in the tactile sensory system, *Somatosensory and Motor Research*, 18, pp. 191–201.
- Gescheider, G. A., Bolanowski Jr., S. J., Verrillo, R. T., Arpajian, D. J., and Ryan, T. F., 1990. Vibrotactile intensity discrimination measured by three methods, *Journal of the Acoustical Society of America*, 87, pp. 330–338.
- Gescheider, G.A., 1997, *Psychophysics: The Fundamentals*, 3rd Edition, Lawrence Erlbaum Associates electronics Ltd, Hailsham, East Sussex.
- Gescheider, G.A., Bolanowski, S.J. and Verrillo, R.T., 2004. Some characteristics of tactile channels. *Behavioural brain research*, 148(1), pp.35-40.

- Gescheider, G.A., Wright, J.H., Weber, B.J. and Barton, W.G., 1971. Absolute thresholds in vibrotactile signal detection. *Attention, Perception, & Psychophysics*, 10(6), pp.413-417.
- Giacomin J. and Onesti, C., 1999. Effect of Frequency and grip force on the perception of steering wheel rotational vibration, *ATA 6th International Conference on the New Role of Experimentation in the Modern Automotive Product Development Process*, Firenze, Italy, Nov. 17 –19.
- Giacomin, J. A. and Berber-Solano, T. P., 2006. Effect of transient event frequency content and scale on the human detection of road surface type. In *Joint Baltic-Nordic Acoustics Meeting*. November 8-10th. Gothenburg, Sweden.
- Giacomin, J. and Abrahams, O. 2000. Human fatigue due to automobile steering wheel vibration, *SIA Conference on Car and Train Comfort*, Nov. 15-16, LeMans, France.
- Giacomin, J. and Berber-Solano, T.P., 2005. Perception enhancement system for automotive steering.
- Giacomin, J. and Fustes, F., 2005. Subjective equivalence of steering wheel vibration and sound. *International Journal of Industrial Ergonomics*, 35(6), pp.517-526.
- Giacomin, J. and Gnanasekaran, S., 2005, Driver estimation of steering wheel vibration intensity: questionnaire-based survey, *Journal of the Engineering Integrity Society*, 18, pp 23-29.
- Giacomin, J. and Screti, A., 2005, Upper body discomfort due to driving: effect of driving experience, gender and vehicle age, *Zeitschrift für Arbeitswissenschaft*, 5, pp 409-418.
- Giacomin, J. and Woo, Y. J., 2004. Beyond comfort: information content and perception enhancement. *Engineering Integrity*, Vol. 16, July, pp. 8–16.
- Giacomin, J. and Woo, Y. J., 2005. A study of the human ability to detect road surface type on the basis of steering wheel vibration feedback. *Proceedings of the Institution of Mechanical Engineers, Part D: Journal of Automobile Engineering*, Vol. 219, No.11, pp. 1259–1270.
- Giacomin, J., 2005. Perception Enhancement for Steer-by-Wire Systems, *ATA Ingegneria dell' Autoveicolo*, Vol. 58, No. 8/9, Sept./Oct.
- Giacomin, J., Shayaa, M. S., Dormegnien, E. and Richard, L., 2004. Frequency weighting for the evaluation of steering wheel rotational vibration. *International Journal of Industrial Ergonomics*. 33, pp. 527–541.

- Giacomin, J., Steinwolf, A. and Staszewski, W.J. 2000. An Algorithm For Mildly Nonstationary Mission Synthesis (MNMS). *Engineering Integrity*, 7(January), pp.44-56.
- Giacomin, J., Steinwolf, A. and Staszewski, W.J., 2000. Application of mildly nonstationary mission synthesis (MNMS) to automotive road data. *Engineering Integrity*, 7, pp.44-56.
- Giacomin, J., Steinwolf, A., and Staszewski, W., 1999. A vibration mission synthesis algorithm for mildly nonstationary road data signal. *ATA 6th International Conference on the New Role of Experimentation in the Modern Automotive Product Development Process*. 17-19 November. Florence, Italy.
- Gibson, E. J., 1969. Principles of perceptual learning and development. New York: Appleton-Century-Crofts.
- Gibson, J. J. and Gibson, E. J., 1955. Perceptual Learning: Differentiation or Enrichment? *Psychological Review* Vol. 62, pp. 32-41.
- Gnanasekaran, S., Ajovalasit, M. and Giacomin, J., 2006. Driver estimation of steering wheel vibration intensity: laboratory-based tests. *Journal of the Engineering Integrity Society*, 20(1), pp.25-31.
- Goodwin, B.C., Browne, M., Rockloff, M. and Loxton, N.J., 2016. Rash impulsivity predicts lower anticipated pleasure response and a preference for the supernormal. *Personality and Individual Differences*, 94, pp.206-210.
- Green, D. M. and Swets, J. A., 1966. Signal detection theory and psychophysics. Reprint edn. Los Altos, CA: Peninsula Publishing.
- Green, P. E., Frank, R. E. and Robinson, P. J., 1967. Cluster analysis in test market selection. *Management science*, 13(8), pp. B-387.
- Griffin, M. J., 1990. *Handbook of Human Vibration*. San Diego, USA: Elsevier Academic Press.
- Griffin, M. J., 2012. Frequency-dependence of Psychophysical and Physiological Responses to Hand-transmitted Vibration. *Review Article of Industrial Health*, 50(5), 354-369.
- Groome, D., 1999. *An introduction to cognitive psychology: Processes and disorders*. East Sussex, England: Psychology Press.
- Grunwald, M. ed., 2008. *Human haptic perception: Basics and applications*. Springer Science & Business Media.

- Gugerty, L. J., & Tirre, W. C. (2000). Individual differences in situation awareness. In M. R. Endsley & D. J. Garland (Eds.), *Situation awareness analysis and measurement* (224–248). Mahwah, NJ: Lawrence Erlbaum.
- Güneş, S., Dursun, M., Polat, K. and Yosunkaya, Ş., 2011. Sleep spindles recognition system based on time and frequency domain features. *Expert Systems with Applications*, 38(3), pp. 2455–2461.
- Hacaambwa, T.M. and Giacomini, J., 2007. Subjective response to seated fore-and-aft direction whole-body vibration. *International journal of industrial ergonomics*, 37(1), pp.61-72.
- Hair, J.F. 2006. *Multivariate data analysis*, 6th edn, Pearson, Upper Saddle River, N.J.
- Halpern, D., & Hakel, M., 2002. *New directions in teaching and learning: Using the principles of cognitive psychology as a pedagogy for higher education*. San Francisco: Jossey-Bass.
- Hamilton, D., 2000. *Frequency domain considerations in vehicle design for optimal structural feel* (No. 2000-01-1344). SAE Technical Paper.
- Hanus, R., Zych, M., Petryka, L., Jaszczur, M. and Hanus, P., 2016. Signals features extraction in liquid-gas flow measurements using gamma densitometry. Part 1: time domain. In EPJ Web of Conferences (Vol. 114, p. 02035). EDP Sciences.
- Harter, W., Pfeiffer, W., Dominke, P., Ruck, G. and Blessing, P., 2000. *Future electrical steering systems: realizations with safety requirements* (No. 2000-01-0822). SAE Technical Paper.
- Heeger, D., 1998. Signal Detection Theory. Available at: <http://www.cns.nyu.edu/~david/handouts/sdt/sdt.html> (Accessed: 13 September 2016).
- Heenan, A., Herdman, C.M., Brown, M.S. and Robert, N., 2014. Effects of conversation on situation awareness and working memory in simulated driving. *Human Factors: The*
- Hekim, M. and Orhan, U., 2011. Subtractive approach to fuzzy c-means clustering method. *Journal of ITU-D*, 10(1).
- Hermawati, S., 2003. *Effect of intermittent unpredictable noise and 2 axis random vibrations on cognitive performance*. Lulea University of Technology. MSc Dissertation.
- Hill, H. and Pollick, F.E., 2000. Exaggerating temporal differences enhances recognition of individuals from point light displays. *Psychological Science*, 11(3), pp.223-228.

- Hodson, F. R., 1971. Numerical typology and prehistoric archaeology. *Mathematics in the archaeological and historical Sciences*, pp. 30–45.
- Hollins, M. and Roy, E. A., 1996. Perceived intensity of vibrotactile stimuli: the role of mechanoreceptive channels, *Somatosensory and Motor Research*, 13 (3–4), pp. 273–286.
- Hollnagel, E. and Woods, D.D., 2005. *Joint cognitive systems: Foundations of cognitive systems engineering*. CRC Press.
- Horiuchi, S., Negishi, H., Abe, K., Kamimura, A. and Fujinawa, Y., 2005. An automatic processing system for broadcasting earthquake alarms. *Bulletin of the Seismological Society of America*, 95(2), pp.708-718.
- Hu, J., Tung, W.W. and Gao, J., 2006. Detection of low observable targets within sea clutter by structure function based multifractal analysis. *Antennas and Propagation, IEEE Transactions on*, 54(1), pp.136-143.
- Hu-ming, D., Kaibin, Z. and Feng, S., 2010, July. Signal trend extraction of road surface profile measurement. In *Signal Processing Systems (ICSPS), 2010 2nd International Conference on* (Vol. 2, pp. V2-694). IEEE.
- Inman, D.J. & Singh, R.C. 2014, *Engineering vibration*, Fourth;International; edn, Pearson, Boston.
- International Organization for Standardization, 2001. *ISO 13091-1 2001 Mechanical Vibration - Vibrotactile perception thresholds for the assessment of nerve dysfunction, Part 1: Methods of measurement at the fingertips*. Geneva, Switzerland.
- Isermann, R., Schwarz, R. and Stolzl, S., 2002. Fault-tolerant drive-by-wire systems. *IEEE Control Systems*, Vol.22, No.5, pp.64-81.
- Jain, A. K., 2010. Data clustering: 50 years beyond K-means. *Pattern recognition letters*, 31(8), pp. 651–666.
- Jain, A.K. and Dubes, R.C. 1988, *Algorithms for clustering data*, Prentice-Hall, Englewood Cliffs.
- Jain, A.K. and Dubes, R.C., 1988. *Algorithms for clustering data*. Prentice-Hall, Inc..
- Jain, A.K., Murty, M.N. and Flynn, P.J., 1999. Data clustering: a review. *ACM computing surveys (CSUR)*, 31(3), pp.264-323.
- Jeon, B.H., 2010. *Proposed automobile steering wheel test method for vibration*. Brunel University School of Engineering and Design. PhD thesis.
- Jeon, B.H., Ajovalasit, M. and Giacomini, J., 2009. Effects of gender differences on the subjective perceived intensity of steering wheel rotational vibration based on a

- multivariate regression model. *International Journal of Industrial Ergonomics*, 39(5), pp.736-743.
- Jiang, F., Bo, Z.Q., Chin, P.S.M., Redfern, M.A. and Chen, Z., 2000, January. Power transformer protection based on transient detection using discrete wavelet transform (DWT). In *Power Engineering Society Winter Meeting, 2000. IEEE* (Vol. 3, pp. 1856-1861). IEEE.
- Jiang, L., Yin, H., Li, X. & Tang, S. 2014. Fault Diagnosis of Rotating Machinery Based on Multisensor Information Fusion Using SVM and Time-Domain Features. *SHOCK AND VIBRATION*, vol. 2014.
- Jing, M., Yan, X., Zengping, W. and Haofang, L., 2006. A novel adaptive scheme of discrimination between internal faults and inrush currents of transformer using Mathematical Morphology. In *Power Engineering Society General Meeting, 2006. IEEE* (pp. 7-pp). IEEE.
- Johannsdottir, K.R. & Herdman, C.M. 2010, "The Role of Working Memory in Supporting Drivers' Situation Awareness for Surrounding Traffic", *Human Factors: The Journal of Human Factors and Ergonomics Society*, vol. 52, no. 6, pp. 663-673.
- Johansson, R. S., Landström, U. and Lundström, R., 1982. Responses of mechanoreceptive afferent units in the glabrous skin of the human hand to sinusoidal skin displacements, *Brain Research*, 244, pp. 17–25.
- Johnson, M., 2002. Waveform based clustering and classification of AE transients in composite laminates using principal component analysis. *NDT & E International*, 35(6), pp.367-376.
- Juliusson, E.Á., Karlsson, N. and Gärling, T., 2005. Weighing the past and the future in decision making. *European Journal of Cognitive Psychology*, 17(4), pp.561-575.
- KAIST., 2014. Fault diagnosis for electric chassis systems, Available at: <http://sdac.kaist.ac.kr/research/index.php?mode=area&act=fdi> (Accessed: 30 August 2016).
- Kashef, R., 2008. Cooperative clustering model and its applications.
- Kerschen, G., Golinval, J.C. and Worden, K., 2001. Theoretical and experimental identification of a non-linear beam. *Journal of Sound and vibration*, 244(4), pp.597-613.
- Kerschen, G., Golinval, J.C. and Worden, K., 2001. Theoretical and experimental identification of a non-linear beam. *Journal of Sound and vibration*, 244(4), pp.597-613.

- Kettenring, J.R., 2006. The practice of cluster analysis. *Journal of classification*, 23(1), pp.3-30.
- Knibestol, M. and Vallbo, A. B., 1970. Single unit analysis of mechanoreceptor activity from the human glabrous skin, *Acta Physiologica Scandinavica*, 80, pp. 178–195
- Köhler, B.U., Hennig, C. and Orglmeister, R., 2002. The principles of software QRS detection. *Engineering in Medicine and Biology Magazine, IEEE*, 21(1), pp.42-57.
- Kulkarni, K.B. and Thyagarajan, R.S., 2001. *Optimizing the effects of body attachment stiffness on steering column in-vehicle modes* (No. 2001-01-0041). SAE Technical Paper.
- Kumar, R. 2005, *Research methodology: a step-by-step guide for beginners*, Second edn, SAGE, Thousand Oaks, London.
- Kunda, Z., 1999. *Social cognition: Making sense of people*. Cambridge, MA: MIT Pres.
- Lambrou, T., Kudumakis, P., Speller, R., Sandler, M. and Linney, A., 1998, May. Classification of audio signals using statistical features on time and wavelet transform domains. In *Acoustics, Speech and Signal Processing*, 1998. Proceedings of the 1998 IEEE International Conference on (Vol. 6, pp. 3621-3624). IEEE.
- Laming, D., 2003. *Human judgment: the eye of the beholder*. Cengage Learning EMEA.
- Lamoré, P. J. J. and Keemink, C. J., 1988. Evidence for different types of mechanoreceptors from measurements of the psychophysical threshold for vibrations under different stimulation conditions, *Journal of the Acoustical Society of America*, 83 (6), pp. 2339–2351.
- Leen, G. and Heffernan, D., 2002. Expanding automotive electronic systems. *Computer*, Vol. 35, No. 1, pp. 88-93.
- Li, C., Zheng, C. and Tai, C., 1995. Detection of ECG characteristic points using wavelet transforms. *Biomedical Engineering, IEEE Transactions on*, 42(1), pp.21-28.
- Li, M.A., Luo, X.Y. and Yang, J.F., 2016. Extracting the nonlinear features of motor imagery EEG using parametric t-SNE. *Neurocomputing*, 218, pp.371-381.
- Lloyd, S., 1982. Least squares quantization in PCM. *IEEE transactions on information theory*, 28(2), pp. 129–137.
- LMS International., 2002. *LMS Cada-X Fourier Monitor Manual*. (3rd Edition). Leuvan
- Logie, R. H., Engelkamp, J., Dehn, D., & Rudkin, S., 2001. Actions, mental actions, and working memory. In M. Denis, R. H. Logie, C. Cornoldi, J Engelkamp, & M.

- De Vega (Eds.), *Imagery, language and visuo-spatial thinking* (pp. 161–184). Hove, England: Psychology Press.
- Loomis, J. M. and Lederman, S. J., 1996. Tactual perception. *Handbook of Human Perception and Performance*, Wiley, NY.
- Louie, J.F. and Mouloua, M., 2015, September. Individual Differences in Cognition as Predictors of Driving Performance. In *Proceedings of the Human Factors and Ergonomics Society Annual Meeting* (Vol. 59, No. 1, pp. 1540-1544). SAGE Publications.
- Luce, R. D. and Raiffa, H., 2012. *Games and decisions: Introduction and critical survey*. Courier Corporation.
- Maaten, L.V.D. and Hinton, G., 2008. Visualizing data using t-SNE. *Journal of Machine Learning Research*, 9(Nov), pp.2579-2605.
- Mallory-Greenough, L. M., Greenough, J. D. and Owen, J. V., 1998. New data for old pots: trace-element characterization of ancient Egyptian pottery using ICP-MS. *Journal of Archaeological Science*, 25(1), pp. 85–97.
- Mansfield, N.J. 2005, *Human response to vibration*, Taylor & Francis, London.
- Mansfield, N.J. and Griffin, M.J., 2000. Difference thresholds for automobile seat vibration. *Applied Ergonomics*, 31(3), pp.255-261.
- March, J. G., 1991. Exploration and exploitation in organizational learning. *Organization science*, 2(1), pp. 71–87.
- Marchesiello, S. and Fasana, A., 2001. A frequency domain versus a time domain identification technique for nonlinear parameters applied to wire rope isolators.
- Marchesiello, S. and Fasana, A., 2001. A frequency domain versus a time domain identification technique for nonlinear parameters applied to wire rope isolators.
- Massaro, D. W. and Cowan, N., 1993. Information processing models: Microscopes of the mind. *Annual Review of Psychology*, 44, pp. 383-425
- Matlin, M.W. 2005, *Cognition*, 6th edn, J. Wiley & Sons, New York
- McCann, R., 2000. *Variable effort steering for vehicle stability enhancement using an electric power steering system* (No. 2000-01-0817). SAE Technical Paper.
- McClelland, J. L., and Rumelhart, D. E., 1985. Distributed memory and the representation of general and specific information. *Journal of Experimental Psychology: General*, 114, 159–188.
- McCOWAN, B.R.E.N.D.A., Hanser, S.F. and Doyle, L.R., 1999. Quantitative tools for comparing animal communication systems: information theory applied to bottlenose dolphin whistle repertoires. *Animal behaviour*, 57(2), pp.409-419.

- McLeod, S., 2009. Short Term Memory. Available at: <http://www.simplypsychology.org/short-term-memory.html>. (Accessed: 26 October 2016).
- Medin, D. L., and Ross, B., H., 1992. *Cognitive psychology*. Orlando, FL: Harcourt Brace Jovanovich.
- Mercer., C (2011). Vibration: Measure Acceleration, Velocity or Displacement? Available at: <http://blog.prosig.com/2011/09/05/vibration-analysis-should-we-measure-acceleration-velocity-or-displacement/>. (Accessed: 16 April 2017).
- Miles, J., 2014. On the job robot was. As driving becomes more automated, A concerned John Mikes Takes Cover. *Vehicle Dynamics*. Annual Showcase 2014. UKIP Media & Events Ltd.
- Miller, G. A., 1956. The magical number seven plus or minus two: Some limits on our capacity for processing information. *Psychological Review*, 63, pp. 81–97.
- Miller, G., 2006. The emotional brain weighs its options. *Science*, 313(5787), pp. 600–601.
- Miura, T., Morioka, M., Kimura, K. and Akuta, A., 1959. On the occupational hazards by vibrating tools (Report IV) - On the vibration of vibrating tools and the tentative threshold limit value of vibration, *Journal of Science of Labour*, 35, pp. 760–767.
- Miwa, T., 1967. Evaluation methods for vibration effect, Part 3: Measurements of threshold and equal sensation contours on hand for vertical and horizontal sinusoidal vibration, *Industrial Health*, 5, pp. 213–220.
- Miwa, T., 1968. Evaluation methods for vibration effect, Part 7: The vibration greatness of the pulses, *Industrial Health*, 7, pp. 143–164.
- Moore, B. C. J., 1997. *An Introduction to the Psychology of Hearing*, 4th Edition, London: Academic Press.
- Mordor Intelligence, 2016. Report structure of global automotive electric power steering systems market. Available at: <http://www.mordorintelligence.com> (Accessed: 22 September 2016)
- Morioka, M. and Griffin, M. J., 2006. Magnitude-dependence of equivalent comfort contours for fore-and-aft, lateral and vertical hand-transmitted vibration. *Sound and Vibration*, 295(3–5), 633–648.
- Morioka, M. and Griffin, M. J., 2007. Frequency dependence of perceived intensity of steering wheel vibration: effect of grip force. *Second Joint EuroHaptics*

Conference and Symposium on Haptic Interfaces for Virtual Environment and Teleoperator Systems, (pp. 50–55).

- Morioka, M. and Griffin, M. J., 2008. Absolute thresholds for the perception of fore-and-aft, lateral, and vertical vibration at the hand, the seat, and the foot. *Journal of Sound and Vibration*, 314(1–2), 357–370.
- Morioka, M. and Griffin, M. J., 2009. Equivalent comfort contours for vertical vibration of steering wheels: effect of vibration magnitude, grip force, and hand position. *Applied Ergonomics*, 40(5), 817–825.
- Morioka, M. and Griffin, M.J., 2000. Difference thresholds for intensity perception of whole-body vertical vibration: Effect of frequency and magnitude. *The Journal of the Acoustical Society of America*, 107(1), pp.620-624.
- Morioka, M., 1998. Difference thresholds for intensity perception of hand-transmitted vibration. *Proceedings of the 33rd Meeting of the UK Group on Human Response to Vibration, The Health and Safety Executive*. Buxton, Derbyshire. 16-18 September
- Morioka, M., 2004. Magnitude dependence of equivalent comfort contours for vertical steering wheel vibration, 39th Meeting of the UK Group on Human Response to Vibration, Ludlow, UK, 15–17 Sep., 2004.
- Mountcastle, V. B, LaMotte, R. H. and Carli, G., 1972. Detection thresholds for stimuli in humans and monkeys: comparison with threshold events in mechanoreceptive afferent fibres innervating the monkey hand, *Journal of Neurophysiology*, 35, pp. 122–136.
- Murphy, G. L., and Medin, D. L., 1985. The role of theories in conceptual coherence. *Psychological Review*, 92, 289–316.
- Mwangi, B., Soares, J.C. and Hasan, K.M., 2014. Visualization and unsupervised predictive clustering of high-dimensional multimodal neuroimaging data. *Journal of neuroscience methods*, 236, pp.19-25.
- Mwasiagi, J.I., Wang, X.H. and Huang, X.B., 2009. The use of k-means and artificial neural network to classify cotton lint. *Fibers and Polymers*, 10(3), pp.379-383.
- Nakamura, Y., 1988, August. On the urgent earthquake detection and alarm system (UrEDAS). In *Proc. of the 9th World Conference on Earthquake Engineering* (Vol. 7, pp. 673-678).
- Nakayama, O., Futami, T., Nakamura, T. and Boer, E.R., 1999. *Development of a steering entropy method for evaluating driver workload* (No. 1999-01-0892). SAE Technical Paper.

- Neely, G. and Burström, L., 2006. Gender differences in subjective responses to hand–arm vibration. *International journal of industrial ergonomics*, 36(2), pp.135-140.
- Newell, A., 1990. *Unified Theories of Cognition*, Harvard University Press.
- Niedenthal, P. M., and Halberstadt, J. B., 2000. Grounding categories in emotional response. In J. P. Forgas (Ed.), *Feeling and thinking: The role of affect in social cognition* (pp. 357–386). Cambridge, UK: Cambridge University Press.
- Niedenthal, P. M., Halberstadt, J. B., and Innes-Ker, A. H., 1999. Emotional response categorization. *Psychological Review*, 106, 337–361.
- Noguchi, M., 2002. Trend and future prospect regarding steering system technology. *KOYO Engineering Journal English Edition*.
- Norman, D. A., 1970. Introduction: Models of Human Memory. In D. A. Norman (Ed.), *Models of Human Memory*. p. 1–15. New York: Academic Press.
- Orasanu, J. and Martin, L., 1998. Errors in aviation decision making: A factor in accidents and incidents. In *Proceedings of the Workshop on Human Error, Safety, and Systems Development* (pp. 100–107).
- Orhan, U. and Hekim, M., 2007. Mass action based data clustering method and its weighted fuzzification. In *5th International conference on electrical and electronics engineering* (pp. 386-390).
- Orhan, U., Hekim, M. and Ozer, M., 2011. EEG signals classification using the K-means clustering and a multilayer perceptron neural network model. *Expert Systems with Applications*, 38(10), pp. 13475–13481.
- Orhan, U., Hekim, M., and Ibrikci, T., 2008. Gravitational fuzzy clustering. *Lecture Notes in Artificial Intelligence*, 5317, 524–531.
- Osman, O.A., Codjoe, J. and Ishak, S., 2015. Impact of Time-to-Collision Information on Driving Behavior in Connected Vehicle Environments Using A Driving Simulator Test Bed. *Journal of Traffic and Logistics Engineering Vol, 3*(1). pair comparison task. *Perception & psychophysics*, 58(5), pp.680-692.
- Oxford University Press, 2004. *Oxford Advanced Learner’s Dictionary Sixth edition*. Oxford: Oxford University Press.
- Oxford University Press, 2013. *Accuracy. A Dictionary of Mechanical Engineering*, 1st edn.
- Pak, C.H., Lee, U.S., Hong, S.C., Song, S.K., Kim, J.H. and Kim, K.S., 1991. *A study on the tangential vibration of the steering wheel of passenger car* (No. 912565). SAE Technical Paper.

- Palmer, S. E., 1999. *Vision science: Photons to phenomenology*. Cambridge, MA:MIT Press.
- Panagopoulos, S. and Soraghan, J.J., 2004. Small-target detection in sea clutter. *Geoscience and Remote Sensing, IEEE Transactions on*, 42(7), pp.1355-1361.
- Parsania, P., and Saradava, K., 2012. Drive by-wire systems in automobiles. *Journal of systematic computing, At VVP Engineering College, Rajkot, Gujarat, India*, Volume: 6.
- Parsons, K.C. and Griffin, M.J., 1988. Whole-body vibration perception thresholds. *Journal of sound and Vibration*, 121(2), pp.237-258.
- Patten, C.J., Kircher, A., Östlund, J., Nilsson, L. and Svenson, O., 2006. Driver experience and cognitive workload in different traffic environments. *Accident Analysis & Prevention*, 38(5), pp.887-894.
- Paykel, E.S., 1971. Classification of depressed patients: a cluster analysis derived grouping. *The British Journal of Psychiatry*, 118(544), pp.275-288.
- Peng, Z.K., Peter, W.T. and Chu, F.L., 2005. An improved Hilbert–Huang transform and its application in vibration signal analysis. *Journal of sound and vibration*, 286(1), pp.187-205.
- Perez, O., Mukamel, R., Tankus, A., Rosenblatt, J. D., Yeshurun, Y. and Fried, I., 2015. Preconscious prediction of a driver's decision using intracranial recordings. *Journal of cognitive neuroscience*.
- Peruzzetto, P., 1988. Assessing the relative importance of hand vibration with respect to whole-body vibration, The U.K and French joint meeting on human resources to vibration, I.N.R.S., Vandoeuvre, France, 26–28 Sep. 1988, pp. 1–11.
- Peter, D. and Gerhard, R., 1999. *Electric power steering-the first step on the way to “steer by wire”* (No. 1999-01-0401). SAE Technical Paper.
- Peterson, L. and Peterson, M. J., 1959. Short-term retention of individual verbal items. *Journal of experimental psychology*, 58(3), p. 193.
- Peterson, W. W. T. G., Birdsall, T. and Fox, W., 1954. The theory of signal detectability. *Transactions of the IRE professional group on information theory*, 4(4), pp. 171–212.
- Pheasant, S. and Haslegrave, C. M., 2005. *Bodyspace: Anthropometry, Ergonomics and the Design of Work*. (3rd Edition). USA: Taylor & Francis
- Phillips, J. R., Johansson, R. S. and Johansson, O., 1992. Responses on human mechanoreceptive afferents to embossed dot array scanned across fingerpad skin, *Journal of Neuroscience*, 12, pp. 827–839.

- Pierson, L., Swannstrom, R. and Anderson, C., 2015. *Data Science for Dummies*. John Wiley & Sons.
- Pilowsky, I., Levine, S. and Boulton, D. M., 1969. The classification of depression by numerical taxonomy. *The British Journal of Psychiatry*, 115(525), pp. 937–945.
- Pittenger, J.B. and Shaw, R.E., 1975. Aging faces as viscal-elastic events: implications for a theory of nonrigid shape perception. *Journal of Experimental Psychology: Human perception and performance*, 1(4), p.374.
- Platzer, A., 2013. Visualization of SNPs with t-SNE. *PloS one*, 8(2), p.e56883.
- Pongrac, H., 2008. Vibrotactile perception: examining the coding of vibrations and the just noticeable difference under various conditions. *Multimedia systems*, 13(4), pp. 297–307.
- Pottinger, M.G., Marshall, K.D., Lawther, J.M. and Thrasher, D.B., 1986. A review of tire/pavement interaction induced noise and vibration. In *The Tire Pavement Interface*. ASTM International.
- PR Newswire Association., 2015. Global Automotive Steering System Market 2015-2019. Available at: <http://www.prnewswire.com/news-releases/global-automotive-steering-system-market-2015-2019-300136156.html>. (Accessed: 28 October 2016).
- Rabiner, L.R. and Juang, B.H. 1993, *Fundamentals of speech recognition*, Prentice Hall PTR, Upper Saddle River, N.J.
- Raphisak, P., Schuckers, S.C. and de Jongh Curry, A., 2004, September. An algorithm for EMG noise detection in large ECG data. In *Computers in Cardiology, 2004* (pp. 369-372). IEEE.
- Rayner, K., Foorman, B.R., Perfetti, C.A., Pesetsky, D. and Seidenberg, M.S., 2001. How psychological science informs the teaching of reading. *Psychological science in the public interest*, 2(2), pp.31-74.
- Reed, S.K., 1977. Facilitation of problem solving. *Cognitive theory*, 2, pp.3-20.
- Reynolds, D. D., Standlee, K. G. and Angevine, E. N., 1977. Hand-arm vibration, Part III: Subjective response characteristics of individuals to hand-induced vibration. *Journal of sound and vibration*, 51(2), pp. 267–282.
- Rizun, N. and Taranenko, Y., 2014. Simulation models of human decision-making processes. *Management Dynamics in the Knowledge Economy*, 2(2), p.241.
- Roberts, D., 2002. *Signals and perception: The fundamentals of human sensation*. Basingstoke: Open University Press and Palgrave.

- Rosch, E., 1975. Cognitive representations of semantic categories. *Journal of Experimental Psychology: General*, 104, 192–233.
- Rosch, E., 1978. Principles of categorization. In E. Rosch and B. B. Lloyd (Eds.), *Cognition and categorization* (pp. 27–48). Hillsdale, NJ: Lawrence Erlbaum Associates, Inc.
- Rosch, E., Mervis, C., Gray, W. D., Johnson, D. M. and Boyes-Braem, P., 1976. Basic objects in natural categories. *Cognitive Psychology*, 8, 382–439.
- Ross, T.J., 2009. *Fuzzy logic with engineering applications*. John Wiley & Sons.
- Rouillard, V., Sek, M.A. and Bruscella, B., 2001. Simulation of road surface profiles. *Journal of transportation engineering*, 127(3), pp.247-253.
- Russo, J. E., Meloy, M. G. and Medvec, V. H., 1998. Predecisional distortion of product information. *Journal of Marketing Research*, pp. 438–452.
- Saadatpour, A., Lai, S., Guo, G. and Yuan, G.C., 2015. Single-cell analysis in cancer genomics. *Trends in Genetics*, 31(10), pp.576-586.
- Saniie, J. and Mohamed, M.A., 1994. Ultrasonic flaw detection based on Mathematical Morphology. *Ultrasonics, Ferroelectrics, and Frequency Control, IEEE Transactions on*, 41(1), pp.150-160.
- Saroj, K.A., 2009. Decision Making: Meaning and Definition. Available at: <http://www.excellentguru.com/index.php>. (Accessed: 26 October 2016).
- Satriano, C., Wu, Y.M., Zollo, A. and Kanamori, H., 2011. Earthquake early warning: Concepts, methods and physical grounds. *Soil Dynamics and Earthquake Engineering*, 31(2), pp.106-118.
- Schacter, D. L., 2002. *The seven sins of memory: How the mind forgets and remembers*. Houghton Mifflin Harcourt.
- Schröder, F. and Zhang, T., 1997. Objective and subjective evaluation of suspension harshness, In *6th European Automobile cooperation International Congress*, Cernobbio, Italy, Paper 97A068, pp. 63–72.
- Sebastián-Gallés, N. 2006, "Native-language sensitivities: evolution in the first year of life", *Trends in Cognitive Sciences*, vol. 10, no. 6, pp. 239-241
- Sedighi, A.R. and Haghifam, M.R., 2005. Detection of inrush current in distribution transformer using wavelet transform. *International Journal of Electrical Power & Energy Systems*, 27(5), pp.361-370.
- Silverman, B.W. 1986, *Density estimation for statistics and data analysis*, Chapman and Hall, London.
- Simon, H. A., 1957. *Models of Man*. New York: Wiley.

- Simon, H. A., 1957. *The Administrative Behavior*. New York: Free Press.
- Simon, H.A., 1979. Information processing models of cognition. *Annual review of psychology*, 30(1), pp.363-396.
- Sinclair, R.J. and Burton, H., 1996. Discrimination of vibrotactile frequencies in a delayed
- Sinha, P.K. 2012, "Appendix C Discrete Fourier Transform" in SPIE Press, , pp. 683-692.
- Smith, E.E., 2000. Neural bases of human working memory. *Current Directions in Psychological Science*, 9(2), pp.45-49.
- Smyth, A.W. and Pei, J.S., 2000, October. Integration of response measurements for nonlinear structural health monitoring. In *Proceedings of 3rd US-Japan Workshop on Nonlinear System Identification and Structural Health Monitoring* (pp. 20-21).
- Song, J., Yan, H. and Xiao, Z., 2010, October. Research on T-wave morphology analysis in ECG signal. In *Biomedical Engineering and Informatics (BMEI), 2010 3rd International Conference on* (Vol. 3, pp. 1033-1036). IEEE.
- Song, S.P. and Que, P.W., 2006. Wavelet based noise suppression technique and its application to ultrasonic flaw detection. *Ultrasonics*, 44(2), pp.188-193.
- Soualhi, A., Razik, H., Clerc, G. and Doan, D.D., 2014. Prognosis of bearing failures using hidden Markov models and the adaptive neuro-fuzzy inference system. *IEEE Transactions on Industrial Electronics*, 61(6), pp.2864-2874.
- Spatz, C. 2008, *Basic statistics: tales of distributions*, 9th edn, Thomson/Wadsworth, Belmont, Calif.
- Squire, L.R., Knowlton, B. and Musen, G., 1993. The structure and organization of memory. *Annual review of psychology*, 44(1), pp.453-495.
- Stanovich, K.E. and West, R.F., 2008. On the relative independence of thinking biases and cognitive ability. *Journal of personality and social psychology*, 94(4), p.672.
- Stevens, S. S., 1986. *Psychophysics: introduction to its perceptual, neural and social prospects*, G. Stevens, New Brunswick, U.S.A., Transaction Books.
- Stokes, A. F., Kemper, K. L. and Marsh, R., 1992. *Time-stressed flight decision making: A study of expert and novice aviators*.
- Subasi, A., 2007. EEG signal classification using wavelet feature extraction and a mixture of expert model. *Expert Systems with Applications*, 32(4), pp.1084-1093.
- Swets, J.A., Tanner Jr, W.P. and Birdsall, T.G., 1961. Decision processes in perception. *Psychological review*, 68(5), p.301.

- Tajima, J., Yuhara, N., Sano, S. and Takimoto, S., 1999. *Effects of steering system characteristics on control performance from the viewpoint of steer-by-wire system design* (No. 1999-01-0821). SAE Technical Paper.
- Talbot, W. H., Darien-Smith, I., Kornhuber, H. H. and Mountcastle, V. B., 1968. The sense of flutter-vibration: Comparison of the human capacity with response patterns of mechanoreceptive afferents from the monkey hand, *Journal of Neurophysiology*, 31, pp. 301–304.
- Taneda, A. and Yamanaka, T., 1998. *Design of actuator for active-rear-steer system* (No. 981114). SAE Technical Paper.
- Tang, Y., Zhang, Z. and Jiang, W., 2016, October. Two-Dimensional Soft Linear Discriminant Projection for Robust Image Feature Extraction and Recognition. In *International Conference on Neural Information Processing* (pp. 514-521). Springer International Publishing.
- Tanner, W. and Swets, J., 1954. The human use of information--I: Signal detection for the case of the signal known exactly. *Transactions of the IRE Professional Group on Information Theory*, 4(4), pp. 213–221.
- Technavio, 2016. Overview the global automotive steer-by-wire (SBW) market systems. Available at: <http://www.technavio.com/report/global-automotive-electronics-automotive-steer-wire-system-market>. (Accessed: 17 October 2016).
- ten Cate, C. and Rowe, C., 2007. Biases in signal evolution: learning makes a difference. *Trends in ecology & evolution*, 22(7), pp.380-387.
- Towler M., 2010. *Rational Decision Making: An introduction*. Wiley, New York, NY.
- Trahanias, P.E., 1993. An approach to QRS complex detection using Mathematical Morphology. *Biomedical Engineering, IEEE Transactions on*, 40(2), pp.201-205.
- Tulving, E., 1972. Episodic and semantic memory. In: Tulving E., Donaldson W., eds. *Organization of Memory*. New York: Academic Press 1972
- van der Maaten, L., 2009. Learning a parametric embedding by preserving local structure. *RBM*, 500(500), p.26.
- Vandeurzen, U., Leuridan, J. and Mergeay, M., 1988. Versatile computer workstation for multiple input/output structural testing and analysis. In *Proc. of 18th Int. Symp. on Automotive Technology and Automation, Florence, Italy. period for Modern Apprenticeships or other recognised training within the industry*.
- VanVoorhis, C.W. and Morgan, B.L., 2007. Understanding power and rules of thumb for determining sample sizes. *Tutorials in Quantitative Methods for Psychology*, 3(2), pp.43-50.

- Verhoeff, L., Verschuren, R. and Zuurbier, J., 2004. Tire Force Estimation for Improved Steering Feel in EPAS and Steer-By-Wire. (No. 2004- 05-0157). SAE Technical Paper.
- Verrillo, R. T., 1966, Vibrotactile sensitivity and the frequency response of the Pacinian corpuscle, *Psychonomics Science* 4, pp. 135–136.
- Verrillo, R. T., 1985, Psychophysics of vibrotactile stimulation, *Journal of the Acoustical Society of America*, 77 (1), pp. 225–232.
- Verrillo, R. T., Fraioli, A. J. and Smith, R. L., 1969. Sensation magnitude of vibrotactile stimuli, *Perception & Psychophysics*, 6, pp. 366–372.
- Verrillo, R. T., 1965. Temporal summation in vibrotactile sensitivity, *Journal of the Acoustical Society of America*, 37 (5), pp. 843–846.
- Ward, D. and Woodgate, R., 2004. Meeting the challenge of drive-by-wire electronics, Aerosystems International. Available at: <http://mira.atalink.co.uk/articles/104>. (Accessed: 20 September 2016).
- Warner, H.W. and Åberg, L., 2008. Drivers' beliefs about exceeding the speed limits. *Transportation Research Part F: Traffic Psychology and Behaviour*, 11(5), pp.376-389.
- Weick, K. E., 2012. *Making sense of the organization, Volume 2: The impermanent organization* (Vol. 2). John Wiley & Sons.
- Wickens, C. D., Gordon, S. E., Liu, Y. and Lee, J., 1998. *An introduction to human factors engineering.*, 2nd Edition, New Jersey: Pearson Education, Inc.
- Wicklin, R., 2011. The trapezoidal rule of integration. Available at: <http://blogs.sas.com/content/iml/2011/06/01/the-trapezoidal-rule-of-integration.html>. (Accessed: 11 February 2017).
- Wolfram Research, 2017. Numerical Differentiation. Available at: <http://mathworld.wolfram.com/NumericalDifferentiation.html>. (Accessed: 18 February 2017)
- Woo, Y. and Giacomini, J., 2006. The role of the scale and the frequency bandwidth of steering wheel vibration on road surface recognition. In *8th International Symposium on Advance Vehicle Control, AVEC'06Taipei*.
- Worden, K. and Tomlinson, G.R., 2000. *Nonlinearity in structural dynamics: detection, identification and modelling*. CRC Press.
- Worden, K., 1990. Data processing and experiment design for the restoring force surface method, part I: integration and differentiation of measured time data. *Mechanical Systems and Signal Processing*, 4(4), pp.295-319.

- Wos, H., Wangenheim, M., Borg, G. and Samuelson, B., 1988. Perceptual rating of local vibration: A psychophysical study of hand-arm vibration of short duration (Part I). *International Journal of Industrial Ergonomics*, 2(2), pp. 143–150.
- Wright, P., 1974. The harassed decision maker: Time pressures, distractions, and the use of evidence. *Journal of applied psychology*, 59(5), p. 555
- Wu, W.C., Ji, T.Y., Li, M.S., Zhang, L.L. and Wu, Q.H., 2013a, July. Inrush identification by applying improved Morphological Gradient Algorithm. In *Power and Energy Society General Meeting (PES), 2013 IEEE* (pp. 1-5). IEEE.
- Wu, W.C., Li, M.S., Ji, T.Y. and Wu, Q.H., 2013b, December. Fast identification of inrush current using a weighted morphological approach. In *Power and Energy Engineering Conference (APPEEC), 2013 IEEE PES Asia-Pacific* (pp. 1-5). IEEE.
- Wyer, R., S., 1998, *Stetrotpe activation and inhibition*. Mahwah, NJ: Erlbaum.
- Yang, C. and Fricker, J., 2001. Using human information processing principles to design advanced traveler information systems. *Transportation Research Record: Journal of the Transportation Research Board*, (1759), pp.1-8.
- Yang, J., Zhang, H. and Peng, G., 2016. Time-domain period detection in short-duration videos. *Signal, Image and Video Processing*, 10(4), pp.695-702.
- Yiakopoulos, C. T., Gryllias, K. C. and Antoniadis, I. A., 2011. Rolling element bearing fault detection in industrial environments based on a K-means clustering approach. *Expert Systems with Applications*, 38(3), pp. 2888–2911.
- Yoshida, Y., Ohwada, H., Mizoguchi, F. and Iwasaki, H., 2014. Classifying Cognitive Load and Driving Situation with Machine Learning. *International Journal of Machine Learning and Computing*, 4(3), p.210.
- Zhang, H., Wen, J.F., Liu, P. and Malik, O.P., 2002. Discrimination between fault and magnetizing inrush current in transformers using short-time correlation transform. *International journal of electrical power & energy systems*, 24(7), pp.557-562.
- Zhang, L., Huang, X., Wang, B., Li, F. and Zhang, Z., 2016, October. Hidden Space Neighbourhood Component Analysis for Cancer Classification. In *International Conference on Neural Information Processing* (pp. 44-51). Springer International Publishing.
- Zhao, N., Chen, W., Xuan, Y., Mehler, B., Reimer, B. and Fu, X., 2014. Drivers' and non-drivers' performance in a change detection task with static driving scenes: is there a benefit of experience?. *Ergonomics*, 57(7), pp.998-1007.

Zwislocki, J. J., 1960, Theory of temporal auditory summation, *Journal of the Acoustical Society of America*, 32, pp. 1046–1060.

APPENDICES

Appendix 1: Laboratory test sheet



PARTICIPANTS INFORMATION SHEET

We would like to invite you to join a research study entitled **"What are the effect of the vibrational energy distribution on the level of driver detection"** Before you decide it is important for you to understand why the research is being done and what it will involve. This document gives detailed information about the research study, and is yours to keep. Please take time to read the following information carefully and discuss it with others if you wish before you decide whether or not you wish to take part. Ask us if there is anything that is not clear or if you would like more information.

What is the purpose of the study?

Since changes in the size of the vibration and in other characteristics of the vibration signal are known to affect people's perception of the steering wheel vibration, this experiment involves several vibration signals whose size or frequency content have been modified. Therefore, the objective of this experiment is to establish how much the human detection changes as a function of the changes which are made to the signal characteristics.

Why have been invited to participate?

The researcher is asking you to consider participating in this study because you are a healthy person with no history of pain and most importantly you have driving experience.

Do I have to take part?

No, this is entirely up to you. If you would like to take part, you will be asked to sign a consent form. Even after you have signed this consent form and agreed to join the study, you are free to withdraw from the study at any time. If you decide not to take part, or withdraw from the study, it will not affect any future interactions that you may have with Brunel University and Perception Enhancement Group. Please inform the research if you no longer wish to participate in the study.

What will happen to me if I take part?

Once you have decided to take part in this research, you will be asked to come to the Human Centred Design Lab (Room TA043), Brunel University, London UB8 3PH, where the researcher will discuss the study with you and answer any questions you may have. You will be asked to attend one session lasting approximately half an hour. If you are still happy to take part, we will ask you to sign the consent form. We will ask you to provide us with information regarding your age, sex, height, weight, and any driving history. Please note that with your consent, photographic and/or video recordings might be taken during the experiment for use within the study. There is a specific section in the consent form to provide permission for these to be taken.

What do I have to do?

During the experiment, you will be asked to sit in a specially-designed steering wheel simulator (Refer Figure 1) where you will be exposed to rotational steering wheel vibration experienced in real driving situations. The whole test involves 400 detection of road surface vibration. You will be asked to judge whether you felt the same (or different) for each of the vibrations was coming from the road surface shown on the photograph on the board directly in front of the test bench which take approximately 10 seconds. After each vibration, you will have a pause of 5 seconds and to response to the vibration. The total test duration is approximately 45-minutes per session.

Appendix 1.1 Participants information sheet for Experiment 1 (Chapter 7)



Figure 1: Steering wheel simulator

What are the possible disadvantages and risks of taking part?

Both total number of vibration and time were designed to take into consideration the learning and the fatigue effects. Additionally, the safety features of the steering wheel simulator, and the acceleration levels used, conform to the health and safety recommendations outlined by British Standard 7085 (1989). However, if you experience any muscle or joint pain and/or discomfort during the session please inform the researcher, and if you need to rest and/or want to stop, you can do so at any time.

What are the possible benefits of taking part?

There are no clear benefits to you of taking part. However, the information from this research will enable the researcher to provide the guidelines for the feedback properties which an automotive steering system should have.

What if something goes wrong?

If you have a concern about any aspect of this study, you should ask to speak to the researcher who will do their best to answer your questions (Sabariah.MohdYusoff@brunel.ac.uk). In the event that something does go wrong and you are harmed during the research and this is due to someone's negligence then you may have grounds for a legal action for compensation against Brunel University, London but you may have to pay your legal costs. The person to be contacted if the participant wishes to complain about the experience should be the Chair of the principal investigator's College Research Ethics Committee.

Will my taking part in this study be kept confidential?

Any information you provide to the researcher will be kept confidential. If the study is published in a book or scientific journal, no individual will be identified in any way. Physical data will be kept in locked drawers and will be destroyed once the study has taken place or if it cannot be scheduled at the end of the data collection phase. All electronics files which can or may contain personally identifying information will be stored only on Brunel computer systems with username and password access by the researcher. Personally identifying data will be removed and transcriptions are anonymised at the earliest opportunity possible (e.g., by replacing any names mentioned with pseudonyms). Once transcribed and once the transcription is checked, the electronic files will be destroyed. The transcription will therefore not contain any personally identifying information. The procedures for handling, processing, storage and destruction of data are compliant with the Data Protection Act 1998.

What will happen to the results of the research study?

The results of the study will be written up for a PhD thesis. In addition, data will be presented at an appropriate scientific conference and written up as a scientific paper for publication in a peer reviewed journal. No individual subject will be identified in any report or presentation arising from the research. The researcher is unable to provide you with your individual results; however, you can be provided with a summary report of our findings at the end of the study, upon your request.

Will I be paid for taking part in the study?

You will not be paid for your participation in the study. Your participation in this study is entirely voluntary. You have the right to withdraw from the study at any time.

Who has reviewed the study?

This study was reviewed and been approved by the research ethics committee of the College of Engineering, Design and Physical Sciences, Brunel University, London UB8 3PH.

Passage on Research Integrity

Brunel University, London is committed to compliance with the Universities UK [Research Integrity Concordat](#). You are entitled to expect the highest level of integrity from our researchers during the course of their research.

Contact for further information and complaints

If you would like to consider this study further before you make your decision, please take your time to do so. To request further information please contact Sabariah Mohd Yusoff, who may be reached by email at Sabariah.MohdYusoff@brunel.ac.uk. [Supervised by: Professor Joseph Giacomini, Joseph.Giacomini@brunel.ac.uk]

PARTICIPANT INFORMATION SHEET



We would like to invite you to join a research study entitled **identification of optimal approach for human to detect the road surface**. Before you decide it is important for you to understand why the research is being done and what it will involve. This document gives detailed information about the research study, and is yours to keep. Please take time to read the following information carefully and discuss it with others if you wish before you decide whether or not you wish to take part. Ask us if there is anything that is not clear or if you would like more information.

What is the purpose of the study?

When driving, drivers experience with a number of vibrations on the steering wheel. The vibrations on the steering wheel suspected could affect the driver's ability to detect the road surfaces. The aim of this study is to anticipate the optimal degree of road surfaces vibrations which can be differentiated by the drivers. Therefore, this study will evaluate the difference of response by drivers on various types of vibration caused by road surfaces.

Why have been invited to participate?

The researcher is asking you to consider participating in this study because you are a healthy person with no history of pain and most importantly you have driving experience.

Do I have to take part?

No, this is entirely up to you. If you would like to take part, you will be asked to sign a consent form. Even after you have signed this consent form and agreed to join the study, you are free to withdraw from the study at any time. If you decide not to take part, or withdraw from the study, it will not affect any future interactions that you may have with Brunel University and Perception Enhancement Group. Please inform the research if you no longer wish to participate in the study.

What will happen to me if I take part?

Once you have decided to take part in this research, you will be asked to come to the Human Centred Design Lab (Room TA043), Brunel University, London UB8 3PH, where the researcher will discuss the study with you and answer any questions you may have. You will be asked to attend one session lasting approximately an hour. If you are still happy to take part, we will ask you to sign the consent form. We will ask you to provide us with information regarding your age, sex, height, weight, and any driving history. Please note that with your consent, photographic and/or video recordings might be taken during the experiment for use within the study. There is a specific section in the consent form to provide permission for these to be taken.

What do I have to do?

During the experiment, you will be asked to sit in a specially-designed steering wheel simulator (Refer Figure 2) where you will be exposed to rotational steering wheel vibration experienced in real driving situations. The whole test involves 5 sets of 30 different types of road surfaces vibration, bringing the total number of the vibrations to be evaluated to 150 (Refer Figure 1). Each set of road surfaces vibration will take approximately 9 minutes to test. After each vibration you will have a pause of 5 second to rest your hands and to response to the vibrations, and after each set you will have a break of 1 minute. Therefore, the total test duration is approximately 45 minutes. Images of road surfaces will be displayed in front of you (Refer Figure 3). You will then be asked to respond "yes" or "no" on each vibration your experience whether the vibrations caused by the road surfaces displayed.

Appendix 1.2 Participants information sheet for Experiment 2 (Chapter 8)



Figure 1: Experiment Design



Figure 2: Steering wheel simulator

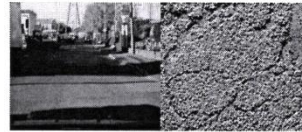


Figure 3: Example of road surface picture

What are the possible disadvantages and risks of taking part?

Both total number of vibration and time were designed to take into consideration the learning and the fatigue effects (Giacomin & Abrahams, 2000; Giacomin & Woo, 2004; Giacomin & Screti, 2005). Additionally, the safety features of the steering wheel simulator, and the acceleration levels used, conform to the health and safety recommendations outlined by British Standard 7085 (1989). However, if you experience any muscle or joint pain and/or discomfort during the session please inform the researcher, and if you need to rest and/or want to stop, you can do so at any time.

What are the possible benefits of taking part?

There are no clear benefits to you of taking part. However, the information from this research will enable the researcher to provide the guidelines for the feedback properties which an automotive steering system should have.

What if something goes wrong?

If you have a concern about any aspect of this study, you should ask to speak to the researcher who will do their best to answer your questions (Sabariah.MohdYusoff@brunel.ac.uk). In the event that something does go wrong and you are harmed during the research and this is due to someone's negligence then you may have grounds for a legal action for compensation against Brunel University, London but you may have to pay your legal costs. The person to be contacted if the participant wishes to complain about the experience should be the Chair of the principal investigator's College Research Ethics Committee.

Will my taking part in this study be kept confidential?

Any information you provide to the researcher will be kept confidential. If the study is published in a book or scientific journal, no individual will be identified in any way. Physical data will be kept in locked drawers and will be destroyed once the study has taken place or if it cannot be scheduled at the end of the data collection phase. All electronics files which can or may contain personally identifying information will be stored only on Brunel computer systems with username and password access by the researcher. Personally identifying data will be removed and transcriptions are anonymised at the earliest opportunity possible (e.g., by replacing any names mentioned with pseudonyms). Once transcribed and once the transcription is checked, the electronic files will be destroyed. The transcription will therefore not contain any personally identifying information. The procedures for handling, processing, storage and destruction of data are compliant with the Data Protection Act 1998.

What will happen to the results of the research study?

The results of the study will be written up for a PhD thesis. In addition, data will be presented at an appropriate scientific conference and written up as a scientific paper for publication in a peer reviewed journal. No individual subject will be identified in any report or presentation arising from the research. The researcher is unable to provide you with your individual results; however, you can be provided with a summary report of our findings at the end of the study, upon your request.

Will I be paid for taking part in the study?

You will not be paid for your participation in the study. Your participation in this study is entirely voluntary. You have the right to withdraw from the study at any time.

Who has reviewed the study?

This study was reviewed and been approved by the research ethics committee of the College of Engineering, Design and Physical Sciences, Brunel University, London UB8 3PH.

Passage on Research Integrity

Brunel University, London is committed to compliance with the Universities UK [Research Integrity Concordat](#). You are entitled to expect the highest level of integrity from our researchers during the course of their research.

Contact for further information and complaints

If you would like to consider this study further before you make your decision, please take your time to do so. To request further information please contact Sabariah Mohd Yusoff, who may be reached by email at Sabariah.MohdYusoff@brunel.ac.uk. [Supervised by: Professor Joseph Giacomin, Joseph.Giacomin@brunel.ac.uk]

1. **Welcome**, thank you for taking part in this experiment.
2. The experiment will be performed using the wheel simulator that you see in front of you. This simulator consists of a rigid frame, a rigid steering wheel, an automobile seat, an electrodynamic shaker unit, a power amplifier and a signal generator (Refer Figure 2).
3. The simulator has **numerous features/ which guarantee your safety**. The control software was built-in safety limits which restrict the maximum vibration output to safe values. The power amplifier has similar limiting circuits, and the vibrator is incapable of physically exceeding health and safety limits. The safety features of the steering wheel simulator, and the acceleration levels used, conform to the health and safety recommendations outlined by British Standard 7085 (1989).
4. I would like now to ask if you can please **read** carefully and a **complete consent form** and a participant information form for the experiment. It is particularly important that you provide a signature to authorize your participation in my research study.
5. Before we start, let me brief again the **purpose** of this test. The objective this experiment is to establish how much the human perception detection as a function of the changes which are made to the signal characteristics.
6. The whole test contains 400 vibrations to be detected which 10-second length for each. After every each stimuli you will have a pause of 5-second to relax your hands and response to the vibrations. Therefore the total experiment will takes half an hour.
7. Ok, now I will explain **how to response to the road surface vibration**. Your driving experience is very important to determine the vibration.
8. There are five possible answers for the vibration response. You need to state, by means of your level of detection from 'not similar at all (1)' to 'extremely similar (5)', whether you can detect the source of the vibration which you are feeling through the steering wheel are from the photograph shown.
9. If at any time before or during the experiment you should decide that you wish to **stop**, please state this and the procedure will be brought to a halt.
10. Please now remove any articles of **heavy clothing**, any **watches** and any **jewellery, glasses** or other items, which might effect your perception of road surface vibration.
11. Please now sit in the simulator and adjust the **sitting posture** to the **same position** as you are driving. Please don't touch the simulator frame with your legs or feet (Refer Figure 2).

Appendix 1.3 Test procedure for Experiment 1 (Chapter 7)

12. Please now **hold the steering wheel in the middle of the hand grips** using both hands and **maintain a constant palm grip**, avoiding touching the lower and upper arms. You should try to adopt a posture which is as close as possible to the one you use in your own car (Refer Figure 2).



Figure 2: Steering wheel simulator and position of participant

13. In order to familiarise with the test procedure you asked to judge 3 sets of vibration signal which consists of exposure vibration signal and manipulated vibration signal to be judge.
14. Do you have any questions before the formal testing starts?
15. Now, I will send to you the 20-seconds of vibration signal or I can say as a exposure vibration signal from the photograph road shown in front of you. At this stage, you need to try to remember or really feel the vibration to be used for the testing after this. Are you ready?
16. Now, we start the testing. Are you ready?
17. Can you detect the vibration signal same as the exposure that you felt before? At what level you indicate your level of detection?
18. Ok, now the testing is complete.
19. Before you leave, please complete the questionnaire related to the **vibrational sickness**.
20. Thank you very much for having taken part in this experiment.

Appendix 1.3 (continued) Test procedure for Experiment 1 (Chapter 7)

Test Procedure

1. **Welcome**, thank you for taking part in this experiment.
2. The experiment will be performed using the wheel simulator that you see in front of you. This simulator consists of a rigid frame, a rigid steering wheel, an automobile seat, an electrodynamic shaker unit, a power amplifier and a signal generator (Refer Figure 3).
3. The simulator has **numerous features/ which guarantee your safety**. The control software was built-in safety limits which restrict the maximum vibration output to safe values. The power amplifier has similar limiting circuits, and the vibrator is incapable of physically exceeding health and safety limits. The safety features of the steering wheel simulator, and the acceleration levels used, conform to the health and safety recommendations outlined by British Standard 7085 (1989).
4. I would like now to ask if you can please **read** carefully and a **complete consent form** and a participant information form for the experiment. It is particularly important that you provide a signature to authorize your participation in my research study.
5. Before we start, let me brief again the **background and purpose** of this test. When driving, drivers experience with a number of vibrations on the steering wheel. The vibrations on the steering wheel suspected could affect the driver's ability to detect the road surfaces. The aim of this study is to anticipate the optimal degree of road surfaces vibrations which can be differentiated by the drivers. Therefore, this study will evaluate the difference of response by drivers on various types of vibration caused by road surfaces.
6. The whole test involves 5 sets of 30 different types of road surfaces vibration, bringing the total number of the vibrations to be evaluated to 150 (Refer Figure 1). Each set of road surfaces vibration will take approximately 9 minutes to test. After each vibration they will have a pause of 5 second to rest their hands and to response to the vibrations, and after each set they will have a break of 1 minute. Therefore, the total test duration is approximately 45 minutes. Images of road surfaces will be displayed in front of you (Refer Figure 2 and 3). You will then be asked to respond "yes" or "no" on each vibration your experience whether the vibrations caused by the road surfaces displayed. Both total number of stimuli and time were designed to take into consideration the learning the fatigue effects.

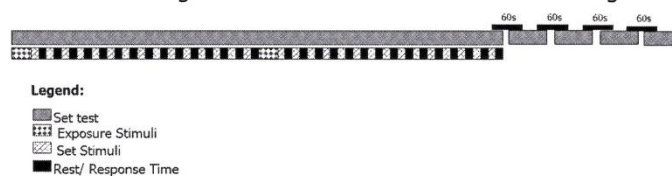


Figure 1: Experiment design

7. Ok, now I will explain **how to response to the vibrations**.

Appendix 1.4 Test procedure for Experiment 2 (Chapter 8)

8. There are **two possible answers** for the response. Your driving experience is very important to determine the vibration. You need to state:

- i. **Yes** – You are experiencing vibrations represent the picture shown (Refer Figure 2)
- ii. **No** – You are experiencing vibration does not represent the picture shown (Refer Figure 2)



Figure 2: Example of road surface picture

9. If at any time before or during the experiment you should decide that you wish to **stop**, please state this and the procedure will be brought to a halt.

10. Please now remove any articles of **heavy clothing**, any **watches** and any **jewellery, glasses** or other items, which might effect your perception of road surface vibration.

11. Please now sit in the simulator and adjust the **sitting posture** to the **same position** as you are driving. Please don't touch the simulator frame with your legs or feet (Refer Figure 3).

12. Please now **hold the steering wheel in the middle of the hand grips** using both hands and **maintain a constant palm grip**, avoiding touching the lower and upper arms. You should try to adopt a posture which is as close as possible to the one you use in your own car (Refer Figure 3).



Figure 3: Steering wheel simulator and position of participant

13. Do you have any questions before the formal testing starts?

14. Now, I will send to you the 20-seconds of vibration signal or I can say as a **exposure vibration signal** from the photograph road shown in front of you (Refer Figure 2). At this stage, you need to try to **remember or really feel** the vibration to be used for the testing after this. Are you ready?

15. Now, we start the testing. Are you ready?

16. Can you detect the vibration signal same as the exposure that you felt before? Yes or No?

17. Ok, now the **testing is complete**.

18. Before you leave, please complete the questionnaire related to the **vibrational sickness**.

19. Thank you very much for having taken part in this experiment.

Appendix 1.4 (continued) Test procedure for Experiment 2 (Chapter 8)

PARTICIPANTS CONSENT FORM

Please read carefully the information below which summarises the experiment which you are being requested to perform. Please tick appropriate box and indicate your agreement to participate by providing your signature and the date at the bottom.

The purpose of this experiment is to investigate the human perception of road surface stimuli. You will be asked to sit in a specially-designed simulator where you will be exposed to rotational steering wheel vibrations similar in level to those experienced in automobiles.

The experiments will last approximately one hour and half, in which time you will be exposed to a set of vibration stimuli. You will be asked to state, by means of your detection, at each and every stimulus sent to you.

The data you provide will be used to develop measure of the information contained in the stimuli. All information will be considered fully confidential and only tabulated general statistics will be used in reports and publications.

<i>The participant should complete the whole of this sheet him/herself</i>		
	YES	NO
Have you read the Research Participants Information Sheet?	<input type="checkbox"/>	<input type="checkbox"/>
Have you had an opportunity to ask questions and discuss this study?	<input type="checkbox"/>	<input type="checkbox"/>
Have you received satisfactory answers to all your questions?	<input type="checkbox"/>	<input type="checkbox"/>
Do you understand that you will not be referred to by name in any report concerning the study?		
• at any time?	<input type="checkbox"/>	<input type="checkbox"/>
• without having to give a reason for withdrawing?	<input type="checkbox"/>	<input type="checkbox"/>
I agree to my interview being recorded.	<input type="checkbox"/>	<input type="checkbox"/>
I agree to the use of non-attributable direct quotes when the study is written up or published.	<input type="checkbox"/>	<input type="checkbox"/>
Do you agree to take part in this study?	<input type="checkbox"/>	<input type="checkbox"/>
Signature of Research Participant:		
Name in capitals:	Date:	

Appendix 1.5 Participants consent form for Experiment 1 (Chapter 7)

PARTICIPANTS CONSENT FORM

Please read carefully the information below which summarises the experiment which you are being requested to perform. Please tick appropriate box and indicate your agreement to participate by providing your signature and the date at the bottom.

The purpose of this experiment is to investigate the human perception of road surface stimuli. You will be asked to sit in a specially-designed simulator where you will be exposed to rotational steering wheel vibrations similar in level to those experienced in automobiles.

The experiments will last approximately 45 minutes, in which time you will be exposed to a set of vibration stimuli. You will be asked to state, by means of your detection, at each and every stimulus sent to you.

The data you provide will be used to develop measure of the information contained in the stimuli. All information will be considered fully confidential and only tabulated general statistics will be used in reports and publications.

<i>The participant should complete the whole of this sheet him/herself</i>		
	YES	NO
Have you read the Research Participants Information Sheet?	<input type="checkbox"/>	<input type="checkbox"/>
Have you had an opportunity to ask questions and discuss this study?	<input type="checkbox"/>	<input type="checkbox"/>
Have you received satisfactory answers to all your questions?	<input type="checkbox"/>	<input type="checkbox"/>
Do you understand that you will not be referred to by name in any report concerning the study?		
• at any time?	<input type="checkbox"/>	<input type="checkbox"/>
• without having to give a reason for withdrawing?	<input type="checkbox"/>	<input type="checkbox"/>
I agree to my interview being recorded.	<input type="checkbox"/>	<input type="checkbox"/>
I agree to the use of non-attributable direct quotes when the study is written up or published.	<input type="checkbox"/>	<input type="checkbox"/>
Do you agree to take part in this study?	<input type="checkbox"/>	<input type="checkbox"/>
Signature of Research Participant:		
Name in capitals:	Date:	

Appendix 1.6 Participants consent form for Experiment 2 (Chapter 8)

PARTICIPANTS INFORMATION FORM

Section A: Personal Details					
(1) Full Name: _____					
(2) Age (years): _____	(3) Gender:	<input type="checkbox"/> Male	<input type="checkbox"/> Female		
(4) Height (m): _____	(5) Weight (kg): _____				
(6) Driving experience (years): _____					
Section B: Health Information					
(1) Are you often exposed to vibrations, or do you regular use vibration-producing tools as part of work or hobbies (i.e. drills, hand phone vibration)?					
<input type="checkbox"/> Yes		<input type="checkbox"/> No			
If Yes, please specify: _____					
(2) Do you have any physical condition which you feel may affect your vibration test responses?					
<input type="checkbox"/> Yes		<input type="checkbox"/> No			
If Yes, please specify: _____					
(3) Did you consume alcohol or coffee in the last hour before the experiment?					
<input type="checkbox"/> Yes		<input type="checkbox"/> No			
If Yes, please specify: _____					
Section C: Vibrational Sickness (After Experiment)					
		None	Slight	Moderate	Severe
(i)	General discomfort	<input type="checkbox"/>	<input type="checkbox"/>	<input type="checkbox"/>	<input type="checkbox"/>
(ii)	Fatigue	<input type="checkbox"/>	<input type="checkbox"/>	<input type="checkbox"/>	<input type="checkbox"/>
(iii)	Headache	<input type="checkbox"/>	<input type="checkbox"/>	<input type="checkbox"/>	<input type="checkbox"/>
(iv)	Nausea	<input type="checkbox"/>	<input type="checkbox"/>	<input type="checkbox"/>	<input type="checkbox"/>
(v)	Stomach awareness	<input type="checkbox"/>	<input type="checkbox"/>	<input type="checkbox"/>	<input type="checkbox"/>
(vi)	Dizziness	<input type="checkbox"/>	<input type="checkbox"/>	<input type="checkbox"/>	<input type="checkbox"/>
(vii)	Increased salivation	<input type="checkbox"/>	<input type="checkbox"/>	<input type="checkbox"/>	<input type="checkbox"/>
(viii)	Drowsiness	<input type="checkbox"/>	<input type="checkbox"/>	<input type="checkbox"/>	<input type="checkbox"/>
Signature of Research Participant: _____		Date: _____			

Appendix 1.7 Participants information form for both Experiment 1 (Chapter 7) and Experiment 2 (Chapter 8)

Subject: Volunteers sought for a study of the human perception of steering wheel vibration

I am seeking volunteers who have at least two years of automobile driving experience for a study regarding the human ability to understand road surfaces from the vibration of the automobile steering wheel.

The experiment will be held at the Human Centred Design Lab (Room TA043), Brunel University, London UB8 3PH. During the experiment, you will be asked to sit in a specially-designed simulator where you will be exposed to rotational steering wheel vibration of the type experienced in automobiles. During the experiment you will be shown photograph of a road surface, and will be asked whether you can detect the source of the vibration which you are feeling through the steering wheel are from the photograph shown.

This experiment has been approved by the College of Engineering, Design and Physical Sciences Research Ethics Committee, Brunel University, London UB8 3PH.

If you are interested in taking part in the experiment or seek further information, please contact:

Sabariah Mohd Yusoff
PhD Design Research Student
Perception Enhancement Research Group
College of Engineering, Design and Physical Science
Brunel University, London
Email: Sabariah.MohdYusoff@brunel.ac.uk
Tel.: +44 (0) 741 744 2331

Appendix 1.8 Advertisement on the “Get Involved” section of the intraBrunel home page to seek for participants

